1-1-2011

A Molecular Basis for Divergent, Unstable Actin Filaments in Toxoplasma gondii

Kristen Skillman
Washington University in St. Louis

WASHINGTON UNIVERSITY IN ST. LOUIS

Division of Biology and Biomedical Sciences

Program in Molecular Microbiology

Dissertation Examination Committee:
L. David Sibley, Chairperson
John A. Cooper
Tamara L. Doering
Daniel E. Goldberg
Petra A. Levin
David Sept

A MOLECULAR BASIS FOR DIVERGENT, UNSTABLE ACTIN FILAMENTS IN *TOXOPLASMA GONDII*

by

Kristen Michelle Skillman

A dissertation presented to the
Graduate School of Arts and Sciences
of Washington University
in partial fulfillment of the
requirements for the degree
of Doctor of Philosophy

August 2011

Saint Louis, Missouri

ABSTRACT OF THE DISSERTATION

A Molecular Basis for Divergent, Unstable Actin Filaments

in *Toxoplasma gondii*

by

Kristen Michelle Skillman

Doctor of Philosophy in Biology and Biomedical Sciences

(Molecular Microbiology and Microbial Pathogenesis)

Washington University in St. Louis, 2011

Dr. L. David Sibley, Chairperson

Toxoplasma gondii is an important parasitic pathogen of the phylum Apicomplexa. Parasite invasion of host cells involves a unique gliding motility mechanism that is dependent on polymerization of parasite actin. However, in non-motile parasites, the majority of actin is monomeric and filaments only assemble upon initiation of gliding motility. Actin filament turnover is crucial for motility as shown by the detrimental effects of jasplakinolide, an agent that stabilizes actin filaments. *T. gondii* actin (TgACTI) is functionally highly divergent from conventional actin and only polymerizes into very short filaments. To understand why *T. gondii* actin does not form long filaments and uncover what contributes to its unusual polymerization kinetics, TgACTI filaments were examined using molecular modeling and biochemical assays. Phalloidin binding to parasite actins rescued the short filaments demonstrating that although TgACTI naturally forms short, unstable filaments on its own, it is capable of forming longer, conventional filaments when stabilized. Molecular docking was used to identify

divergent residues within apicomplexan actin that may impart filament stability and revealed critical substitutions in the hydrophobic plug and phalloidin-binding pocket that are predicted to affect subunit interactions within the filament. Mutations were made within TgACTI to replace residues unique to apicomplexan actins with those from muscle actin resulting in formation of longer actin filaments *in vitro*. When this substituted, stabilized actin was expressed within the parasite, it had a deleterious impact on gliding motility exhibited by aberrant forms of both circular and helical gliding combined with a decrease in speed. The ability of TgACTI to polymerize is also controlled by a minimal set of canonical actin-binding proteins. *T. gondii* encodes two formin proteins, TgFRM1 and TgFRM2, and interaction of these proteins with TgACTI results in a dramatic increase in polymerization. However, *T. gondii* profilin (TgPRF) acts to sequester TgACTI from the growing filament. Finally, examination of concentration dependent polymerization has revealed evidence that TgACTI is utilizing an isodesmic mechanism for polymerization. Collectively, these results demonstrate that *T. gondii* has evolved multiple mechanisms for controlling the length of actin filaments within the parasite and these adaptations appear to be critical for productive gliding motility.

ACKNOWLEDGEMENTS

The completion of this dissertation would not have been possible without contributions from many individuals. I am indebted to my committee members for all of their valuable advice, it was a unique opportunity to interact with so many experts in various fields. I especially want to thank my advisor, David Sibley, for his excellent mentorship. In addition to being an inspiring scientist, David is a fantastic teacher who puts enormous energy into mentoring each student in his lab and I am grateful to have had the opportunity to learn from him. Graduate school would not have been the same without all of the amazing colleagues I have been fortunate enough to work with over the years. Lab members, past and present, made the lab an amazing scientific, as well as entertaining, atmosphere. I am also appreciative of the members of the microbiology department for their assistance and comradery. My friends have been an amazing support system for this journey by lending an ear or a hand, celebrating victories, big or small, and helping to drown sorrows when things got tough. Last but not least, I cannot thank my family enough for all their encouragement. A special thank you goes to my mom and dad who have offered me unending guidance and cheered me on in anything I have undertaken.

TABLE OF CONTENTS

LIST OF FIGURES

Chapter I: Introduction

Chapter 2: Divergent, Unstable Actin Filaments in Apicomplexan Parasites are Rescued by Phalloidin

Chapter III: Mutations that Increase Actin Filament Stability Disrupt Motility in *Toxoplasma gondii*

LIST OF TABLES

Chapter I

Introduction

This chapter was composed entirely by Kristen Skillman. Comments from David Sibley are incorporated into the final version presented here.

The Phylum Apicomplexa

Apicomplexan parasites are obligate intracellular protozoan pathogens of humans and animals, many of agricultural importance (Dubey, 2010). There are over 5000 species within this phylum that infect a broad range of hosts (Levine, 1988). Noteable members include the tissue-cyst forming coccidia *Toxoplasma* (the causative agent of toxoplasmosis) and *Sarcocystis* (animal pathogen), enteric coccidia *Eimeria* (animal pathogen largely afflicting poultry) and *Cyclospora* (food-borne diarrheal disease), haemosporinids including *Plasmodium (*the agent of malaria), piroplasms *Thelieria* (cattle parasites) and *Babesia* (tick-borne fever), cryptosporidians *Cryptosporidium* (water-borne diarrheal disease) and Gregarines, the most ancient members of the phylum (Levine, 1988).

Toxoplasma gondii

Toxoplasma gondii is a ubiquitous member of the Apicomplexa and it is estimated that as much as one third of the world population has been exposed to the parasite (Tenter et al., 2000). *T. gondii* also infects all warm-blooded animals making it one of the most common parasitic diseases to inflict humans and animals (Hill and Dubey 2002). The prevalence of infection with *T. gondii* is highly dependent on the geographical region examined with an estimated 11-16% of the population infected in the United States (Dubey and Jones, 2008), and 8-22% of the population infected in the United Kingdom while there is a much greater prevalence, 51-72%, in Central and South America and 37-58% in Europe (Tenter et al., 2000). Despite its ubiquitous presence in the human

population, *T. gondii* is an opportunistic pathogen and disease symptoms are normally more severe in immunocompromised individuals and developing fetuses.

Different isolates of *T. gondii* exhibit high similarity to one another and genotyping strains from North America and Europe revealed that the parasite exists in three clonal lineages, each differing in the extent of virulence toward the host (Howe and Sibley, 1995). Type I comprises the most highly virulent parasites. Type II and Type III are avirulent and differ in the host they infect; Type II parasites are mainly found in animal and human infections while Type III parasites have been found primarily in animals (Howe and Sibley, 1995). This division in virulence can be partly attributed to differential expression of virulence factors among these lineages (Saeij et al., 2006; Su et al., 2002; Taylor et al., 2006). Recent analysis has added a fourth clonal lineage for North American strains (Khan et al., 2011). Isolates collected from South America appear to have more variability and group into a number of separate haplogroups (Dubey and Su, 2009; Khan et al., 2007; Lehmann et al., 2006).

Toxoplasma gondii **Life Cycle**

The *T. gondii* life cycle consists of a feline definitive host and non-feline intermediate host (Frenkel et al., 1970). The parasite has been isolated from intermediate hosts ranging from mammals to birds. Unlike many pathogens, disease caused by *T. gondii* is less severe within the definitive host as compared to the intermediate host (Dubey, 2010). Within these hosts, *T. gondii* progresses through various stages of development including sporozoites (within the oocyst), tachyzoite and bradyzoite (within the tissue cyst).

Sexual Cycle

T. gondii sporozoites undergo the sexual stage of the parasite life cycle within the intestine of the cat, its definitive host (Frenkel et al., 1970). Infected cats then shed oocysts containing sporozoites in their feces and these oocysts can be infective to humans or other animals if water or food is contaminated and ingested. Oocysts are very resilient and can survive harsh environmental conditions for up to 18 months (Dubey, 2010). Oocyst ingestion by mammals leads to the asexual stage of the *Toxoplasma* life cycle where the parasite develops into tachyzoites and can replicate within the non-feline host (Dubey, 2010).

Asexual Cycle

Following oral ingestion, the tachyzoites, the rapidly multiplying stage of the parasite, cross the intestinal epithelium to move into deeper tissues and can eventually cross other barriers like the placenta, blood brain barrier or central nervous system where it can infect virtually any nucleated cell. The acute stage of infection results in the host mounting a strong inflammatory response leading to the clinical manifestations of disease (Montoya and Liesenfeld, 2004). In healthy hosts, the immune response leads to transformation of the tachyzoites into bradyzoites that replicate slowly and persist within tissue cysts in the brain, skeletal and cardiac muscle and liver (Dubey, 1994). The cysts persist for the life of the host establishing the potential for reactivation if there is a change in the integrity of the immune system.

Tissue cysts may be transmitted between hosts upon ingestion of undercooked contaminated meat thereby continuing the asexual cycle or sexual cycle if a cat ingests

cysts (Dubey, 2010). Upon ingestion, the cyst wall dissolves releasing bradyzoites enabling them to infect the intestinal epithelia and differentiate back into tachyzoites for dissemination throughout the host.

Toxoplasmosis

Non-congential infections with *T. gondii* occur after ingesting tissue cysts in undercooked meat or drinking water that is contaminated with oocysts shed in cat feces. There is evidence that the infection from ingestion of oocysts is more severe than that from tissue cysts. The first sign of toxoplasmosis is enlarged lymph nodes often combined with flu-like symptoms of fever, sore muscles, sore throat and headaches.

Infection with the parasite often goes unnoticed in the majority of its otherwise healthy hosts, but infection becomes a severe problem in immunocompromised patients and children who are congenitally infected. Patients with a suppressed immune system are unable to slow tissue destruction of the rapidly multiplying tachyzoite stage. Immune suppression is a large problem due to progression of the infection to toxoplasmic encephalitis. Toxoplasmosis is a leading cause of death associated with patients who have acquired immunodeficiency syndrome (AIDS) where infection of the brain is common. Encephalitis, if left untreated, is often fatal for AIDS patients (Luft and Remington, 1992). Ocular pathology (Roberts and McLeod, 1999) and neurological problems (Luft et al., 1993) are other consequences of toxoplasmosis that manifest in immunocompromised patients. Additionally, as a consequence of the high natural burden of chronic infection in otherwise healthy hosts, organ transplant patients may become infected with *T. gondii* via a seronegative recipient receiving an organ from a seropositive

donor. For seropositive patients, immunosuppresion from the transplant may result in undergoing reactivation of a latent infection. The parasite can also cause blindness, mental retardation, or prenatal abortion if a pregnant woman is exposed to the parasite. The severity of congential infection decreases through later trimesters (Desmonts and Couvreur, 1974).

Treatment

Pyrimethamine and sulfonamides can control replication of *Toxoplasma* but do not eradicate chronic infection (McCabe, 2001). Spiramycin does not cross the placenta and may be used to prevent transferring infection from mother to fetus (Desmonts and Couvreur, 1974) although it is not marketed in the United States and it does not appear to be effective against established fetal infections (Wong and Remington, 1994). Clindamycin, atovaquone, and azinthromycin also have antitoxoplasmic effects and can be used for treatment (McCabe, 2001). Many of these drugs have numerous side effects demonstrating a need for new treatments.

Apicomplexan Apical Complex and Cytoskeleton

T. gondii, as well as the other members of the apicomplexan phylum, have an elongated shape with a specialized apical region (Morrissette and Sibley, 2002). *T. gondii* encounters a number of treacherous environments throughout its life cycle including the gastrointestinal tract and must be able to maintain its cell shape in stressful niches. Cell shape is maintained structurally by a number of elements of the apicomplexan cytoskeleton that are conserved within the members of the phylum. In

addition to providing structural integrity of the parasite, maintaining the cytoskeleton is critical for invasion of host cells and replication within them. *T. gondii* has an apical complex comprised of an apical polar ring, two preconoidal rings, a conoid, and secretory organelles (Morrissette and Sibley, 2002). The cytoskeletal make-up of the parasite includes microtubules, a network of intermediate-like filaments and inner membrane complex (IMC) to create the parasite's shape (Figure 1A).

Apical Polar Rings

T. gondii contains two preconoidal rings, an inner and outer ring. The outer ring is found at the top of the conoid in its resting state and covers the apical rim of the IMC. An apical polar ring is also presents beneath the conoid serving as a microtubule organizing center and acts to anchor the 22 singlet, subpellicular microtubules that emanate through the parasite (Morrissette and Sibley, 2002). Ultrastructural examination of the polar ring of *Eimeria* suggested that it controlled the number, spacing, directionality and orientation of the microtubules (Russell and Burns, 1984). Depressions were seen within the ring where the ends of the microtubules attached leading to predictions that the polar ring caps the microtubules (Russell and Burns, 1984).

Conoid

The conoid is a tube-like hollow cylinder of spirally woven microtubules that moves up and down through the preconoidal polar rings. The conoid microtubules are unusual in that they wind into a counterclockwise spiral where the filaments are asymmetrical and form 9 protofilaments (Hu et al., 2002). The conoid is an element unique to *Toxoplasma*,

Eimeria and *Sarcocystis* and protrudes at the time of host cell invasion suggesting it may aid these parasites in penetrating intestinal epithelium (Morrissette and Sibley, 2002). Conoid extrusion is dependent upon calcium fluxations within the parasite (Mondragon and Frixione, 1996) and actin and myosin but not microtubules play a role in regulating extrusion (Del Carmen et al., 2009). Following detergent extraction and sonication, conoid-enriched preparations were subjected to MudPit analysis to identify the proteins associated with the complex. These studies identified TgMORN1 as a protein that concentrates at the conoid but additionally as the first structural marker for the basal end of the parasite. Two centrins, dynein light chain (TgDLC) and calcium binding proteins (TgCAM-1 and –2) were also identified as part of the complex with the later three proteins suggested to be potential regulators of conoid extrusion in *T. gondii* (Hu et al., 2006).

Subpellicular Microtubules

The subpellicular microtubules of *T. gondii*, organized via the apical polar ring, are unusually stable and form filaments around 5 μM long that run along two-thirds the length of the parasite ending just past the nucleus (Nichols and Chiappino, 1987). *T. gondii* contains 22 singlet microtubules, comprised of 13 tubulin-containing protofilaments, creating 22 nm hollow tubes that are equally spaced around the parasite (Nichols and Chiappino, 1987). The number of microtubules as well as their distribution differs among members of the apicomplexa with notable differences seen in *P. falciparum*, which has only 3 microtubules that emanate down one side of the parasite (Fowler et al., 2001), or other *Plasmodium* spp. where all but one microtubule is spaced

across two-thirds of the parasite (Morrissette and Sibley, 2002). Despite the varied arrangements, the subpellicular microtubules are thought to contribute to structural stability of the parasites as demonstrated by the fact that depolymerization of microtubules using chemical agents disrupts cell shape and polarity (Morrissette and Roos, 1998). Additionally, *T. gondii* microtubules are highly stable and resistant to many microtubule destabilizing drugs when parasites are extracellular, but intracellular replicating parasites are sensitive to high concentrations of colchicines and dinitroanilines, such as oryzalin (Morrissette and Sibley, 2002). Drug-treated intracellular parasites are unable to assemble proper subpellicular microtubules and fail to infect host cells, demonstrating the need for proper cell shape and rigidity in host cell invasion.

Cryoelectron tomography of the *P. berghei* microtubule lattice revealed 8 nm periodicities that were not observed with the more conventional pig brain tubulin (Cyrklaff et al., 2007). Similar periodicities were also seen along microtubules extracted from *T. gondii* tachyzoites. It was hypothesized that the microtubules of these parasites must be elastic to undergo turns and movement into host cells. These studies revealed that *P. berghei* microtubules could undergo turns with radii as small as 86 nm demonstrating these microtubules are not only stable but also highly elastic. Visualization of increased luminal density of the microtubules lead to identification of an unconventional microtubule associated protein (MAP). The microtubule structure of *T. gondii* was examined using Fourier methods and a 32 nm periodicity of particles was found, also suggesting interaction with a MAP (Morrissette et al., 1997). In *P. berghei*, uncapped microtubule ends were visualized but depolymerization was not seen

suggesting this unidentified factor may bind to aid in preventing breakage of the microtubules (Cyrklaff et al., 2007). Similar phenomena have previously been seen in other organisms with reduced microtubule treadmilling such as chlamydmonas and trypanosomes (Nicastro et al., 2006; Vaughan et al., 2006).

Secretory organelles

Situated at the apical end of the parasite are secretory organelles containing proteins that are discharged in a specific order to aid with various portions of the parasite life cycle (Carruthers and Sibley, 1997). The micronemes are small rod-shaped structures that release microneme (MIC) proteins important for host cell attachment, motility and host cell invasion. Rhoptries are club-shaped organelles with a long neck. Proteins secreted from the rhoptries play a role host cell invasion, creation of the parasitophorous vacuole (PV) and immune evasion. The proteins are secreted in a hierarchical manner with the proteins in the rhoptry neck (RONs) secreted first, followed by those in the rhoptry bulb (ROPs). Dense granules are found throughout the parasite but are more highly concentrated at the apical end. The dense granule proteins (GRAs) from this organelle are typically associated with the parasitophorous vacuole membrane (PVM).

Subpellicular Network

It is clear that cytoskeletal components provide the structure to apicomplexan cells; however, the fact that the subpellicular microtubules do not extend the entire length of the parasite body suggests that another element existed to provide further mechanical stability. Experiments extracting the cytoskeleton of *T. gondii* to examine protein

composition identified a network of interwoven filaments (8-10 nm in diameter) that extends from the polar ring along the entire length of the parasite and is anchored into a cup-like structure at the parasite posterior (Mann and Beckers, 2001; Porchet and Torpier, 1977). The extremely stable complex formed by this filamentous network, surrounds the microtubule cytoskeleton and was aptly named the subpellicular network. Further analysis of the protein make up of the network identified the novel protein TgIMC1 as a major component as well as a homolog in *Plasmodium* species (Mann and Beckers, 2001).

Inner Membrane Complex

Apicomplexans also contain a double membranous inner membrane complex (IMC) comprised of flattened vesicles originating from the endoplasmic reticulum that are sutured together. An exception is the sporozoite stage of *Plasmodium* where the IMC is created by one large flattened vesicle (Morrissette and Sibley, 2002). Together with the outer plasmalemma, the IMC creates a three membrane pellicle surrounding the parasite. The IMC extends to cover the intermediate filaments that make up the subpellicular network and delineates a compartment beneath the plasma membrane. Cytoskeletal components such as actin and myosin have been shown to localize to the inner membrane space possibly for their role in parasite motility.

Intramembranous particles (IMPs) run in parallel rows down the length of the parasite throughout the IMC and are arranged in single and double rows with a 32 nm periodicity (Morrissette et al., 1997). Twenty-two double rows of IMPs are present in the IMC cytoplasmic face and follow the path of the subpellicular microtubules (Morrissette et al.,

1997). The double rows are thought to associate with microtubules but the IMPs extend the full length of the parasite even though the microtubules only reach 2/3 of the length suggesting there is also an interaction with the subpellicular network. The single rows of IMPs are a likely candidate for linkage of the subpellicular network to the IMC (Mann and Beckers, 2001).

Apicomplexan Host Cell Invasion

The ability of *T. gondii* and other apicomplexan parasites to enter into host cells is essential for their development. The conserved apical complex and cytoskeleton among the members of this phylum leads to a conserved mechanism for host cell entry. Invasion is an active process controlled by the parasite as seen by an absence of membrane ruffling and host actin rearrangement that are associated with phagocytosis (Morisaki et al., 1995). In order to complete a full lytic cycle, *T. gondii* must undergo gliding motility to find a cell to invade, attach to and enter the cell, establish a parasitophorous vacuole in which to replicate and then egress from the cell in order to repeat the cycle and continue infection within the host.

Gliding motility

The force for invasion of apicomplexans through host cell membranes is dependent on forward motility of the parasite (Morisaki et al., 1995). Typically, cells undergo one of two types of motility: swimming, which requires flagella or cilia to propel a microorganism through an environment or amoeboid crawling which relies on rearrangement of host cell actin to create lamellipodia which moves in response to certain

stimuli. However, apicomplexans lack flagella or cilia for swimming motility and do not undergo a change in cell shape as the parasite migrates as in amoeboid motility. Rather, apicomplexans employ a gliding motility mechanism that is dependent on polymerization of their own actin into filaments instead of utilizing host cell powered machinery for entry (Dobrowolski and Sibley, 1996).

Gliding motility is unique to apicomplexans and conserved among the phylum. It is a fast, ~1 μm/sec, substrate dependent process (Håkansson et al., 1999). Initial evidence of gliding was seen by visualization of protein trails that these parasites leave behind as they glide on glass coverslips. For *T. gondii*, these trails can be visualized by immunofluorescence staining with antibodies again surface antigen-1 (SAG1) (Dobrowolski and Sibley, 1996). Similar surface-protein laden trails have also been reported from other apicomplexans including *Plasmodium* sporozoites (Vanderberg, 1974), *Eimeria* (Russell and Sinden, 1981) and *Cryptosporidium* (Arrowood et al., 1991). These trails appear to be formed as a result of membrane shedding during motility and contain proteins found on the parasite surface, but normally not those that are secreted (Håkansson et al., 1999). Interestingly, despite the high conservation of gliding motility among the apicomplexans, one member of the phylum, *Theileria*, does not appear to utilize gliding motility for host cell entry and instead relies on an zippering mechanism for invasion that requires host cell actin, suggesting a more passive entry process (Shaw, 1999).

Further investigation of gliding motility in *T. gondii* using videomicroscopy observed that the parasites undergo three distinct types of gliding motility: circular, helical and twirling (Håkansson et al., 1999). During circular gliding, the parasite lies on its right

side and moves in a counterclockwise circle. Circular gliding motility does not net any forward movement and as a result does not allow host cell invasion. In order to undergo productive forward motion and entry into host cells, the parasite relies on the helical form of gliding motility. Helical gliding is a biphasic process that begins when the parasite lies on its left side and undergoes a clockwise corkscrew motion of 180 degrees and nets a forward motion of one body length. Once the parasite turns to its concave face, it can no longer contact the substrate so it raises itself onto its posterior end and flips back to its left side to reinitiate the process. The second phase of helical gliding yields no net forward motion. Twirling motility occurs when the parasite attaches its posterior to substrate and spins in a clockwise motion. This movement is similar to helical gliding but in the z-plane and results in no forward progress. Videomicroscopy studies were also used to visualize parasites utilizing gliding motility as a means to drive themselves into host cells for invasion (Håkansson et al., 1999). *Plasmodium* sporozoites have been observed to undergo similar types of motion after injection into the dermis (Amino et al., 2006). *Plasmodium* ookinetes also undergo gliding within the mosquito midgut (Vlachou et al., 2004), although the speed of movement for the ookinetes was slower than that observed for *T.gondii* tachyzoites (0.1 μm/sec vs 1-3 μm/sec) (Siden-Kiamos et al., 2006).

Further studies into the movements of *Plasmodium* sporozoites using reflection interference contrast and traction force microscopy observed that the parasites undergo stick-and-slip movements from specific adhesion sites that require turnover for movement to occur (Munter et al., 2009). Initial attachment sites at both poles where seen to form (stick) as well as an adhesion site located more centrally. The front patch

then disengaged with the central patch appearing to provide some force for movement. As the posterior patch released, the parasite moved (slide) forward.

Numerous studies of the molecular components of gliding have led to a model where cytoskeletal elements within the parasite pellicle are capped by adhesive proteins on the outer surface of the parasite that mediate motility. The proteins involved in this process have been dubbed components of the "glideosome" and are described in more detail below. At the onset of *T. gondii* gliding, the parasite secretes the micronemal adhesin, MIC2, from its apical end, which makes contacts with receptors on the substratum or host cell surface (Figure 1B). Beneath the membrane of the parasite, the cytoplasmic tail of MIC2 is linked to actin filaments via interaction with aldolase, which has been shown to interact with both MIC2 and actin (Jewett and Sibley, 2003). Non-processive myosin motors that are anchored in the inner membrane complex of the parasite, translocate these actin filaments rearward through the cell, causing movement of MIC2 along the surface. As MIC2 moves along the parasite surface, it is cleaved by a rhomboid protein localized in the cell membrane allowing the "conveyor belt" to continue moving (Brossier et al., 2005; Buguliskis et al., 2010). The final result of this process is forward motion of the parasite and entry into host cells. Gliding motility plays a role in transmigration of polarized cell layers such as the intestinal epithelium, allowing greater dissemination through the host (Barragan and Sibley, 2002).

Host attachment

The parasite must tightly attach to the host cell prior to invasion. When the apical end of the parasite comes into contact with the host cell, it discharges it secretory

organelles, first the micronemes followed by the rhoptries (Carruthers and Sibley, 1997). Many microneme proteins appear to play a role in attachment to the host cell. Depletion of the micronemal proteins TgMIC2 or TgAMA1 disrupts the ability of *T. gondii* to attach to host cells thereby reducing invasion (Huynh et al., 2004; Mital et al., 2005). After initial attachment has been established, the rhoptry proteins are discharged into the host cell that play a role in establishing the parasitophorous vacuole (below). The parasite then creates a ring-shaped zone of intimate attachment between the parasite and host cell known as the moving junction. Many proteins involved in invasion localize to this junction forming a ring around the parasite including the rhoptry neck proteins (RONs), which form a complex with TgAMA1 at the moving junction (Alexander et al., 2005; Lebrun et al., 2005). The moving junction moves toward the posterior of the parasite as invasion progresses and it enters into the host cell. Recent evidence suggests RON proteins may insert into the host cell membrane thereby creating a receptor for the parasite (Besteiro et al., 2009).

Vacuole formation

As the parasite invades the host cell through the moving junction, it creates and enters into a parasitophorous vacuole (PV), which is non-fusogenic and acts as a barrier to provide separatation from the host cell cytoplasm (Mordue and Sibley, 1997). The PV initially forms via an invagination of the host cell membrane (Suss-Toby et al., 1996). However, the moving junction is predicted to play a role in selecting what components are present in the parasitophorous vacuole membrane (PVM) and many host cell components appear to be excluded from the PVM. Selective exclusion is largely based

on how proteins are anchored in the membrane (Mordue et al., 1999). The rhoptry contents secreted just prior to invasion form vesicles that fuse with the PVM and further modify it (Håkansson et al., 2001). Eventually the PV becomes associated with the host cell ER and mitochondria (Jones et al., 1972). Once the PV is established, dense granules release GRAs to modify the intracellular face of the PV (Carruthers and Sibley, 1997).

Replication

Replication of *T. gondii* occurs within the PV by the mechanism of endodyogeny, a process of internal budding (Striepen et al., 2007). One of the first steps in budding is the formation of the IMC, which provides a scaffold for daughter cell formation. Much of the mother's cytoplasm is incorporated into the two daughter cells while other structures such as the conoid and secretory organelles are broken down (Striepen et al., 2007). Actin traditionally plays a role in cell division but in *T. gondii*, disruption of actin dynamics has no impact on parasite replication (Shaw et al., 2000). However, disruption of microtubule polymerization is detrimental to the budding of daughter cells demonstrating *T. gondii* replication is a microtubule-driven process (Shaw et al., 2000).

Egress

Egress from host cells is again dependent on microneme secretion and gliding motility. As *T. gondii* undergoes its intracellular cycle, abscisic acid accumulates signaling for egress by cADPR production and increases in intracellular calcium (Nagamune et al., 2008). Calcium increase stimulates the release of micronemal proteins including TgPLP1, a perforin-like protein that aids to permeabilize the PVM and host

membrane for parasite egress (Kafsack et al., 2009). Many calcium dependent processes are regulated by calcium dependent protein kinases (CDPKs). Depletion of TgCDPK1 results in loss of microneme secretion and inability to egress from host cells (Lourido et al., 2010). In addition to abscisic acid accumulation, there is evidence that the parasite can sense the loss of potassium in the host cytosol as the host cell membrane is broken down (Moudy et al., 2001). Decreasing potassium raises the intracellular calcium concentration within the parasite to aid in triggering parasite egress. Once egress from the host cell has occurred, *T. gondii* employs gliding motility to move to a new host cell and reinitiate the invasion process.

Apicomplexan Glideosome

The protein components involved in gliding motility have been termed the glideosome (Opitz and Soldati, 2002). The glideosome is comprised of the actomyosin motor as well as the structural and functional proteins linking the complex together. Glideosome proteins are localized to the pellicle in the space between the inner membrane complex and parasite plasma membrane (Figure 1B). The specific function of glideosome proteins MIC2, aldolase, myosin, glideosome associated proteins and actin are described in more detail below.

MIC2/TRAP

Microneme secretion is required for *T. gondii* to undergo proper invasion (Carruthers et al., 1999). Microneme protein 2, MIC2, has been shown to be critical in gliding motility and host cell attachment (Huynh and Carruthers, 2006). MIC2 contains

extracellular adhesive domains such as integrin-like I domain (A domain) and thrombospondin type I-like (TSP) repeats as well as an acidic cytoplasmic domain, referred to as the C-terminal tail (Ménard, 2001). Thrombospondin-related adhesive protein, TRAP, was identified as the MIC2 homolog in *Plasmodium* sporozoites and knockouts of TRAP revealed it is required for gliding in sporozoites (Sultan et al., 1997). The TRAP knockouts were unable to complete proper gliding motility and instead moved in a pendulum-like motion. The C-terminal tails of MIC2 and TRAP are functionally homologous (Kappe et al., 1999). Additionally, MIC2 interacts with the accessory protein MIC2 associated protein, M2AP, (Jewett and Sibley, 2004) whereas TRAP has no binding partner. Further proof of the conservation of gliding motility among the apicomplexans came with identification of MIC2/TRAP homologs in Plasmodium merozoites (MTRAP) (Baum et al., 2006b) and CTRAP in oocysts (Dessens et al., 1999). MIC2 contains transmembrane domains that are cleaved by rhomboid proteins located within the membrane of the parasite (Brossier et al., 2005; Buguliskis et al., 2010). Cleavage of MIC2 is predicted to be important for continuation of gliding motility.

Aldolase

The glycolytic enzyme aldolase was identified as the bridge that links the C-terminal tail of the extracellular adhesin to the cytoskeleton (Jewett and Sibley, 2003). MIC2 contains two acidic stretches in its C-terminal tail that are important for parasite survival and one of these domains is required for interaction with aldolase (Starnes et al., 2006). Mutants of aldolase were identified that could uncouple its role in glycolysis from its role in MIC2 C-terminal tail binding (Starnes et al., 2009). Parasites expressing the aldolase

mutants that were unable to perform their role in glycolysis had severe motility defects. Additionally, parasites expressing aldolase mutants that were unable to interact with MIC2 showed a reduced ability to invade host cells demonstrating the bridging function of aldolase is important for efficient invasion (Starnes et al., 2009).

Myosin

T. gondii encodes eleven myosins in total: two belonging to class VI (MyoJ and K), five within class XIV (MyoA, B, C, D, E), and one each within classes XXII (MyoF), XXIII (MyoG) and XXIV (MyoI) (Foth et al., 2006). MyoB and MyoC are derived from differential RNA splicing (Heintzelman and Schwartzman, 1997) and may be involved in cell division (Delbac et al., 2001). MyoA is the best studied of these myosins and has been characterized as a fast-step, single headed, plus-end directed motor similar to muscle myosins (Herm-Gotz et al., 2002). However, this myosin is quite unusual with a short neck and C-terminal tail domain, no conserved glycine at the pivot point, does not follow TEDS rule (a position of a loop in the head domain always contains a negatively charged amino acid) and contains degenerate IQ containing motifs in the region that traditionally anchors the regulatory light chain.

The finding that known myosin inhibitors, butanedione monoxime (BDM) (myosin ATPase inhibitor), and myosin light chain inhibitor KT5926, disrupted invasion and gliding was the first evidence that MyoA was an important component in gliding motility (Dobrowolski et al., 1997a) although the specificity of these drugs is not clear. Use of a tetracycline-inducible protein expression system to create parasites that conditionally

express MyoA, confirmed this finding by revealing that depletion of MyoA disrupted gliding motility (Meissner et al., 2002).

T. gondii myosin light chain 1, TgMLC1, was identified as the regulatory light chain for MyoA (Herm-Gotz et al., 2002). A homolog of this protein was identified in *Plasmodium* sporozoites and named MyoA tail domain interacting protein (MTIP) (Bergman et al., 2003). MTIP was localized to the IMC within the sporozoites and similar findings in T.gondii demonstrate MyoA is linked to the inner membrane complex via MLC1, glidesome associated protein 45 and 50 (GAP45 and GAP50) (below).

Glideosome Associated Proteins

Glideosome associated protein (GAP) 45 and 50 were isolated from the *T. gondii* pellicle and determined to play a role in anchoring MyoA to the inner membrane complex (Gaskins et al., 2004). MyoA interacts with the N-terminus of MLC1, which in turn binds to the C-terminus of GAP45 (Frenal et al., 2010). GAP45 is regulated through phospohorylation and this controls the final assembly step of the motor complex as phosphorylation of this protein blocks association of GAP45-MyoA-MLC1 with GAP50 (Gilk et al., 2009). In addition to its interaction with the IMC, GAP45 has an N-terminal lipid modification that anchors it to the PM, thereby spanning the entire inner membrane space. Knockout of GAP45 in *T. gondii* disrupts gliding and invasion demonstrating a role for GAP45 in pellicle integrity (Frenal et al., 2010). GAP40 was recently identified as an additional member of this complex (Frenal et al., 2010).

Actin

Actin is an essential protein in eukaryotic cells and its sequence is highly conserved among organisms (Pollard et al., 2000). *T. gondii* contains one actin gene, TgACTI, (Dobrowolski et al., 1997b), while *Plasmodium* contains two actin alleles, PfACTI and PfACTII (Gordon and Sibley, 2005). TgACTI has 93.1% sequence identity with PfACTI and 83% with mammalian actin (Dobrowolski et al., 1997b). PfACTI and PfACTII have 79% sequence similarity to one another (Morrissette and Sibley, 2002), which is the lowest similarity for any organism containing multiple actins. The *Plasmodium* genes also differ in their transcription profiles as PfACTI is expressed throughout the parasite life cycle but PfACTII is upregulated in the sexual stages (Kissinger et al., 2003). The conservation of actins is low and numerous apicomplexan-specific amino acid substitutions have been identified by phylogenic comparisons (Sahoo et al., 2006). Phylogenetic analysis also revealed that apicomplexan actins form their own branch away from more conventional actins. Actin monomers from higher eukaryotes have four subdomains with the nucleotide binding pocket located between subdomains 1 and 3, a DNaseI binding loop within subdomain 2 and a hydrophobic loop between subdomains 3 and 4. Many substitutions within apicomplexan actin are found within the DNaseI loop of subdomain 2 resulting in limited flexibility, between subdomains 3 and 4, which are predicted to impact monomer-monomer contacts or within the face of subdomain 1 near the N-terminus, potentially impacting myosin binding (Schüler et al., 2005). Additionally, PfACTI isolated from the parasite was analyzed for post-translational modifications. The only modification seen was N-terminal acetylation, methylation

typically seen on histidine 73, which is normally important for nucleotide binding, was noteably absent (Schmitz et al., 2005).

Role of Parasite Actin in Gliding Motility

Actin polymerization was first determined to be a critical component of apicomplexan gliding motility through studies using cytochalasins, drugs derived from fungal cells, which bind the barbed end of actin filaments thereby preventing further monomer association or dissociation (Cooper, 1987). Cytochalasin D (CytD) treatment has been shown not to prevent attachment of *T.gondii* to host cells but does inhibit entry into phagocytic cells (Dobrowolski and Sibley, 1996). Initially, this finding was interpreted as a requirement for host cell actin polymerization during *T. gondii* invasion (Ryning and Remington, 1978). However, CytD treatment of the parasites was shown to block parasite motility on coverslips (Dobrowolski and Sibley, 1996). The critical experiment to resolve the role of actin in invasion was that upon infection of CytD-resistant host cells, wild type parasites were unable to invade in the presence of CytD even though the host actin would be unimpaired (Dobrowolski and Sibley, 1996). However, when the converse was done and a mutant *T. gondii* strain conferring resistance to CytD was used to infect sensitive host cells, the parasites were able to invade. Differential sensitivity to CytD demonstrated that the parasite actin, not the host cell actin, is responsible for cell entry as the functionality of the parasite actin dictated whether invasion could occur. A similar phenomena has been seen for other apicomplexans as cytochalasin B blocked *P. knowlesi* invasion of red blood cells (Miller et al., 1979), *P. falciparum* invasion (Field et al., 1993) and gliding and invasion of

Eimeria sporozoites (Russell and Sinden, 1981). It has also been suggested that dynamic host cell actin is required for invasion as treatment with CytD can disrupt *T. gondii* invasion at certain concentrations (Gonzalez et al., 2009). Alternatively, this data can be interpreted to mean that upon invasion, the actin cytoskeleton is required within the host cell to provide an anchor for the parasite to initiate the formation of its PV.

Unusual Apicomplexan Actin

Actin exists in two states, globular actin (G-actin), which is the monomeric state, and filamentous actin (F-actin). The G-actin pool conventionally polymerizes into filaments composed of two strands forming a right-handed helix containing monomers assembled in a head to tail conformation (Pollard et al., 2000). In actin systems of higher eukaryotes, there is a dynamic equilibrium between the G-actin and F-actin states with much of the actin found in a filamentous form. Despite the requirement for actin polymerization in order to undergo host cell invasion, a large majority of *T. gondii* actin has been shown to exist in an unpolymerized state (Dobrowolski et al., 1997b; Wetzel et al., 2003). Consistent with this, attempts to visualize filaments in non-motile parasites have been unsuccessful (Shaw and Tilney, 1999). However, freeze fracture EM was used to show actin filaments form beneath the plasma membrane and are deposited in the membrane left behind in trails during gliding (Wetzel et al., 2003). These filaments appear straight and lay parallel to one another and disappear upon treatment with CytD. Such a discrepancy demonstrates that the polymerization process is tightly regulated and that actin filaments are very transient.

It was also confirmed in more recent studies involving both TgACTI and PfACTI that parasite actins do not readily polymerize and form only short filaments (Sahoo et al., 2006; Schmitz et al., 2005; Schüler et al., 2005). Tryptophan quenching assays demonstrated that baculovirus-expressed TgACTI is capable of polymerization through addition of cation or salt, conditions used for polymerization of conventional actins (Sahoo et al., 2006). The critical concentration (Cc) of this actin was found to be 0.04 μM, 3-4 fold below the value traditionally seen for vertebrate and yeast actin (Pollard et al., 2000). This low Cc suggests that TgACTI should polymerize at low protein concentration. However, when TgACTI was incubated in F buffer, stained with fluorescent phalloidin, and visualized using microscopy, only small foci were seen. Under comparable conditions, rabbit actin underwent extensive filament formation. TgACTI was incubated in buffer conducive for polymerization and centrifuged at 100,000 x g, a speed which will sediment conventional actin filaments. The contents of the pellet were subsequently analyzed by electron microscopy and short actin-like filaments were detected (0.1 μm), although the morphology was somewhat broken. If phalloidin was added after polymerization but prior to the EM analysis, the filaments that formed appeared more normal and were slightly longer (0.2 μm) (Sahoo et al., 2006). Phalloidin is a cyclic peptide derived from the fungus *Amanita phalloides* (Dancker et al., 1975), which stabilizes monomer interactions and increases the rate of polymerization by lowering the critical concentration.

Results similar to those for TgACTI have been demonstrated for PfACTI using protein isolated by sedimenting actin filaments from parasite lysates (Schmitz et al., 2005) or expression in yeast (Schüler et al., 2005). One study suggested that

centrifugation at 100,000 × *g* was not sufficient to pellet PfACTI and centrifugation at 500,000 × *g* was required to sediment these filaments (Schmitz et al., 2005). These sedimentation assays were also used to estimate the Cc for PfACTI to be 0.2 μM. However, because the PfACTI was isolated from the parasite, other actin-binding proteins are likely to be present confounding these calculations. Additionally, recombinant PfACTI purified from yeast was shown to polymerize slowly, and only in the presence of gelsolin and phalloidin to form short, punctate filaments (Schüler et al., 2005). However, this system is artificial due to the fact that neither of these stabilizing agents is found in *Plasmodium*. It has also been predicted that there is a change in the rotational angle of the helix between PfACTI filaments and rabbit skeletal actin filaments (Schmitz et al., 2010). Modeling to examine the changes in rotational angle predicted different monomer stacking within the parasite actin filament thereby forming a double helix with a pitch that is 10% larger within the parasite actin filament compared to a conventional filament (Schmitz et al., 2010).

Apicomplexans and Jasplakinolide

Jasplakinolide (JAS) is a membrane permeable cyclic peptide isolated from the marine sponge, *Jaspis johnstoni* (Crews et al., 1986). JAS induces actin polymerization by decreasing the critical concentration of actin, releasing monomers from sequestering proteins and binding to filaments for stabilization (Bubb et al., 1994; Bubb et al., 2000). Treatment of *T. gondii* with JAS induces a large projection from the apical end of the cell, which is membrane enclosed and appears to be associated with the conoid (Shaw and Tilney, 1999). JAS-induced projections were confirmed to contain actin that was

decorated with myosin subfragment 1. *P. falciparium* treated with JAS also induced apical protrusions with filaments visualized within them (Mizuno et al., 2002). It has been suggested that the actin polymerized as a result of JAS treatment leads to a build up of pressure that deforms the membrane (Mizuno et al., 2002).

Additionally, stabilization of TgACTI filaments with (JAS) disrupts parasite motility and cell invasion (Poupel and Tardieux, 1999). As JAS concentration increases, more actin is seen in pellet, trail lengths decrease and invasion decreases (Wetzel et al., 2003). Similarly, addition of JAS to *P. falciparum* culture resulted in decreased parasiteamia (Mizuno et al., 2002). Merozoites could be released from red blood cells but reinvasion did not occur in the presence of JAS. JAS treatment also causes *T. gondii* to become hypermotile, however, these parasites lose directionality, often reversing direction, and no longer proceed with forward movement (Wetzel et al., 2003), demonstrating that highly stable filaments may have a toxic effect on the gliding process. JAS treatment of *T.gondii* resulted in actin relocalization to the apical and posterior poles as well as causing a spiral pattern to emanate from the posterior end of the parasite. Freeze fracture EM of filaments below the plasma membrane following JAS treatment showed they became intertwined and tangled in appearance (Wetzel et al., 2003). These findings demonstrate that actin polymerization within *T. gondii* controls directionality and speed of the parasite. Collectively, these results are consistent with a requirement for dynamic actin turnover.

Other Unconventional Actins

In addition to the members of the Apicomplexa, there are other examples among the protozoa, as well as the ciliates, bacteria and plants where actin homologs are quite divergent in sequence from conventional actins and this may impact their behavior.

Protozoa

Leishmania donovani has been probed with an anti-actin antibody to determine the intracellular localization of actin, which was seen in conjunction with the flagella, flagellar pocket, nucleus, kinetoplast and plasma membrane (Sahasrabuddhe et al., 2004). Filaments were formed by LdACT but they were not stained by phalloidin and were unaffected by both CytD and another actin destabilizing agent, latrunculin B (Sahasrabuddhe et al., 2004). Similar to what has been seen with apicomplexan actins, LdACT shows sequence divergence in the DNase I loop and hydrophobic plug (Sahasrabuddhe et al., 2004). LdACT appears to have a critical concentration three to four fold lower than conventional actins and only forms actin bundles, individual filaments are not observed during *in vitro* polymerization (Mizuno et al., 2002).

Giardia intestinalis encodes an extremely divergent actin (giActin) and the parasite genome lacks all canonical actin-binding proteins (Paredez et al., 2011). Purified giActin was shown to form filaments during *in vitro* polymerization, some filaments of conventional diameter and also those of half this diameter were observed suggesting that in some cases, individual protofilaments were formed (Paredez et al., 2011). Overall the filaments appeared to be shorter and more curved than rabbit actin filaments polymerized under the same conditions. Interestingly, giActin appears to be resistant to

depolymerization by conventional agents such as CytD or LatB, potentially due to divergent residues in the regions these drugs are known to interact with actin (Paredez et al., 2011). Knockdown of giActin resulted in numerous defects within the parasite including abnormal cell morphogenesis, as well as disruption of membrane trafficking and cytokinesis (Paredez, 2011).

Ciliates

Sequence divergence has also been observed in Karyorelictean, Heterotrich, Listostome (Kim et al., 2004) and Hypotrich (Perez-Romero et al., 1999) ciliate actins. However, microinjection of rhodamine-labeled phalloidin into the organism allowed visualization of label within the cell and some localization to filamentous structures within bundles (Kersken et al., 1986). Actin is not an abundant protein in these organisms and tubulin may be more involved in cellular processes allowing actin to evolve at a higher mutation rate and potentially take on novel functions. This is supported by the fact that although ciliate actins are quite unconserved in terms of sequence, ciliate tubulins are much more conserved with conventional tubulin (Villalobo et al., 2001).

Sequence analysis of *Tetrahymena* actins have also revealed many substituted residues (Cupples and Pearlman, 1986) and actins are not highly conserved among species *T. thermophila* and *T. pyriformis* (Hirono et al., 1987). Along with PACTII, *Tetrahymena* actin is the least conserved known (Wesseling et al., 1988). *T. pyriformis* actin polymerizes *in vitro*, is dependent on cation and binds myosin but attempts to visualize the actin using phalloidin have failed and no inhibition of DNase I binding was

observed (Hirono et al., 1989). *Tetrahymena* actin does copolymerize with skeletal muscle actin but there is reduced binding with muscle alpha-actinin and no binding with muscle tropomyosin (Hirono et al., 1990).

Bacteria and Plants

Bacteria have extremely divergent actin homologs including MreB and ParM. ParM, a bacterial actin homolog that plays a role in plasmid segregation, exhibits dynamic instability in a manner similar to tubulin (Garner et al., 2004), although it is regulated by ATP hydrolysis rather than GTP. MreB plays a role in maintaining cell shape of *E. coli* (Doi et al., 1988) and has been shown to be capable of forming filaments *in vitro* although these appear to be single helices rather then conventional double helices (Jones et al., 2001). There is some speculation that MreB may form more conventional helices *in vivo* due to interaction with other proteins, while it only forms linear polymers on its own (Shaevitz and Gitai, 2010).

Plant actins have also been shown to be highly monomeric and lack an equilibrium between monomers and filamentous actin (Staiger and Blanchoin, 2006). Maize and field poppy only polymerize 5-10% of their actin (Gibbon et al., 1999; Snowman et al., 2002) while tobacco only polymerizes 1-2% of its actin (Staiger and Blanchoin, 2006).

Regulation of Apicomplexan Actin Polymerization by Actin-binding Proteins

Many proteins are involved in regulation of actin filamentation in conventional systems (Pollard and Borisy, 2003). Because *T. gondii* actin diverges from conventional actin and is critical for gliding motility, one might postulate that polymerization of these

filaments is a highly regulated process. However, searches of the *T. gondii* genome reveal that it contains far fewer actin-binding proteins than are found in other systems. The only conventional regulatory proteins that are found include: the monomer-binding proteins profilin, actin depolymerizing factor (ADF), and cyclase-associated protein (CAP), as well as formins, but without a highly conserved FH1 domain, coronin, capping protein, toxofilin, and actin-like proteins (Baum et al., 2006a; Schüler and Matuschewski, 2006).

Profilin

Profilin is a small actin-binding protein that is essential in all eukaryotes in which it has been studied (Witke, 2004). It has been shown to bind monomeric actin and to facilitate nucleotide exchange resulting in transition from ADP-actin to ATP-actin (Figure 2). Nucleotide exchange prepares the actin monomer for addition to the growing filament. When profilin is bound to the monomer it also aids in inhibiting the hydrolysis of ATP-bound actin allowing the monomers to maintain a high affinity for addition to the filament (Witke, 2004). Profilin binds directly to actin monomers but utilizes formin proteins for interaction with the growing actin filament (Figure 2).

Profilin homologs have also been identified in apicomplexans, however, they have low sequence conservation with profilins characterized in other systems (18-24%) suggesting a divergent function (Kucera et al., 2010). Conditional knockouts of *T. gondii* profilin (TgPRF) were made in the parasite using the tetracycline-transactivator system. While intracellular growth and replication were unaffected, gliding, invasion and egress were impaired (Plattner et al., 2008). Additionally, if the profilin depleted parasites were

used to infect animals, there was complete loss of parasite lethality as all the animals survived. *Plasmodium* profilin (PfPFN) also appears to be essential as it cannot be knocked out in the parasite red blood cell stages (Kursula et al., 2008). PfPFN and TgPRF must have somewhat similar functions as PfPFN can be used to complement the defects of the TgPRF depletion (Plattner et al., 2008). Additionally, *P. berghei* profilin (PbPFN) deletions can be complemented with human profilin (HsPFN1) (Kursula et al., 2008), but conversely TgPRF cannot complement depletion of yeast profilin (ScPRF) (Plattner et al., 2008).

Biochemical analysis was also performed to determine if TgPRF, PfPFN and CpPRF (from *C. parvum*) had behaviors consistent with canonical profilins. Filament growth at the barbed and pointed ends was monitored as well as steady state assembly using free and gelsolin capped ends. No growth was recorded at the pointed ends when the barbed ends were capped but enhancement of polymerization was seen at free barbed ends, consistent with conventional profilin function. At steady state, if the barbed end was capped, filament depolymerization was observed suggesting actin monomers were sequestered (Plattner et al., 2008). These assays were used to calculate dissociation constant (K_d) of 5μM for TgPRF, 8.7 μM for CpPRF and 26 μM for PfPFN (Plattner et al., 2008). These K_d are higher than more conventional profilins, for example, *Acanthamoeba* profilin binds amoeba actin with a K_d of 1 μM (Vinson et al., 1998). Sedimentation analysis also demonstrated that PfPFN sequesters actin monomers and bound polyproline sepharose, although both activities were performed less efficiently than HsPfn1 (Kursula et al., 2008).

Crystal structures have been solved for TgPRF and PfPFN (Kucera et al., 2010; Kursula et al., 2008). The PfPRF structure was also solved in conjunction with a polyproline peptide. The C-terminal helix within conventional profilin contributes to interaction with polyprolines, however the PfPFN interaction with polyproline is mediated by an N-terminal tyrosine. Contributions from the C-terminal helix, plays a role in the interaction. The structural folds for both PfPFN and TgPRF look like canonical profilins, however, the apicomplexan profilins contain a unique minidomain containing an acidic loop followed by a beta-hairpin. The acidic loop is slightly longer in PfPRF (Kursula et al., 2008) but more acidic in TgPRF (Kucera et al., 2010). Additionally, the side chains contributed from actin for profilin binding appear to be conserved while the side chain contributions from profilin for this interaction are not.

Studies with TgPRF demonstrated decreased nucleotide exchange on rabbit actin and weak binding with a K_d of 13.9 +/-5.0 μM (Kucera et al., 2010). The minidomain is located within the binding region, diverging from conventional actins and potentially impacting the nucleotide exchange. However, if this hairpin region is deleted, even weaker binding is observed with a K_d of >150 μM (Kucera et al., 2010).

Another interesting feature of TgPRF is that it has been identified as the ligand for toll-like receptor 11 (TLR11) leading to interleukin-12 (IL-12) production (Yarovinsky et al., 2005). *T. gondii* depeleted for profilin does not induce the TLR11 dependent IL-12 response and when these conditional knockouts are complemented with PfPRF, the parasites still do not elicit an IL-12 response (Plattner, 2008). Mutants with TgPRF demonstrate the acidic loop is needed for TLR11. If the beta-hairpin and acidic loop are deleted, there is no IL-12 secretion (Kucera et al., 2010). However, if these features are

added to ScPRF, this protein can now activate TLR11. Replacing the TgPRF loop from *C. parvum*, which has only two amino acid differences, results in wildtype activation and replacement with the loop from *P. falciparum* still results in activation but produces lower levels of IL-12 (Kucera et al., 2010).

Formin

Formins are actin-binding proteins that accelerate de novo actin nucleation, alter the elongation and depolymerization rate of actin filaments and prevent barbed end capping by capping proteins (Higgs, 2005). Traditionally, formins contain a FH2 domain that interacts with the actin filament, FH1 domain that bind to monomeric profilin for recruitment to the growing filament and diaphanous autoinhibitory domains (DAD) for autoregulation (Kovar, 2006) (Figure 2). The FH2 domain is approx 400 residues and forms homodimers to interact with the actin filament. The FH2 domain is necessary and sufficient to nucleate actin. It is predicted that each formin subunit interacts with one actin monomer and then steps along as the filament elongates. FH1 domains contain polyproline stretches that are involved in profilin/actin recruitment. Formin interaction with profilin increases the rate of barbed end nucleation 5-10 fold (Kovar, 2006). However, of these components, apicomplexans contain FH2 domains but have degenerate FH1 domains, PfFRM1 has two pairs of proline residues while PfFRM2 has two proline stretches, further evidence that the role of profilin in these organisms may act differently than those from other eukaryotes (Schüler and Matuschewski, 2006). Additionally, the apicomplexan formins do not have Rho-GTPase domains or DAD for autoregulation (Schüler and Matuschewski, 2006).

T. gondii expresses three formins, TgFRM1, TgFRM2, TgFRM3 and *P. falciparum* also expresses three formins, PfFRM1, PfFRM2 and MISFIT, although the third formin from each organism has not yet been examined for a role in actin nucleation. PfFRM1 and PfFRM2 are both expressed during the erythocyte stage but are differentially expressed. PfFRM1 is expressed later, around 40-48 hours into the cycle while PfFRM2 is most highly expressed around 24 hours. Incidentally, PfPFN expression peaks with PfFRM1 and is reduced during PfFRM2 expression. Both PfFRM1 and TgFRM1 localize at the apical tip of the parasite as well as colocalize with the moving junction marker RON4, whereas PfFRM2 had a more cytoplasmic localization (Baum et al., 2008). It remains to be determined whether formin interaction with actin occurs at the apical tip then allowing actin filaments to move along parasite via myosin or if the interaction occurs at the moving junction as filaments are needed for gliding motility.

Pull-down assays demonstrate that the FH2 domains of PfFRM1 and PfFRM2 do associate with heterologous chicken skeletal muscle actin and modeling of these dimers revealed that the primary interfaces that interact with conventional actins are conserved (Baum et al., 2008). Biochemical assays were used to examine the ability of PfFRM1 and PfFRM2 to nucleate chicken skeletal muscle actin and both formins stimulated actin polymerization, although FRM2 was a less potent nucleator. Total internal reflection fluorescence microscopy was also used to show barbed end nucleation activity, and the results were suggestive of a mechanism of processive association where the formin stays associated with the barbed end as the filament grows.

Promoter exchange experiments within *T. gondii* were used to demonstrate that TgFRM1 is essential for *T. gondii* to undergo gliding and invasion. Pull-down assays

also revealed interaction between the formin FH2 domains and TgACTI. Expression of dominant negative mutants of the FH2 domains demonstrate that both TgFRM1 and TgFRM2 are required for gliding motility and invasion (Daher et al., 2010). Biochemical analysis also revealed that when combined with chicken muscle actin, both formins exhibit the properties of potent actin nucleators (Daher et al., 2010). The contribution of TgPRF to the TgFRM mediated nucleation remains to be determined but it has been shown that a peptide of the TgFRM2-FH1 (MPPPPPPGLTP) does not bind to TgPRF (Kucera et al., 2010).

Actin Depolymerizing Factor

Members of the actin depolymerizing factor (ADF)/cofilin superfamily play a role in monomer sequestering, filament severing, and enhancement of depolymerization from the pointed end. The severing mechanism increases filaments ends and increases the rate constant for dissociation from ends (Pollard et al., 2000). The ADF/cofilin family of proteins is often regulated by phosphorylation but apicomplexans are lacking the conventional kinases involved in this process, LIM or TES kinase. Recombinant TgADF was initially shown to bind heterologous actin monomers and aid in depolymerizing actin filaments (Allen et al., 1997). Additionally, TgADF was localized below the plasma membrane. More extensive biochemical analysis of TgADF reveals that it has only weak severing activity on both rabbit actin and TgACTI (Mehta and Sibley, 2010). TgADF binds to TgACTI and negatively impacts polymerization suggestive of a sequestering mechanism. TgADF also acts to inhibit nucleotide exchange on both rabbit actin and TgACTI (Mehta and Sibley, 2010). Combined these results show an unconventional role

for TgADF where its mechanism in *T. gondii* is to sequester actin monomers rather than to sever preformed actin filaments. Conditional knockdowns of TgADF have a dramatic impact on the ability of the parasite to undergo gliding motility (Mehta and Sibley, 2011). These parasites displayed aberrant forms of both circular and helical motility and a reduction in the speed of both forms of motility. This likely led to the phenotype of invasion and egress defects exhibited by the ADF-depleted parasites. Strikingly, longer actin filaments were visualized within the ADF-depeleted parasites demonstrating a role for TgADF in regulation of TgACTI filament formation (Mehta and Sibley, 2011).

PfADF1 has also been shown to bind G-actin, not to have severing activity and it does not enhance depolymerization, instead it slightly enhances nucleotide exchange from ADP-actin to ATP-actin (Schuler et al., 2005), differing from the functions seen for TgADF. Additionally, a second ADF in *Plasmodium*, PfADF2, appears to play a role in transitioning from the ookinete life stage to oocyst as well as sporozoite transformation to the infectious stage (Doi et al., 2010).

Capping protein

Capping protein is a stable heterodimer of α and β subunits that binds to the barbed ends of actin filaments to cap the end, inhibit filament growth and prevent monomer dissociation (Cooper and Sept, 2008). The only apicomplexan capping protein to be examined thus far is that from Plasmodium. PfCPβ was initially identified in a screen for genes that are upregulated in salivary gland *P. falciparum* sporozoites. The function of CPβ, along with CPα, were then examined in the *P. berghei* system. Using heterologous non-muscle β actin, it was demonstrated that the presence of the CP heterodimer leads to

the formation of shorter actin filaments than those formed in its absence, showing these proteins function as canonical capping proteins (Ganter et al., 2009). Knockouts of PbCPβ had no impact on the erythrocytic portion of the parasite life cycle but these knockout parasites showed reduced ookinete motility. Additionally, sporozoites did not have proper forward motility and as a result, there was no sporozoite transmission to the mammaliam host from the mosquito (Ganter, 2009).

Coronin

Coronin is a bundling and crosslinking protein that binds F- actin (ATP and ADP-P_i bound). It has been shown to regulate Arp2/3 binding to filaments in order to mediate actin assembly, although in the absence of filaments it appears to negatively regulate Arp2/3 (Gandhi and Goode, 2008). Coronin also plays a role in protecting actin filaments from cofilin-mediated actin disassembly. The net effect of its function is to protect newly formed actin filaments and enable filament expansion (Gandhi and Goode, 2008). Coronin has been identified within the apicomplexans, including *Toxoplasma*, and examination of the *Plasmodium* coronin revealed it contains 3 WD40 repeats identifying it into this class of proteins and has been shown to cosediment with filamentous rabbit muscle actin (Tardieux et al., 1998). The *Plasmodium* protein also cross reacts with an antibody against coronin in *Dictyostelium discoideum* further verifying it as a coronin (Tardieux et al., 1998). Coronin could play a regulatory role in apicomplexan parasite by acting to stabilize F-actin.

CAP

Adenylate cyclase associated protein (CAP) is a G-actin binding protein that plays a role in filament turnover and recycling of actin monomers (Paavilainen et al., 2004). The CAP proteins found within the apicomplexans are short and only have a conserved C-terminal domain which binds to actin, while they are missing the N-terminal adenylate cyclase binding domain and proline-rich domain traditionally found in CAP proteins (Baum et al., 2006a). In *Cryptosporidium*, CAP is a dimer forming protein that binds G-actin and sequesters it from polymerization (Hliscs et al., 2010). Knockouts of CAP in *P. berghei* demonstrate the protein is not required in the blood cell stage, however appear to be required for development into oocysts within the mosquito midgut (Hliscs et al., 2010).

Actin-like Proteins

Actin-like proteins (ALPs) have been classified as actin related proteins (Arps) that are unique to the Apicomplexa. The members of the phylum contain between 8-10 ALPs (Gordon and Sibley, 2005). TgALP1 forms a phylogentic branch between traditional Arp2 and Arp3 proteins that are absent within apicomplexan genomes. The phylogentic placement of ALP1 gave the appearance that it may potentially act as an actin nucleator within the apicomplexans (Gordon and Sibley, 2005). However, rather than playing a role in actin polymerization, TgALP1 appears to have a role in *T. gondii* cell division (Gordon et al., 2008). Localization of ALP1 is seen with the IMC early in its formation during endodyogeny, even prior to early markers such as IMC-1. Additionally,

overexpression of ALP1 disrupted daughter cell formation (Gordon et al., 2008). TgALP1 was also identified to exist in two states, as a soluble protein with the cytoplasm as well as a part of a high molecular weight complex. The presence of these two states likely represents recycling from a soluble state to interaction with the IMC (Gordon et al., 2010).

Toxofilin

Toxofilin is an actin-binding protein unique to *T. gondii*. Toxofilin binds muscle G-actin, sequesters monomers to inhibit actin polymerization as well as slowing down muscle actin filament disassembly by capping filament ends (Poupel et al., 2000). Injection of toxofilin into mammalian cells resulted in stress fiber disassembly. Toxofilin was also shown to bind G-actin from *T. gondii* lysates and co-sediments with *T. gondii* F-actin. Localization patterns show toxofilin diffuse the throughout cytoplasm but also localizing at the apical end just prior to egress (Poupel et al., 2000). Structural analysis of the protein demonstrated an interaction of toxofilin with an antiparallel actin dimer in a 1:2 toxofilin to actin binding ratio (Lee et al., 2007). It was also shown to inhibit nucleotide exchange on actin, which may be due to the dimer formation blocking the ability of the nucleotide to dissociate.

Despite the results that toxofilin interacts with actin within the parasite, this protein has been found in the rhoptries and is likely secreted into the host (Bradley et al., 2005). As a result, it is more likely to modulate host actin and less likely to play a role in regulating TgACTI. Toxofilin was also identified as a secreted protein during infection in a FRET-based assay (Lodoen et al., 2010). Furthermore, a knockout of toxofilin had

no effect on growth, invasion, motility or egress. Additionally, infections of host cells with the toxofilin knockout demonstrated no deleterious impact on the ability of macrophages to migrate or perform phagocytosis (Lodoen et al., 2010). Hence, the definite role of toxofilin in *T. gondii* infection remains to be determined.

Aim and Scope of Thesis

Despite the fact that apicomplexan parasites produce unusually short filaments, they are still able to glide at a speed of about 1 μm/sec. Moreover, highly stable filaments have a toxic effect on the gliding process. These seemingly contradictory findings raise the questions of why parasites assemble such short filaments and if they are only capable of forming short filaments. One of the central questions of this thesis was to uncover whether formation of short filaments is an inherent property of the apicomplexan actins. The requirement for short filaments in the gliding motility mechanism was further investigated through mutational analysis of divergent residues within *Toxoplasma* actin.

The highly unpolymerized nature of apicomplexan actins also reveals a large requirement for regulation of filamentous actin. It has been suggested that shorter filaments allow for faster polymerization and depolymerization and that rapid depolymerization may occur at the rear of the parasite where the actin can be sequestered until required for motility (Schmitz et al., 2005). Actin-binding proteins have now been identified with the genomes of apicomplexan parasites and studies have been undertaken to reveal their functions. However, due to the difficulties of apicomplexan actin purification, these studies have largely relied on the use of heterologous actin. Because of the divergent nature of these actins, it is likely there will be differences in the

interactions of actin-binding proteins with apicomplexan actin as compared to more conventional actins. The present thesis aims to uncover the role of actin-binding proteins from *T. gondii*, specifically TgPRF, TgFRM1 and TgFRM2, and their interactions with TgACTI to determine if these proteins undergo canonical roles or have evolved a more specialized function to regulate parasite actin.

Examining the underlying structural instabilities of actin in apicomplexans as well as regulation of the filamentation process will improve our understanding of the ability of apicomplexan parasites to enter into host cells, spread to other cells and establish subsequent infection. Uncovering critical elements of this process will enable a better understanding of apicomplexan biology including cell entry and spread and potentially provide a target unique for use to block infection. Due to conservation of gliding motility in apicomplexan parasites, examining how the gliding motility process is regulated in *Toxoplasma* will also have a broader impact on our understanding of actin-based motility in eukaryotic cells.

REFERENCES

Alexander, D.L., Mital, J., Ward, G.E., Bradley, P.J., and Boothroyd, J.C. (2005). Identification of the moving junction complex of *Toxoplasma gondii*: a collaboration between distinct secretory organelles. PLoS Pathog *1*, 137-149.

Allen, M.L., Dobrowolski, J.M., Muller, H., Sibley, L.D., and Mansour, T.E. (1997). Cloning and characterization of actin depolymerizing factor from *Toxoplasma gondii*. Mol Biochem Parasitol *88*, 43-52.

Amino, R., Thiberge, S., Martin, B., Celli, S., Shorte, S., Frishknecht, F., and Menard, R. (2006). Quantitative imaging of *Plasmodium* transmission from mosquito to mammal. Nat Med *12*, 220-224.

Arrowood, M.J., Sterling, C.R., and Healey, M.C. (1991). Immunofluorescent microscopical visualization of trails left by gliding *Cryptosporidium parvum* sporozoites. J Parasitol *77*, 315-317.

Barragan, A., and Sibley, L.D. (2002). Transepithelial migration of *Toxoplasma gondii* is linked to parasite motility and virulence. J Exp Med *195*, 1625-1633.

Baum, J., Papenfuss, A.T., Baum, B., Speed, T.P., and Cowman, A.F. (2006a). Regulation of apicomplexan actin-based motility. Nat Rev Microbiol *4*, 621-628.

Baum, J., Richard, D., Healer, J., Rug, M., Krnajski, Z., Gilberger, T.W., Green, J.L., Holder, A.A., and Cowman, A.F. (2006b). A conserved molecular motor drives cell invasion and gliding motility across malaria life cycle stages and other apicomplexan parasites. J Biol Chem *281*, 5197-5208.

Baum, J., Tonkin, C.J., Paul, A.S., Rug, M., Smith, B.J., Gould, S.B., Richard, D., Pollard, T.D., and Cowman, A.F. (2008). A malaria parasite formin regulates actin polymerization and localizes to the parasite-erythrocyte moving junction during invasion. Cell Host Microbe *3*, 188-198.

Bergman, L.W., Kaiser, K., Fujioka, H., Coppens, I., Daly, T.M., Fox, S., Matuschewski, K., Nussenzweig, V., and Kappe, S.H. (2003). Myosin A tail domain interacting protein (MTIP) localizes to the inner membrane complex of Plasmodium sporozoites. J Cell Sci *116*, 39-49.

Besteiro, S., Michelin, A., Poncet, J., Dubremetz, J., and Lebrun, M. (2009). Export of a *Toxoplasma gondii* rhoptry neck protein complex at the host cell membrane to form the moving junction during invasion. PLoS Path *5*, e1000309.

Bradley, P.J., Ward, C., Cheng, S.J., Alexander, D.L., Coller, S., Coombs, G.H., Dunn, J.D., Ferguson, D.J., Sanderson, S.J., Wastling, J.M., *et al*. (2005). Proteomic analysis of

rhoptry organelles reveals many novel constituents for host-parasite interactions in *T. gondii*. J Biol Chem *280*, 34245-34258.

Brossier, F., Jewett, T.J., Sibley, L.D., and Urban, S. (2005). A spatially-localized rhomboid protease cleaves cell surface adhesins essential for invasion by *Toxoplasma*. Proc Natl Acad Sci (USA) *102*, 4146-4151.

Bubb, M.R., Senderowicz, A.M.J., Sausville, E.A., Duncan, K.L.K., and Korn, E.D. (1994). Jasplakinolide, a cytotoxic natural product, induces actin polymerization and competitively inhibits the binding of phalloidin to F-actin. J Biol Chem *269*, 14869-14871.

Bubb, M.R., Spector, I., Beyer, B.B., and Fosen, K.M. (2000). Effects of jasplakinolide on the kinetics of actin polymerization: an explanation for certain *in vivo* observations. J Biol Chem *275*, 5163-5170.

Buguliskis, J.S., Brossier, F., Shuman, J., and Sibley, L.D. (2010). Rhomboid 4 (ROM4) affects the processing of surface adhesins and facilitates host cell invasion by *Toxoplasma gondii*. PLoS Pathog *6*, e1000858.

Carruthers, V.B., Giddings, O.K., and Sibley, L.D. (1999). Secretion of micronemal proteins is associated with Toxoplasma invasion of host cells. Cell Microbiol *1*, 225-236.

Carruthers, V.B., and Sibley, L.D. (1997). Sequential protein secretion from three distinct organelles of *Toxoplasma gondii* accompanies invasion of human fibroblasts. Eur J Cell Biol *73*, 114-123.

Cooper, J.A. (1987). Effects of cytochalasin and phalloidin on actin. J Cell Biol *105*, 1473-1478.

Cooper, J.A., and Sept, D. (2008). New insights into mechanism and regulation of actin capping protein. Int Rev Cell Mol Biol *267*, 183-206.

Crews, P., Manes, L.V., and Boehler, M. (1986). Jasplakinolide, a cyclodepsipeptide from the marine sponge, *Jaspis* spp. Tetrahedron Lett *27*, 2797-2800.

Cupples, C.G., and Pearlman, R.E. (1986). Isolation and characterization of the actin gene from Tetrahymena thermophila. Proc Natl Acad Sci U S A *83*, 5160-5164.

Cyrklaff, M., Kudryashev, M., Leis, A., Leonard, K., Baumeister, W., Menard, R., Meissner, M., and Frischknecht, F. (2007). Cryoelectron tomography reveals periodic material at the inner side of subpellicular microtubules in apicomplexan parasites. J Exp Med *204*, 1281-1287.

Daher, W., Plattner, F., Carlier, M.F., and Soldati-Favre, D. (2010). Concerted action of two formins in gliding motility and host cell invasion by *Toxoplasma gondii*. PLoS Pathog *6*.

Dancker, P., Low, I., Hasselbach, W., and Wieland, T. (1975). Interaction of actin with phalloidin: polymerization and stabilization of F-actin. Biochim Biophys Acta *400*, 407-414.

Del Carmen, M.G., Mondragon, M., Gonzalez, S., and Mondragon, R. (2009). Induction and regulation of conoid extrusion in Toxoplasma gondii. Cell Microbiol *11*, 967-982.

Delbac, F., Sanger, A., Neuhaus, E.M., Stratmann, R., Ajioka, J.W., Toursel, C., Herm-Gotz, A., Tomavo, S., Soldati, T., and Soldati, D. (2001). *Toxoplasma gondii* myosins B/C: one gene, two tails, two localizations, and a role in parasite division. J Cell Biol *155*, 613-623.

Desmonts, G., and Couvreur, J. (1974). Congenital toxoplasmosis: a prospective study of 378 pregnancies. N Engl J Med *290*, 1110-1116.

Dessens, J.T., Beetsma, A., Dimopoulos, G., Wengelnik, K., Crisanti, A., Kafatos, F.C., and Sinden, R.E. (1999). CTRP is essential for mosquito infection by malaria ookinetes. EMBO J *18*, 6221-6227.

Dobrowolski, J.M., Carruthers, V.B., and Sibley, L.D. (1997a). Participation of myosin in gliding motility and host cell invasion by *Toxoplasma gondii*. Mol Microbiol *26*, 163-173.

Dobrowolski, J.M., Niesman, I.R., and Sibley, L.D. (1997b). Actin in the parasite *Toxoplasma gondii* is encoded by a single copy gene, *ACT1* and exists primarily in a globular form. Cell Motil Cytoskel *37*, 253-262.

Dobrowolski, J.M., and Sibley, L.D. (1996). Toxoplasma invasion of mammalian cells is powered by the actin cytoskeleton of the parasite. Cell *84*, 933-939.

Doi, M., Wachi, M., Ishino, F., Tomioka, S., Ito, M., Sakagami, Y., Suzuki, A., and Matsuhashi, M. (1988). Determinations of the DNA sequence of the mreB gene and of the gene products of the mre region that function in formation of the rod shape of Escherichia coli cells. J Bacteriol *170*, 4619-4624.

Doi, Y., Shinzawa, N., Fukumoto, S., Okano, H., and Kanuka, H. (2010). ADF2 is required for transformation of the ookinete and sporozoite in malaria parasite development. Biochem Biophys Res Commun *397*, 668-672.

Dubey, J.P. (1994). Toxoplasmosis. J Am Vet Med Assoc *205*, 1593-1598.

Dubey, J.P. (2010). Toxoplasmosis of animals and humans (Boca Raton, CRC Press).

Dubey, J.P., and Jones, J.L. (2008). Toxoplasma gondii infection in humans and animals in the United States. Int J Parasitol *38*, 1257-1278.

Dubey, J.P., and Su, C. (2009). Population biology of Toxoplasma gondii: what's out and where did they come from. Mem Inst Oswaldo Cruz *104*, 190-195.

Field, S.J., Pinder, J.C., Clough, B., Dluuzewski, A.R., Wilson, R.J.M., and Gratzer, W.B. (1993). Actin in the merozoite of the malaria parasite, *Plasmodium falciparum*. Cell Motil Cytoskel *25*, 43-48.

Foth, B.J., Goedecke, M.C., and Soldati, D. (2006). New insights into myosin evolution and classification. Proc Natl Acad Sci (USA) *103*, 3681-3686.

Fowler, R.E., Smith, A.M.C., Whitehorn, J., Williams, I.T., Bannister, L.H., and Mitchell, G.H. (2001). Microtubule associated motor proteins of *Plasmodium falciparum* merozoites. Mol Biochem Parasitol *117*, 187-200.

Frenal, K., Polonais, V., Marq, J.B., Stratmann, R., Limenitakis, J., and Soldati-Favre, D. (2010). Functional dissection of the apicomplexan glideosome molecular architecture. Cell Host Microbe *8*, 343-357.

Frenkel, J.K., Dubey, J.P., and Miller, N.L. (1970). *Toxoplasma gondii* in cats: fecal stages identified as coccidian oocysts. Science *167*, 893-896.

Gandhi, M., and Goode, B.L. (2008). Coronin: the double-edged sword of actin dynamics. Subcell Biochem *48*, 72-87.

Ganter, M., Schuler, H., and Matuschewski, K. (2009). Vital role for the Plasmodium actin capping protein (CP) beta-subunit in motility of malaria sporozoites. Mol Microbiol, d.o.i. 10.1111/j.1365-2958.2009.06828.x.

Garner, E.C., Campbell, C.S., and Mullins, R.D. (2004). Dynamic instability in a DNA-segregating prokaryotic actin homolog. Science *306*, 1021-1025.

Gaskins, E., Gilk, S., DeVore, N., Mann, T., Ward, G.E., and Beckers, C. (2004). Identification of the membrane receptor of a class XIV myosin *Toxoplasma gondii*. J Cell Biol *165*, 383-393.

Gibbon, B.C., Kovar, D.R., and Staiger, C.J. (1999). Latrunculin B has different effects on pollen germination and tube growth. Plant Cell *11*, 2349-2363.

Gilk, S.D., Gaskins, E., Ward, G.E., and Beckers, C.J. (2009). GAP45 phosphorylation controls assembly of the Toxoplasma myosin XIV complex. Eukaryot Cell *8*, 190-196.

Gonzalez, V., Combe, A., David, V., Malmquist, N.A., Delorme, V., Leroy, C., Blazquez, S., Menard, R., and Tardieux, I. (2009). Host cell entry by apicomplexa parasites requires actin polymerization in the host cell. Cell Host Microbe *5*, 259-272.

Gordon, J.L., Beatty, W.L., and Sibley, L.D. (2008). A novel actin-related protein is associated with daughter cell formation in Toxoplasma. Euk Cell *7*, 1500-1512.

Gordon, J.L., Buguliskis, J.S., Buske, P.J., and Sibley, L.D. (2010). Actin-like protein 1 (ALP1) is a component of dynamic, high molecular weight complexes in Toxoplasma gondii. Cytoskeleton *67*, 23-31.

Gordon, J.L., and Sibley, L.D. (2005). Comparative genome analysis reveals a conserved family of actin-like proteins in apicomplexan parasites. BMC Genomics *6*, e179.

Håkansson, S., Charron, A.J., and Sibley, L.D. (2001). *Toxoplasma* evacuoles: a two-step process of secretion and fusion forms the parasitophorous vacuole. EMBO J *20*, 3132-3144.

Håkansson, S., Morisaki, H., Heuser, J.E., and Sibley, L.D. (1999). Time-lapse video microscopy of gliding motility in *Toxoplasma gondii* reveals a novel, biphasic mechanism of cell locomotion. Mol Biol Cell *10*, 3539-3547.

Heintzelman, M.B., and Schwartzman, J.D. (1997). A novel class of unconventional myosins from *Toxoplasma gondii*. J Mol Biol *271*, 139-146.

Herm-Gotz, A., Weiss, S., Stratmann, R., Fujita-Becker, S., Ruff, C., Meyhofer, E., Soldati, T., Manstein, D.J., Geeves, M.A., and Soldati, D. (2002). *Toxoplasma gondii* myosin A and its light chain: a fast, single-headed, plus-end-directed motor. EMBO J *21*, 2149-2158.

Higgs, H.N. (2005). Formin proteins: a domain-based approach. Trends Biochem Sci *30*, 342-353.

Hill, D., and Dubey , J.P. (2002). *Toxoplasma gondii* transmission, diagnosis and prevention. Clin Microbiol Infect *8*, 634-640.

Hirono, M., Endoh, H., Okada, N., Numata, O., and Watanabe, Y. (1987). Tetrahymena actin. Cloning and sequencing of the Tetrahymena actin gene and identification of its gene product. J Mol Biol *194*, 181-192.

Hirono, M., Kamagai, Y., Numata, O., and Watanabe, Y. (1989). Purification of Tetrahymena actin reveals some unusual properties. Proc Natl Acad Sci (USA) *86*, 75-79.

Hirono, M., Tanaka, R., and Watanabe, Y. (1990). Tetrahymena actin: copolymerization with skeletal muscle actin and interactions with muscle actin-binding proteins. J Biochem *107*, 3236.

Hliscs, M., Sattler, J.M., Tempel, W., Artz, J.D., Dong, A., Hui, R., Matuschewski, K., and Schuler, H. (2010). Structure and function of a G-actin sequestering protein with a vital role in malaria oocyst development inside the mosquito vector. J Biol Chem *285*, 11572-11583.

Howe, D.K., and Sibley, L.D. (1995). *Toxoplasma gondii* comprises three clonal lineages: correlation of parasite genotype with human disease. J Infect Dis *172*, 1561-1566.

Hu, K., Johnson, J., Florens, L., Franholz, M., Suravajjala, S., Dilullo, C., Yates, J.R., Roos, D.S., and Murray, J.M. (2006). Cytoskeletal components of an invasion machine - the apical complex of *Toxoplasma gondii*. PLoS Path *2*, 121-138.

Hu, K., Roos, D.S., and Murray, J.M. (2002). A novel polymer of tubulin forms the conoid of *Toxoplasma gondii*. J Cell Biol *156*, 1039-1050.

Huynh, M.H., and Carruthers, V.B. (2006). *Toxoplasma* MIC2 is a major determinant of invasion and virulence. PloS Pathog *2*, 753-762.

Huynh, M.H., Opitz, C., Kwok, L.Y., Tomley, F.M., Carruthers, V.B., and Soldati, D. (2004). Trans-genera reconstitution and complementation of an adhesin complex in *Toxoplasma gondii*. Cell Micro *6*, 771-782.

Jewett, T.J., and Sibley, L.D. (2003). Aldolase forms a bridge between cell surface adhesins and the actin cytoskeleton in apicomplexan parasites. Molec Cell *11*, 885-894.

Jewett, T.J., and Sibley, L.D. (2004). The Toxoplasma proteins MIC2 and M2AP for a hexameric complex necessary for intracellular survival. J Biol Chem *275*, 9362-9369.

Jones, L.J., Carballido-Lopez, R., and Errington, J. (2001). Control of cell shape in bacteria: helical, actin-like filaments in Bacillus subtilis. Cell *104*, 913-922.

Jones, T.C., Yeh, S., and Hirsch, J.G. (1972). The interaction between *Toxoplasma gondii* and mammalian cells. I. Mechanism of entry and intracellular fate of the parasite. J Exp Med *136*, 1157-1172.

Kafsack, B.F., Pena, J.D., Coppens, I., Ravindran, S., Boothroyd, J.C., and Carruthers, V.B. (2009). Rapid membrane disruption by a perforin-like protein facilitates parasite exit from host cells. Science *323*, 530-533.

Kappe, S., Bruderer, T., Gantt, S., Fujioka, H., Nussenzweig, V., and Ménard, R. (1999). Conservation of a gliding motility and cell invasion machinery in apicomplexan parasites. J Cell Biol *147*, 937-943.

Kersken, H., Momayezi, M., Braun, C., and Plattner, H. (1986). Filamentous actin in paramecium cells: functional and structural changes correlated with phalloidin affinity labeling in vivo. J Histochem Cytochem *34*, 455-465.

Khan, A., Dubey , J.P., Su, C., Ajioka, J.W., Rosenthal, B.M., and Sibley, L.D. (2011). Genetic analyses of atypical *Toxoplasma gondii* strains reveals a fourth clonal lineage in North America. Int J Parasitol *in press*.

Khan, A., Fux, B., Su, C., Dubey , J.P., Darde, M.L., Ajioka, J.W., Rosenthal, B.M., and Sibley, L.D. (2007). Recent transcontinental sweep of *Toxoplasma gondii* driven by a single monomorphic chromosome. Proc Natl Acad Sci (USA) *104*, 14872-14877.

Kim, O.T., Yura, K., Go, N., and Harumoto, T. (2004). Highly divergent actins from karyorelictean, heterotrich, and litostome ciliates. J Eukaryot Microbiol *51*, 227-233.

Kissinger, J.C., Gajria, B., Li, L., Paulsen, I.T., and Roos, D.S. (2003). ToxoDB: Accessing the *Toxoplasma gondii* genome. Nucleic Acids Res *31*, 234-236.

Kovar, D.R. (2006). Molecular details of formin-mediated actin assembly. Curr Opin Cell Biol *18*, 11-17.

Kucera, K., Koblansky, A.A., Saunders, L.P., Frederick, K.B., De La Cruz, E.M., Ghosh, S., and Modis, Y. (2010). Structure-based analysis of Toxoplasma gondii profilin: a parasite-specific motif is required for recognition by Toll-like receptor 11. J Mol Biol *403*, 616-629.

Kursula, I., Kursula, P., Ganter, M., Panjikar, S., Matuschewski, K., and Schuler, H. (2008). Structural basis for parasite-specific functions of the divergent profilin of Plasmodium falciparum. Structure *16*, 1638-1648.

Lebrun, M., Michelin, A., El Hajj, H., Poncet, J., Bradley, P.J., Vial, H.J., and Dubremetz, J.F. (2005). The rhoptry neck protein RON4 relocalizes at the moving junction during *Toxoplasma gondii* invasion. Cell Micro *7*, 1823-1833.

Lee, S.H., Hayes, D.B., Rebowski, G., Tardieux, I., and Dominguez, R. (2007). Toxofilin from Toxoplasma gondii forms a ternary complex with an antiparallel actin dimer. Proc Natl Acad Sci U S A *104*, 16122-16127.

Lehmann, T., Marcet, P.L., Graham, D.H., Dahl, E.R., and Dubey, J.P. (2006). Globalization and the population structure of *Toxoplasma gondii*. Proc Natl Acad Sci (USA) *103*, 11423-11428.

Levine, N.D. (1988). The Protozoan Phylum Apicomplexa, Vol 1,2 (Boca Raton, CRC Press).

Lodoen, M.B., Gerke, C., and Boothroyd, J.C. (2010). A highly sensitive FRET-based approach reveals secretion of the actin-binding protein toxofilin during Toxoplasma gondii infection. Cell Microbiol *12*, 55-66.

Lourido, S., Shuman, J., Zhang, C., Shokat, K.M., Hui, R., and Sibley, L.D. (2010). Calcium-dependent protein kinase 1 is an essential regulator of exocytosis in Toxoplasma. Nature *465*, 359-362.

Luft, B.J., Hafner, R., Korzun, A.H., Leport, C., Antoniskis, D., Bosler, E.M., Bourland, D.D., Uttamchandani, R., Fuhrer, J., Jacobson, J., *et al*. (1993). Toxoplasmic encephalitis in patients with the acquired immunodeficiency syndrome. N Engl J Med *329*, 995-1000.

Luft, B.J., and Remington, J.S. (1992). Toxoplasmic encephalitis in AIDS. Clin Infect Dis *15*, 211-222.

Mann, T., and Beckers, C. (2001). Characterization of the subpellicular network, a filamentous membrane skeletal component in the parasite *Toxoplasma gondii*. Molec Biochem Parasitol *115*, 257-268.

McCabe, R.E. (2001). Antitoxoplasma chemotherapy. In Toxoplasmosis: a comprehensive clinical guide, D.H.M. Joynson, and T.G. Wreghitt, eds. (Cambridge, Cambridge Univ. Press), pp. 319-359.

Mehta, S., and Sibley, L.D. (2010). *Toxoplasma gondii* actin depolymerizing factor acts primarily to sequester G-actin. J Biol Chem *285*, 6835-6847.

Mehta, S., and Sibley, L.D. (2011). Actin depolymerizing factor controls actin turnover and gliding motility in Toxoplasma gondii. Molc Biol Cell *22*, 1290-1299.

Meissner, M., Schluter, D., and Soldati, D. (2002). Role of *Toxoplasma gondii* myosin A in powering parasite gliding and host cell invasion. Science *298*, 837-840.

Ménard, R. (2001). Gliding motility and cell invasion by Apicomplexa: insights from the Plasmodium sporozoite. Cell Micro *3*, 63-73.

Miller, L.H., Aikawa, M., Johnson, J.G., and Shiroishi, T. (1979). Interaction between cytochalasin B-treated malarial parasites and erythrocytes. J Exp Med *149*, 172-184.

Mital, J., Meissner, M., Soldati, D., and Ward, G.E. (2005). Conditional expression of *Toxoplasma gondii* apical membrane antigen-1 (TgAMA1) demonstrates that TgAMA1 plays a critical role in host cell invasion. Mol Biol Cell *16*, 4341 - 4349.

Mizuno, Y., Makioka, A., Kawazu, S., Kano, S., Kawai, S., Akaki, M., Aikawa, M., and Ohtomo, H. (2002). Effect of jasplakinolide on the growth, invasion, and actin cytoskeleton of *Plasmodium falciparum*. Parasitol Res *88*, 844 - 848.

Mondragon, R., and Frixione, E. (1996). Ca^{2+}-dependence of conoid extrusion in *Toxoplasma gondii* tachyzoites. J Eukaryot Microbiol *43*, 120-127.

Montoya, J.G., and Liesenfeld, O. (2004). Toxoplasmosis. Lancet *363*, 1965-1976.

Mordue, D.G., Desai, N., Dustin, M., and Sibley, L.D. (1999). Invasion by *Toxoplasma gondii* establishes a moving junction that selectively excludes host cell plasma membrane proteins on the basis of their membrane anchoring. J Exp Med *190*, 1783-1792.

Mordue, D.G., and Sibley, L.D. (1997). Intracellular fate of vacuoles containing *Toxoplasma gondii* is determined at the time of formation and depends on the mechanism of entry. J Immunol *159*, 4452-4459.

Morisaki, J.H., Heuser, J.E., and Sibley, L.D. (1995). Invasion of *Toxoplasma gondii* occurs by active penetration of the host cell. J Cell Sci *108*, 2457-2464.

Morrissette, N.S., Murray, J.M., and Roos, D.S. (1997). Subpellicular microtubules associate with an intramembranous particle lattice in the protozoan parasite *Toxoplasma gondii*. J Cell Sci *110*, 35-42.

Morrissette, N.S., and Roos, D.S. (1998). *Toxoplasma gondii*: a family of apical antigens associated with the cytoskeleton. Exp Parasitol *89*, 296-303.

Morrissette, N.S., and Sibley, L.D. (2002). Cytoskeleton of apicomplexan parasites. Microbiol Mol Biol Rev *66*, 21-38.

Moudy, R., Manning, T.J., and Beckers, C.J. (2001). The loss of cytoplasmic potassium upon host cell breakdown triggers egress of *Toxoplasma gondii*. J Biol Chem *276*, 41492-41501.

Munter, S., Sabass, B., Selhuber-Unkel, C., Kudryashev, M., Hegge, S., Engel, U., Spatz, J.P., Matuschewski, K., Schwarz, U.S., and Frischknecht, F. (2009). Plasmodium sporozoite motility is modulated by the turnover of discrete adhesion sites. Cell Host Microbe *6*, 551-562.

Nagamune, K., Hicks, L.M., Fux, B., Broissier, F., Chini, E.N., and Sibley, L.D. (2008). Abscisic acid controls calcium-dependent egress and development in *Toxoplasma gondii*. Nature *451*, 207-211.

Nicastro, D., Schwartz, C., Pierson, J., Gaudette, R., Porter, M.E., and McIntosh, J.R. (2006). The molecular architecture of axonemes revealed by cryoelectron tomography. Science *313*, 944-948.

Nichols, B., and Chiappino, M. (1987). Cytoskeleton of *Toxoplasma gondii*. J Protozool *34*, 217-226.

Opitz, C., and Soldati, D. (2002). 'The glideosome': a dynamic complex powering gliding motion and host cell invasion by *Toxoplasma gondii*. Mol Microbiol *45*, 597-604.

Paavilainen, V.O., Bertling, E., Falck, S., and Lappalainen, P. (2004). Regulation of cytoskeletal dynamics by actin-monomer-binding proteins. Trends Cell Biol *14*, 386-394.

Paredez, A.R., Assaf, Z.J., Sept, D., Timofejeva, L., Dawson, S.C., Wang, C.J.R., and Cande, W.J. (2011). An actin cytoskeleton with evolutionaryly conserved functions in the absence of cannonical actin-binding protiens. PNAS (USA) *in press*.

Perez-Romero, P., Villalobo, E., Diaz-Ramos, C., Calvo, P., and Torres, A. (1999). Actin of Histriculus cavicola: characteristics of the highly divergent hypotrich ciliate actins. J Eukaryot Microbiol *46*, 469-472.

Plattner, F., Yarovinsky, F., Romero, S., Didry, D., Carlier, M.F., Sher, A., and Soldati-Favre, D. (2008). *Toxoplasma* profilin is essential for host cell invasion and TLR11-dependent induction of an interleukin-12 response. Cell Host Microbe *3*, 77-87.

Pollard, T.D., Blanchoin, L., and Mullins, R.D. (2000). Molecular mechanisms controlling actin filament dynamics in nonmuscle cells. Annu Rev Biophys Biomol Struct *29*, 545 - 576.

Pollard, T.D., and Borisy, G.G. (2003). Cellular motility driven by assembly and disassembly of actin filaments. Cell *112*, 453 - 465.

Porchet, E., and Torpier, G. (1977). [Freeze fracture study of Toxoplasma and Sarcocystis infective stages (author's transl)]. Z Parasitenkd *54*, 101-124.

Poupel, O., Boleti, H., Axisa, S., Couture-Tosi, E., and Tardieux, I. (2000). Toxofilin, a novel actin-binding protein from *Toxoplasma gondii*, sequesters actin monomers and caps actin filaments. Mol Biol Cell *11*, 355-368.

Poupel, O., and Tardieux, I. (1999). *Toxoplasma gondii* motility and host cell invasiveness are drastically impaired by jasplakinolide, a cyclic peptide stabilizing F-actin. Microb Infect *1*, 653-662.

Roberts, F., and McLeod, R. (1999). Pathogenesis of toxoplasmic retinochoroiditis. Parasitol Today *15*, 51-57.

Russell, D.G., and Burns, R.G. (1984). The polar ring of coccidian sporozoites: a unique microtubule-organizing centre. J Cell Sci *65*, 193-207.

Russell, D.G., and Sinden, R.E. (1981). The role of the cytoskeleton in the motility of coccidian sporozoites. J Cell Sci *50*, 345-359.

Ryning, F.W., and Remington, J.S. (1978). Effect of cytochalasin D on *Toxoplasma gondii* cell entry. Infect Immun *20*, 739-743.

Saeij, J.P.J., Boyle, J.P., Coller, S., Taylor, S., Sibley, L.D., Brooke-Powell, E.T., Ajioka, J.W., and Boothroyd, J.C. (2006). Polymorphic secreted kinases are key virulence factors in toxoplasmosis. Science *314*, 1780-1783.

Sahasrabuddhe, A.A., Bajpai, V.K., and Gupta, C.M. (2004). A novel form of actin in Leishmania: molecular characterisation, subcellular localisation and association with subpellicular microtubules. Mol Biochem Parasitol *134*, 105-114.

Sahoo, N., Beatty, W.L., Heuser, J.E., Sept, D., and Sibley, L.D. (2006). Unusual kinetic and structural properties control rapid assembly and turnover of actin in the parasite *Toxoplasma gondii*. Mol Biol Cell *17*, 895-906.

Schmitz, S., Grainger, M., Howell, S.A., Calder, L.J., Gaeb, M., Pinder, J.C., Holder, A.A., and Veigel, C. (2005). Malaria parasite actin filaments are very short. J Mol Biol *349*, 113-125.

Schmitz, S., Schaap, I.A., Kleinjung, J., Harder, S., Grainger, M., Calder, L., Rosenthal, P.B., Holder, A.A., and Veigel, C. (2010). Malaria parasite actin polymerisation and filament structure. J Biol Chem.

Schüler, H., and Matuschewski, K. (2006). Regulation of apicomplexan microfilament dynamics by minimal set of actin-binding proteins. Traffic *7*, 1433-1439.

Schuler, H., Mueller, A.K., and Matuschewski, K. (2005). A Plasmodium actin-depolymerizing factor that binds exclusively to actin monomers. Mol Biol Cell *16*, 4013-4023.

Schüler, H., Mueller, A.K., and Matuschewski, K. (2005). Unusual properties of *Plasmodium falciparum* actin: new insights into microfilament dynamics of apicomplexan parasites. FEBS Lett *579*, 655-660.

Shaevitz, J.W., and Gitai, Z. (2010). The structure and function of bacterial actin homologs. Cold Spring Harb Perspect Biol *2*, a000364.

Shaw, M.K. (1999). Theileria parva: sporozoite entry into bovine lymphocytes is not dependent on the parasite cytoskeleton. Exp Parasitol *92*, 24-31.

Shaw, M.K., Compton, H.L., Roos, D.S., and Tilney, L.G. (2000). Microtubules, but not actin filaments, drive daughter cell budding and cell division in *Toxoplasma gondii*. J Cell Sci *113*, 1241-1254.

Shaw, M.K., and Tilney, L.G. (1999). Induction of an acrosomal process in *Toxoplasma gondii*: visualization of actin filaments in a protozoan parasite. Proc Natl Acad Sci U S A *96*, 9095-9099.

Siden-Kiamos, I., Ecker, A., Nyback, S., Louis, C., Sinden, R.E., and Billker, O. (2006). *Plasmodium berghei* calcium-dependent protein kinase 3 is required for ookinate gliding and mosquito midgut invasion. Mol Microbiol *60*, 1355-1363.

Snowman, B.N., Kovar, D.R., Shevchenko, G., Franklin-Tong, V.E., and Staiger, C.J. (2002). Signal-mediated depolymerization of actin in pollen during the self-incompatibility response. Plant Cell *14*, 2613-2626.

Staiger, C.J., and Blanchoin, L. (2006). Actin dynamics: old friends with new stories. Curr Opin Plant Biol *9*, 554-562.

Starnes, G.L., Coincon, M., Sygusch, J., and Sibley, L.D. (2009). Aldolase is essential for energy production and bridging adhesin-actin cytoskeletal interactions during parasite invasion of host cells. Cell Host Microbe *5*, 353-364.

Starnes, G.L., Jewett, T.J., Carruthers, V.B., and Sibley, L.D. (2006). Two separate, conserved acidic amino acid domains within the *Toxoplasma gondii* MIC2 cytoplasmic tail are required for parasite survival. J Biol Chem *281*, 30745-30754.

Striepen, B., Jordan, C.N., Reiff, S., and van Dooren, G.G. (2007). Building the perfect parasite: cell division in Apicomplexa. PLoS Pathog *3*, 691-698.

Su, C., Howe, D.K., Dubey, J.P., Ajioka, J.W., and Sibley, L.D. (2002). Identification of quantitative trait loci controlling acute virulence in *Toxoplasma gondii*. Proc Natl Acad Sci (USA) *99*, 10753-10758.

Sultan, A.A., Thathy, V., Frevert, U., Robson, K.J.H., Crisanti, A., Nussenzweig, V., Nussenzweig, R.S., and Menard, R. (1997). TRAP is necessary for gliding motility and infectivity of Plasmodium sporozoites. Cell *90*, 511-522.

Suss-Toby, E., Zimmerberg, J., and Ward, G.E. (1996). *Toxoplasma* invasion: The parasitophorous vacuole is formed from host cell plasma membrane and pinches off via a fusion pore. Proc Natl Acad Sci USA *93*, 8413-8418.

Tardieux, I., Liu, X., Poupel, O., Parzy, D., Dehoux, P., and Langsley, G. (1998). A *Plasmodium falciparum* novel gene encoding a coronin-like protein which associates with actin filaments. FEBS Lett *441*, 251-256.

Taylor, S., Barragan, A., Su, C., Fux, B., Fentress, S.J., Tang, K., Beatty, W.L., Hajj, E.L., Jerome, M., Behnke, M.S., *et al*. (2006). A secreted serine-threonine kinase determines virulence in the eukaryotic pathogen *Toxoplasma gondii*. Science *314*, 1776-1780.

Tenter, A.M., Heckeroth, A.R., and Weiss, L.M. (2000). *Toxoplasma gondii*: from animals to humans. Int J Parasitol *30*, 1217-1258.

Vanderberg, J.P. (1974). Studies on the motility of *Plasmodium* sporozoites. J Protozool *21*, 527-537.

Vaughan, S., Shaw, M., and Gull, K. (2006). A post-assembly structural modification to the lumen of flagellar microtubule doublets. Curr Biol *16*, R449-450.

Villalobo, E., Perez-Romero, P., Sanchez-Silva, R., and Torres, A. (2001). Unusual characteristics of ciliate actins. Int Microbiol *4*, 167-174.

Vinson, V.K., De La Cruz, E.M., Higgs, H.N., and Pollard, T.D. (1998). Interactions of Acanthamoeba profilin with actin and nucleotides bound to actin. Biochemistry *37*, 10871-10880.

Vlachou, D., Zimmermann, T., Cantera, R., Janse, C.J., Waters, A.P., and Kafatos, F.C. (2004). Real-time, *in vivo* analysis of malaria ookinete locomotions and mosquito midgut invasion. Cell Microbiol *6*, 671-685.

Wesseling, J.G., Smits, M.A., and Schoenmakers (1988). Extremely diverged actin proteins in *Plasmodium falciparum*. Mol Biochem Parasitol *30*, 143-154.

Wetzel, D.M., Håkansson, S., Hu, K., Roos, D.S., and Sibley, L.D. (2003). Actin filament polymerization regulates gliding motility by apicomplexan parasites. Mol Biol Cell *14*, 396-406.

Witke, W. (2004). The role of profilin complexes in cell motility and other cellular processes. Trends Cell Biol *14*, 461-469.

Wong, S., and Remington, J.S. (1994). Toxoplasmosis in pregnancy. Clin Infect Dis *18*, 853-862.

Yarovinsky, F., Zhang, D., Andersen, J.F., Bannenberg, G.L., Serhan, C.N., Hayden, M.S., Hieny, S., Sutterwala, F.S., Flavell, R.A., Ghosh, S., *et al*. (2005). TLR11 activation of dendritic cells by a protozoan profilin-like protein. Science *308*, 1626-1629.

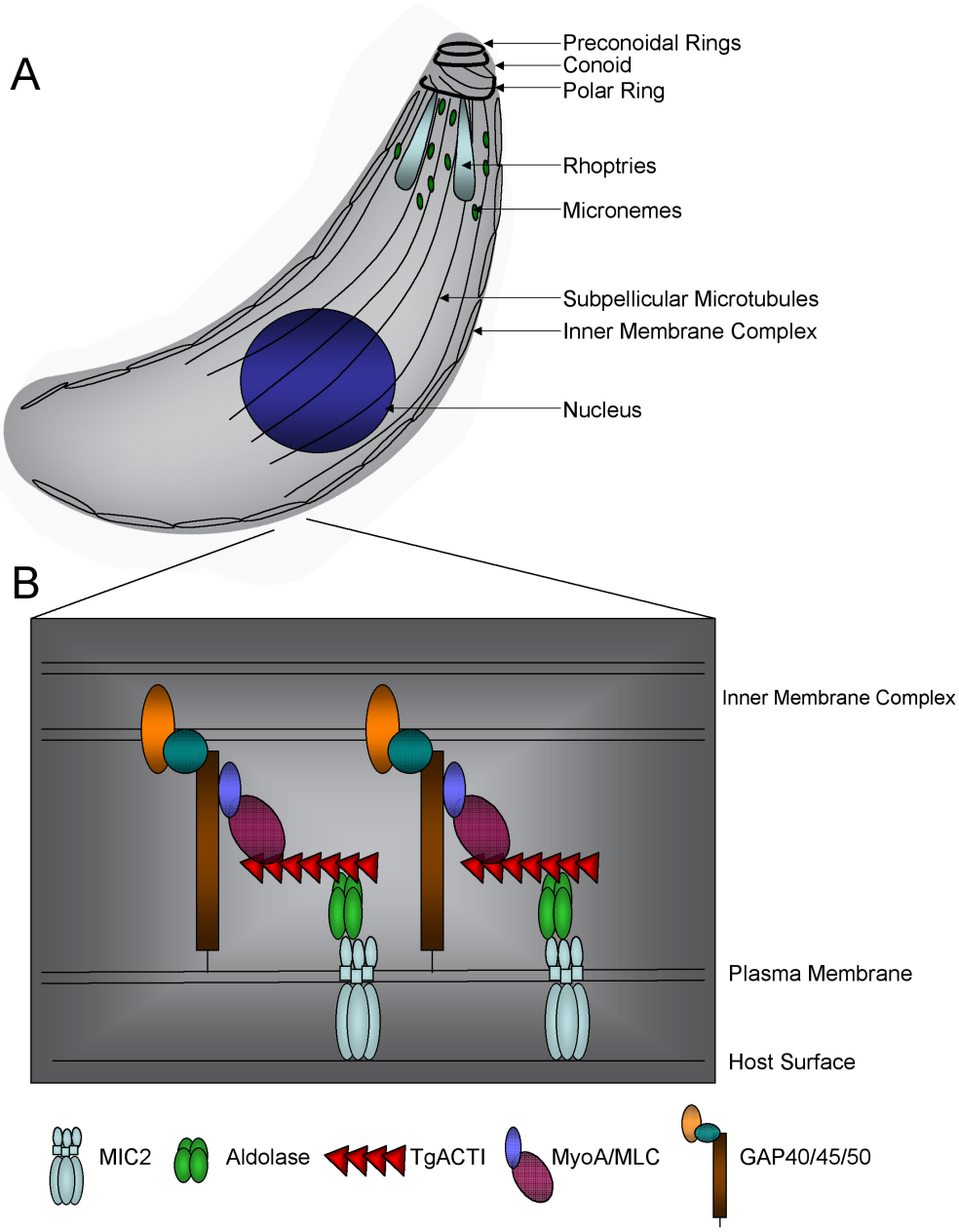

Figure 1. *T. gondii* cytoskeleton and proteins involved in gliding motility.

(A) *T. gondii* cytoskeletal components and apical complex. (B) Zoom in of glideosome proteins beneath the *T. gondii* plasma membrane that play a role in the process of gliding motility.

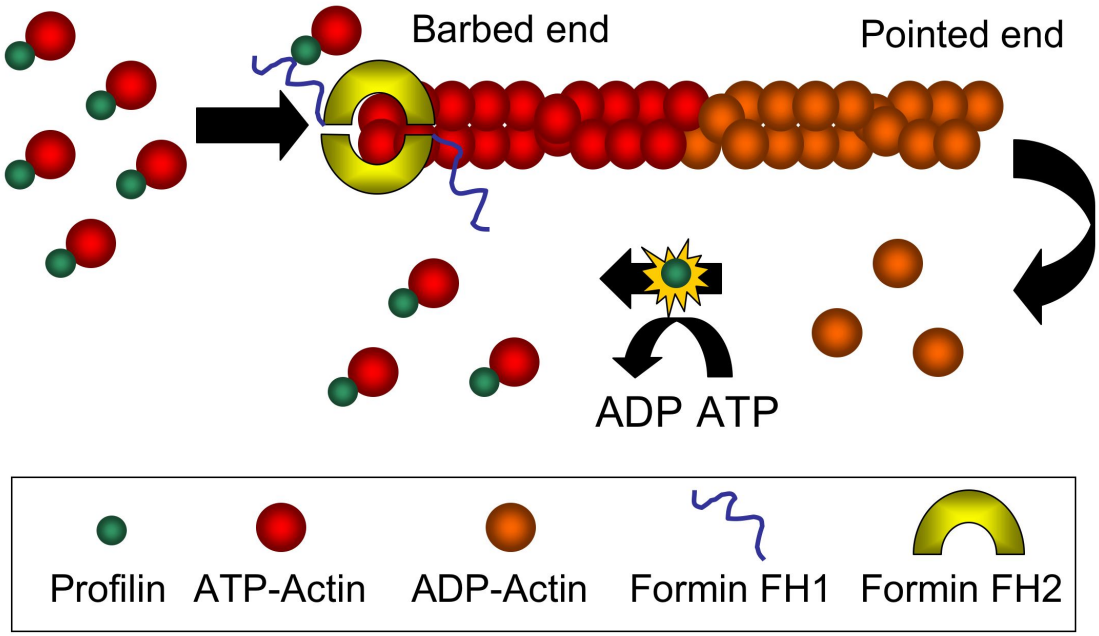

Figure 2. Mechanism of formin and profilin mediated enhancement of actin polymerization.

Chapter II

Divergent, Unstable Actin Filaments in Apicomplexan Parasites are Rescued by Phalloidin

PREFACE

Work presented in this chapter was conducted by KMS and Karthik Diraviyam. KD performed all of the molecular docking and modeling experiments as well as making the parasite actin homology models. Keliang Tang contributed by cloning the actins into baculovirus expression vectors.

The first complete draft of this chapter was written by KMS. Comments from David Sibley, David Sept and Karthik Diraviyam were incorporated into the final version printed here.

Portions of this chapter (Figures 1-5; 8) have been accepted for publication in Plos Pathogens:

Skillman KM, Diraviyam K, Khan A, Tang K, Sept D, Sibley LD. Evolutionarily Divergent, Unstable Filamentous Actin is Essential for Gliding Motility in Apicomplexan Parasites.

ABSTRACT

Apicomplexan parasites, including *Toxoplasma* and *Plasmodium*, invade host cells using a unique gliding motility mechanism that is critically dependent on the polymerization of their own actin. However, previous studies suggest that parasite actins form only short filaments, which contrasts polymerization of more conventional actins. Why parasite actins form short filaments and how this affects their ability to undergo gliding motility remain unresolved. Recombinant *Toxoplasma* (TgACTI) and *Plasmodium* (PfACTI and PfACTII) actins were purified using a baculovirus expression system. When the parasite actins were polymerized in the presence of low levels of phalloidin, only short filaments were observed, although PfACTII filaments were slightly more prevalent. In contrast, when equimolar levels of phalloidin were included during polymerization, long filaments were formed by all three actins. Phalloidin stabilization also impacted the parasite actin filament morphology, ability to sediment and increased the extent of polymerization. Parasite actins contain a conserved phalloidin binding site as determined by molecular modeling and computational docking, yet differ in nearby residues that are predicted to impact filament stability. Our studies document that parasite actins do not polymerize robustly *in vitro*. However, in the presence of the stabilizing agent phalloidin, they are capable of robust polymerization that is more consistent with conventional actin polymerization. The lack of long filament formation by parasite actins suggests that inherent properties within the actin itself contribute to polymerization, which is likely a critical adaptation for rapid turnover needed for gliding motility and host cell invasion.

INTRODUCTION

Apicomplexan parasites are obligate intracellular protozoan pathogens of humans and animals (Cowman and Crabb, 2006; Sibley, 2004). Two notable members of this phylum are *Toxoplasma gondii*, an opportunistic pathogen and model for the phylum and *Plasmodium falciparum,* the cause of malaria, a devastating global disease. The ability of these parasites to enter into host cells is essential for their development. However, rather than utilizing host cell machinery to power entry, apicomplexans employ a unique gliding motility mechanism that is dependent on polymerization of their own actin into filaments (Dobrowolski and Sibley, 1996). Gliding and cell invasion also depend on secretion of adhesins from the apical end that make contacts with receptors on the host cell surface (Cowman and Crabb, 2006; Sibley, 2004). Beneath the parasite membrane, the cytoplasmic tails of the adhesins are linked to actin filaments via interaction with aldolase, which has been shown to interact with both the adhesins MIC2 in *Toxoplasma* (Jewett and Sibley, 2003) and TRAP in *Plasmodium* (Buscaglia et al., 2003), thus bridging these adhesions to actin. Non-processive myosin motors anchored in the inner membrane complex of the parasite (Gaskins et al., 2004) have been shown to be essential (Meissner et al., 2002) and are believed to translocate actin filaments rearward along the cell surface, directing movement of the adhesin. The culmination of this process is forward motion of the parasite and entry into host cells.

Actin polymerization is a critical component of apicomplexan motility and cell invasion but, paradoxically, parasite actins have been shown to exist mostly in an unpolymerized state, as defined by sedimentation at 100,000g (Schmitz et al., 2005; Wetzel et al., 2003). This is in contrast to mammalian, yeast and amoeba cells, in which

the majority of actin is found in a filamentous form (Pollard et al., 2000). This discrepancy suggests that polymerization of parasite actin is tightly regulated and that actin filaments may be very transient. Agents that stabilize actin filaments, such as the drug jasplakinolide, disrupt host cell invasion (Poupel and Tardieux, 1999). Jasplakinolide treatment also causes parasites to become hypermotile, however, they lose directionality and no longer proceed with forward movement (Wetzel et al., 2003). These findings demonstrate that highly stabilized actin filaments have a toxic effect on the gliding process. Fluorescent derivatives of phalloidin, a cyclic peptide that binds to and stabilizes filamentous actin, are often used to visualize conventional actin filaments from purified protein as well as fixed cells (Small et al., 1999). However, when fluorescent phalloidin was used to attempt to stain actin filaments within *Toxoplasma* or the closely related apicomplexan parasite, *Cryptosporidium*, no filaments were observed, suggesting phalloidin may be unable to bind parasite actins or that long, stable filaments do not exist at steady state (Dobrowolski and Sibley, 1996; Forney et al., 1998; Shaw and Tilney, 1999).

Actin is an essential protein in eukaryotic cells and its sequence is highly conserved among organisms (Pollard et al., 2000). *T. gondii* contains a single actin gene, TgACTI, (Dobrowolski et al., 1997), while *P. falciparum* contains two actin genes, PfACTI, that is closely related to TgACTI and PfACTII, which is divergent (Wesseling et al., 1988). Transcriptional analysis demonstrates that PfACTI is expressed throughout the parasite life cycle while PfACTII is most highly expressed in the sexual stages (Wesseling et al., 1989). Previous studies involving both TgACTI and PfACTI have demonstrated that parasite actin does not readily polymerize and forms only short filaments, averaging

around 100 nm in length (Sahoo et al., 2006; Schmitz et al., 2005; Schüler et al., 2005). Only small foci or fragmented filaments were seen when TgACTI was incubated under polymerizing conditions and visualized using microscopy or sedimented and subjected to electron microscopy analysis of the pellet (Sahoo et al., 2006). Similar filament lengths were demonstrated for PfACTI using protein isolated by sedimenting actin filaments from lysates (Schmitz et al., 2005), although actin binding proteins may have influenced this result. Alternatively expression of PfACTI in yeast (Schüler et al., 2005), resulted in slow, inefficient polymerization forming short, punctate filaments only in the presence of phalloidin or gelsolin.

Apicomplexan actins are divergent from vertebrate actin and yet filamentous actin is critical for gliding motility, raising the questions of why *Toxoplasma* and *Plasmodium* actins do not form robust filaments and what contributes to their unusual polymerization properties. Here, we demonstrate that phalloidin can bind to parasite actins and is capable of rescuing the lack of parasite actin polymerization. In addition to the phenotypic impact of phalloidin on parasite actins, the parasite actin polymerization kinetics were also increased in the presence of phalloidin. Collectively, these findings reveal that although the parasite actins do not polymerize robustly on their own, they are capable of forming longer, more conventional filaments when stabilized. This rescue suggests the lack of polymerization may be a result of an intrinsic property within the actins.

RESULTS

Sequence Comparison of TgACTI, PfACTI and PfACTII

Actins are considered to be highly conserved in structure and function. However, apicomplexan actins are functionally divergent from actins in yeast, animals and plants likely due to molecular differences within the parasite actin protein sequence (Figure 1). For example, TgACTI has only 83% sequence identity with mammalian actin while sharing 93% identity with PfACTI (Dobrowolski et al., 1997). In contrast, PfACTI and PfACTII have only 79% sequence similarity to one another, which is relatively low for actin sequences (Wesseling et al., 1988). To visualize the shared sequence differences between these three parasite actins, homology models were created to highlight the substitutions within each actin. TgACTI and PfACTI are highly similar (Figure 2A, yellow spheres) while PfACTII is more divergent (Figure 2B). A sequence alignment of the parasite actins compared to more conventional actins, *Saccharomyces cerevisiae* (ScACT) and *Homo sapiens* muscle actin also demonstrates the areas of divergence between these actins (Figure 1).

Expression and Purification of Parasite Actins

Parasite actins were expressed in baculovirus, similar to a previous report of TgACTI (Sahoo et al., 2006). We set out to make recombinant protein for both PfACTI and PfACTII to analyze them *in vitro* and further characterize their ability to polymerize. While it has been shown that TgACTI and PfACTI form short filaments *in vitro*, the ability of PfACTII to polymerize has not yet been studied. N-terminally HIS_6-tagged TgACTI, PfACTI and PfACTII were expressed within Hi5 insect cells and subsequently

purified using Ni-resin chromatography. Previous studies have shown that the presence of this tag does not appreciably alter polymerization of TgACTI (Sahoo et al., 2006). The yield and purity of the recombinant proteins were analyzed by Sypro Ruby staining of SDS-PAGE gels (Figure 2C), which demonstrated that the parasite actins were well expressed using this system and constituted the large majority of protein seen on the gel. *Saccharomyces cerevisiae* actin (ScACT) was also purified using the baculovirus system to serve as a control for the functionality of virally expressed actin.

Polymerization Kinetics of Parasite Actins

The kinetics of parasite actin polymerization were examined by light scattering following addition of filamentation (F) buffer. TgACTI did not polymerize under these conditions (Figure 3, red), while both PfACTI and PfACTII were capable of low levels of polymerization (Figure 3, blue and green, respectively). These results are consistent with the lack of filamentation reported previously (Sahoo et al., 2006; Schmitz et al., 2005; Schüler et al., 2005). In contrast, polymerization of ScACT (Figure 3, orange) was much more efficient, indicating that the inefficiency of parasite actin polymerization was not a consequence of expression in baculovirus or the N-terminal tag shared by all of the proteins.

Phalloidin Rescues Inherent Instability of Parasite Actins

It has previously been suggested that TgACTI does not bind phalloidin based on the finding that actin filaments have never been visualized when the parasite is stained with fluorescently labeled phalloidin (Heintzelman, 2006). However, it has been shown that

addition of phalloidin to TgACTI after polymerization results in stabilization of short filaments (Sahoo et al., 2006). To test the capability of phalloidin to bind to parasite actin filaments and examine the ability of the actins to polymerize under stabilizing conditions, purified actins were incubated with different amounts of phalloidin during polymerization in F buffer. Consistent with previous reports (Poupel and Tardieux, 1999; Shaw and Tilney, 1999), filaments were not detected for TgACTI in the presence of low levels of fluorescently labeled phalloidin (i.e. 0.13 μM) that was added to visualize filamentous actin (Figure 4A). Short, punctate filaments were observed when a slightly higher level of labeled phalloidin (i.e. 0.33 μM) was added to TgACTI (Figure 4A). In contrast, long clusters of filaments were observed when TgACTI was allowed to polymerize in the presence of equimolar levels of unlabeled phalloidin combined with lower levels of labeled phalloidin for visualization (i.e. 0.33 μM) (Figure 4A). A similar dose-response to increasing phalloidin was seen for PfACTI and PfACTII, although these actins also occasionally formed small clusters of short filaments even in low levels of labeled phalloidin (i.e. 0.13 μM) (although rare, a representative example is shown in Figures 4B and 4C). Both PfACTI and PfACTII formed more abundant clusters of short filaments in slightly higher levels of labeled phalloidin (i.e. 0.33 μM) and these were further stabilized by equimolar unlabeled phalloidin (Figures 4B, 4C). Phenotypically, PfACTII filaments clumped together and appeared to polymerize slightly more extensively than the other actins. As expected for a conventional actin, ScACT formed long filaments regardless of the phalloidin concentration (Figure 4D) confirming that virally-expressed actins can polymerize normally and that the results seen with the parasite actins are not artifacts of the method of purification.

Phalloidin-stabilized Parasite Actin Filaments Resemble Conventional Filaments

To further analyze the filaments formed by parasite actins, negative staining and electron microscopy were used to examine ultrastructural details. Similar to the fluorescent phalloidin assays, EM visualization of abundant parasite actin filaments required incubation in F buffer containing equimolar phalloidin (Figure 5). When TgACTI was incubated in G buffer, globular structures were observed that likely represent aggregates (Figure 5A). Similar structures were seen with TgACTI in F buffer (Figure 5A), and short filaments were rarely observed under the conditions used (data not shown). Polymerization of TgACTI in F buffer with equimolar phalloidin resulted in long filaments that often bundled together (Figure 5A). PfACTI in G buffer also revealed small clusters of protein and similar results were observed when the protein was incubated in F buffer (Figure 5B). Like TgACTI, PfACTI formed long filaments in the presence of equimolar phalloidin (Figure 5B). PfACTII incubated in G buffer also formed small clusters (Figure 5C). Despite the fluorescence microscopy data that suggested PfACTII was capable of forming clusters even in low levels of phalloidin, electron microscopy did not reveal formation of filaments when PfACTII was incubated in F buffer (Figure 5C). This may reflect instability under the conditions used for EM or a low density of filaments. Similar to both TgACTI and PfACTI, long, stable filaments were formed when polymerization occurred in the presence of F buffer and equimolar phalloidin. Enlargement of the phalloidin stabilized filaments formed by the three parasite actins revealed a spiral pattern of the actin helix and striations along the filament, which are typical characteristics of conventional actin filaments (Figure 5).

When ScACT was incubated in G buffer, only small clusters of globular protein were

observed, similar to what was seen with each parasite actin (Figure 5D). In contrast to the parasite actins, long filaments were observed when ScACT was incubated in F buffer. Similar filaments were also seen when ScACT was incubated in F buffer with phalloidin. Closer examination of these filaments revealed striations within the filaments as expected for a conventional actin (Figure 5D). Both the parasite actins and yeast actin showed prominent filament bundles, which are also seen in the fluorescence images mentioned above. Collectively, the fluorescence phalloidin microscopy and electron microscopy studies verify that the instability of parasite actins is an intrinsic property of the protein itself and that this instability can be overcome using a stabilization agent as seen by the fact that polymerization is rescued by high concentrations of phalloidin.

Parasite Actins Exhibit Sedimentation Patterns that Differ from Conventional Actin

When conventional actins are polymerized and centrifuged at 100,000g, the majority of the protein exists in long filaments and therefore sediments in the pellet (Pardee and Spudich, 1982). Previous studies with TgACTI and PfACTI have reported that the proteins require higher force (i.e. 500,000g for 1 hour) for sedimentation of recombinant TgACTI (Sahoo et al., 2006) or *Plasmodium* actin in lysates (Schmitz et al., 2005). We were interested to determine what effect the addition of phalloidin or higher force during centrifugation would have on parasite actins. When TgACTI was incubated in F buffer to induce polymerization and subsequently centrifuged at 100,000g, the majority of the protein remained in the supernatant similar to previous reports (Figure 6A). Addition of phalloidin at equimolar ratio shifted more TgACTI to the pellet (Figure 6A). Centrifugation at 350,000g was sufficient to pellet the majority of TgACTI in F buffer

even in the absence of phalloidin. When TgACTI was polymerized in the presence of phalloidin and subsequently centrifuged at 350,000g, there was essentially no further sedimentation from that seen without phalloidin. PfACTI behaved similarly to TgACTI in responding to higher force and addition of phalloidin (Figure 6B). PfACTII was also found predominantly in the supernatant after polymerization and spinning at 100,000g (Figure 6C). While the addition of phalloidin shifted more protein into the pellet, PfACTII was less responsive to phalloidin than the other parasite actins. However, spinning at 350,000g shifted the majority of PfACTII to the pellet. Addition of phalloidin to the reaction before the 350,000g spin did not further increase the amount of PfACTII in the pellet. These behaviors were not the result of baculovirus expression as ScACT was tested under the same conditions and more than 90% of the protein was found in the pellet regardless of the addition of phalloidin or speed of centrifugation (Figure 6D).

Polymerization Kinetics of TgACTI are Enhanced by Phalloidin

Since microscopy with fluorescent phalloidin-binding revealed the parasite actins are not capable of robust polymerization but can be phenotypically rescued by phalloidin to form long filaments, we wanted to determine what effect adding the stabilizing agent would have on the kinetics of parasite actin polymerization. The extent of TgACTI polymerization was monitored by ninety degree light scattering in the presence or absence of phalloidin. With the addition of only F buffer to TgACTI, very little change was observed in the light scattering (Figure 7, red). When 0.33 μM phalloidin (to mimic the concentration used in the fluorescence phalloidin microscopy) was added with the F

buffer, a minimal increase was observed (Figure 7, green). However, if equimolar phalloidin was added at the time polymerization of TgACTI was induced, the rate of polymerization and maximum light scatter both increased dramatically (Figure 7, blue). However, the levels of TgACTI polymerization were still less robust than what was oberserved when polymerization of ScACTI was induced with F buffer (Figure 7, orange).

Homology Modeling of the Phalloidin-binding Site within Parasite Actins

To investigate the molecular basis of phalloidin binding, we used structures from our MD simulation of the muscle actin filament and performed molecular docking studies with phalloidin (Figures 8A, 8B). Our predicted phalloidin binding site is similar to that reported previously (Oda et al., 2005), but also provides more precise information on specific binding contacts that stem from the following improvements: 1) unconstrained docking analyses were based on a new higher resolution actin filament model (Oda et al., 2009); 2) flexible protein conformations were included by choosing multiple snapshots from MD simulations and multiple binding sites were included within each snapshot; 3) induced fit was accommodated by simulated annealing. Together these analyses precisely mapped the phalloidin binding site in mammalian actin to the loop formed by residues 196-200 in the lower actin monomer, the 72-74 loop of the middle monomer, and the 285-290 loop of the upper monomer (Figure 8A). These three regions closely coincide with those identified in previous experimental studies as important for phalloidin interactions (Faulstich et al., 1993; Oda et al., 2005; Steinmetz et al., 1998). Importantly, residues including D179, Y198, S199, K284, I287 and R290, which were previously

observed to be close to the phalloidin binding site (Oda et al., 2005) were also within 4 Å of phalloidin in our model. Moreover, our more precise placement of the compounds predicts maximum interaction between the Cys3-Pro(OH)4-Ala5-Trp6 ring in phalloidin and actin residues while Leu(OH)7 in phalloidin faces out of the binding pocket and is accessible to solvent. This orientation corresponds well with experimental studies (Faulstich et al., 1993; Oda et al., 2005; Steinmetz et al., 1998) showing that derivatives of phalloidin with a fluorophore linked to Leu(OH)7, bind actin filaments in the same conformation.

Homology models for TgACTI and PfACTII were built using the muscle actin filament obtained by simulated annealing. Docking studies were repeated using TgACTI and PfACTII homology models and they yielded very similar conformations although the specific amino acid contacts lying within 4 Å varied slightly between proteins. Residues previously shown by mutational analysis to mediate phalloidin binding in yeast (Belmont et al., 1999) (*i.e.* R177, D179), were conserved in all three models (Figure 8C). Residues R177 and D179 in mammalian actin, corresponding to R178 and D180 in parasite TgACTI, both lie within 4 Å (Figure 8C). Six specific differences in the residues contacting phalloidin in mammalian muscle actin *vs*. TgACTI and PfACTII were noted (Figure 8C, Figure 1). Together, these differences may mediate the less efficient binding to phalloidin observed for parasite actin filaments.

DISCUSSION

Previous studies have shown that while apicomplexan motility relies on filamentous actin, only short filaments are detected *in vivo* where a majority of actin appears to be non-polymerized (Schmitz et al., 2005; Wetzel et al., 2003). Consequently, we set out to determine if this unusual behavior was due to an inherent property of the actins themselves. Insect cell-expressed *Toxoplasma* (TgACTI) and *Plasmodium* (PfACTI and PfACTII) actins were used to demonstrate that after incubation in polymerization buffer, the actins formed small fluorescent asters that only sedimented at 350,000g suggesting they are small multimers or short filaments. The extent of polymerization of the parasite actins was also less robust than that of conventional actin. However, when high levels of phalloidin were added during polymerization, parasite actin polymerization was rescued and longer filaments that more closely resembled conventional actins were formed. Modeling of the phalloidin binding site within the parasite actins demonstrated it was highly similar to the binding site in conventional actins with only subtle differences that may explain the apparent difference in stability between the actins.

In this study, purified, recombinant TgACTI and PfACTI incubated under conditions known to induce polymerization of conventional actins did not form long filaments as viewed by fluorescence microscopy and detected with low levels of fluorescent phalloidin staining. When subjected to EM, no filaments were detected for TgACTI or PfACTI, rather only small aggregates were observed. Short filaments of TgACTI have been observed through EM in previous studies (Sahoo et al., 2006) but we did not observe any filaments in the current study, suggesting they are rarely detected. Consistent with the lack of extensive filament formation, sedimentation analysis revealed

that when centrifuged at 100,000g, the majority of the parasite actin did not sediment. This is in contrast to the behavior of yeast actin, which sedimented efficiently at this speed. When the parasite actins were centrifuged at 350,000g, the majority of the protein was now found in the pellet, indicating this higher speed was enough to sediment the small filaments. These results are consistent with previous reports investigating the behavior of baculovirus-expressed TgACTI (Sahoo et al., 2006) and PfACTI isolated from parasite lysate (Schmitz et al., 2005), which demonstrated that centrifugation at 500,000g was required to efficiently sediment the polymerized parasite actins. Our findings indicate that while TgACTI and PfACTI do undergo polymerization, they have a very limited capacity to do so in comparison to yeast actin.

Prior to this study, PfACTII had not been purified and there were no reports about the polymerization properties of this actin. Transcriptional analysis demonstrates PfACTII is upregulated in the sexual stages of the *Plasmodium* developmental cycle (Wesseling et al., 1989) and therefore, it may have a different function and extent of polymerization than PfACTI, which is expressed throughout the parasite life cycle. In addition to the differential expression, the amino acid sequences of PfACTI and PfACTII are divergent from one another with only 79% similarity (Wesseling et al., 1988), also suggesting their functions could differ. When recombinant PfACTII was incubated with low levels of phalloidin, it appeared slightly more capable of polymerization compared to either TgACTI or PfACTI, however, the filaments were still shorter than what would be expected from a conventional actin and filaments could still not be detected by EM. Sedimentation analysis was also consistent with the lack of robust polymerization as seen by the small percentage of actin that sedimented after centrifugation at 100,000g. The

finding that PfACTII appears slightly more capable of polymerization could have potential significance *in vivo* if it is involved in processes that are not as prone to turnover as is the mechanism of gliding motility. It may be important for the parasite to contain a more stable actin during stages of the parasite development that are non-motile, such as the gametocyte stage when PfACTII is highly expressed.

In order to determine if the low level of polymerization by parasite actins could be rescued, phalloidin was added to the polymerization reaction. Interestingly, only when equimolar levels of phalloidin were added, long filaments that closely resembled conventional actin were visualized by fluorescence microscopy. When these phalloidin-stabilized filaments were viewed by electron microscopy, the morphology of the filaments was similar to conventional actins. When the phalloidin-stabilized filaments were centrifuged at 100,000g, the majority of the protein was now found in the pellet suggesting that the filaments had sufficient mass to sediment. The extent of polymerization by light scattering was also increased in the presence of phalloidin. The phalloidin rescue suggests there may be a defect in monomer association limiting filament formation or alternatively differences in monomer turnover causing filaments to assemble and disassemble more rapidy. The phalloidin binding site sits at an interface between protomers, and therefore phalloidin may reverse either of these potential effects by stabilizing monomer-monomer contacts within the filament.

Despite previous reports of failed attempts to visualize actin filaments within parasites by staining with phalloidin (Cintra and De Souza, 1985; Dobrowolski et al., 1997; Shaw and Tilney, 1999), the results of this current study demonstrate that purified recombinant actin from *Toxoplasma* and *Plasmodium* are in fact capable of binding phalloidin. The

finding that polymerization of the parasite actins in the presence of phalloidin allows visualization of long filaments suggests that the lack of staining from previous studies was not due to the inability of phalloidin to bind but rather was likely due to the low level of polymerization, which would be difficult to detect by microscopy.

Having demonstrated that parasites actins are capable of binding phalloidin, we used molecular docking to identify the phalloidin binding site and pinpoint residues important for this interaction. Initially, docking was used to model the phalloidin binding site within mammalian actin. The binding site was in agreement with that previously determined (Faulstich et al., 1993; Oda et al., 2005; Steinmetz et al., 1998) but revealed additional details about the orientation of the compound and potent ion contacts between side groups and actin residues. Subsequently, this model was used to compare the binding site for TgACTI and PfACTII. Most residues previously determined to be important for phalloidin binding, including R177 and D179, which extend into the binding pocket and phalloidin binding is disrupted when they are mutated (Belmont et al., 1999), are conserved among all actins compared. It is interesting to note that most of the residues of the three actins that are predicted to interact with phalloidin are also conserved in *Tetrahymena* actin which is reported not to bind phalloidin (Hirono et al., 1989). However, the levels of phalloidin used in this prior study were below what was in the current study and it is possible that higher levels would be required for phalloidin binding to *Tetrahymena* actin. Noteably, *Tetrahymena* shows diversity among some of the residues that also differ when comparing parasite and mammalian actin.

Despite the highly conserved nature of the actin sequence, subtle differences are present in the residues interacting with phalloidin among the three actins studied here that

may affect binding and thus explain why high molar amounts of phalloidin are needed to stabilize the parasite actins. One potentially important predicted difference is M269 in muscle actin, which is changed to K270 and R270 in *Toxoplasma* and *Plasmodium*, respectively. The resulting extra positive charge introduced into the parasite phalloidin binding site could affect interaction with the drug. Interestingly, this residue change has also been suggested to affect stability of the actin filament by introducing a destabilizing force on the actin filament due to its location at the end of the hydrophobic plug region of the actin monomer (Sahoo et al., 2006), which is thought to be important for monomer-monomer interaction and filament stability (Chen et al., 1993). The other important region that differs within the phalloidin binding site of mammalian and parasite actins is the serine at position 200 in mammalian actin, which is glycine or threonine in TgACTI or PfACTII, respectively. In the case of mammalian actin this residue is within hydrogen bonding distance to Pro(OH)4 of the phalloidin ring and actin residue D179. In the case of the glycine substitution in TgACTI and the threonine in PfACTII, this hydrogen bonding with Pro(OH)4 is precluded due to steric hindrances. The role that these substitutions play in the inherent instability has not been tested directly but if mutation of these residues to those found in conventional actins rescues the ability of the parasite actins to form long filaments in the absence of a stabilizing agent, this would provide a molecular explanation for why these actins are short and unstable.

It is apparent that the apicomplexan actins functionally diverge from conventional actins as seen by low levels of *in vitro* polymerization in the present study. Combined with the data that parasite actins are rescued by high concentrations of phalloidin, these results support a model suggesting intrinsic properties are largely responsible for

controlling polymerization of parasite actins. The intrinsic properties of actins may be more significant in controlling dynamics in apicomplexan parasites since they contain only a streamlined set of actin-binding proteins, including profilin, actin depolymerizing factor (ADF), cyclase associated protein (CAP), and capping protein (Baum et al., 2006; Schüler and Matuschewski, 2006).

It has been suggested that shorter filaments allow for faster polymerization and depolymerization and that rapid depolymerization may occur so the actin can be sequestered until required for motility (Schmitz et al., 2005). Our studies are consistent with inherent properties of parasite actins contributing to this behavior. Addition of phalloidin *in vitro* dramatically changes the behavior of the actins to form long filaments. However, phalloidin is not membrane permeable, precluding its use for examination of filaments in live cells. When live parasites are treated with jasplakinolide, another actin stabilizing agent, they are no longer capable of invading host cells (Shaw and Tilney, 1999). The jasplakinolide-treated parasites contain long actin filaments at both poles and become hyper-motile and no longer undergo productive motility (Wetzel et al., 2003). These findings imply that rapidly recycling filaments are actually required for gliding motility and stabilizing these filaments is toxic to the parasite. The demonstration that apicomplexan actins are capable of forming long, stable filaments provides more insight into the mechanism of regulation of the short parasite actin filaments that have previously been observed and enhances the knowledge of actin dynamics in apicomplexans.

MATERIALS AND METHODS

Plasmid Constructions and Transfection

Recombinant *Plasmodium* and yeast actins were expressed in baculovirus, similar to TgACTI as previously described (Sahoo et al., 2006). Recombinant viruses were created for the *Plasmodium* actins by amplification from 3D7 strain of *Plasmodium falciparum* cDNA using primers 5'-CTAGTCTCGAGAATGGGAGAAGAAGTAGTTCAA-3' (forward) and 5'-CTAGTGAGCTCTTAGAAACATTTTCTGTGGACAATAC-3' (reverse) for PfACTI and 5'-CTAGTCTCGAGGATGTCTGAAGAAGCTGTTG-3' (forward) and 5'-CTAGTGAGCTCTTAGAAACATTTTCTATGAACAATACTAGG-3' (reverse) and cloned into the viral transfer vector pAcHLT-C (BD Biosciences Pharmingen, San Jose, CA). The coding sequence of ScACT was amplified from *Saccharomyces cerevisiae* cDNA using primers 5'-CTAGTCATATGCATGGATTCTG AGGTTGCT-3' (forward) and 5'-CTAGTGAATTCTTAGAAACACTTGTGGTGAA CGAT-3' (reverse) and cloned into the viral transfer vector pAcHLT-C (BD Bioscience Pharmingen). Cotransfection of the pAcHLT-C vectors, containing the respective actins, with linearized baculogold genomic DNA into Sf9 insect cells (BD Biosciences Pharmingen), was used to obtain recombinant virus, according to manufacturer's instructions.

Parasite actin homology models and alignment

Homology models for TgACTI, PfACTI, and PfACTII sequences were built on the ADP-actin crystal structure (1J6Z) (Otterbein et al., 2001) using Modeller (Martí-Renom et al., 2000). Homology models were aligned and visualized using VMD (Humphrey et al.,

1996). Protein sequences for actins from *Homo sapiens* (muscle α-actin), gi: 6049633; *Saccharomyces cerevisiae*, gi: 38372623; *Toxoplasma gondii*, gi: 606857; *Plasmodium falciparum* ACTI, gi: 160053; and *Plasmodium falciparum* ACT2, gi: 160057; were aligned using DNASTAR Lasergene MegAlign v7 and modified using Adobe Illustrator v10.

Actin expression and purification

Hi5 insect cells were maintained as suspension cultures in Express-Five SFM media (Invitrogen). Hi5 cells were harvested at 2.5 days postinfection with recombinant virus and lysed in BD BaculoGold Insect Cell Lysis Buffer (BD Biosciences Pharmingen) supplemented with 5 mM $CaCl_2$, 5 mM ATP, 5 mM NaN_3, and protease inhibitor cocktail (E64, 1 μg ml^{-1} AEBSB, 10 μg ml^{-1}; TLCK, 10 μg ml^{-1}; leupeptin, 1μg ml^{-1}). His-tagged actins were purified using Ni-NTA agarose (Invitrogen). After binding for 2 h, the column was washed sequentially with G actin buffer without DTT (G-DTT buffer) (5 mM Tris-Cl, pH 8.0, 0.2 mM $CaCl_2$, 0.2 mM ATP), then G-DTT buffer with 10 mM imidazole, G-DTT buffer with 0.5 M NaCl, G-DTT buffer with 0.5 M KCl buffer, and finally G-DTT buffer with 25 mM imidazole. Proteins were eluted with serial washes of G-DTT buffer containing 50 mM, 100 mM, and 200 mM imidazole, pooled together and dialyzed overnight in G actin buffer containing 0.5 mM DTT with 100 μM sucrose. Purified recombinant actins were clarified by centrifugation at 100,000*g*, 4°C, for 30 min using a TL100 rotor and a Beckman Optima TL ultracentrifuge (Becton Coulter) to remove aggregates. Purified proteins were resolved on 12% SDS-PAGE gels followed by SYPRO Ruby (Molecular Probes) staining, visualized using a FLA-5000

phosphorimager (Fuji Film Medical Systems), and quantified using Image Gauge v4.23. Purified actins were stored at 4°C and used within 2-3 days.

Fluorescence microscopy

Purified recombinant actins were clarified by as described above and incubated (5 μM) in 1/10th 10X F buffer (500 mM KCl, 20 mM $MgCl_2$, 10 mM ATP), and treated with or without equimolar amounts of unlabeled phalloidin (Molecular Probes). Final concentrations of 0.13 μM or 0.33 μM Alexa-488 phalloidin (Molecular Probes) were added to each sample to stain filaments. Following polymerization for 1 h, samples were placed on a slide and viewed with a Zeiss Axioskop (Carl Zeiss) microscope using 63X Plan-NeoFluar oil immersion lens (1.30 NA). Images were collected using a Zeiss Axiocam with Axiovision v3.1 and processed using linear adjustments in Adobe Photoshop v8.0

Negative Staining Electron Microscopy

For ultrastructural analysis of actin filaments, purified recombinant actins were clarified as described above and incubated (5 μM) in F buffer to initiate polymerization for 1 h at room temperature in the absence or presence of equimolar phalloidin (Molecular Probes). Samples were applied to glow-discharged formvar/carbon-coated Cu grids, incubated for 5 min, washed twice with dH_20, and stained with 1% aqueous uranyl acetate (Ted Pella) for 1 min.

Actin Sedimentation Assay

Purified recombinant TgACTI, PfACTI, PfACTII, and ScACT proteins were pre-centrifuged at 100,000g, 4°C for 30 min using a TL100 rotor and a Beckman Optima TL ultracentrifuge (Becton Coulter, Fullerton, CA) to remove aggregates. TgACTI (5 μM), PfACTI (5 μM), PfACTII (3.5 μM), ScACT (5 μM) were incubated in F buffer to initiate polymerization for 1 hr in the presence or absence of equimolar amounts of phalloidin (Molecular Probes) at room temperature. The samples were subsequently centrifuged at 100,000g or 350,000g for 1 hr at room temperature. Protein in the supernatant was acetone precipitated and washed with 70% ethanol. All pellets were resuspended in 1X sample buffer. Proteins were resolved on a 12% SDS-PAGE gels, stained with Sypro-Ruby (Molecular Probes), visualized using a FLA-5000 phosphorimager (Fuji Film Medical Systems), and quantitated using Image Gauge v4.23.

Light scattering

Purified recombinant actins were clarified as described above and incubated (5 μM) in G buffer containing 1 mM EGTA and 50 μM $MgCl_2$ for 10 min (to replace bound Ca^{2+} with Mg^{2+}). Samples were placed in a microcuvette (Starna Cells) and following addition of $1/10^{th}$ volume of F buffer, light scattering was monitored with the PTI Quantmaster spectrofluorometer (Photon Technology International) with excitation 310 nm (1 nm bandpass) and emission 310 nm (1 nm bandpass). For experiments with addition of phalloidin, either methanol diluted 1:8.4 (same dilution as the phalloidin stock), 0.33 μM phalloidin or 5 μM phalloidin were also added to the actin at the same time as the F buffer.

Actin structure for molecular modeling

An atomic model of phalloidin was derived from the solid state structure of a synthetic derivative (Zanotti et al., 2001), modified to contain dihydroxy-Leu7 using Maestro (Schrödinger LLC,) and energy minimized using MacroModel (Schrödinger LLC,) with a MMFF94s forcefield. The model was further optimized in continuum solvent using Jaguar (Schrödinger LLC), with DFT level of theory using a hybrid B3LYP functional and 6-31G** basis set. The actin filament model based on X-ray fiber diffraction data (Oda et al., 2009) was used to create an 8-monomer filament of muscle F-actin. A 50 ns molecular dynamics (MD) simulation in explicit water was carried out using NAMD (Kale et al., 1999) in an NPT ensemble with a pressure of 1 atm and a temperature of 300 K with explicit TIP3P water. CHARMM27 forcefield was used with a 10 Å cut off for van der Waals with a 8.5 Å switching distance, and Particle Mesh Ewald for long-range electrostatics. Bonded hydrogens were kept rigid to allow 2 fs time steps. A simulated annealed structure of muscle filament model with phalloidin in the binding site was used as the template for building parasitic actin filament homology models using Modeller (Martí-Renom et al., 2000).

Docking studies

Docking of phalloidin to different sites along the filament was captured using multiple snapshots taken at intervals of 200 ps from the 50 ns simulation. AutoDock (Morris et al., 1998) was used to perform large scale docking runs with a coarse grid that covered the six binding sites on the filament. To determine the correct orientation of phalloidin in the binding site, higher resolution docking studies were performed on each binding site

using both AutoDock and Glide (Schrödinger LLC) in independent trials and clustered to derive the most probable docking orientation. For AutoDock, flexible ligand docking was performed using Lamarckian genetic algorithm with a population size of 200, 10 million energy evaluations, and a local search probability frequency at 0.2. Grid spacings of 0.325 Å and 0.25 Å were used for coarse and high resolution docking, respectively, and the results were clustered at RMSD of 3.0 Å from the lowest docked energy conformer. Gasteiger-Marsili charges were assigned to the ligand using Sybyl (Tripos Inc.,). Default parameters were used for Glide; ligand charges were derived from the quantum optimization calculation and protein charges were derived from the OPLS2001 forcefield.

ACKNOWLEDGEMENTS

We thank Wandy Beatty for assistance with microscopy, Keli Tang for excellent technical support and the cytoskeletal discussion group for thoughtful comments and advice. This work was supported by predoctoral fellowships from the American Heart Association (0815645G to KMS) and an Institutional Training Grant T32-AI007172 (to KMS), and a grant from the NIH (AI073155 to LDS, DS).

REFERENCES

Baum, J., Papenfuss, A.T., Baum, B., Speed, T.P., and Cowman, A.F. (2006). Regulation of apicomplexan actin-based motility. Nat Rev Microbiol *4*, 621-628.

Belmont, J.D., Patterson, G.M., and Drubin, D.G. (1999). New actin mutants allow further characterization of the nucleotide binding cleft and drug binding sites. J Cell Sci *112*, 1325-1336.

Buscaglia, C.A., Coppens, I., Hol, W.G.J., and Nussenzweig, V. (2003). Site of interaction between aldolase and thrombospondin-related anonymous protein in *Plasmodium*. Mol Biol Cell *14*, 4947-4957.

Chen, X., Cook, R.K., and Rubenstein, P.A. (1993). Yeast actin with a mutation in the hydrophobic plug between subdomains 3 and 4 ($L_{266}D$) displays a cold-sentitive polymerization defect. J Cell Biol *123*, 1185-1195.

Cintra, W.M., and De Souza, W. (1985). Immunocytochemical localization of cytoskeletal proteins and electron microscopy of detergent extracted tachyzoites of *Toxoplasma gondii*. J Submicro Cyt *17*, 503-508.

Cowman, A.F., and Crabb, B.S. (2006). Invasion of red blood cells by malaria parasites. Cell *124*, 755-766.

Dobrowolski, J.M., Niesman, I.R., and Sibley, L.D. (1997). Actin in the parasite *Toxoplasma gondii* is encoded by a single copy gene, *ACT1* and exists primarily in a globular form. Cell Motil Cytoskel *37*, 253-262.

Dobrowolski, J.M., and Sibley, L.D. (1996). Toxoplasma invasion of mammalian cells is powered by the actin cytoskeleton of the parasite. Cell *84*, 933-939.

Faulstich, H., Zobeley, S., Heintz, D., and Drewes, G. (1993). Probing the phalloidin binding site of actin. FEBS Lett *318*, 218-222.

Forney, J.R., Vaughan, D.K., Yang, S., and Healey, M.C. (1998). Actin-dependent motility in *Cryptosporidium parvum* sporozoites. J Parasitol *84*, 908-913.

Gaskins, E., Gilk, S., DeVore, N., Mann, T., Ward, G.E., and Beckers, C. (2004). Identification of the membrane receptor of a class XIV myosin *Toxoplasma gondii*. J Cell Biol *165*, 383-393.

Heintzelman, M.B. (2006). Cellular and molecular mechanics of gliding locomotion in eukaryotes. Int Rev Cytol *251*, 79-129.

Hirono, M., Kamagai, Y., Numata, O., and Watanabe, Y. (1989). Purification of Tetrahymena actin reveals some unusual properties. Proc Natl Acad Sci (USA) *86*, 75-79.

Humphrey, W., Dalke, A., and Schulten, K. (1996). VMD: visual modeling dynamics. Graph *14*, 33-38.

Jewett, T.J., and Sibley, L.D. (2003). Aldolase forms a bridge between cell surface adhesins and the actin cytoskeleton in apicomplexan parasites. Molec Cell *11*, 885-894.

Kale, L., Skeel, R., Bhandarkar, M., Brunner, R., Gursoy, A., Krawetz, N., Phillips, J., Shinozaki, A., Varadarajan, K., and Schulten, K. (1999). NAMD2: Greater scalability for parallel molecular dynamics. J Comp Physics *151*, 283-312.

Martí-Renom, M.A., Stuart, A.C., Fiser, A., Sánchez, R., Melo, F., and Sali, A. (2000). Comparative protein structure modeling of genes and genomes. Annu Rev Biophys Biomol Struct *29*, 291-325.

Meissner, M., Schluter, D., and Soldati, D. (2002). Role of *Toxoplasma gondii* myosin A in powering parasite gliding and host cell invasion. Science *298*, 837-840.

Morris, G.M., Goodsell, D.S., Halliday, R.S., Huey, R., Hart, W.E., Belew, R.K., and Olson, A.J. (1998). Automated docking using a Lamarkian genetic algorithm and emperical binding free energy function. J Comp Chem *19*, 1639-1662.

Oda, T., Iwasa, M., Aihara, T., Maeda, Y., and Narita, A. (2009). The nature of the globular- to fibrous-actin transition. Nature *457*, 441-445.

Oda, T., Namba, K., and Maeda, Y. (2005). Position and orientation of phalloidin in F-actin determined by X-Ray fiber diffraction analysis. Biophys J *88*, 2727-2736.

Otterbein, L.R., Graceffa, P., and Dominguez, R. (2001). The crysal structure of uncomplexed actin in the ADP bound state. Science *293*, 708-711.

Pardee, J.D., and Spudich, J.A. (1982). Purification of muscle actin. Methods Cell Biol *24*, 271-289.

Pollard, T.D., Blanchoin, L., and Mullins, R.D. (2000). Molecular mechanisms controlling actin filament dynamics in nonmuscle cells. Annu Rev Biophys Biomol Struct *29*, 545 - 576.

Poupel, O., and Tardieux, I. (1999). *Toxoplasma gondii* motility and host cell invasiveness are drastically impaired by jasplakinolide, a cyclic peptide stabilizing F-actin. Microb Infect *1*, 653-662.

Sahoo, N., Beatty, W.L., Heuser, J.E., Sept, D., and Sibley, L.D. (2006). Unusual kinetic and structural properties control rapid assembly and turnover of actin in the parasite *Toxoplasma gondii*. Mol Biol Cell *17*, 895-906.

Schmitz, S., Grainger, M., Howell, S.A., Calder, L.J., Gaeb, M., Pinder, J.C., Holder, A.A., and Veigel, C. (2005). Malaria parasite actin filaments are very short. J Mol Biol *349*, 113-125.

Schüler, H., and Matuschewski, K. (2006). Regulation of apicomplexan microfilament dynamics by minimal set of actin-binding proteins. Traffic *7*, 1433-1439.

Schüler, H., Mueller, A.K., and Matuschewski, K. (2005). Unusual properties of *Plasmodium falciparum* actin: new insights into microfilament dynamics of apicomplexan parasites. FEBS Lett *579*, 655-660.

Shaw, M.K., and Tilney, L.G. (1999). Induction of an acrosomal process in *Toxoplasma gondii*: visualization of actin filaments in a protozoan parasite. Proc Natl Acad Sci U S A *96*, 9095-9099.

Sibley, L.D. (2004). Invasion strategies of intracellular parasites. Science *304*, 248-253.
Small, J., Rottner, K., Hahne, P., and Anderson, K.I. (1999). Visualising the actin cytoskeleton. Microsc Res Tech *47*, 3-17.

Steinmetz, M.O., Stoffler, D., Müller, S.A., Jahn, W., Wolpensinger, B., Goldie, K.N., Engel, A., Faulstich, H., and Aebi, U. (1998). Evaluating atomic models of F-actin with an undecagold-tagged phalloidin derivative. J Mol Biol *276*, 1-6.

Wesseling, J.G., Smits, M.A., and Schoenmakers (1988). Extremely diverged actin proteins in *Plasmodium falciparum*. Mol Biochem Parasitol *30*, 143-154.

Wesseling, J.G., Snijders, P.J.F., van Someren, P., Jansen, J., Smits, M.A., and Schoenmakers, J.G.G. (1989). Stage-specific expression and genomic organization of the actin genes of the malaria parasite *Plasmodium falciparum*. Mol Biochem Parasitol *35*, 167-176.

Wetzel, D.M., Håkansson, S., Hu, K., Roos, D.S., and Sibley, L.D. (2003). Actin filament polymerization regulates gliding motility by apicomplexan parasites. Mol Biol Cell *14*, 396-406.

Zanotti, G., Falcigno, L., Saviano, M., D'Auria, G., Bruno, B.M., Campanile, T., and Paolillo, L. (2001). Solid state and solution conformation of [Ala7]-phalloidin: a synthetic phallotoxin analogue. Chemistry *7*, 1479-1485.

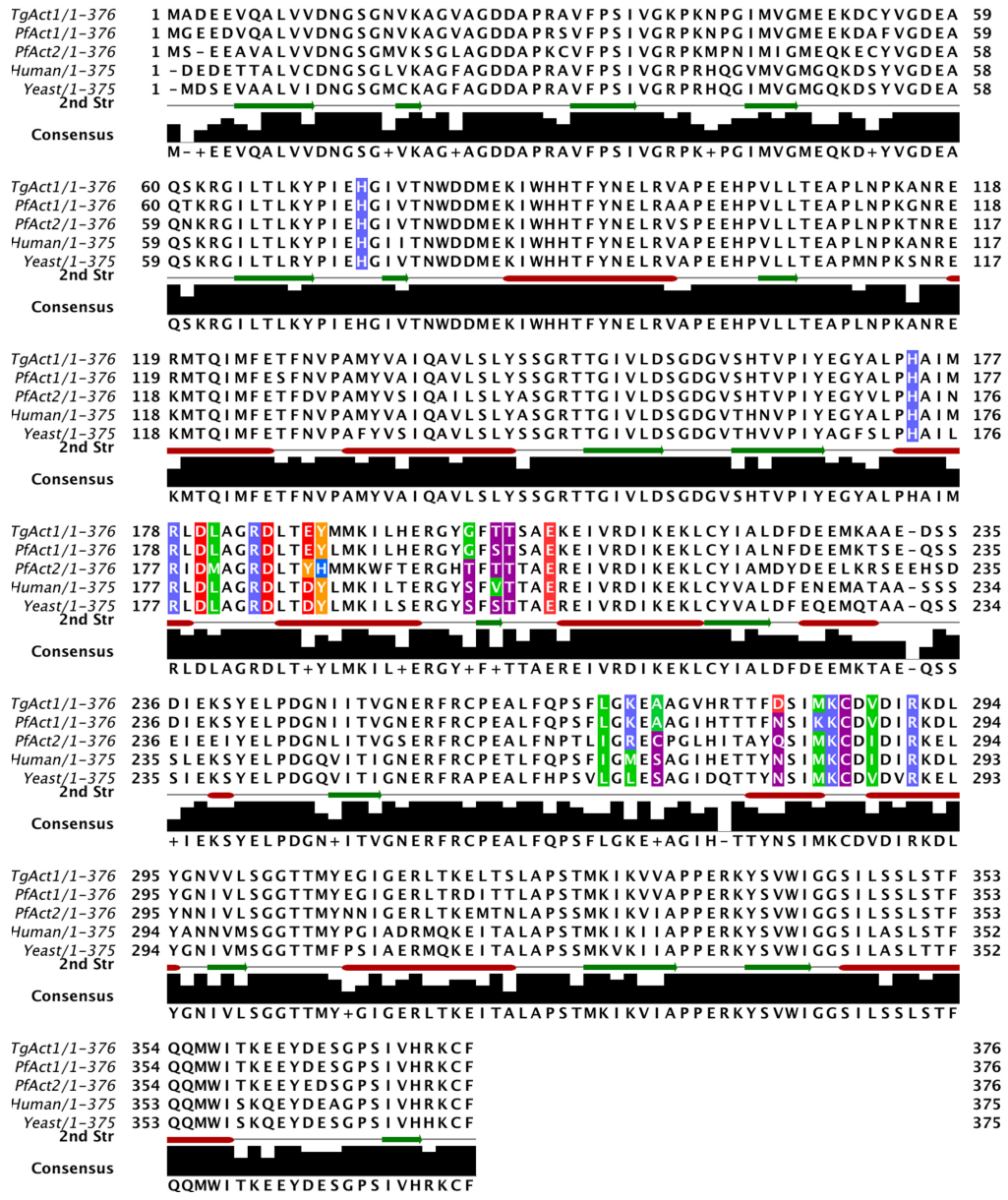

Figure 1. Sequence alignment for comparison of actins from *Homo sapiens* (muscle) (Human), *Saccharomyces cerevisiae (Yeast)*, *Toxoplasma gondii (TgACTI)*, *Plasmodium falciparum* (PfACTI or PfACTII). Residues that were mapped to within 4 Å of the phalloidin-binding site in muscle actin are highlighted. Color code: Blue – positive charged residues (including His), Red - negative charged, Green – hydrophobic, Purple – polar residues, Orange – aromatic.

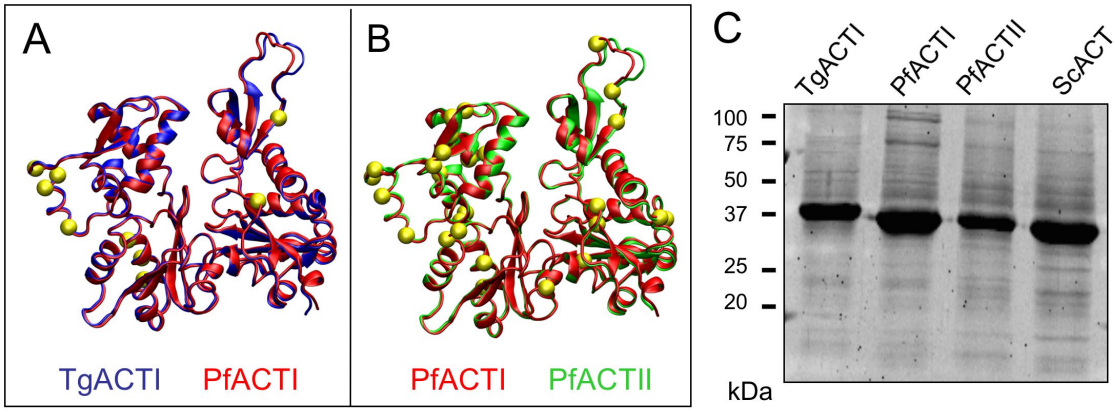

Figure 2. Comparison of TgACTI, PfACTI and PfACTII conservation of residues. (A) Model of TgACTI (blue) mapped onto PfACTI (red) highlighting amino acid differences (yellow). (B) Model of PfACTI (red) mapped onto PfACTII (green) highlighting amino acid differences (yellow). (C) Baculovirus-expressed, His_6-tagged actins were purified by Ni-chromatography, resolved using a 12% SDS-PAGE gel, and stained with Sypro Ruby (Lane 1: TgACTI, Lane 2: PfACTI, Lane 3: PfACTII, Lane 4: ScACT).

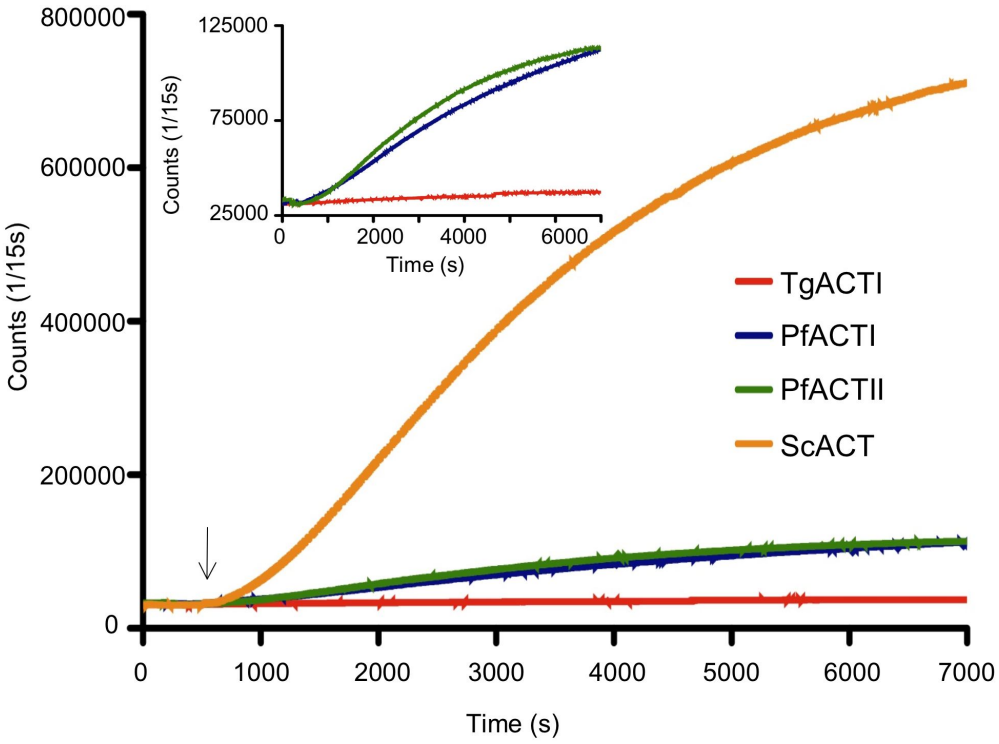

Figure 3. Comparison of actin polymerization kinetics.

Polymerization of 5 μM TgACTI (red), PfACTI (blue), PfACTII (green) or ScACT (orange) was induced by the addition of F buffer (arrow) and monitored by light scattering. Insert shows parasite actins on the expanded Y-axis.

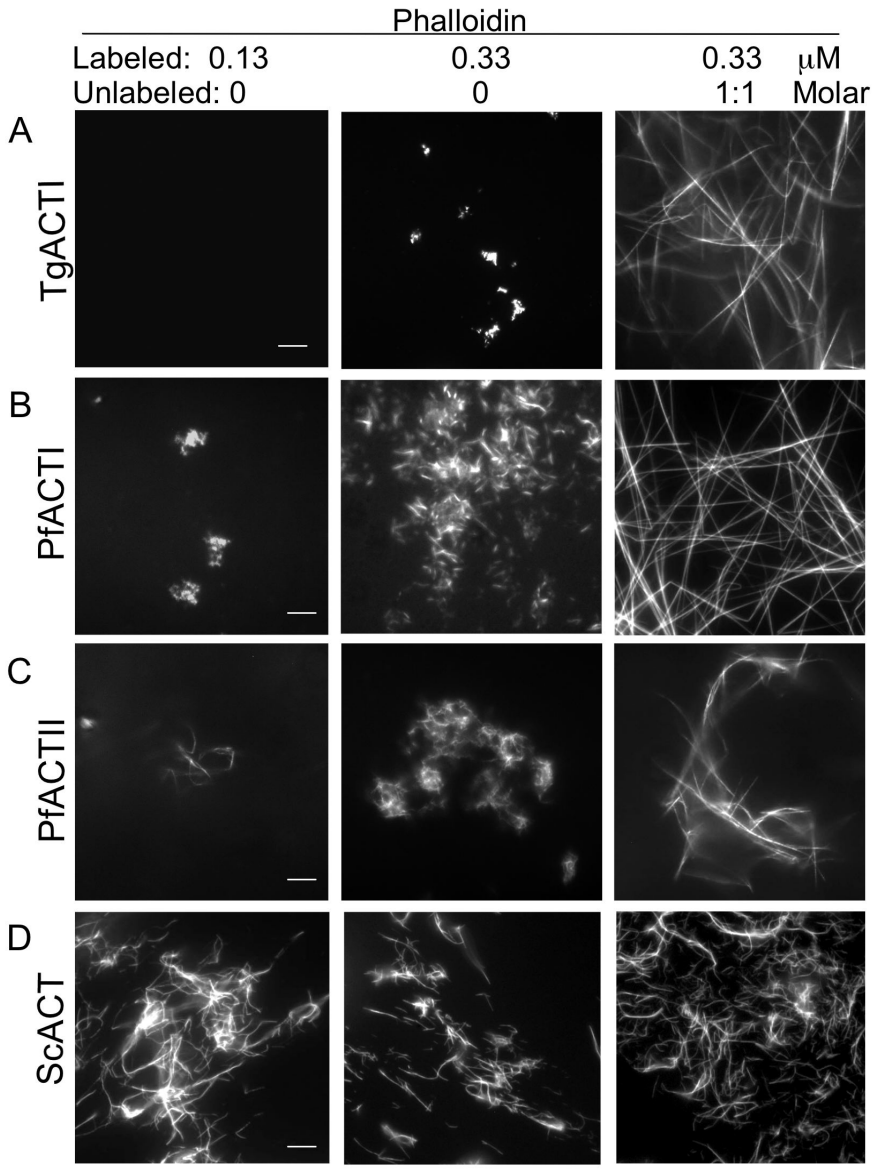

Figure 4. *In vitro* polymerization of parasite actins visualized by fluorescence microscopy of phalloidin stained actin.

(A) TgACTI, (B) PfACTI, (C) PfACTII or (D) ScACT were incubated at 5 μM with no addition (0) or with equimolar unlabeled phalloidin (1:1) and visualized by addition of low levels of Alexa-488 labeled phalloidin and visualized by fluorescence microscopy. Scale bars, 5 μm. Representative of three or more similar experiments.

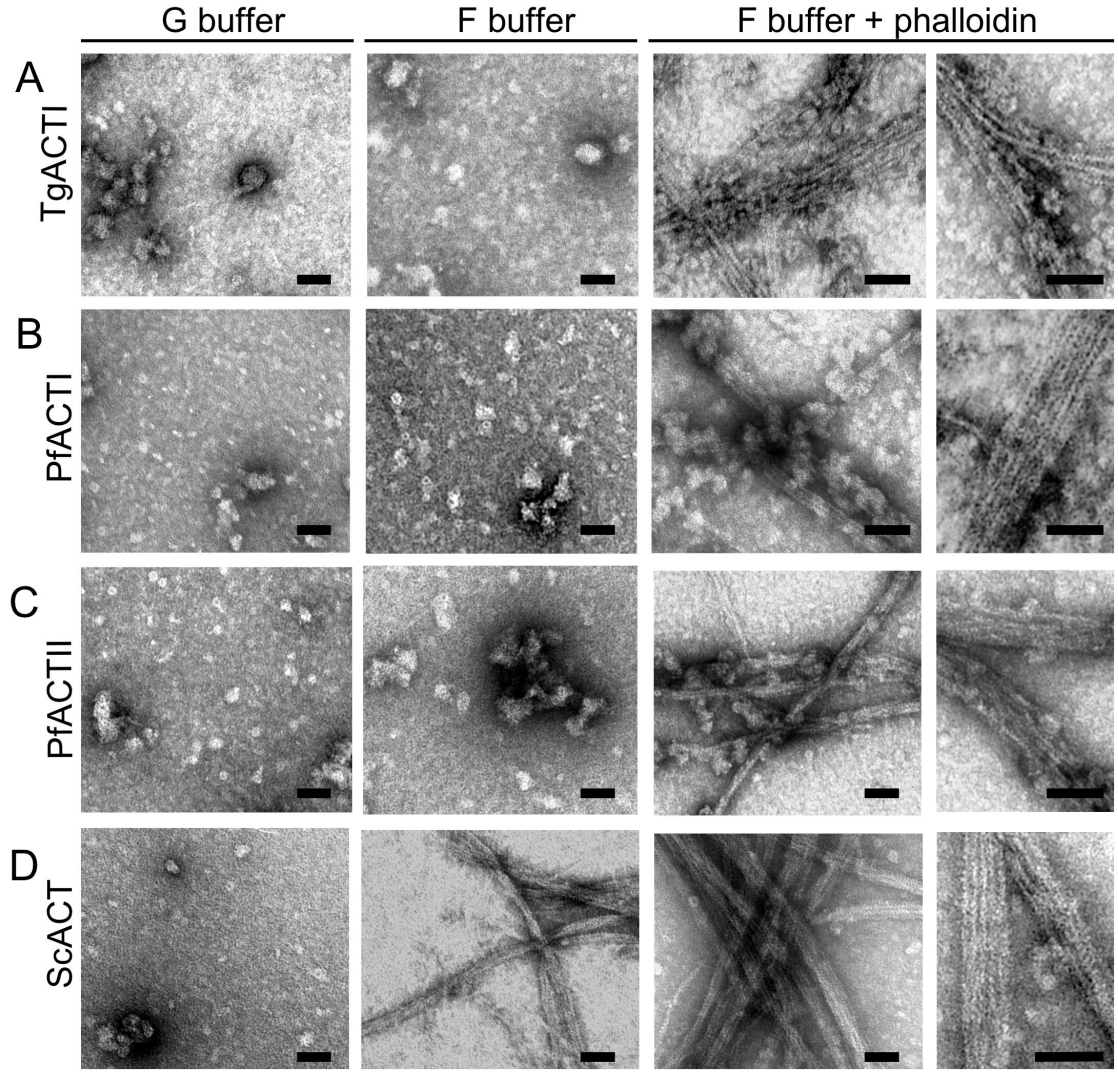

Figure 5. Ultrastructural features of parasite actins revealed by electron microscopy. (A) TgACTI was incubated in G buffer or F buffer with or without equimolar concentration of phalloidin for 1 h. The reactions were added to grids, negatively stained with uranyl acetate and examined by EM. Identical conditions were used to observe (B) PfACTI, (C) PfACTII, and (D) ScACT. Images are representative of 3 or more experiments. Scale bars, 50 nm.

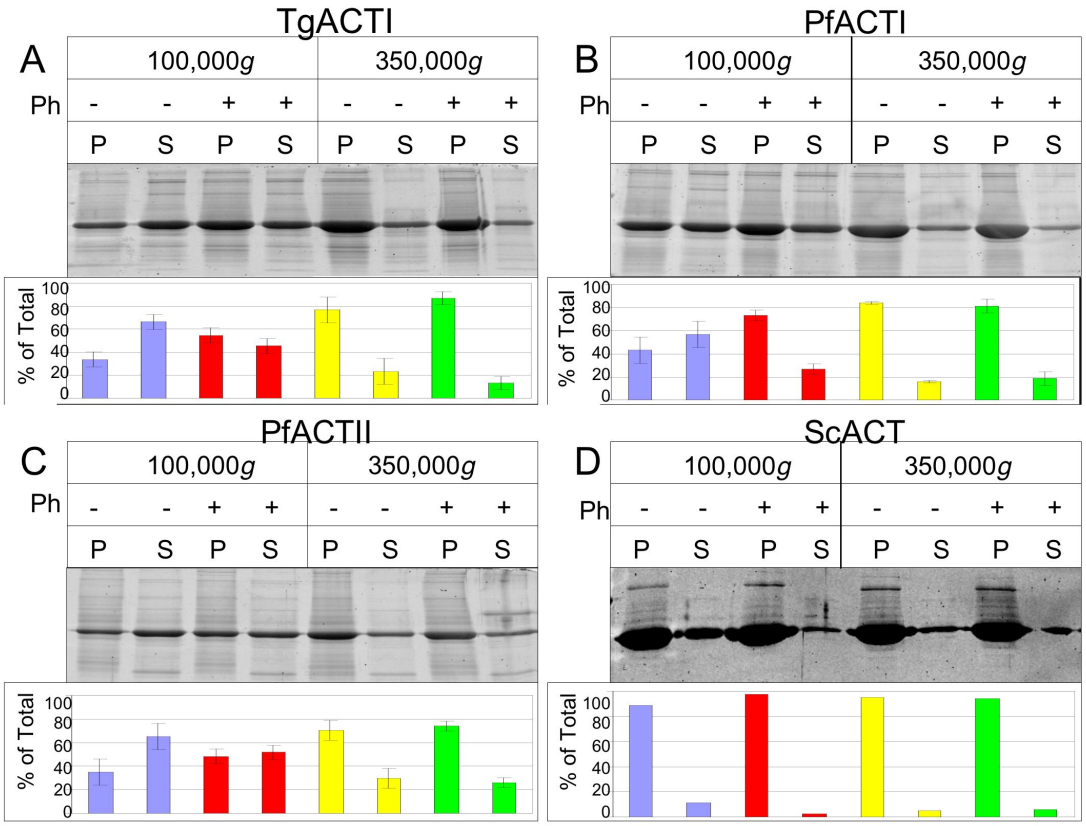

Figure 6. Sedimentation analysis of TgACTI, PfACTI, PfACTII and ScACT.

(A) TgACTI was polymerized in F buffer +/- equimolar phalloidin, centrifuged at 100,000g or 350,000g to pellet actin filaments formed during the incubation, and protein in the pellet or supernatants of all samples was resolved on a 12% SDS-PAGE gel, stained with SYPRO Ruby and quantified by phosphorimager analysis. (B) PfACTI, (C) PfACTII and (D) ScACT were tested under the same conditions as TgACTI. The percentages above represent averages of 3 or more experiments and the gel shown is representative.

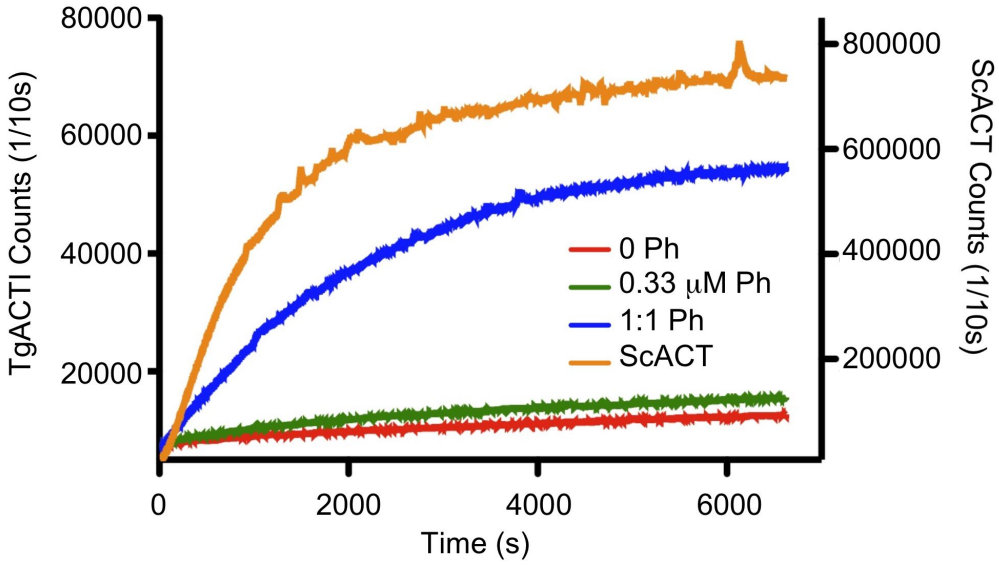

Figure 7. Effect of phalloidin on the extent of TgACTI polymerization.

Light scattering was conducted to determine the kinetics of polymerization of TgACTI in the presence and absence of phalloidin. TgACTI polymerization was induced by the addition of F buffer alone (red), 0.33 μM phalloidin (green) or equimolar phalloidin (blue) and the level of polymerization was then monitored by measuring changes in light scattering. ScACT polymerization was induced with F buffer as a control (orange).

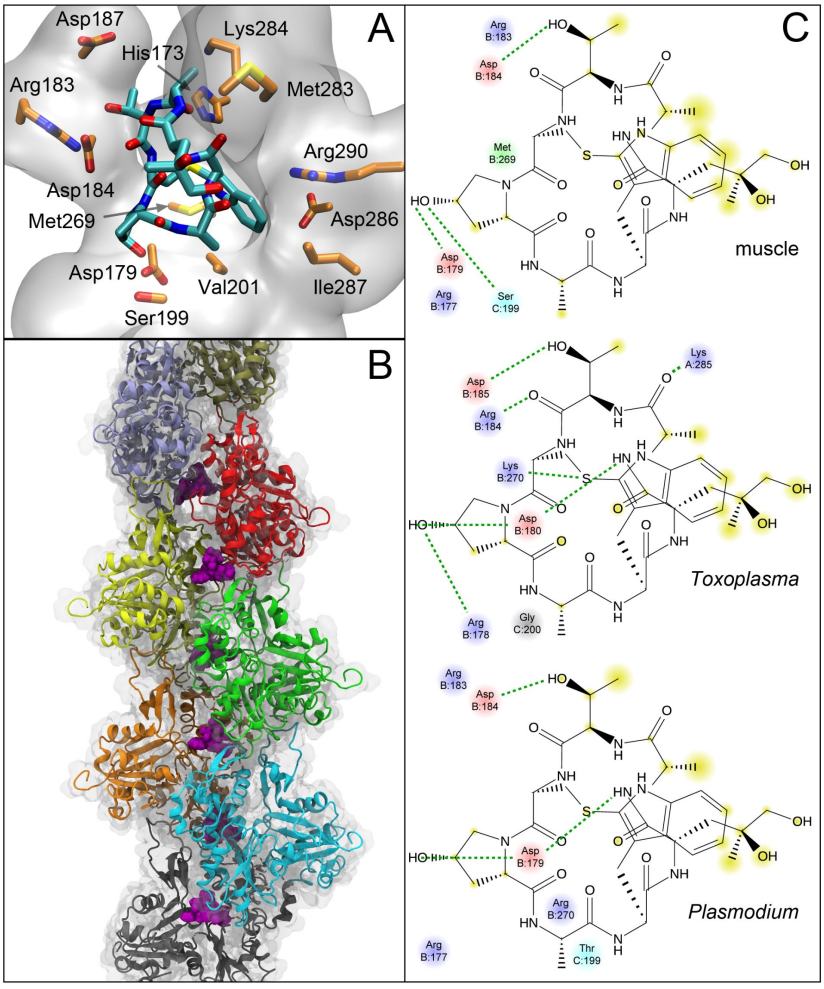

Figure 8. Predicted binding site of phalloidin in muscle and parasite actin filaments. (A) Molecular details of the interaction of phalloidin in the muscle actin filament. Side chains of amino acids within 3.5 Å are explicitly shown and the protein around phalloidin is depicted as a transparent surface. Hydrogens are omitted for clarity. (B) Position of phalloidin (purple) in the filament showing its interaction with three individual protomers. (C) 2D interaction diagrams showing the interaction differences between muscle, TgACTI and PfACTII. Hydrogen bonding interaction are depicted by dashed green lines and portions of the molecule that are solvent accessible are highlighted in yellow. Color code: blue - basic residues; red - acidic residues; cyan - polar residues.

Chapter III

Mutations that Increase Actin Filament Stability Disrupt Motility in *Toxoplasma gondii*

PREFACE

Work presented in this chapter was conducted by KMS. Molecular modeling to identify residues with potential to impact filament stability was performed by Karthik Diraviyam.

The first complete draft of this chapter was written by KMS. Comments from David Sibley, David Sept and Karthik Diraviyam were incorporated into the final version printed here.

Portions of this chapter (Figures 1-3; 6-7; 11) have been accepted for publication in PloS Pathogens:
Skillman KM, Diraviyam K, Khan A, Tang K, Sept D, Sibley LD. Evolutionarily Divergent, Unstable Filamentous Actin is Essential for Gliding Motility in Apicomplexan Parasites.

ABSTRACT

Apicomplexan parasites rely on a novel form of actin-based motility called gliding to migrate through their hosts and invade cells. This form of motility depends on parasite actin polymerization, however, parasite actins are divergent both in sequence and function and only form short, unstable filaments in contrast to the stability of conventional actins. The molecular basis for parasite actin filament instability and its relationship to gliding motility remain unresolved. Parasite actins contain several divergent residues that are predicted to impact filament length and stability. Two residues that differ from conventional actins were conserved in apicomplexan parasites that rely on gliding motility. Substitution of divergent residues found in *Toxoplasma gondii* actin (TgACTI) with those from mammalian actin resulted in formation of long filaments *in vitro*. Expression of these stabilized actins in *T. gondii* increased sensitivity to actin-stabilizing compounds and disrupted normal gliding motility in the absence of treatment. These results identify the molecular basis for short, dynamic filaments in apicomplexan parasites and demonstrate that inherent instability of parasite actin filaments is a critical adaptation for gliding motility.

INTRODUCTION

Actin is an essential protein that is highly conserved in sequence and function in eukaryotic cells. Despite this conservation, parasites within the phylum Apicomplexa encode divergent actins that remain largely in an unpolymerized state *in vivo* (Dobrowolski et al., 1997; Schmitz et al., 2005; Wetzel et al., 2003) and only form short, unstable filaments *in vitro* (Sahoo et al., 2006; Schüler et al., 2005), in contrast to conventional actins from yeast to mammals. Apicomplexan parasites are obligate intracellular protozoan pathogens of animals including humans. Apicomplexans move by a unique form of gliding motility that is dependent on polymerization of parasite actin filaments (Dobrowolski and Sibley, 1996). Gliding motility is considered to be a conserved feature of the phylum (Heintzelman, 2006) and has been described in *Toxoplasma gondii* tachyzoites (Håkansson et al., 1999), *Plasmodium* spp. sporozoites (Vanderberg, 1974), *Cryptosporidium* spp. sporozoites (Wetzel et al., 2005) and gregarines (King, 1981). Gliding motility powers migration through tissues, traversal of biological barriers, and invasion into and egress from host cells (Sibley, 2010).

T. gondii contains a single actin gene, TgACTI, which shows 83% amino acid identity with mammalian muscle actin (Dobrowolski et al., 1997). Parasite actins have been shown to exist mostly in an unpolymerized state, as defined by sedimentation at 100,000*g* and an absence of staining in fixed cells with fluorescently-labeled phalloidin (Schmitz et al., 2005; Wetzel et al., 2003). In contrast, the majority of actin in mammalian, yeast, and amoeba cells is found in long filaments, branched networks, or bundled fibers, which are readily stained with phalloidin and sedimented by centrifugation at 100,000*g* (Pollard et al., 2000). Although uncommon in apicomplexans,

when actin filaments have been visualized, they are short and unbranched, in keeping with the absence of Arp2/3 in these organisms (Gordon and Sibley, 2005). Actin filaments in *T. gondii* are only transiently detected beneath the parasite membrane during gliding motility, as visualized by freeze fracture electron microscopy (Wetzel et al., 2003). PfACTI from *P. falciparum* has been shown to form short filaments *in vitro* (Schüler et al., 2005), and similar short filaments of ~100 nm in length were detected in parasite lysates following sedimentation at 500,000*g* (Schmitz et al., 2005).

The annealing process of actin monomers into filaments has been described in vertebrate muscle actin as resulting from increased intermolecular contacts that cinch the filament into a tighter, more stable conformation (Schoenenberger et al., 2002). In contrast, *in vitro* polymerization of TgACTI results in formation of short, irregular filaments that rapidly disassemble in the absence of stabilizing compounds such as phalloidin (Sahoo et al., 2006). TgACTI fails to copolymerize with mammalian actin (Sahoo et al., 2006); however, copolymerization of PfACTI with rabbit muscle actin reveals differences in monomer stacking and a larger helical pitch in parasite actin (Schmitz et al., 2005). Consistent with this, previous modeling studies have suggested that instability of parasite actin filaments might arise from structural changes (Sahoo et al., 2006), although this hypothesis has not been directly tested.

Highly motile cells often exhibit rapid actin turnover (Pollard et al., 2000), suggesting that the unusual dynamics of apicomplexan actins may be important in gliding motility. Indirect evidence that actin turnover is important comes from treatment with agents that stabilize actin filaments, such as the heterocyclic compound jasplakinolide (JAS), which is produced by marine sponges and acts to stabilize actin filaments (Crews et al., 1986).

JAS treatment disrupts motility and cell invasion in *T. gondii* (Poupel and Tardieux, 1999; Wetzel et al., 2003), as well as invasion of merozoites (Mizuno et al., 2002), motility of ookinetes (Siden-Kiamos et al., 2006), and endocytic trafficking in trophozoites (Smythe et al., 2008) of *Plasmodium*. Collectively, previous studies indicate that apicomplexan actins spontaneously polymerize into short filaments that appear to be intrinsically unstable; however, the molecular basis and functional significance of these unusual properties are largely unknown.

The present study was undertaken to address two important questions: 1) what intrinsic properties govern actin filament instability in apicomplexans? and 2) are the unusual dynamic properties of filamentous actin important for efficient motility in apicomplexans? Here, we demonstrate that several divergent residues partially explain the inherent instability of parasite actin filaments and reveal that this feature is important for efficient gliding motility.

RESULTS

Divergent residues within apicomplexan actins may impact filament stability

T. gondii actin (TgACTI) and mammalian muscle actin have an 83% sequence identity, which is low for this highly conserved class of proteins. Molecular modeling and molecular dynamic simulations were used to identify residues that differ between human muscle actin and TgACTI in regions that are critical for stabilizing the actin filament. Divergent residues at positions G200 and K270 in *T. gondii* were identified as candidates that likely affect monomer-monomer interactions across the filament. However, the previously identified difference R277 in TgACTI, corresponding to glutamate in muscle (Sahoo et al., 2006), no longer made close contact in the new filament model, and consistent with this, no change in polymerization of substituted TgACTI-R277E was observed (data not shown). Instead, our refined model now points to S199 in human muscle actin as forming an important hydrogen bond with D179 of a monomer across the filament (Figure 1A). This hydrogen bonding was observed in a majority of inter-monomer contacts predicted in the molecular dynamic simulations of the filament. However, at this position TgACTI contains a glycine that would eliminate the hydrogen bond and potentially impact filament stability (Figure 1B). The second residue of interest identified was M269 in muscle actin (Figure 1A) that corresponds to K270 in TgACTI (Figure 1B). Mutational studies in yeast have previously demonstrated that loss of hydrophobicity in this loop leads to destabilization of the actin filament (Chen et al., 1993), and it has previously been suggested that this change may affect parasite actin stability (Sahoo et al., 2006). In comparing other actins to TgACTI, the alteration in G200 seen in *T. gondii* is conserved only in ACTI homologues found in a subset of

apicomplexans that rely on gliding motility (Figure 2). Noteably, PfACTII has a threonine at this position. In contrast, the substitution of K/R in the hydrophobic plug at residue 269/270 is seen in a wider variety of protozoa including dinoflagelates, ciliates, and apicomplexans (Figure 2).

TgACTI filament stability is restored by substitution with conventional residues

We tested the impact these residues have on TgACTI filament stability by substituting TgACTI residues with the corresponding amino acids from human muscle actin. The substituted proteins TgACTI-G200S (hydrogen bond substitution), TgACTI-K270M (hydrophobic loop substitution) and TgACTI-G200S/K270M (double substitution) were expressed using baculovirus and purified with Ni-affinity chromatography (Figure 3A). To examine the polymerization kinetics of the substituted TgACTI alleles, purified proteins were incubated in F buffer and light scattering was used to examine polymerization. Wild type TgACTI underwent only limited polymerization while the TgACTI-K270M substituted protein showed a modest enhancement (Figure 3B). However, TgACTI-G200S and TgACTI-G200S/K270M showed significantly increased polymerization, with both the rate (slope of the initial phase) and maximum extent being greater than wild type protein (Figure 3B).

The results of the light scattering assays were confirmed using fluorescent phalloidin staining and visualization via fluorescence microscopy. In all cases, filaments were visualized by addition of low levels of labeled phalloidin (0.33 mM) combined with different molar ratios of unlabeled phalloidin. As shown above, wild type actin (WT) required 1:20 molar ratio of unlabeled phalloidin to form clusters of short filaments and

long filaments only formed at a 1:1 molar ratio (Figure 3C, top panel). The TgACTI-K270M protein showed a slight enhancement in polymerization with small filaments appearing even in the absence of unlabeled phalloidin and reaching conventional lengths with addition of 1:5 molar ratio of unlabeled phalloidin (Figure 3C, second panel). Interestingly, the TgACTI-G200S substitution showed much more robust polymerization with short filaments being detected even with addition of only low levels of labeled phalloidin (0.33 mM) and conventional length filaments appearing with addition of 1:20 molar ratio of unlabeled phalloidin (Figure 3C, third panel). TgACTI-G200S/K270M also formed longer filaments than seen with wild type TgACTI, similar to the TgACTI-G200S single mutant (Figure 3C, bottom panel). Taken together, these results show that TgACTI filaments may be less capable of polymerizing due to the presence of only a few differences from conventional actins and that mutations designed to mimic mammalian actin in TgACTI result in formation of more stable actin filaments *in vitro*.

The G200 and K270 substitutions have previously been mapped to the phalloidin-binding pocket in TgACTI, therefore, we looked into the influence of phalloidin-binding on polymerization. Light scattering was used to determine if polymerization of the mutants alone differed from that in the presence of low levels of phalloidin (corresponding to the concentration used for filament visualization in the phalloidin microscopy assays). This level of phalloidin had no influence on the ability of TgACTI to polymerize but did show a slight enhancement of polymerization of TgACTI-K270M and a large enhancement for the polymerization of TgACTI-G200S and TgACTI-G200S/K270M (Figure 4).

Due to the positive effect the tested TgACTI substitutions had on polymerization, we wanted to determine if the converse substitutions would adversely effect yeast actin (ScACT) polymerization. S199G, L269K and S199G/L270K substitutions were made in ScACT and expressed in bacuolovirus to obtain recombinant protein. ScACT-S199G was first compared to wild type ScACT using light scattering and polymerization was unchanged by the substitution (Figure 5A). Polymerization of S199G was then compared to polymerization of L269K and S199G/L269K. All three actins polymerized to roughly the same extent, demonstrating the TgACTI-like substitutions did not impede the robustness of ScACT polymerization (Figure 5B).

Expression of Stabilized TgACTI in *T. gondii*

To examine the effect of expressing stabilized mutants of TgACTI in *T. gondii*, we generated transgenic parasites expressing a second copy of TgACTI fused to an N-terminal degradation domain (DD), which allows regulated expression in the presence of Shield-1 (Herm-Gotz et al., 2007). This approach was chosen over allelic replacement, since we reasoned that the mutant alleles might be detrimental, hence compromising attempts to evaluate their functions. The regulated nature of the DD-stabilized proteins also allows the timing of expression to be controlled, thus minimizing the chance for pleomorphic downstream effects or compensatory changes that can occur using conventional dominant negative strategies. Transgenic lines expressing the DD-fusion proteins were tested for regulated expression by Western blot using an antibody against TgACTI (Figure 6A) and by immunofluorescence detection of the c-myc tag (Figure 6B). The level of DD-tagged actins was approximately 50% of wild type actin and the patterns

of staining was diffuse in the cytosol, similar to the pattern for endogenous actin described previously (Dobrowolski et al., 1997).

The impact of expressing DD-TgACTI fusions on the life cycle of the parasite was tested using a plaque assay, which monitors the normal intracellular growth cycle (Figure 6C). Although parasites expressing DD-G200S or DD-G200S/K270M formed plaques comparable to the controls in the absence of Shield-1, plaque formation was almost non-existent when parasites were treated with Shield-1 (Figure 6C), demonstrating that expression of stabilized TgACTI disrupts the parasite life cycle. In contrast, expression of the wild type DD-TgACTI (DD-wild type) had no effect on plaque formation either in the absence or presence of Shield-1 (Figure 6C).

Following growth in Shield-1, parasites expressing DD-TgACT1 fusion proteins revealed a diffuse pattern of actin staining with some discrete puncta (Figure 7A; data not shown). The absence of detectable long filaments in cells expressing mutant stabilized actins suggest that they behave somewhat differently *in vivo* than *in vitro*, perhaps as a result of other proteins that regulate actin turnover. Actin dynamics are highly sensitive to actin-stabilizing compounds like JAS, which permeates cells stabilizes actin filaments (Bubb et al., 1994). Hence, we examined the distribution of actins in parasites expressing DD-TgACTI alleles following treatment with low levels of JAS. Remarkably, filamentous actin structures were revealed emanating from both the apical and posterior poles in parasites expressing the stabilized TgACTI mutants grown in the presence of Shield-1, whereas staining of wild type DD-TgACTI relocalized to the poles without forming visible filaments (Figure 7A). The actin filaments seen in parasites expressing stabilized mutants of TgACTI formed spiral patterns beneath the surface of the parasite,

as visualized in sequential slices of a z-series (Figure 7B).

To determine if the stabilized DD-TgACTI alleles polymerized more readily *in vivo*, we examined the proportion of globular and filamentous actin based on sedimentation at 350,000*g*, conditions previously found to be necessary to pellet short filaments that form in parasites (Schmitz et al., 2005). Although no change in sedimented actin was detected in control lysates, treatment with low levels of JAS induced much greater polymerization of the DD-G200S and DD-G200S/K270M mutants compared to DD-wild type (Figure 7C). Collectively, these studies demonstrate that stabilized forms of TgACTI were more sensitive to JAS-induced polymerization *in vivo*.

Consistent with previous reports (Shaw and Tilney, 1999; Wetzel et al., 2003), actin relocalized to the poles in parasites treated with higher concentrations of JAS, leading to characteristic apical projections (Figure 8A; Figure 9). JAS-induced actin polymerization was also accentuated in parasites expressing stabilized TgACTI alleles, however, treatment resulted in actin-rich projections from both ends of the parasite (Figure 8A; Figure 9C). Quantitation of parasites stained with anti-TgACTI revealed that while double protrusions are rarely seen in control parasites, there was a significant increase in the number of double protrusions seen in the parasites expressing the more stable TgACTI alleles (Figure 8B). Further examination of these projections by electron microscopy revealed electron dense filament structures within the projections from the apical end of control parasites (Figure 9A,B) that resemble actin protrusions reported previously (Shaw and Tilney, 1999). Additionally the posterior extensions also contained tightly clustered bundles of filaments protruding through the base of the cell where the inner membrane complex was interrupted (Figure 9C-F). These results are consistent with the idea that the mutant actin alleles are hypersensitive to jasplakinolide. Additionally, to determine if phenotypic changes could be observed in the absence of jasplakinolide, parasites expressing DD-wildtype, DD-G200S and DD-G200S/K270M,

but untreated with JAS, were subjected to EM. Interestingly, small blebs were visualized projecting from the apical end of the DD-G200S and DD-G200S/K270M parasites but not DD-wildtype parasites (Figure 10). These blebs appear to contain electron dense material although the nature of this material has not been determined (Figure 10).

Toxoplasma expressing stabilized actin undergo aberrant gliding motility

To examine the impact of stabilized TgACTI alleles on parasite motility, we employed video microscopy to analyze the typical circular and helical motions that are characteristic of gliding, as described previously (Håkansson et al., 1999). In contrast to DD-wild type expressing parasites that underwent normal circular gliding (Figure 11A), a large percentage of the circular movements in parasites expressing DD-G200S and DD-G200S/K270M actins were aberrant (Figures 11B, 11C). For example, DD-G200S and DD-G200S/K270M expressing parasites often stalled, were unable to complete circles, or went off-track during gliding (Figures 11B, 11C).

Quantification of these results indicated that expression of the DD-wild type allele resulted in a higher frequency of circular gliding than helical, relative to untransfected parasites, however these movements were largely normal (Figure 11D). Although parasites expressing DD-G200S and DD-G200S/K270M underwent wild type motility in the absence of Shield-1, significantly more cells exhibited aberrant forms of gliding motility in the presence of Shield-1 (Figure 11D). Comparison of the radii of tracks made by DD- wild type and DD-G200S and DD-G200S/K270M expressing parasites, revealed that parasites expressing these mutant actins traced out partial arcs that were significantly larger than circular tracks formed by wild type parasites (Figure 11E). Collectively, these results indicate that expression of the mutant DD-G200S and DD-G200S/K270M forms

of TgACTI disrupts normal circular gliding motility. Consistent with previous descriptions of normal helical motility (Håkansson et al., 1999), DD-wild type expressing parasites underwent helical gliding at a relatively fast rate and moved through numerous corkscrew motions, noted in the example shown (Figure 11A). In contrast, DD-G200S and DD-G200S/K270M expressing parasites were delayed in their movements and went through fewer flips and turns (Figures 11B, 11C). Parasites expressing the stabilized TgACTI alleles were significantly slower in both helical and circular gliding compared to the untransfected or DD-wild type parasites (Table 1). Taken together, these findings reveal that expression of stabilized mutants of TgACTI significantly disrupts gliding motility in *T. gondii*.

DISCUSSION

Our studies are in agreement with previous work on the polymerization properties of parasite actins and extend these findings by examining the molecular basis for instability of actin filaments. TgACTI filaments form upon initiation of gliding motility but a stable pool of filamentous actin does not exist within the parasite (Dobrowolski et al., 1997; Wetzel et al., 2005), suggesting TgACTI is unstable. The findings from the current studies demonstrate that the instability of parasite actin filaments is an inherent property that results in part from differences in monomer-monomer interactions that normally stabilize the filament. The inefficient polymerization of TgACTI was rescued *in vitro* by reversion of several key residues in *T. gondii* actin to match those predicted to stabilize mammalian muscle actin. Furthermore, *in vivo* expression of these stabilized actins led to disruption of gliding in *T. gondii*. These findings provide insight into the molecular basis of parasite actin filament dynamics and reveal formation of short, highly dynamic actin filaments is an important adaptation for parasite motility.

Molecular modeling predicts that actin filaments are stabilized by interactions across the width (inter-strand) of the filament through two key regions including the "hydrophobic plug" encompassing residues 265-270 and a helix from residues 191-199 (Fujii et al., 2010; Oda et al., 2009). Our studies suggest that relatively few changes in these critical regions account for the instability of parasite actin filaments. Among these alterations, a change in the hydrophobic plug (*i.e.* K270 in *T. gondii*) plays a modest role while an alteration in the helix (*i.e.* G200) has a larger affect on filament stability. The substitution of K270M in TgACTI resulted in filaments that were detected by fluorescent staining at low concentrations of phalloidin, although this change had less effect on actin

polymerization as monitored by light scattering assays in the absence of phalloidin. As this residue lies within the phalloidin pocket, it suggests that hydrophobic residues here result in enhanced phalloidin binding. Light scattering experiments demonstrate a slight increase in the polymerization kinetics of TgACTI-K270M in presence of low levels of phalloidin compared to the kinetics in its absence whereas the polymerization of wild type TgACTI is unaffected by addition of this level of phalloidin. Mutations designed to reduce hydrophobicity in the corresponding residue in yeast actin (*i.e.* L269) have no affect on polymerization, while those at the other end of the hydrophobic plug are much more severe (Kuang and Rubenstein, 1997). Hence, these results indicate that K270 contributes to naturally low phalloidin binding of parasite actins, while it likely plays a lesser role in intrinsic filament instability.

Modeling predictions also indicate that S199 in muscle actin plays a role in intra-filament stabilization via a hydrogen bond network with R177 and D179. Consistent with this, fluorescence microscopy revealed formation of longer, more stable filaments when the G200S substitution was present in TgACTI. When low levels of phalloidin were added to protein and monitored by light scattering, a large increase in polymerization was observed. Because of cooperativity in binding of phalloidin to actin, it is difficult to differentiate whether this larger increase is due to an influence of the mutation on the ability to bind phalloidin or the fact that these filaments are longer and therefore contain more phalloidin binding sites, leading to the further enhancement of polymerization. Regardless, mutation of G200S had a larger impact on the *in vitro* polymerization of TgACTI as shown by increased light scattering, even in the absence of phalloidin. Collectively, the absence of these two stabilizing interactions in TgACTI

partially explains the inherent instability of parasite actin filaments.

Filament instability is evidently an important adaptation since expression of stabilized TgACTI within the parasite had a detrimental effect on gliding motility. Consistent with this, previous studies using actin stabilizing agents have revealed that increased polymerization of TgACTI filaments adversely effects motility and host cell invasion (Poupel and Tardieux, 1999; Shaw and Tilney, 1999; Wetzel et al., 2003). In the present study, stabilized mutants of TgACTI were more sensitive than wild type to JAS, as shown by formation of spiral actin filaments and increased sedimentation at 350,000g. The spiral patterns seen here are similar to those reported previously from wild type *T. gondii* treated with high levels of JAS (Wetzel et al., 2003); however, notably here they occur with low levels of JAS and are only seen in parasites expressing stabilized TgACTI forms. Unexpectedly, with higher levels of JAS treatment, they also formed actin filament bundles at the posterior ends of the cell that protruded through posterior cap that closes off the end of the inner membrane, a structure that forms as the last step in cell division (Anderson-White et al., 2010). Even without addition of jasplakinolide, changes in the integrity of the parasite membrane where electron dense material is protruding from the parasite were seen using EM of parasites expressing the stabilized DD-TgACTI alleles.

Stabilized DD-TgACTI mutants also had a significant effect on disrupting normal motility in the absence of treatment, revealing that this phenotype is not simply due to enhanced binding to JAS or phalloidin. Intriguingly, parasites expressing stabilized actins formed circles with larger radii, moved more slowly, and stalled in the process of gliding. This suggests that short, highly dynamic actin filaments are required for parasites to

complete the tight arcs and corkscrew turns that are characteristic for circular and helical gliding (Håkansson et al., 1999) (Figure 12A).

The current model for gliding motility predicts that short, highly dynamic actin filaments attached to transmembrane adhesive proteins are translocated along the surface of the parasite by a small myosin (Frenal and Soldati-Favre, 2009). The myosin motor, which is anchored in the inner membrane complex (Gaskins et al., 2004), is also highly nonprocessive (Herm-Gotz et al., 2002), meaning it does not stay attached to a single filament for long periods. Instead, this model predicts that short actin filaments, tethered to transmembrane adhesins, are passed sequentially between motor complexes that operate independently. Consistent with this model, where actin filaments have been seen in parasites, they are quite short (*i.e.* 50-100 nm) (Sahoo et al., 2006; Schmitz et al., 2005). Actin in apicomplexans may be adapted for rapid turnover of short filaments, since long filaments would increase the likelihood of multiple motors being engaged simultaneously, potentially leading to conflicting forces on the same filament. Although we were not able to discern distinct filaments in parasites expressing DD-TgACTI proteins, the observed punctate staining pattern may reflect clusters of short filaments that are below the resolving power of the light miscroscope (in theory ~200 nm, but in practice likely ~400 nm). Nonetheless, we would predict based on their *in vitro* properties that the G200S and G200S/K270M mutants would form more stable filaments, which could inhibit motility by reducing free monomers needed for new filament assembly, or by physically disrupting productive motor-actin filament complexes (Figure 12B). Alternatively, stabilized DD-TgACTI mutants could affect interactions with actin-binding proteins *in vivo*, including those involved in polymerization or depolymerization

(Figure 12C). Although apicomplexans lack an Arp2/3 complex (Gordon and Sibley, 2005), they express several formins that act to increase actin polymerization (Baum et al., 2008; Daher et al., 2010) and actin depolymerization factor (ADF), which acts primarily to sequester monomers and prevent polymerization (Mehta and Sibley, 2011). Regardless of the exact mechanism, our results indicate that even subtle changes in actin filament stability significantly affect function, underscoring the importance of rapid actin dynamics in apicomplexans.

In comparing apicomplexans to other organisms, the alteration in G200 is conserved only in ACTI homologues found in a subset of parasites that rely on gliding motility. In contrast, the substitution of K/R in the hydrophobic plug at residue 269/270 is seen in a wider variety of protozoa including dinoflagelates, ciliates, and apicomplexans. Consistent with this, diverse actins from protozoans *Leishmania* (Kapoor et al., 2008), *Giardia* (Paredez et al., 2011), and *Tetrahymena* (Hirono et al., 1989) have also been reported not to bind well to phalloidin and display unusual polymerization kinetics or novel actin structures. This pattern further suggests that stable actin filaments are a more recent evolutionary development, found in amoeba, yeast, plants and animals, but not shared by many protozoans. These differences likely reflect adaptations for stable *vs*. dynamic actin cytoskeletons that are designed for very different life strategies. The importance of such adaptations is shown by introduction of stabilizing residues in TgACTI, changes that were sufficient to dramatically slow the speed of gliding and result in aberrant forms of motility.

Collectively, these findings demonstrate that actin filament instability and rapid turnover are important adaptations for productive gliding in apicomplexans, and suggest

that small molecules designed to selectively stabilize parasite actins may have potential for preventing infection.

MATERIALS AND METHODS

Plasmid constructions and transfection

Recombinant *Toxoplasma* actins were expressed in baculovirus, as previously described (Sahoo et al., 2006). Recombinant viruses for mutant TgACTI alleles and were created via site-directed mutagenesis using wild type TgACTI as a template and allele-specific primers. For TgACTI-K270M primers 5'-AGCCCTCCTTCTTGGGCATGGAGGCTG CAGGTGTCCA-3' (forward) and 5'-TGGACACCTGCAGCCTCCATGCCCAAGAA GGAGGGCT-3' (reverse) were used to amplify from the wild type TgACTI template. For TgACTI-G200S and TgACTI-G200S/K270M (using K270M as template) primers 5'-CTCCACGAGAGAGGATACTCCTTCACCACCTCCGCCGAG-3' (forward) and 5'-CTCGGCGGAGGTGGTGAAGGAGTATCCTCTCTCGTGGAG-3' (reverse) were used. The resulting products were cloned into the viral transfer vector pAcHLT-C (BD Biosciences Pharmingen). Recombinant viruses were obtained by cotransfection with linearized baculogold genomic DNA into Sf9 insect cells (BD Biosciences Pharmingen), according to manufacturer's instructions.

Actin structure for molecular modeling

An atomic model of phalloidin was derived from the solid state structure of a synthetic derivative (Zanotti et al., 2001), modified to contain dihydroxy-Leu7 using Maestro (Schrödinger LLC,) and energy minimized using MacroModel (Schrödinger LLC,) with a MMFF94s forcefield. The model was further optimized in continuum solvent using Jaguar (Schrödinger LLC), with DFT level of theory using a hybrid B3LYP functional and 6-31G** basis set. The actin filament model based on X-ray fiber diffraction data (Oda et al., 2009) was used to create an 8-monomer filament of muscle F-actin. A 50 ns molecular dynamics (MD) simulation in explicit water was carried out using NAMD

(Kale et al., 1999) in an NPT ensemble with a pressure of 1 atm and a temperature of 300 K with explicit TIP3P water. CHARMM27 forcefield was used with a 10 Å cut off for van der Waals with a 8.5 Å switching distance, and Particle Mesh Ewald for long-range electrostatics. Bonded hydrogens were kept rigid to allow 2 fs time steps. A simulated annealed structure of muscle filament model with phalloidin in the binding site was used as the template for building parasitic actin filament homology models using Modeller (Martí-Renom et al., 2000).

Actin expression and purification

Hi5 insect cells were maintained as suspension cultures in Express-Five SFM media (Invitrogen). Hi5 cells were harvested at 2.5 days postinfection with recombinant virus and lysed in BD BaculoGold Insect Cell Lysis Buffer (BD Biosciences Pharmingen) supplemented with 5 mM $CaCl_2$, 5 mM ATP, 5 mM NaN_3, and protease inhibitor cocktail (E64, 1 μg ml^{-1} AEBSB, 10 μg ml^{-1}; TLCK, 10 μg ml^{-1}; leupeptin, 1μg ml^{-1}). His-tagged actins were purified using Ni-NTA agarose (Invitrogen). After binding for 2 h, the column was washed sequentially with G actin buffer without DTT (G-DTT buffer) (5 mM Tris-Cl, pH 8.0, 0.2 mM $CaCl_2$, 0.2 mM ATP), then G-DTT buffer with 10 mM imidazole, G-DTT buffer with 0.5 M NaCl, G-DTT buffer with 0.5 M KCl buffer, and finally G-DTT buffer with 25 mM imidazole. Proteins were eluted with serial washes of G-DTT buffer containing 50 mM, 100 mM, and 200 mM imidazole, pooled together and dialyzed overnight in G-actin buffer containing 0.5 mM DTT with 100 μM sucrose. Purified recombinant actins were clarified by centrifugation at 100,000*g*, 4°C, for 30 min using a TL100 rotor and a Beckman Optima TL ultracentrifuge (Becton Coulter) to remove aggregates. Purified proteins were resolved on 12% SDS-PAGE gels followed

by SYPRO Ruby (Molecular Probes) staining, visualized using a FLA-5000 phosphorimager (Fuji Film Medical Systems), and quantified using Image Gauge v4.23. Purified actins were stored at 4°C and used within 2-3 days.

Light scattering

Purified recombinant actins were clarified as described above and incubated (5 μM) in G buffer containing 1 mM EGTA and 50 μM $MgCl_2$ for 10 min (to replace bound Ca^{2+} with Mg^{2+}). Samples were placed in a microcuvette (Starna Cells) and following addition of $1/10^{th}$ volume of F-buffer, light scattering was monitored with the PTI Quantmaster spectrofluorometer (Photon Technology International) with excitation 310 nm (1 nm bandpass) and emission 310 nm (1 nm bandpass). When examining the influence of phalloidin, 0.33 μM phalloidin was added at the time of F-buffer addition.

Fluorescence microscopy of actin filaments

Purified recombinant actins were clarified by as described above and incubated (5 mM) in F-buffer (50 mM KCl, 2 mM $MgCl_2$, 1 mM ATP), and treated with different molar ratios of unlabeled phalloidin to actin from 0:1 to 1:1 (Molecular Probes). In addition, final concentrations of 0.13 mM or 0.33 mM Alexa-488 phalloidin (Molecular Probes) were added to each sample to visualize filaments. Following polymerization for 1 h, samples were placed on a slide and viewed with a Zeiss Axioskop (Carl Zeiss) microscope using 63X Plan-NeoFluar oil immersion lens (1.30 NA). Images were collected using a Zeiss Axiocam with Axiovision v3.1 and processed using linear adjustments in Adobe Photoshop v8.0.

Conditional expression system

TgACTI alleles were amplified by PCR inserted into a modified vector pTUB-DD-myc-YFP-CAT-Pst1 (Herm-Gotz et al., 2007) at unique Pst1-AvrII sites to generate DD-TgACTI fusions using primers 5'-GCGCCTAGGATGGCGGATGAAGAAGTGCAA-3' (forward) 5'-CTAGTCTGCAGTTAGAAGCACTTGCGGTGGA-3' (reverse). The resulting plasmids were transfected into tachyzoites of the RH strain of *Toxoplasma* and parasites were single celled cloned on monolayers of HFF cells and propagated as previously described (Morisaki et al., 1995).

Immunofluorescence microscopy

For intracellular staining, parasites were allowed to invade HFF monolayers on glass coverslips for 24 h in the presence or absence of 4 μM Shield-1. The coverslips were then fixed with 4% formaldehyde and stained with mouse anti-c-myc (Zymed) to detect the DD-fusion proteins followed by goat anti-mouse IgG conjugated to AlexaFluor488 (Molecular Probes) and mAB DG52 (anti-TgSAG1) directly conjugated to AlexaFluor 594 to detect the parasite. For actin staining, parasites were treated ± 0.25μM JAS (Invitrogen) for 15 min and allowed to glide for 15 min on glass coverslips coated with 50 μg ml^{-1} BSA. Coverslips were fixed and stained with mouse anti-c-myc (Zymed) followed by goat anti-mouse IgG conjugated to AlexaFlour 488 and mAb DG52 labeled with AlexaFlour 594. For projection staining, parasites were treated ± 2.5μM JAS (Invitrogen) for 15 min and allowed to glide for 15 min on glass coverslips coated with 50 μg ml^{-1} BSA. Coverslips were fixed and stained with rabbit anti-TgACTI (Sahoo et al., 2006) followed by goat anti-rabbit IgG conjugated to AlexaFlour 488 and mAb DG52

labeled with AlexaFlour 594. Coverslips were mounted in Pro-Long Gold anti-fade reagent (Invitrogen) and viewed with a Zeiss Axioskop (Carl Zeiss) microscope using 63X Plan-NeoFluar oil immersion lens (1.30 NA). Images were collected using a Zeiss Axiocam and deconvolved using a nearest neighbor algorithm in Axiovision v3.1. Images were processed using linear adjustments in Adobe Photoshop v8.0.

Plaque assay

Plaque assays were conducted by adding 300 purified parasites to HFF monolayers in 6-well dishes containing medium + DMSO or medium +3 μM Shield-1 in DMSO and incubated at 37°C with 5% CO_2 for 7 days. Plates were then fixed with 70% ethanol and stained with 0.01% crystal violet to visualize plaques.

Actin sedimentation analysis

Parasite strains expressing DD-tagged actins were treated ± 0.5 μM JAS for 30 min, lysed with Triton-X-100 for 1 h, centrifuged at 1,000*g*, 4°C for 2 min and supernatants centrifuged at 350,000*g*, 4°C for 1 h using a TL100 rotor and a Beckman Optima TL ultracentrifuge (Becton Coulter). Supernatant proteins were acetone precipitated and washed with 70% ethanol. All pellets were resuspended in 1X sample buffer, resolved on a 12% SDS-PAGE gels, Western blotted with anti-TgACTI antibody, visualized using a FLA-5000 phosphorimager (Fuji Film Medical Systems), and quantified using Image Gauge v4.23.

Electron microscopy

For examination of JAS-induced actin projections, parasites were grown in the presence of Shield-1 for 40 h, harvested and treated with 2.5 μM JAS for 15 min, and fixed in 2% paraformaldehyde/2.5% glutaraldehyde (Polysciences Inc) in 100 mM phosphate buffer, pH 7.2 for 1 hr at room temperature. Samples were washed in phosphate buffer and postfixed in 1% osmium tetroxide (Polysciences Inc) for 1 h. Following extensive washing in dH20, samples were en bloc stained with 1% aqueous uranyl acetate (Ted Pella Inc) for 1 h. Samples were then dehydrated in a graded series of ethanol and embedded in Eponate 12 resin (Ted Pella Inc). Sections of 95 nm were cut with a Leica Ultracut UCT ultramicrotome (Leica Microsystems Inc), stained with uranyl acetate and lead citrate. Samples were viewed and photographed on a JEOL 1200 EX transmission electron microscope (JEOL USA) and images adjusted linearly using Adobe Photoshop v8.0. The same procedure but without JAS treatment was used to analyze membrane blebs.

Video microscopy

Parasite gliding was monitored by video microscopy as previously described (Håkansson et al., 1999). Parasites were treated with DMSO or 4 μM Shield-1 for 40 h, resuspended in Ringer's solution and allowed to glide on uncoated glass coverslips. Images were captured with 50 - 100 ms exposure times at 1 sec intervals, combined into composites with Openlab v4.1 (Improvision), analyzed using ImageJ and saved as QuickTime movies. Cell motility was tracked using the ParticleTracker plug-in to evaluate average speeds from a 3-15 tracks. The percentage of parasites undergoing different forms of motility was quantified from 4 separate movies containing 10-40 motile parasites each

using Cell Counter, as described (Lourido et al., 2010). Radii of circular patterns were measured using the measurement feature of Axiovision software (Zeiss).

Statistical Analysis

Statistics were calculated in Excel or Prism (Graph Pad) using unpaired, two-tailed Student's *t*-tests for normally distributed data with equal variances, and two-tailed Mann-Whitney analysis for analysis of samples with small samples sizes of unknown distribution. Significant differences were defined as $P \leq 0.05$.

ACKNOWLEDGEMENTS

We are grateful to John Cooper, Guy Genin, Emil Reisler, and Peter Rubenstein for helpful comments and suggestions. We thank Markus Meissner and Daniel Goldberg for reagents, Wandy Beatty, Microbiology Imaging Center, Washington University, for assistance with imaging, Jennifer Barks, Julie Nawas and Keli Tang for excellent technical support, Simren Mehta for thoughtful discussions and Joel Shuman for development of protocols for videomicroscopy and data analysis. This work was supported by predoctoral fellowships from the American Heart Association (0815645G to KMS) and an Institutional Training Grant T32-AI007172 (to KMS), and a grant from the NIH (AI073155 to LDS, DS).

REFERENCES

Anderson-White, B.R., Ivey, F.D., Cheng, K., Szatanek, T., Lorestani, A., Beckers, C.J., Ferguson, D.J., Sahoo, N., and Gubbels, M.J. (2010). A family of intermediate filament-like proteins is sequentially assembled into the cytoskeleton of Toxoplasma gondii. Cell Microbiol.

Baum, J., Tonkin, C.J., Paul, A.S., Rug, M., Smith, B.J., Gould, S.B., Richard, D., Pollard, T.D., and Cowman, A.F. (2008). A malaria parasite formin regulates actin polymerization and localizes to the parasite-erythrocyte moving junction during invasion. Cell Host Microbe *3*, 188-198.

Bubb, M.R., Senderowicz, A.M.J., Sausville, E.A., Duncan, K.L.K., and Korn, E.D. (1994). Jasplakinolide, a cytotoxic natural product, induces actin polymerization and competitively inhibits the binding of phalloidin to F-actin. J Biol Chem *269*, 14869-14871.

Chen, X., Cook, R.K., and Rubenstein, P.A. (1993). Yeast actin with a mutation in the hydrophobic plug between subdomains 3 and 4 ($L_{266}D$) displays a cold-sentitive polymerization defect. J Cell Biol *123*, 1185-1195.

Crews, P., Manes, L.V., and Boehler, M. (1986). Jasplakinolide, a cyclodepsipeptide from the marine sponge, *Jaspis* spp. Tetrahedron Lett *27*, 2797-2800.

Daher, W., Plattner, F., Carlier, M.F., and Soldati-Favre, D. (2010). Concerted action of two formins in gliding motility and host cell invasion by *Toxoplasma gondii*. PLoS Pathog *6*.

Dobrowolski, J.M., Niesman, I.R., and Sibley, L.D. (1997). Actin in the parasite *Toxoplasma gondii* is encoded by a single copy gene, *ACT1* and exists primarily in a globular form. Cell Motil Cytoskel *37*, 253-262.

Dobrowolski, J.M., and Sibley, L.D. (1996). Toxoplasma invasion of mammalian cells is powered by the actin cytoskeleton of the parasite. Cell *84*, 933-939.

Frenal, K., and Soldati-Favre, D. (2009). Role of the parasite and host cytoskeleton in apicomplexa parasitism. Cell Host Microbe *5*, 602-611.

Fujii, T., Iwane, A.H., Yanagida, T., and Namba, K. (2010). Direct visualization of secondary structures of F-actin by electron cryomicroscopy. Nature.
Gaskins, E., Gilk, S., DeVore, N., Mann, T., Ward, G.E., and Beckers, C. (2004). Identification of the membrane receptor of a class XIV myosin *Toxoplasma gondii*. J Cell Biol *165*, 383-393.

Gordon, J.L., and Sibley, L.D. (2005). Comparative genome analysis reveals a conserved family of actin-like proteins in apicomplexan parasites. BMC Genomics *6*, e179.

Håkansson, S., Morisaki, H., Heuser, J.E., and Sibley, L.D. (1999). Time-lapse video microscopy of gliding motility in *Toxoplasma gondii* reveals a novel, biphasic mechanism of cell locomotion. Mol Biol Cell *10*, 3539-3547.

Heintzelman, M.B. (2006). Cellular and molecular mechanics of gliding locomotion in eukaryotes. Int Rev Cytol *251*, 79-129.

Herm-Gotz, A., Agop-Nersesian, C., Munter, S., Grimley, J.S., Wandless, T.J., Frischknecht, F., and Meissner, M. (2007). Rapid control of protein level in the apicomplexan *Toxoplasma gondii*. Nat Methods *4*, 1003-1005.

Herm-Gotz, A., Weiss, S., Stratmann, R., Fujita-Becker, S., Ruff, C., Meyhofer, E., Soldati, T., Manstein, D.J., Geeves, M.A., and Soldati, D. (2002). *Toxoplasma gondii* myosin A and its light chain: a fast, single-headed, plus-end-directed motor. EMBO J *21*, 2149-2158.

Hirono, M., Kamagai, Y., Numata, O., and Watanabe, Y. (1989). Purification of Tetrahymena actin reveals some unusual properties. Proc Natl Acad Sci (USA) *86*, 75-79.

Kale, L., Skeel, R., Bhandarkar, M., Brunner, R., Gursoy, A., Krawetz, N., Phillips, J., Shinozaki, A., Varadarajan, K., and Schulten, K. (1999). NAMD2: Greater scalability for parallel molecular dynamics. J Comp Physics *151*, 283-312.

Kapoor, P., Sahasrabuddhe, A.A., Kumar, A., Mitra, K., Siddiqi, M.I., and Gupta, C.M. (2008). An unconventional form of actin in protozoan hemoflagellate, Leishmania. J Biol Chem *283*, 22760-22773.

King, C.A. (1981). Cell surface interaction of the protozoan Gregarina with Concanavalin A beads - implications for models of gregarine gliding. Cell Biol Intl Rep *5*, 297-305.

Kuang, B., and Rubenstein, P.A. (1997). Beryllium fluoride and phalloidin retore polymerizability of a mutant yeast actin (V266G, L267G) with severely decreased hydrophobicty in a subdomain 3/4 loop. J Biol Chem *272*, 1237-1247.

Lourido, S., Shuman, J., Zhang, C., Shokat, K.M., Hui, R., and Sibley, L.D. (2010). Calcium-dependent protein kinase 1 is an essential regulator of exocytosis in Toxoplasma. Nature *465*, 359-362.

Martí-Renom, M.A., Stuart, A.C., Fiser, A., Sánchez, R., Melo, F., and Sali, A. (2000). Comparative protein structure modeling of genes and genomes. Annu Rev Biophys Biomol Struct *29*, 291-325.

Mehta, S., and Sibley, L.D. (2011). Actin depolymerizing factor controls actin turnover and gliding motility in *Toxoplasma gondii*. Molc Biol Cell *In press*.

Mizuno, Y., Makioka, A., Kawazu, S., Kano, S., Kawai, S., Akaki, M., Aikawa, M., and Ohtomo, H. (2002). Effect of jasplakinolide on the growth, invasion, and actin cytoskeleton of *Plasmodium falciparum*. Parasitol Res *88*, 844 - 848.

Morisaki, J.H., Heuser, J.E., and Sibley, L.D. (1995). Invasion of *Toxoplasma gondii* occurs by active penetration of the host cell. J Cell Sci *108*, 2457-2464.

Oda, T., Iwasa, M., Aihara, T., Maeda, Y., and Narita, A. (2009). The nature of the globular- to fibrous-actin transition. Nature *457*, 441-445.

Paredez, A.R., Assaf, Z.J., Sept, D., Timofejeva, L., Dawson, S.C., Wang, C.J.R., and Cande, W.J. (2011). An actin cytoskeleton with evolutionaryly conserved functions in the absence of cannonical actin-binding protiens. PNAS (USA) *in press*.

Pollard, T.D., Blanchoin, L., and Mullins, R.D. (2000). Molecular mechanisms controlling actin filament dynamics in nonmuscle cells. Annu Rev Biophys Biomol Struct *29*, 545 - 576.

Poupel, O., and Tardieux, I. (1999). *Toxoplasma gondii* motility and host cell invasiveness are drastically impaired by jasplakinolide, a cyclic peptide stabilizing F-actin. Microb Infect *1*, 653-662.

Sahoo, N., Beatty, W.L., Heuser, J.E., Sept, D., and Sibley, L.D. (2006). Unusual kinetic and structural properties control rapid assembly and turnover of actin in the parasite *Toxoplasma gondii*. Mol Biol Cell *17*, 895-906.

Schmitz, S., Grainger, M., Howell, S.A., Calder, L.J., Gaeb, M., Pinder, J.C., Holder, A.A., and Veigel, C. (2005). Malaria parasite actin filaments are very short. J Mol Biol *349*, 113-125.

Schoenenberger, C.A., Bischler, N., Fahrenkrog, B., and Aebi, U. (2002). Actin's propensity for dynamic filament patterning. FEBS Lett *529*, 27-33.

Schüler, H., Mueller, A.K., and Matuschewski, K. (2005). Unusual properties of *Plasmodium falciparum* actin: new insights into microfilament dynamics of apicomplexan parasites. FEBS Lett *579*, 655-660.

Shaw, M.K., and Tilney, L.G. (1999). Induction of an acrosomal process in *Toxoplasma gondii*: visualization of actin filaments in a protozoan parasite. Proc Natl Acad Sci U S A *96*, 9095-9099.

Sibley, L.D. (2010). How apicomplexan parasites move in and out of cells. Curr Opin Biotechnol *21*, 592-598.

Siden-Kiamos, I., Pinder, J.C., and Louis, C. (2006). Involvement of actin and myosins in *Plasmodium berghei* ookinete motility. Mol Biochem Parasitol *150*, 308-317.

Smythe, W.A., Joiner, K.A., and Hoppe, H.C. (2008). Actin is required for endocytic trafficking in the malaria parasite Plasmodium falciparum. Cell Microbiol *10*, 452-464.

Vanderberg, J.P. (1974). Studies on the motility of *Plasmodium* sporozoites. J Protozool *21*, 527-537.

Wetzel, D.M., Håkansson, S., Hu, K., Roos, D.S., and Sibley, L.D. (2003). Actin filament polymerization regulates gliding motility by apicomplexan parasites. Mol Biol Cell *14*, 396-406.

Wetzel, D.M., Schmidt, J., Kuhlenschmidt, M., Dubey, J.P., and Sibley, L.D. (2005). Gliding motility leads to active cellular invasion by *Cryptosporidium parvum* sporozoites. Infect Immun *73*, 5379-5387.

Zanotti, G., Falcigno, L., Saviano, M., D'Auria, G., Bruno, B.M., Campanile, T., and Paolillo, L. (2001). Solid state and solution conformation of [Ala7]-phalloidin: a synthetic phallotoxin analogue. Chemistry *7*, 1479-1485.

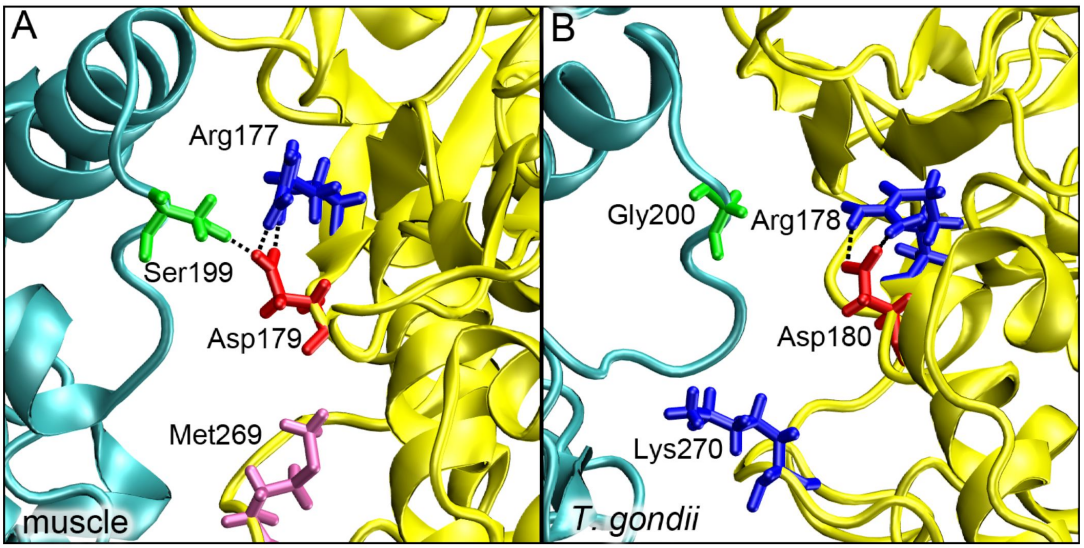

Figure 1. Identification of substitutions within TgACTI that may affect filament stability. (A) Modeling of S199-D179 hydrogen bond and M269 in the hydrophobic loop of mammalian actin. (B) Modeling of loss of hydrogen bond with G200 substitution and reduced hydrophobicity at position 270 in TgACTI.

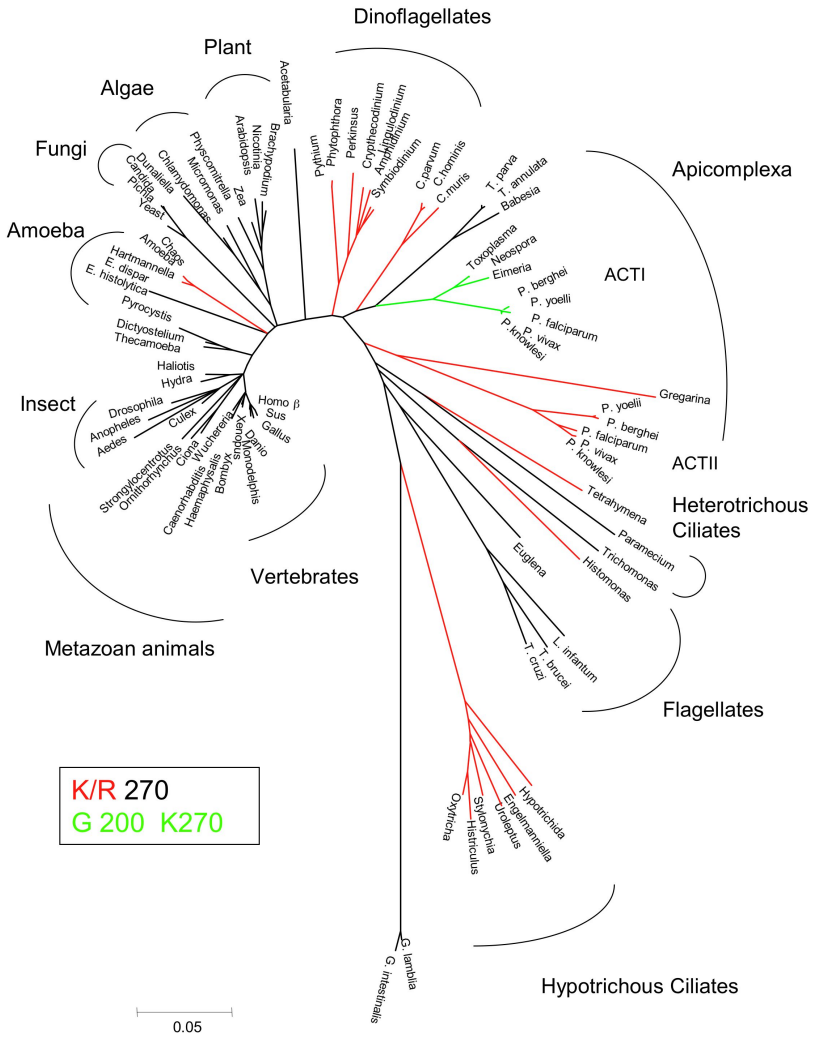

Figure 2. Phylogenetic tree highlighting the diversity of actins.

Actin sequences were retrieved from Genbank and aligned using Clustal. Neighbor joining with PAUP* was used to assemble the sequences into phylogenetic tree. The branches are color coded to show phylogenetic differences. Red represents branches containing a lysine or arginine at position 270, which is conventionally a methionine. Green represents branches that contain the 270 substitution as well as a glycine at position 200, which is conventionally a serine or threonine. Numbering based on the TgACTI sequence.

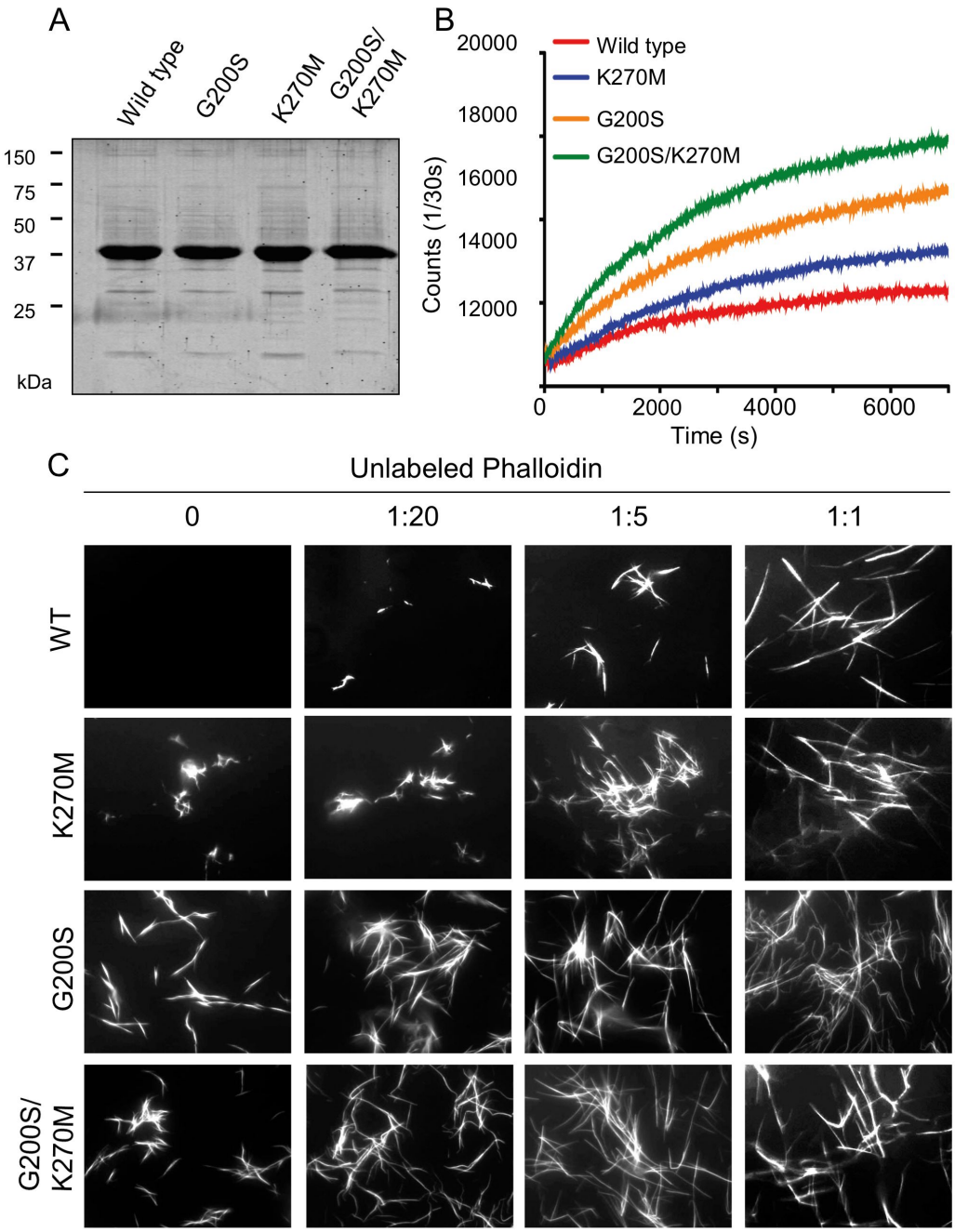
A
Wild type
G200S
K270M
G200S/
K270M
150
75
50
37
25
kDa
B
20000
18000
16000
14000
12000
Counts (1/30s)
Wild type
K270M
G200S
G200S/K270M
0
2000
4000
6000
Time (s)
C
Unlabeled Phalloidin
0
1:20
1:5
1:1
WT
K270M
G200S
G200S/
K270M

Figure 3. Single substitutions with TgACTI restore filament stability.

(A) Expression of TgACTI recombinant proteins containing mammalian-like substitutions in baculovirus, resolved using a 12% SDS-PAGE gel, and stained with SYPRO Ruby. (B) Comparison of polymerization kinetics of TgACTI substitutions. F buffer was added to induce polymerization of 5 μM actin and polymerization was monitored by light scattering. (C) *In vitro* polymerization of TgACTI substituted with mammalian actin residues. 5 μM actins were visualized by fluorescence microscopy using 0.33 μM Alexa 488-phalloidin and different molar ratios of unlabeled phalloidin to actin. Scale bars, 5 μm. Representative of three or more similar experiments.

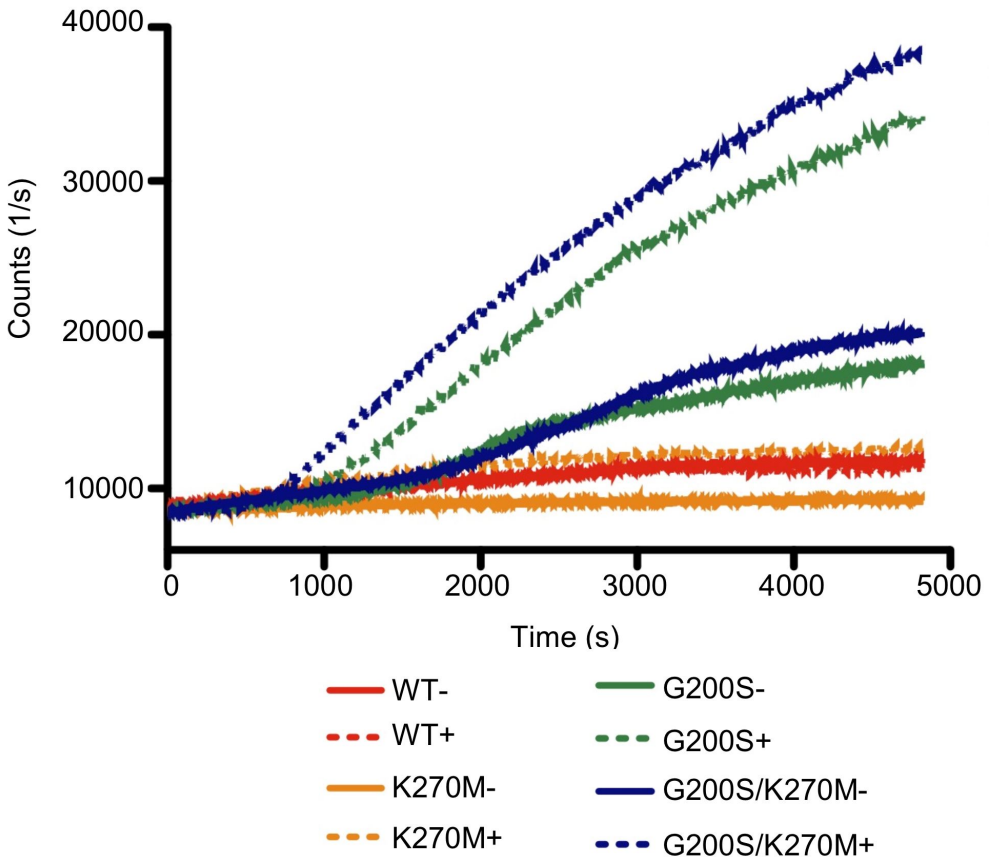

Figure 4. Comparison of polymerization kinetics of TgACTI substitutions +/- phalloidin. F buffer +/- 0.33 μM phalloidin was added to induce polymerization of 5 μM actin and polymerization was monitored by light scattering. Solid lines represent no phalloidin addition and dashed lines represent samples where phalloidin was added.

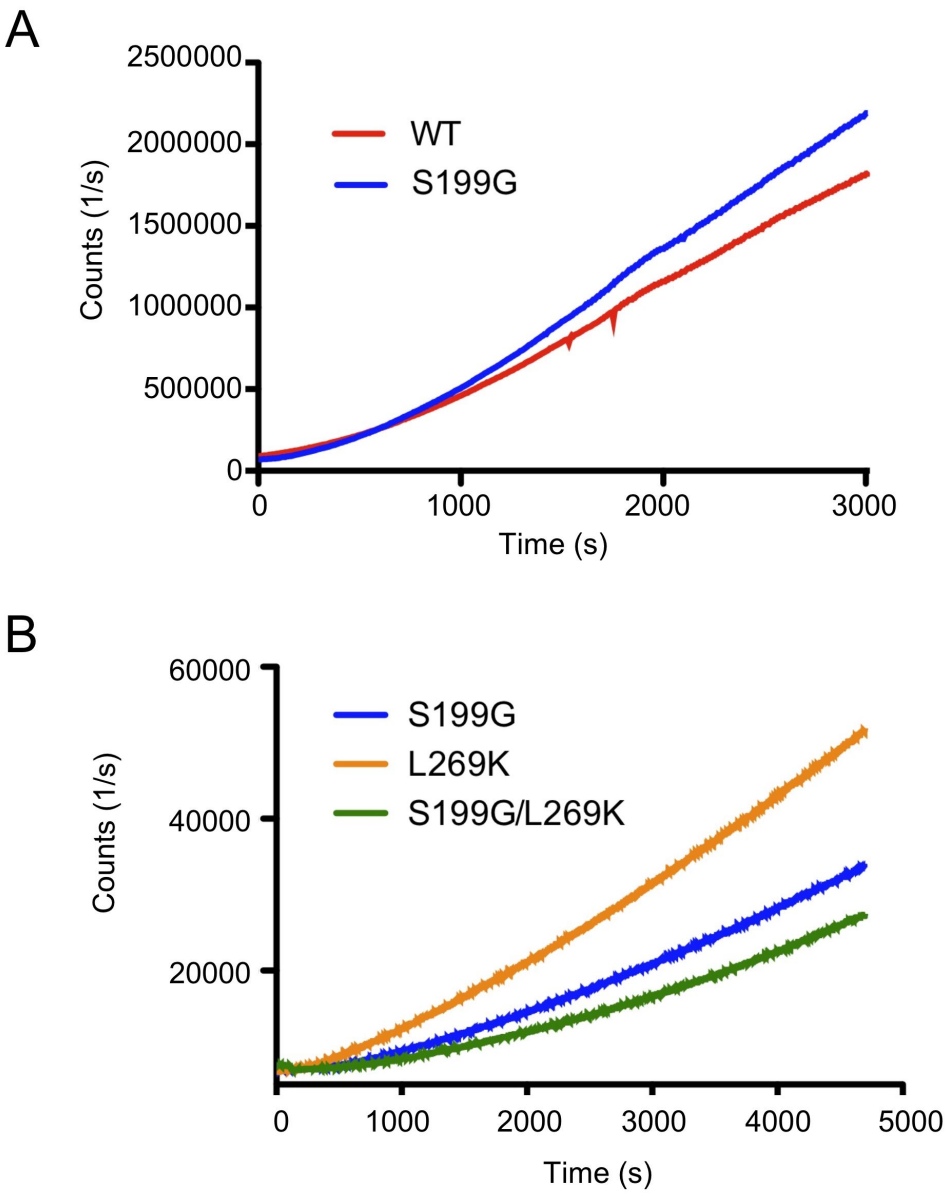

Figure 5. Comparison of polymerization kinetics of ScACT substitutions.

(A) F buffer was added to induce polymerization of 5 μM ScACT or ScACT-S199G and polymerization was monitored by light scattering. (B) F buffer was added to induce polymerization of 5 μM ScACT substitutions and polymerization was monitored by light scattering.

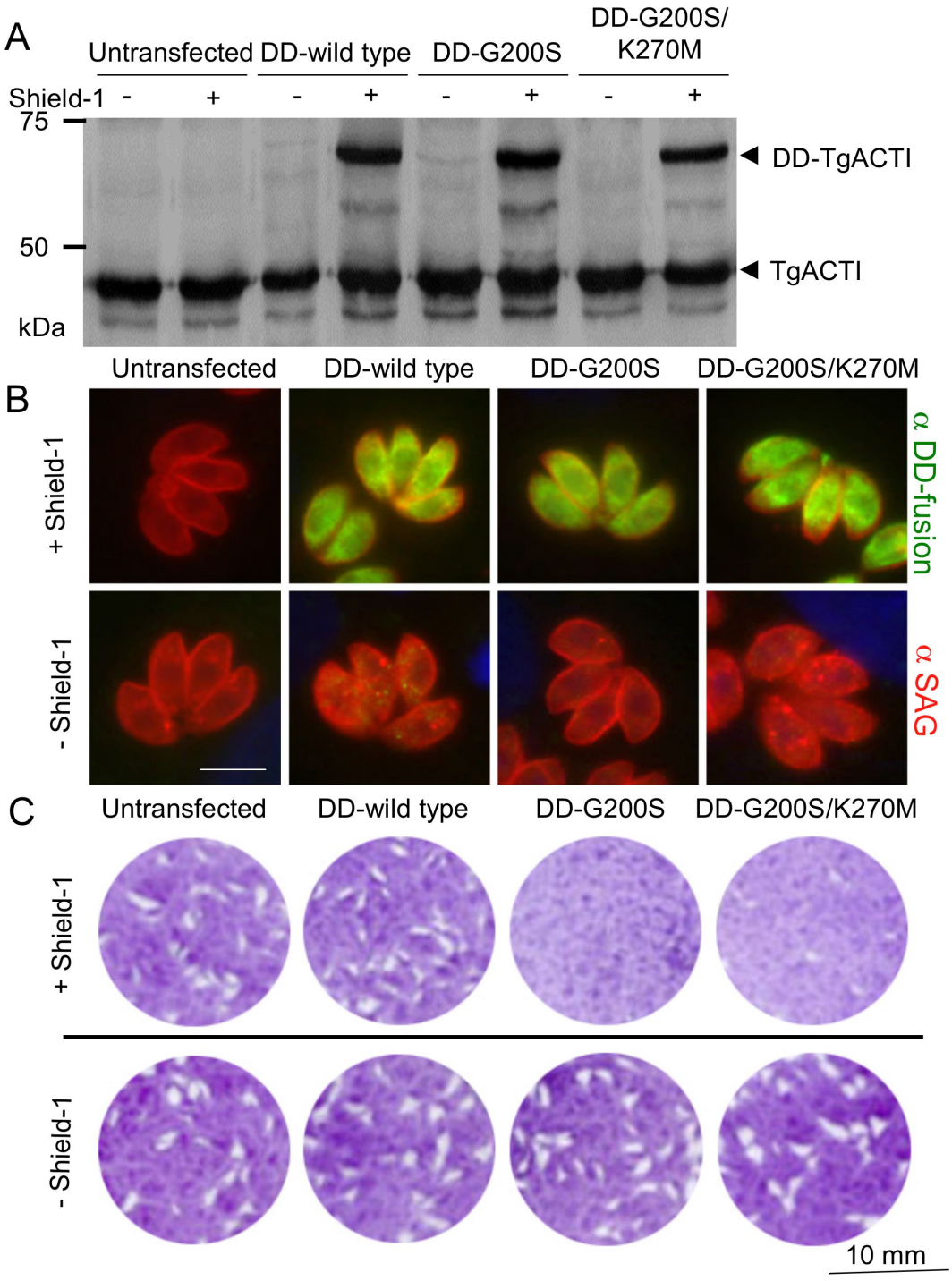
A
Untransfected
DD-wild type
DD-G200S
DD-G200S/
K270M
Shield-1 - + - + - + - +
75
50
kDa
DD-TgACTI
TgACTI
B
Untransfected
DD-wild type
DD-G200S
DD-G200S/K270M
+ Shield-1
- Shield-1
α DD-fusion
α SAG
C
Untransfected
DD-wild type
DD-G200S
DD-G200S/K270M
+ Shield-1
- Shield-1
10 mm

Figure 6. Expression of degradation domain (DD)-tagged TgACTI alleles in *Toxoplasma*. (A) Expression of DD-TgACTI fusion proteins following treatment ± Shield-1 for 40 h and detected by Western blot with anti-TgACTI antibody. All strains express the endogenous TgACTI while the fusion proteins (DD-TgACTI) were only expressed by the transfected strains in the presence of Shield-1. (B) Expression of DD-tagged TgACTI alleles following treatment ± Shield-1 for 24 h and stained for immunofluorescence with anti-SAG1 (surface antigen 1, red) and anti-c-myc (green) to detect the DDTgACTI fusion protein. (C) Effects of DD-TgACTI allele expression on plaque formation. HFF monolayers were infected with untransfected parasites or those expressing DD-TgACTI alleles ± Shield-1 for 7 days and visualized by crystal violet staining. Representative of three or more similar experiments.

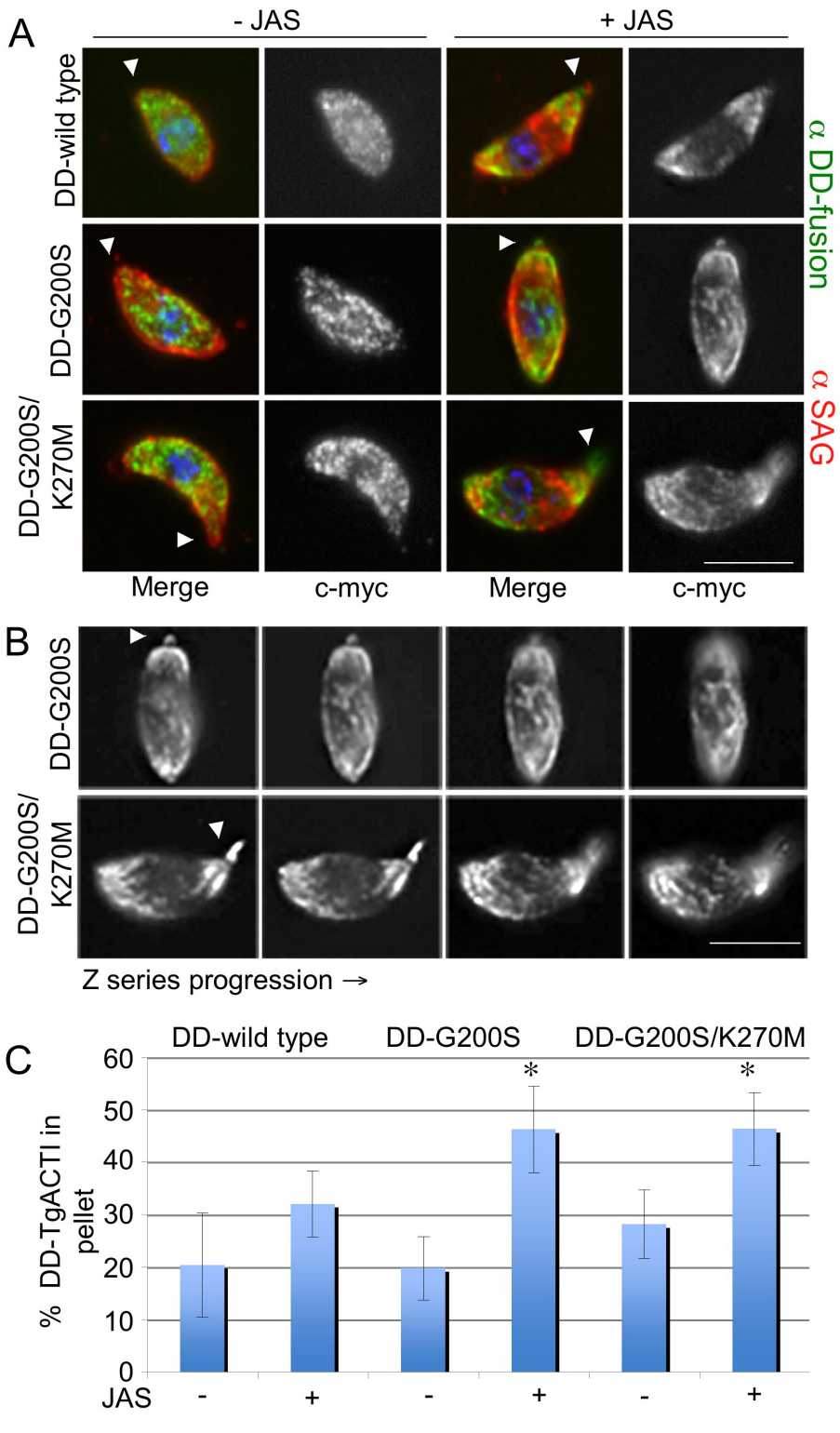
A
- JAS
+ JAS
DD-wild type
DD-G200S
DD-G200S/ K270M
α DD-fusion
α SAG
Merge
c-myc
Merge
c-myc
B
DD-G200S
DD-G200S/ K270M
Z series progression →
C
DD-wild type
DD-G200S
DD-G200S/K270M
% DD-TgACTI in pellet
60
50
40
30
20
10
0
JAS
-
+
-
+
-
+
*
*

Figure 7. Stabilized actin alleles are more sensitive to JAS-stabilization than endogenous TgACTI in *Toxoplasma*.

(A) Localization of c-myc-tagged DD-TgACTI alleles in parasites treated with Shield-1 for 40 h as visualized by immunofluorescence with anti-c-myc antibody (green) and SAG1 (red). Treatment with low levels of JAS (*i.e.* 0.25 μM) induced spiral patterns of filaments in parasites expressing stabilized actin alleles (right). Apical end noted with arrowhead. Scale bar, 5.0 μm. (B) Images from (A) shown as z-slices (~0.3 μm). Actin spirals in JAS-treated parasites were visualized by staining with anti-c-myc antibody. Apical end noted with arrowhead. Scale bar 5 μm. (C) Sedimentation analysis of F actin in parasites expressing DD-TgACTI fusions and treated ± Shield-1 for 40 h. Cell lysates were prepared ± 0.5 μM JAS, sedimented for 1 h at 350,000*g* and analyzed by SDSPAGE and quantitative Western blotting. Mean ± S.D., n = 3 experiments with a single replicate each. $*P < 0.05$ (Student's *t*-test) *vs*. DD-wild type.

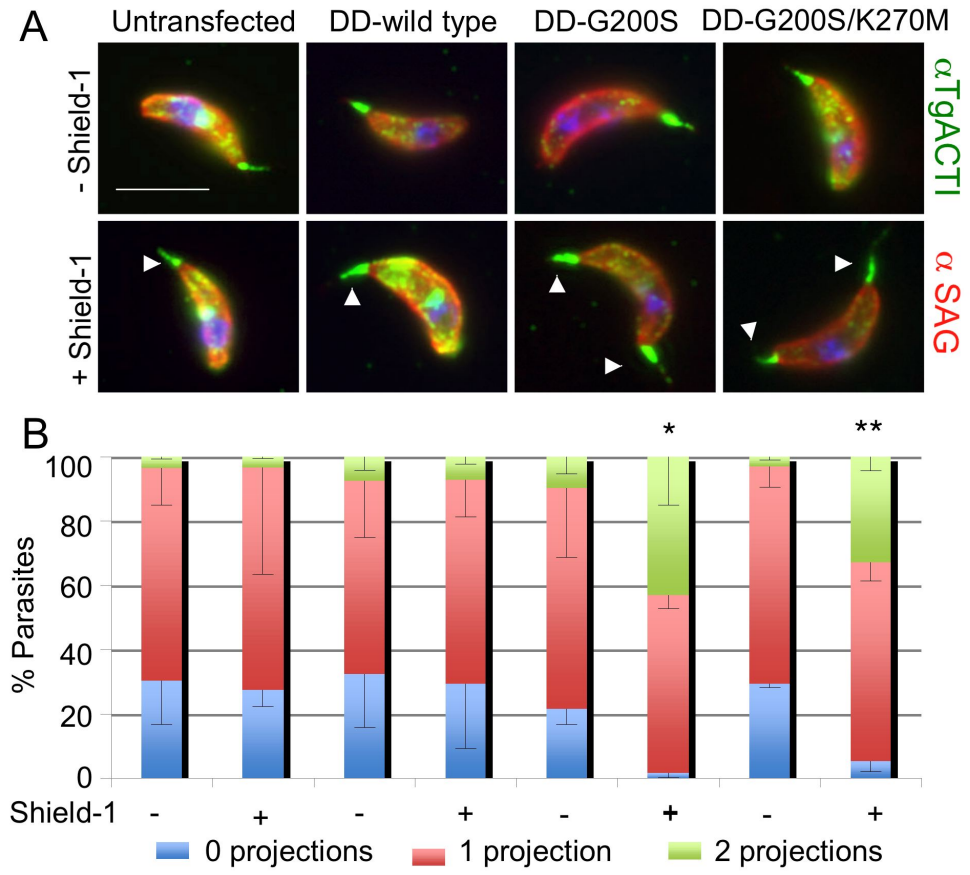

Figure 8. Immunofluorescence staining of actin-rich projections in JAS-treated parasites. (A) Parasites expressing stabilized TgACTI and treated ± Shield-1 for 40 h formed actin-rich projections from their apical and posterior ends as visualized by immunofluorescence with anti-TgACTI antibody (green) and SAG1 (red). Untransfected and DD-fusion expressing parasites were treated with 2.5 µM JAS (top panel). Scale bar, 5 µm. (B) The percentage of parasites with one or two projections were counted from cells after growth ± Shield-1 for 40 h. The frequency of cells expressing two actin projections in DD-G200S and DD-G200S/K270M –expressing parasites was significantly in the presence *vs*. absence of Shield-1 (bottom panel), * $P < 0.05$ (Student's *t*-test), ** $P < 0.001$ (Student's *t*-test). Mean ± S.E.M., n =3 experiments.

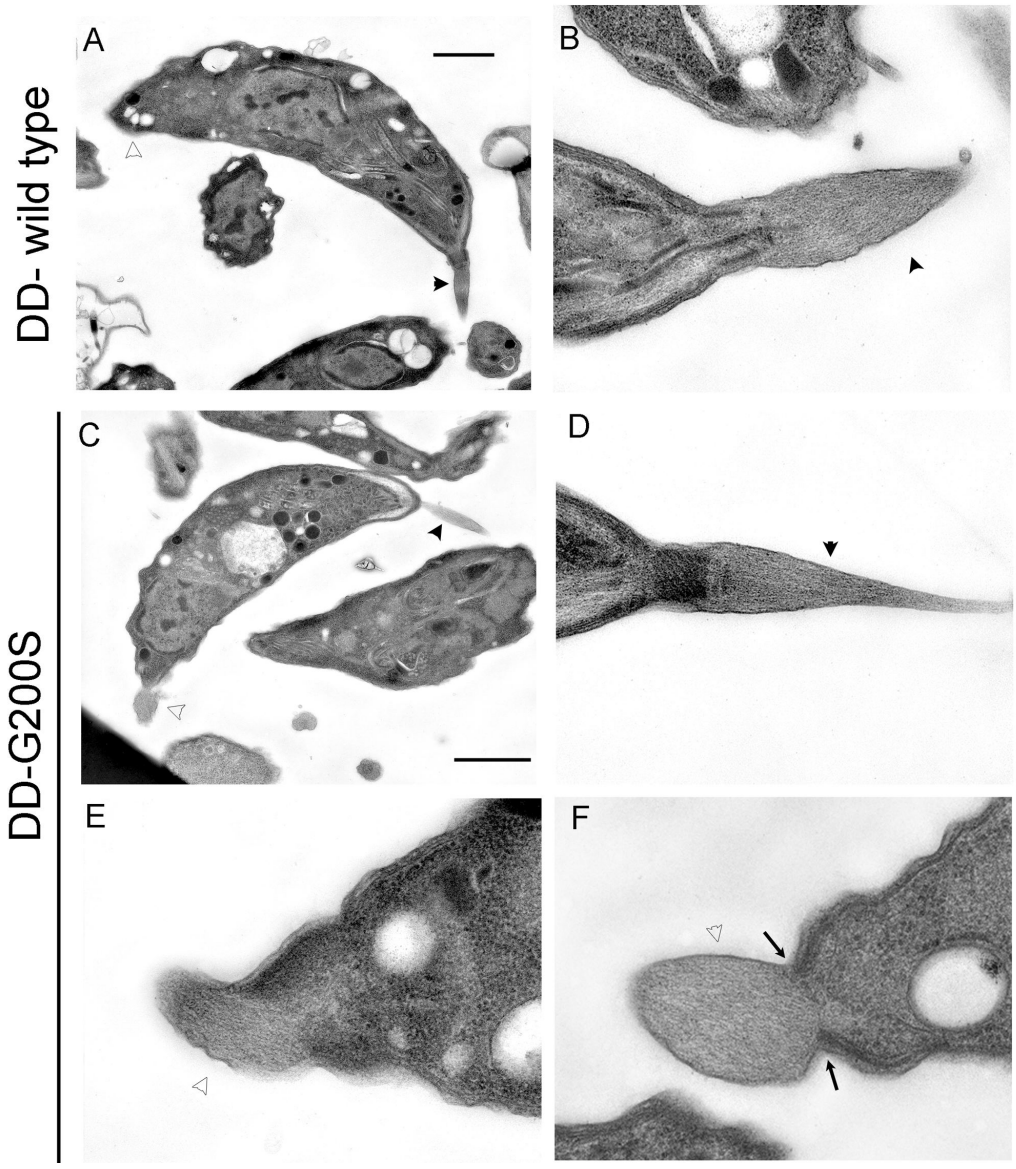

Figure 9. EM examination of F-actin in parasites expressing DD fusions and treated with JAS.

(A,B) DD- wild type expressing parasites showing apical projections (black arrowheads). (C-F) DD-G200S expressing parasites showing apical (black arrowheads) and posterior (white arrowheads) actin projections. F, Posterior projection of filaments protrudes through the dense inner membrane complex (arrows). Scale bars = 1 μm A, C, 0.5 μm, B, D-F.

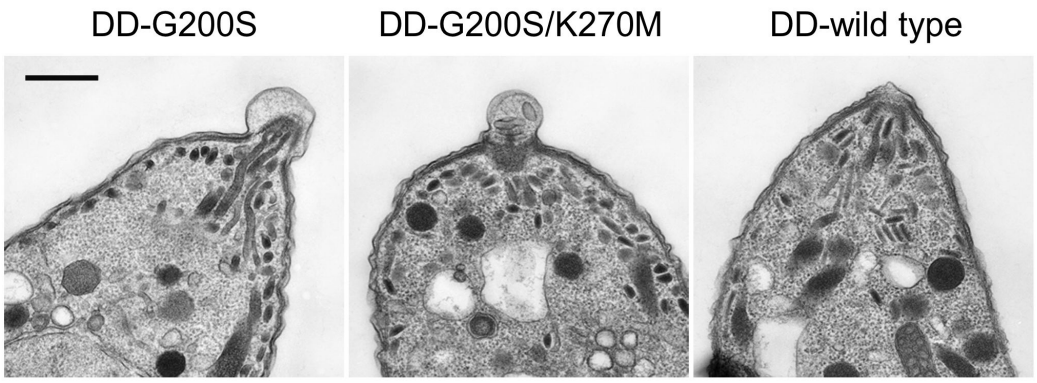

Figure 10. EM examination of parasites expressing DD-fusions in the absence of JAS. DD-G200S, DD-G200S/K270M and DD-wild type expressing parasites showing apical membrane blebs. Scale bar = 0.5μm.

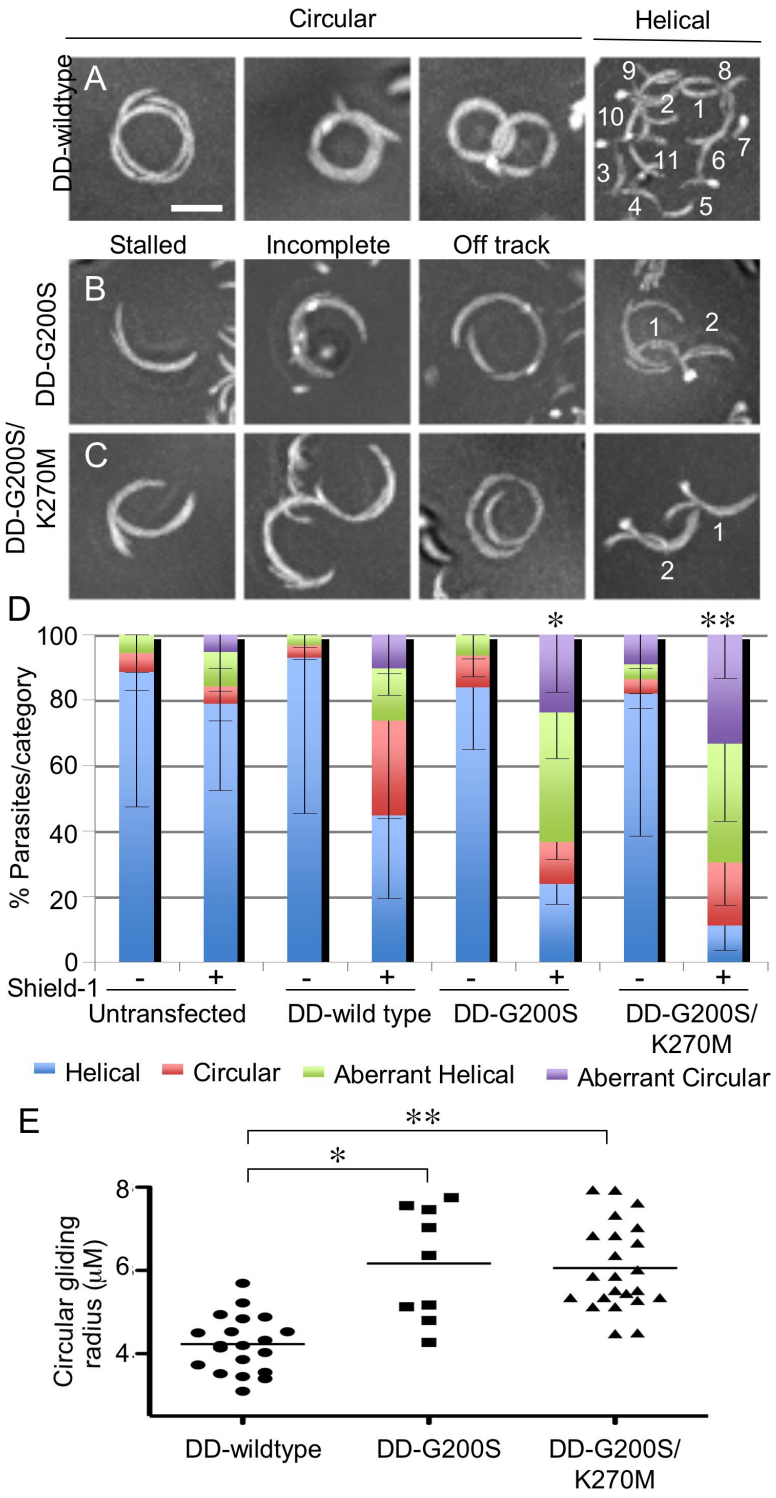
Circular
Helical
DD-wildtype
A
9
8
10
2
1
7
3
11
6
4
5
Stalled
Incomplete
Off track
DD-G200S
B
1
2
DD-G200S/
K270M
C
1
2
D
*
**
100
80
60
40
20
0
% Parasites/category
Shield-1
-
+
-
+
-
+
-
+
Untransfected
DD-wild type
DD-G200S
DD-G200S/
K270M
Helical
Circular
Aberrant Helical
Aberrant Circular
E
**
*
8
6
4
Circular gliding
radius (μM)
DD-wildtype
DD-G200S
DD-G200S/
K270M

Figure 11. Parasites expressing stabilized actin undergo aberrant gliding motility.

(A) Representative composite videos of normal gliding motility by parasites expressing DD-wild type TgACTI. (B,C) Representative composite videos of gliding by parasites expressing stabilized actin mutants revealed examples of stalled, incomplete or off-track circular patterns and disrupted helical patterns that were classified as aberrant. For helical gliding, the number of complete turns made during the time-lapse sequence are numbered. Images are composite frames from 60 sec of video recording. Scale bars, 5 μm. (D) Quantification of number of parasites undergoing each category of gliding motility following treatment ± Shield-1 for 40 h. The percentage of parasites undergoing aberrant gliding (as defined in B,C) increased in the presence *vs*. absence of Shield-1 in the mutant actins, * $P < 0.005$ (Student's *t*-test). Mean ± S.D. (E) Comparison of radii of circular tracks formed during normal gliding by DD- wild type expressing parasites *vs*. parasites expressing mutant actins that formed aberrant circular tracks (i.e. stalled, incomplete, or off-track). * $P < 0.001$ ** $P < 0.0001$ (Mann-Whitney test). Mean shown by horizontal line.

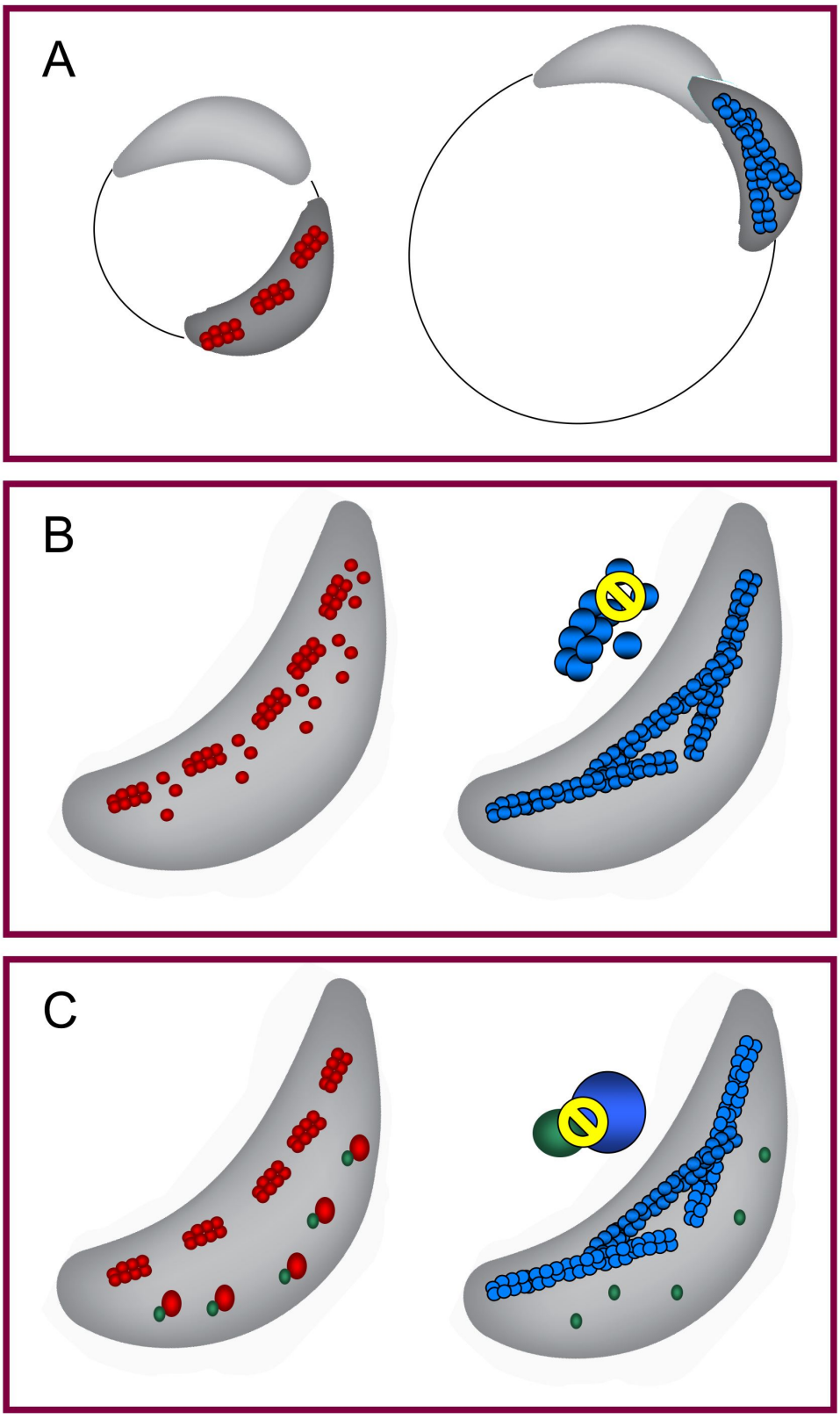
A
B
C

Figure 12. Models for mechanism by which substitutions within TgACTI influence gliding motility of *T. gondii*.

(A) Wild type TgACTI (red) forms short filaments providing flexibility for the parasite to undergoe a tight turning radius. TgACTI containing stabilizing substitutions (blue) is not flexible enough to allow the parasite to undergo tight turns and corkscrew motions resulting in aberrant forms of gliding motility. (B) Turnover of stabilized TgACTI from the filament is slowed due to the amino acid substitutions thereby disrupting normal motility by reducing the pool of free actin monomers. (C) Substitutions within TgACTI might also interfere with wild type binding of actin-binding proteins (green) and therefore alter their role in actin polymerization.

Table 1. Quantification of *T. gondii* gliding motility rates from video microscopy

Strain/Shield-1	Normal Helical[a]	Aberrant Helical	Normal Circular	Aberrant Circular
Untransfected/**-**	1.34 ± 0.23[b]	-[c]	-	-
Untransfected/**+**[d]	1.50 ± 0.44	-	-	-
DD-wild type/**-**	1.54 ± 0.29	-	-	-
DD-wild type/**+**	1.35 ± 0.28	-	1.09 ± 0.40	-
DD-G200S/**-**	1.49 ± 0.32	-	1.35 ± 0.46	-
DD-G200S/**+**	-	0.72 ± 0.32***	-	0.71±0.35*
DD-G200S/K270M/**-**	1.59 ± 0.41	-	1.32 ± 0.26	-
DD-G200S/K270M/**+**	-	0.73 ± 0.22***	-	0.64 ± 0.28**

[a] μm/sec

[b] Mean ± S.D.

[c] Too infrequent for analysis

[d] 4 μM Shield-1

* Comparison of circular gliding by DD-G200S ± Shield-1, $P < 0.05$, Student's *t*-test.

** Comparison of circular gliding by DD-G200S/K270M ± Shield-1, $P < 0.01$, Student's *t*-test.

***Comparison of helical gliding by DD-G200S or DD-G200S/K270M ± Shield-1, $P < 0.005$, Student's *t*-test.

Chapter IV

Influence of Formin and Profilin on Polymerization of Actin in *Toxoplasma gondii*

PREFACE

Work presented in this chapter was conducted by KMS. Wassim Daher contributed by cloning and purification of the formin proteins and the profilin used in the formin assays. Profilin in characterization assays was cloned and purified by KMS.

The first complete draft of this chapter was written by KMS. Comments from David Sibley were incorporated into the final version printed here.

ABSTRACT

Apicomplexan parasites employ a gliding motility mechanism that is dependent on the polymerization of parasite actin in order to enter into host cells. Paradoxically, intracellular actin populations are predominantly unpolymerized and actin filaments appear to only assemble when required for gliding and host cell entry. Actin polymerization is therefore likely a tightly regulated process; however, apicomplexans encode fewer actin-binding proteins than typically found in other eukaryotes. Previous studies have examined the behavior of apicomplexan formins and profilin on heterologous actin and demonstrate these proteins exhibit canonical functions to those of homologs in higher eukaryotes. However, the function of apicomplexan formins and profilin on divergent apicomplexan actins is still undetermined. We therefore analyzed the impact of *T. gondii* profilin (TgPRF) and two formin isoforms (TgFRM1 and TgFRM2) on the polymerization of *T. gondii* actin (TgACTI). Light scattering assays were used to demonstrate TgFRM1 and TgFRM2 enhanced TgACTI polymerization. TgPRF sequestered TgACTI and hence inhibited polymerization and also slightly inhibited nucleotide exchange, both unconventional properties. Determination that TgPRF sequesters TgACTI while TgFRMs enhance polymerization provides insight into TgACTI regulation *in vivo* and helps to explain the unconventional actin dynamics observed within the parasite.

INTRODUCTION

Toxoplasma gondii is a protozoan pathogen of the phylum Apicomplexa. *T. gondii* has an obligate intracellular life cycle and must therefore enter into host cells for replication. Along with the other members of the phylum, *T. gondii* employs a unique form of motility for active invasion of host cells. In the current model for this mechanism, termed gliding motility, the parasite has been proposed to utilize myosin motors anchored within the parasite inner membrane complex (Gaskins et al., 2004) to translocate actin filaments toward the posterior of the parasite. The actin filaments are coupled to extracellular adhesions via aldolase (Jewett and Sibley, 2003), and contact of these adhesins with the host surface results in rearward pulling of the adhesins to facilitate forward motion of the parasite into the host cell (Sibley, 2004).

Treatment of *T. gondii* with cytochalasin-D (cytD) to depolymerize actin filaments disrupts gliding motility and inhibits host cell invasion (Dobrowolski and Sibley, 1996). Despite the apparent requirement for filamentous actin to successfully enter host cells, intracellular parasites have been shown to maintain a highly unpolymerized population of actin (Dobrowolski et al., 1997; Wetzel et al., 2003). However, cytD-sensitive filaments have been visualized within trails formed by gliding parasites using sonication and rapid freezing followed by electron microscopy (Wetzel et al., 2003). *T. gondii* contains one actin, TgACTI, and studies with recombinant baculovirus-expressed TgACTI have revealed formation of unconventionally short actin filaments (Sahoo et al., 2006). Additionally, treatment with jasplakinolide to stabilize actin filaments, results in hypermotile kinetic motility and disrupts host cell invasion (Wetzel et al., 2003). Therefore, it appears that actin filaments within the parasite control the proper

directionality of motility and the timing of polymerization within the parasite so that filaments only form when required for gliding. These features raise the questions of how apicomplexan actin polymerization is regulated and what factors contribute to their unusual polymerization properties.

Formation of actin filaments is regulated by either controlling the concentration of the free actin monomer pool that can contribute to a growing filament or by controlling the accessibility of free filament ends for addition of monomers. This regulation is critical for maintaining proper actin networks within cells and therefore, eukaryotic organisms have evolved numerous actin-binding proteins to ensure proper regulation of actin polymerization. Searches within the genomes of apicomplexan parasites have revealed a minimal set of actin-binding proteins as compared to other organisms (Schüler and Matuschewski, 2006). Noteably absent is the actin nucleator Arp 2/3 (Gordon and Sibley, 2005). However, two actin-binding proteins that have been identified are profilin and formin, which collectively may be important for the regulation of parasite actin polymerization.

Profilins are small monomeric actin binding proteins that play multiple roles in regulation of actin polymerization. Profilins were initially shown to sequester G-actin resulting in filament depolymerization (Carlsson et al., 1977). However, profilin also plays a role in promoting polymerization by enhancing nucleotide exchange to convert ADP-actin to ATP-actin, thus creating a polymerization competent state and lowering the critical concentration for polymerization (Pantaloni and Carlier, 1993). More recently, profilin has been shown to enhance polymerization through interaction with the FH1 domain of formin (Sagot et al., 2002). Profilin has previously been demonstrated to be

essential for gliding motility in *T. gondii* through the use of a conditional knockout (Plattner et al., 2008). Depletion of *T. gondii* profilin, TgPRF, results in reduced gliding and defects in parasite egress from host cells (Plattner et al., 2008). Biochemical assays also demonstrate that TgPRF aids in the assembly of skeletal muscle actin filaments at free barbed ends but not at the pointed end (Plattner et al., 2008). Despite a conventional interaction with heterologous actin, TgPRF is unable to complement depletion of profilin in yeast (Plattner et al., 2008). Additionally, unlike conventional profilins, TgPRF was shown to inhibit nucleotide exchange by rabbit actin (Kucera et al., 2010). Finally, the profilin from another apicomplexan, *P. falciparum*, has also been shown to be essential in the blood-stage of the parasite life-cycle (Kursula et al., 2008).

Conventional formins contain a formin-homology 2 (FH2) domain that assembles into a homodimer that binds barbed ends of actin filaments. Upstream of the FH2 domain is the formin-homology 1 (FH1) domain that typically contains a number of polyproline stretches involved in recruitment of profilin-actin complexes (Higgs, 2005). Formins have been shown to enhance actin polymerization by moving processively along actin filaments, allowing addition of actin monomers that are donated by profilin (Romero et al., 2004). In the absence of homologs of other nucleating proteins in apicomplexans, such as Arp2/3, formins have become the suspected candidate to nucleate parasite actin filament formation. There are three formins in *T. gondii* and the functions of two of them, TgFRM1 and TgFRM2, have been examined and shown to act as nucleators of rabbit actin and contribute to parasite motility (Daher et al., 2010). *P. falciparum* also encodes three formins, PfFormin1 and PfFormin2 have been shown to act as a barbed end nucleators of chicken actin (Baum et al., 2008).

The overall sequences of TgACTI as well as those for TgPRF, TgFRM1 and TgFRM2 diverge from their counterparts in higher eukaryotes (Daher et al., 2010; Plattner et al., 2008). Hence, these regulatory actin-binding proteins may differ in their interaction with TgACTI from what has been observed with heterologous actins in previous studies. Therefore, we tested the function of TgPRF along with TgFRM1 and TgFRM2 on the regulation of TgACTI polymerization. We observed that while *T. gondii* formins are capable of enhancing TgACTI polymerization, the role of TgPRF appears to be primarily in actin sequestration.

RESULTS

Localization and Concentration of Profilin within *T. gondii*

Recombinant His-tagged *T. gondii* profilin (TgPRF) was purified using Ni-chromatography and used for polyclonal antibody generation. Rabbit anti-TgPRF (Rb αTgPRF) was specific for recognition of TgPRF and recognized the recombinant protein (Figure 1A, lane 1) and a band at the corresponding molecular weight to profilin within *T. gondii* lysate (Figure 1A, lane 3), but did not detect anything in control host cell lysate (Figure 1A, lane 2). Rabbit αTgPRF was used to determine the localization of TgPRF within intracellular parasites and revealed a punctate staining pattern throughout the parasite (Figure 1B). The localization of TgPRF was also examined in extracellular gliding parasites and TgPRF was again seen in a punctate pattern within the parasite but also in the protein trails deposited on coverslips as the parasite undergoes gliding motility. Interestingly, the TgPRF found within the trails was also within punctae (Figure 1C). The TgPRF punctae observed in extracellular parasites appeared closer to the parasite membrane than that seen within intracellular parasites. We therefore measured the distance of the TgPRF punctae from the parasite membrane using images of intracellular and extracellular gliding parasites using the measurement tool in the Volocity software (Perkin Elmer). The distance of TgPRF from the parasite membrane was significantly less in extracellular parasites (0.40 μm) than in intracellular parasites (0.67 μm) (Figure 1D). Other proteins involved in actin polymerization (TgACTI, TgADF) have been demonstrated to relocalize to the inner membrane space beneath the parasite plasma membrane (Mehta and Sibley, unpublished data). This relocalization

suggests that TgPRF may also move to this region upon initiation of gliding motility, potentially to interact with other proteins involved in motility.

The intracellular concentration of TgACTI has previously been estimated to be 40 μM (Mehta and Sibley, 2011). To compare this concentration with that of TgPRF, we compared the levels of TgPRF in *T. gondii* lysate of known parasite concentration on a Western blot also containing recombinant TgPRF and probed with anti-TgPRF (Figure 2A) to establish a standard curve (Figure 2B). We estimate the intracellular concentration of TgPRF to be ~ 43 μM, about a 1:1 concentration ratio to TgACTI.

TgPRF acts to sequester *T. gondii* actin

Conventional profilins bind actin monomers, sequestering them to prevent polymerization of filaments (Carlsson et al., 1977). To determine how TgACTI polymerization is influenced in the presence of TgPRF, sedimentation assays were used to monitor polymerization. We have previously demonstrated that TgPRF does not polymerize robustly at 5 μM (Chapter 2), but is able to form longer filaments and polymerize more extensively at 25 μM (Chapter 6, Figure 3A). Therefore, we chose to monitor sedimentation at 350,000g with 25 μM TgACTI in order to better observe changes. TgACTI was polymerized for 1 hr in the presence of varying concentrations of TgPRF prior to sedimentation. A dose-dependent decrease in TgACTI in the pellet fraction was observed with increasing concentrations of TgPRF demonstrating TgPRF inhibited polymerization (Figure 3A). Steady state sedimentation was used to further examine the effect of TgPRF on TgACTI polymerization. Varying concentrations of TgACTI were polymerized in the presence of equimolar TgPRF for 20 hrs and

subsequently centrifuged at 350,000g. Increasing the TgACTI concentration led to a greater mass of protein collected in the pellet (Figure 1B). However, addition of equimolar TgPRF resulted in reduced mass in the pellet demonstrating decreased levels of polymerization (Figure 1B). Collectively, these results provide evidence that TgPRF sequesters TgACTI from polymerization.

TgFormins Enhance TgACTI Polymerization

Recent studies have demonstrated the *T. gondii* formins act in a conventional manner in the presence of rabbit actin to enhance polymerization (Daher et al., 2010); however, it is yet unknown if their influence on TgACTI polymerization will be similar. A range of concentrations of recombinant *T.gondii* FRM1 and FRM2 were added to TgACTI and polymerization was monitored by light scattering. Consistent with results from previous studies, polymerization of 5 μM TgACTI alone was not robust (Figure 4A and 4B). Upon addition of 1 nM and 10 nM TgFRM1, light scattering was increased slightly, however, a substantial increase in polymerization was observed with addition of 100 nM TgFRM1 to TgACTI (Figure 4A). The same concentrations were used to test the effects of TgFRM2, and extremely robust polymerization occurred even with addition of only 10 nM TgFRM2 and an even greater increase in light scattering was observed at 100 nM (Figure 4B). Concentrations of 100 nM FRM1 (1:50 molar ratio with TgACTI) and 10 nM FRM2 (1:500 molar ratio with TgACTI) were chosen for use in subsequent experiments due to their ability to similarly increase TgACTI polymerization (Figure 4C). Upon completion of light scattering, the samples were centrifuged at 100,000g for 1 hour and the amount of TgACTI in the pellet and supernatant were calculated using SDS-

PAGE. A significant increase in pelletable actin was observed in the TgACTI samples incubated with TgFRM1 (1:50 molar ratio) or TgFRM2 (1:500 molar ratio) (Figure 4D). These results demonstrate that the presence of formins during TgACTI polymerization enhances TgACTI polymerization.

To examine the extent of polymerization, we visualized TgACTI filaments in the absence and presence of TgFRM1 and TgFRM2 using fluorescence microscopy. TgACTI (25 μM) was incubated in F buffer alone, with TgFRM1 (1:50 molar ratio) or with TgFRM2 (1:500 molar ratio) and 0.33 μM Alexa-488 phalloidin was added to all samples to allow for actin filament visualization. On its own, TgACTI polymerized into filaments of various lengths (Figure 5A). However, in the presence of TgFRM1 or TgFRM2, there were many more clusters of filaments, although the length of these filaments was shorter than with TgACTI alone (Figure 5A). Combination of TgFRM1 and TgFRM2 together resulted in more filaments (Figure 5A). These observations, combined with data from both light scattering and sedimentation analysis, demonstrate that although the TgACTI appears to form shorter filaments in the presence of formins, the amount of total filaments increases, consistent with conventional formin function.

TgProfilin Inhibits Formin-mediated TgACTI Polymerization

Biochemical assays have previously shown that TgPRF acts in a conventional manner to promote polymerization at rabbit actin barbed, but not pointed, ends (Plattner et al., 2008). To determine what effect TgPRF plays on formin-mediated enhancement of TgACTI polymerization, we used fluorescence microscopy to observe TgACTI filamentation in the presence of TgPRF. Consistent with the sequestering observed by

TgPRF in light scattering assays, the addition of TgPRF to TgACTI resulted in complete loss of filaments by microscopy (Figure 5B). Addition of TgFRM1 and TgFRM2 to the TgACTI/TgPRF reaction restored filaments slightly, but polymerization was not as robust as TgACTI alone or in the presence of either formin without profilin (Figure 5B). This decrease in polymerization was surprising since profilin has been shown to interact with formin to enhance actin polymerization (Sagot et al., 2002). We therefore added profilin to light scattering reactions with TgACTI and TgFRM1, TgFRM2, or both, to examine the effect on light scattering. In contrast to what was seen with TgFRM1 and TgFRM2 alone, addition of TgPRF to the TgACTI polymerization reaction at a 1:1 concentration resulted in decreased light scatter (Figure 6A). Addition of both TgFRM1 and TgFRM2 simultaneously with TgACTI resulted in an even larger increase than with either formin alone (Figure 6B). However, decreased TgACTI polymerization was also seen upon TgPRF addition to TgACTI in the presence of both TgFRM1 and TgFRM2 together (Figure 6B). Therefore, at equimolar concentration to TgACTI, TgPRF does not contribute to the formin-nucleated polymerization. To determine if this inhibition is a concentration-dependent effect, TgPRF was added at a 1:10 ratio to TgACTI in the presence of either TgFRM1 or TgFRM2. At this lower ratio of TgPRF, TgACTI had a slight enhancement in polymerization suggesting there is an optimal profilin concentration where a percentage of actin monomers are free of sequestration and instead interact with formin to enhance polymerization.

TgPRF does not enhance nucleotide exchange of TgACTI

Profilins conventionally enhance actin polymerization by converting ADP-actin monomers following depolymerization to ATP-actin, preparing it for addition to the growing barbed end (Pantaloni and Carlier, 1993). ε-ATP labeled actin can be used to monitor the ability of profilins to exchange nucleotide by monitoring the decrease in fluorescence of the actin upon addition of unlabeled ATP. It was recently demonstrated that when combined with heterologous actin, TgPRF acts unconventionally and inhibits nucleotide exchange (Kucera et al., 2010). The ability of TgPRF to exchange nucleotide from ATP-TgACTI was examined over a range of concentrations. At a 2:1 ratio of TgPRF to ATP-TgACTI or lower, no change in nucleotide exchange was observed (Figure 7, inset). However, when the concentration of TgPRF was increased to 10 times the level of TgACTI, slight inhibition of nucleotide exchange was observed by a slower rate of loss of ε-ATP fluorescence (Figure 7). An affinity of ~ 2.9 μM was calculated for TgPRF interaction with TgACTI. This affinity exceeds that typically observed for conventional profilin/actin interaction, but consistent with previous calculations of TgPRF binding to rabbit actin (Plattner et al., 2008).

DISCUSSION

Previous studies have shown that while apicomplexan motility relies on filamentous actin, filaments are only transiently detected *in vivo* where the majority of actin appears to be unpolymerized (Schmitz et al., 2005; Wetzel et al., 2003). The current studies attempt to uncover regulatory mechanisms utilized within the parasite to maintain this steady state pool and assemble filaments at the time they are required for gliding motility. The genome of apicomplexan parasites contains few actin-binding proteins, such as formins, profilins, actin depolymerizing factor (ADF) and capping protein, which may be critical for regulating the state of polymerized actin and may contribute to turnover in the parasite (Schüler and Matuschewski, 2006). We have analyzed the effects of *T. gondii* formins and profilin on polymerization of TgACTI. TgFRM1 and TgFRM2 enhance filamentation by forming filaments that are otherwise not observed for TgACTI alone. TgPRF was shown to function primarily in sequestration of TgACTI. These properties help to explain both previously observed *in vitro* and *in vivo* behavior of instability and turnover of parasite actin filaments, which are likely important adaptations for gliding motility.

Conventional profilins have been shown to bind actin monomers and sequester them from filament assembly making this protein an interesting candidate for regulation of TgACTI polymerization. Here, we demonstrate TgPRF inhibits TgACTI polymerization in a dose-dependent manner consistent with canonical profilin activity. However, at equimolar concentrations to TgACTI, TgPRF decreased polymerization enhancement caused by either TgFRM. This was an unexpected finding as conventional profilins have been reported to interact synergistically with formins to further enhance polymerization

(Sagot et al., 2002). When a TgPRF concentration at 1:10 molar ratio of TgACTI was added with TgFRM for polymerization, the inhibition was not observed, suggesting high concentration of TgPRF is required for efficient sequesteration. Previous studies have used biochemical assays to demonstrate that profilin interacts with the barbed end of growing heterologous actin filaments to promote polymerization and report the affinity of TgPRF for rabbit actin to be ~ 5 μM (Plattner et al., 2008). Our studies find a similar affinity of TgPRF for TgACTI, indicating that the sequestering activity on TgACTI is not explained by a change in binding affinity between TgACTI and rabbit actin. It is possible that the lack of polymerization enhancement in the presence of TgFRMs could be due to the degenerate sequences of the *T. gondii* formin FH1 domains, which contain fewer prolines than conserved FH1 domains (Daher et al., 2010). Biochemical analysis has previously revealed that TgPRF had a very low binding affinity for peptides of the TgFRM2 FH1 domain (Kucera et al., 2010) and while TgFRMs were able to bind TgACTI within parasite lysates, they did not pull down TgPRF (Daher et al., 2010).

In contrast to conventional function of profilins, TgPRF slightly inhibited nucleotide exchange on TgACTI, consistent with the action of TgPRF on rabbit actin (Kucera et al., 2010). While the inhibition of nucleotide exchange diverges from the function of most non-plant profilins, the profilins from Arabidopsis (Perelroizen et al., 1996) and Chlamydomonas (Kovar et al., 2001) are also unconventional and either inhibit or have no effect on actin nucleotide exchange. It has been speculated that plant actin may have fast enough intrinsic nucleotide turnover rate that profilin does not require this function and the same may also be true for TgACTI.

Our data suggestTgPRF functions mainly to sequester TgACTI from polymerization. Such a model is especially significant in light of previous studies using TgPRF depletion to demonstrate that profilin is required for proper host cell invasion (Plattner et al., 2008). One interpretation of this data would be that without TgPRF to aid in keeping the actin monomer pool high and filamentation low, the process of host cell invasion is inhibited. Long filaments were not immediately apparent in TgPRF depleted parasites (Plattner et al., 2008), but further microscopy would be required to carefully examine filaments within these parasites. Recent work with the actin depolymerizing factor from *T. gondii,* TgADF, also shows that this actin-binding protein functions to sequester TgACTI (Mehta and Sibley, 2010). Depletion of TgADF leads to visualization of long actin filaments extending throughout the parasite as well as aberrant forms of motility that are detrimental to host cell invasion and egress (Mehta and Sibley, 2011). It was previously calculated that the intracellular concentration of TgACTI is around 40 μM (Mehta and Sibley, 2011). Similar concentrations have been calculated for TgADF (35 μM) (Mehta and Sibley, 2010) and TgPRF (43 μM) (this study). Based on these levels, sequestration by both TgPRF and TgADF is expected to complex nearly all of TgACTI, ensuring there is a small free monomer pool for polymerization. Hence, these monomer-binding proteins are predicted to contribute to the lack of long, stable actin filaments seen within the parasite.

Formins traditionally aid in nucleation of actin filaments through dimerization and interaction with the actin nucleus via the FH2 domain and interaction with the profilin/actin complex via its FH1 domain (Higgs, 2005). Previous work has shown that the *T. gondii* formins TgFRM1 and TgFRM2 act as nucleators of heterologous actin

(Daher et al., 2010). In the present study, we demonstrate that they also act to enhance polymerization of TgACTI. The increase in light scattering observed upon addition of TgFRM1 or TgFRM2 to TgACTI is the first observation of robust TgACTI polymerization on its own without a requirement for stabilizing agents.

When the effect of TgFRM1 and TgFRM2 on actin was studied using rabbit actin, TgFRM1 proved to be a more potent nucleator that TgFRM2 (Daher et al., 2010). This trend was also observed when the formins from *P. falciparum* were tested for their impact on chicken actin polymerization (Baum et al., 2008). Conversely, in the current studies, TgFRM2 appears about 10 times more potent than TgFRM1 for increasing light scattering of TgACTI. However, the increase in light scatter from ninety degree light scattering assays is not necessarily equivalent to polymerization alone, as filament bundling will also register as an increase in light scatter. Sedimentation assays highlight this caveat as the amount of pelletable TgACTI after incubation with TgFRMs was less than what would be expected from light scattering. This discrepancy could be attributed to TgFRMs increasing polymerization, but not filament length, leading to formation of many small TgACTI filaments that do not sediment at 100,000g. Alternatively, the formins from *T. gondii* may not function only to interact with the barbed end of the actin filament, but could have side binding activity as well that would contribute to filament bundles. Bundling has been previously reported to occur with mammalian formins FRL1 and mDia2 (Harris et al., 2006) and with Formin1 from *Arabidopsis thaliana* (AFH1) (Michelot et al., 2006; Michelot et al., 2005). AFH1 interacts with the barbed end of the actin filament in a non-processive manner and binds to the side of the filament following nucleation allowing the formin to faciliate formation of filament bundles (Michelot et al.,

2006). The Formin2 family of apicomplexan formins is phylogenetically more related to AFH1 (Baum et al., 2008) and it remains to be seen if this formin contributes to TgACTI filament side binding and bundling.

The similar functions of apicomplexan formins and profilin to those in plants is not surprising considering other unconventional actin dynamics shared between this phylum of parasites and plants. Like the apicomplexans, plant cells maintain a highly unpolymerized population of actin (Gibbon et al., 1999; Snowman et al., 2002). Plant profilins are also maintained at a high concentration within the cell and appear to be at about a 1:1 ratio with actin (Staiger and Blanchoin, 2006). It may turn out that apicomplexan actin function and regulation is more closely related to that of plants, rather than yeast or mammals.

The transition between unpolymerized actin pools and filament formation appears to be a highly regulated process in *T. gondii*, despite a minimal set of actin-binding proteins. These studies reveal two actin-binding proteins within the parasite that have opposing impacts on TgACTI polymerization. TgPRF primarily sequesters TgACTI while TgFRM1 and TgFRM2 enhance polymerization. The presence of regulatory proteins with these opposite functions likely aid in maintaining the precise balance between monomeric actin and polymerized filaments within the parasite.

MATERIALS AND METHODS

Recombinant Profilin and Formins

For the characterization of profilin, profilin was amplified from *T. gondii* RH strain cDNA using primers 5'-GCGCGCCCATATGTCCGACTGGGACCCTGTTGT-3' (forward) and 5'-CGCGGATCCTTAGTACCCAGACTGGTGAA-3' (reverse) and cloned into pET16b vector using the NdeI and BamHI sites to incorporate a 10X His tag at the N-terminus. The resulting construct was electroporated into BL21 *E. coli* for protein expression. Recombinant protein was obtained using ProBond Nickel beads and was used for polyclonal antibody production (Covance). Antibody specificity was examined by running 12% SDS-PAGE gels with recombinant TgPRF, HFF cell lysate, or *T. gondii* lysate, transferring to nitrocellulose, probing with the anti-TgPRF antibody, followed by detection with anti-rabbit horse radish peroxidase antibody using a FLA-5000 phosphorimager (Fuji Film Medical Systems). TgFRM1 (gene ID: 20.m03963) and TgFRM2 (gene ID: 20.m05986) were bacterially expressed by cloning the FH2 domain and upstream proline rich domain into pETM-30 vector between NcoI and EcoRI. GST-tagged profilin, TgFRM1 **(**amino acids numbers 4582-5051**)** and TgFRM2 **(**amino acids numbers 3317–4043**)** were purified using Amersham Glutation sepharose 4 Fast Flow according to manufacturer's instructions. The GST tag was cleaved with Precission protease.

Immunofluorescence Microscopy

For intracellular staining, parasites were allowed to invade HFF monolayers on glass coverslips for 24 h. The coverslips were then fixed with 4% formaldehyde and stained

with rabbit anti-TgPRF to detect profilin followed by goat anti-mouse IgG conjugated to AlexaFluor488 (Molecular Probes) and mAB DG52 (anti-TgSAG1) directly conjugated to AlexaFluor 594 to detect the parasite. For extracellular staining, parasites were allowed to glide for 15 min on glass coverslips coated with 50 μg ml^{-1} BSA. Coverslips were fixed and stained with rabbit anti-TgPRF followed by goat anti-mouse IgG conjugated to AlexaFlour 488 and mAb DG52 labeled with AlexaFlour 594. Coverslips were mounted in Pro-Long Gold anti-fade reagent (Invitrogen) and viewed with a Zeiss Axioskop (Carl Zeiss) microscope using 63X Plan-NeoFluar oil immersion lens (1.30 NA). Images were collected using a Zeiss Axiocam and deconvolved using a nearest neighbor algorithm in Axiovision v3.1. Images were processed using linear adjustments in Adobe Photoshop v8.0. Measurements to compare the distance of TgPRF from the parasite membrane in intracellular and extracellular parasites were made using the measurement tool in the Volocity software (Perkin Elmer).

Quantitation of Profilin Intracellular Concentration in *T. gondii*

To estimate the intracellular concentration of profilin within *T. gondii*, egressed parasite cultures were lysed in actin stabilization buffer (60 mM PIPES, 25 mM HEPES, 10 mM EGTA, 2mM $MgCl_2$, 125 mM KCl) containing 1% Triton-X-100 and 1X protease inhibitor cocktail (1 μg/ml E64, 10 μg/ml AEBSF, 10 μg/ml TLCK and 1 μg/ml leupeptin) for 30 min followed by centrifugation at 14,000 rpm for 10 min to remove the insoluble material. The lysate was then resuspended in 1X sample buffer and run at various concentrations of parasites on 12% SDS-PAGE gels along with a range of recombinant TgPRF at known concentration, Western blotted with anti-TgPRF antibody,

visualized using a FLA-5000 phosphorimager (Fuji Film Medical Systems), and quantified using Image Gauge v4.23. The recombinant protein was used to create a standard curve for comparison with the parasite lysate to estimate the amount of TgPRF within a single parasite. *T. gondii* tachyzoites are estimated to be 7 μm long and 2 μM wide, therefore the volume of a single parasite can be calculated as:

Volume = 4/3 π (1/2 length) x $(1/2 \text{ width})^2$ = 1.47 x 10^{-11} ml

After calculating the amount of TgPRF within one parasite, the following equation was used to calculate the intracellular concentration of the protein (Rodrigues et al., 2002):

$$\text{Molarity (M)} = \frac{\text{protein concentration per cell in grams}}{\text{molecular weight in grams x } (1.47 \times 10^{-14} \text{ L})}$$

Time-based Ninety Degree Light Scattering

Purified recombinant actin was pre-centrifuged at 100,000g, 4°C, for 30 min using a TL100 rotor and a Beckman Optima TL ultracentrifuge (Becton Coulter, Fullerton, CA) to remove aggregates. TgACTI was diluted to 5 μM in G buffer and preincubated with 1 mM EGTA and 50 μM $MgCl_2$ for 10 min (to replace bound Ca^{2+} with Mg^{2+}). Samples were placed in a 100 μl cuvette (Submicro Quartz Fluorometer cell, Starna Cells, Atascadero, CA) and light scattering was monitored with the PTI Quantmaster spectrofluorometer (Photon Technology International, Santa Clara, CA): excitation 310 nm (1 nm bandpass), emission 310 nm (1 nm bandpass). Once a steady reading was obtained, the acquistition was paused and $1/10^{th}$ volume of 10X F-buffer (500mM KCl, 20mM $MgCl_2$, 10mM ATP) was added to induce polymerization. At the same time the F buffer was added, combinations of TgFRM1-FH1FH2, TgFRM2-FH1FH2 or TgPRF

were added. The acquisition was restarted and counts collected until the readings reached a plateau. Light scattering curves were smoothed by averaging 10 neighbors and normalized by subtracting the values of TgFRM1-FH1FH2, TgFRM2-FH1FH2 or TgPRF added to G buffer in the absence of TgACTI.

Sedimentation Analysis

Samples were prepared for light scattering analysis as described above and counts were read for the stated time. Following light scattering, the sample was transferred from the cuvette to a centrifuge tube and subsequently centrifuged at 100,000g or 350,000g for 1 hr at room temperature. Protein in the supernatant was precipitated in 2 volumes acetone overnight, centrifuged at 14,000 rpm for 30 min, washed with 70% ethanol followed by centrifugation at 14,000 for for 10 min. All pellets were resuspended in 1X sample buffer. Proteins were resolved on a 12% SDS-PAGE gels, stained with Sypro-Ruby (Molecular Probes), visualized using a FLA-5000 phosphorimager (Fuji Film Medical Systems), and quantitated using Image Gauge v4.23.

Fluorescence Microscopy

Purified recombinant TgACTI was clarified as described above and various concentrations were diluted to final molarity with $1/10^{th}$ 10X F buffer, treated with or without equimolar amounts of unlabeled phalloidin (Molecular Probes, Eugene, OR). In experiments to analyze formins, 25 μM TgACTI was incubated with 500nM TgFRM1-FH1FH2 or 50nM TgFRM2-FH1FH2. Final concentration of 0.33μM Alexa-488 phalloidin (Molecular Probes) was added to each sample to allow visualization of actin

filaments. Polymerization was then allowed to proceed for 1 hr at room temperature in the dark following which 6 μl of the reaction was placed on a slide and viewed with a Zeiss Axioskop (Carl Zeiss, Thornwood, NY) microscope using 63X Plan-NeoFluar oil immersion lens (1.30 NA). Images were collected using a Zeiss Axiocam with Axiovision v3.1. All Images were processed by linear adjustment in the same manner using Adobe Photoshop v8.0.

Nucleotide Exchange

Protocol used was as previously described (Mehta and Sibley, 2010). Briefly, purified recombinant TgACTI was clarified as described above and treated with 10% volume of 50% slurry 1X8 Cl (200-400 mesh, Sigma Aldrich) Dowex beads to remove ATP. Actin was then incubated with 500 μM 1,N^6-ethenoadenosine 5'triphosphate (εATP, Molecular Probes) for 1 hr at 4°C. Dowex beads were again added to removed unbound eATP followed by addition of 20 μM εATP to maintain the actin. εATP TgACTI was diluted to 1 μM, preincubated with varying concentrations of TgPRF for 10 min, Mg^{2+} was exchanged for Ca^{2+} with 1 mM EGTA and 50 μM $MgCl_2$ for 5 min. The sample was placed in a submicrocuvette and read in a PTI spectrofluorometer at 360 nm excitation and 410 nm emission until a steady reading was reached. 1.25 mM unlabeled ATP was then added to compete with the εATP and measurements were continued. The affinity of TgPRF for TgACTI was calculated by curve fitting using nonlinear regression analysis of first order exponential decay using Prism Software (GraphPad).

Statistical Analysis

Statistics were calculated in Excel or Prism (Graph Pad) using unpaired, two-tailed Student's *t*-tests for normally distributed data with equal variances. Significant differences were defined as $P \leq 0.05$.

ACKNOWLEDGEMENTS

We thank Nivedita Sahoo for assistance with the initial TgPRF characterization and are grateful to John Cooper and Marie-France Carlier for helpful suggestions. This work was supported by predoctoral fellowships from the American Heart Association (0815645G to KMS) and an Institutional Training Grant T32-AI007172 (to KMS), and a grant from the NIH (AI073155 to LDS, DS).

REFERENCES

Baum, J., Tonkin, C.J., Paul, A.S., Rug, M., Smith, B.J., Gould, S.B., Richard, D., Pollard, T.D., and Cowman, A.F. (2008). A malaria parasite formin regulates actin polymerization and localizes to the parasite-erythrocyte moving junction during invasion. Cell Host Microbe *3*, 188-198.

Carlsson, L., Nystrom, L.E., Sundkvist, I., Markey, F., and Lindberg, U. (1977). Actin polymerizability is influenced by profilin, a low molecular weight protein in non-muscle cells. J Mol Biol *115*, 465-483.

Daher, W., Plattner, F., Carlier, M.F., and Soldati-Favre, D. (2010). Concerted action of two formins in gliding motility and host cell invasion by *Toxoplasma gondii*. PLoS Pathog *6*.

Dobrowolski, J.M., Niesman, I.R., and Sibley, L.D. (1997). Actin in the parasite *Toxoplasma gondii* is encoded by a single copy gene, *ACT1* and exists primarily in a globular form. Cell Motil Cytoskel *37*, 253-262.

Dobrowolski, J.M., and Sibley, L.D. (1996). Toxoplasma invasion of mammalian cells is powered by the actin cytoskeleton of the parasite. Cell *84*, 933-939.

Gaskins, E., Gilk, S., DeVore, N., Mann, T., Ward, G.E., and Beckers, C. (2004). Identification of the membrane receptor of a class XIV myosin *Toxoplasma gondii*. J Cell Biol *165*, 383-393.

Gibbon, B.C., Kovar, D.R., and Staiger, C.J. (1999). Latrunculin B has different effects on pollen germination and tube growth. Plant Cell *11*, 2349-2363.

Gordon, J.L., and Sibley, L.D. (2005). Comparative genome analysis reveals a conserved family of actin-like proteins in apicomplexan parasites. BMC Genomics *6*, e179.

Harris, E.S., Rouiller, I., Hanein, D., and Higgs, H.N. (2006). Mechanistic differences in actin bundling activity of two mammalian formins, FRL1 and mDia2. J Biol Chem *281*, 14383-14392.

Higgs, H.N. (2005). Formin proteins: a domain-based approach. Trends Biochem Sci *30*, 342-353.

Jewett, T.J., and Sibley, L.D. (2003). Aldolase forms a bridge between cell surface adhesins and the actin cytoskeleton in apicomplexan parasites. Molec Cell *11*, 885-894.

Kovar, D.R., Yang, P., Sale, W.S., Drobak, B.K., and Staiger, C.J. (2001). Chlamydomonas reinhardtii produces a profilin with unusual biochemical properties. J Cell Sci *114*, 4293-4305.

Kucera, K., Koblansky, A.A., Saunders, L.P., Frederick, K.B., De La Cruz, E.M., Ghosh, S., and Modis, Y. (2010). Structure-based analysis of Toxoplasma gondii profilin: a parasite-specific motif is required for recognition by Toll-like receptor 11. J Mol Biol *403*, 616-629.

Kursula, I., Kursula, P., Ganter, M., Panjikar, S., Matuschewski, K., and Schuler, H. (2008). Structural basis for parasite-specific functions of the divergent profilin of Plasmodium falciparum. Structure *16*, 1638-1648.

Mehta, S., and Sibley, L.D. (2010). *Toxoplasma gondii* actin depolymerizing factor acts primarily to sequester G-actin. J Biol Chem *285*, 6835-6847.

Mehta, S., and Sibley, L.D. (2011). Actin depolymerizing factor controls actin turnover and gliding motility in Toxoplasma gondii. Molc Biol Cell *22*, 1290-1299.

Michelot, A., Derivery, E., Paterski-Boujemaa, R., Guerin, C., Huang, S., Parcy, F., Staiger, C.J., and Blanchoin, L. (2006). A novel mechanism for the formation of actin-filament bundles by a nonprocessive formin. Curr Biol *16*, 1924-1930.

Michelot, A., Guerin, C., Huang, S., Ingouff, M., Richard, S., Rodiuc, N., Staiger, C.J., and Blanchoin, L. (2005). The formin homology 1 domain modulates the actin nucleation and bundling activity of Arabidopsis FORMIN1. Plant Cell *17*, 2296-2313.

Pantaloni, D., and Carlier, M.F. (1993). How profilin promotes actin filament assembly in the presence of thymosin beta 4. Cell *75*, 1007-1014.

Perelroizen, I., Didry, D., Christensen, H., Chua, N.H., and Carlier, M.F. (1996). Role of nucleotide exchange and hydrolysis in the function of profilin in actin assembly. J Bio Chem *271*, 12302-12309.

Plattner, F., Yarovinsky, F., Romero, S., Didry, D., Carlier, M.F., Sher, A., and Soldati-Favre, D. (2008). *Toxoplasma* profilin is essential for host cell invasion and TLR11-dependent induction of an interleukin-12 response. Cell Host Microbe *3*, 77-87.

Rodrigues, C.O., Ruiz, F.A., Rohloff, P., Scott, D.A., and Moreno, S.N.J. (2002). Characterization of isolated acidocalcisomes from *Toxoplasma gondii* tachyzoites reveals a novel pool of hydrolyzable polyphosphate. J Biol Chem *277*, 48650-48656.

Romero, S., Le Clainche, C., Didry, D., Egile, C., Pantaloni, D., and Carlier, M.F. (2004). Formin is a processive motor that requires profilin to accelerate actin assembly and associated ATP hydrolysis. Cell *119*, 419-429.

Sagot, I., Rodal, A.A., Mosely, J., Goode, B.L., and Pellman, D. (2002). An actin nucleation mechanism mediated by bni1 and profilin. Nat Cell Biol *4*, 626 - 631.

Sahoo, N., Beatty, W.L., Heuser, J.E., Sept, D., and Sibley, L.D. (2006). Unusual kinetic and structural properties control rapid assembly and turnover of actin in the parasite *Toxoplasma gondii*. Mol Biol Cell *17*, 895-906.

Schmitz, S., Grainger, M., Howell, S.A., Calder, L.J., Gaeb, M., Pinder, J.C., Holder, A.A., and Veigel, C. (2005). Malaria parasite actin filaments are very short. J Mol Biol *349*, 113-125.

Schüler, H., and Matuschewski, K. (2006). Regulation of apicomplexan microfilament dynamics by minimal set of actin-binding proteins. Traffic *7*, 1433-1439.

Sibley, L.D. (2004). Invasion strategies of intracellular parasites. Science *304*, 248-253.

Snowman, B.N., Kovar, D.R., Shevchenko, G., Franklin-Tong, V.E., and Staiger, C.J. (2002). Signal-mediated depolymerization of actin in pollen during the self-incompatibility response. Plant Cell *14*, 2613-2626.

Staiger, C.J., and Blanchoin, L. (2006). Actin dynamics: old friends with new stories. Curr Opin Plant Biol *9*, 554-562.

Wetzel, D.M., Håkansson, S., Hu, K., Roos, D.S., and Sibley, L.D. (2003). Actin filament polymerization regulates gliding motility by apicomplexan parasites. Mol Biol Cell *14*, 396-406.

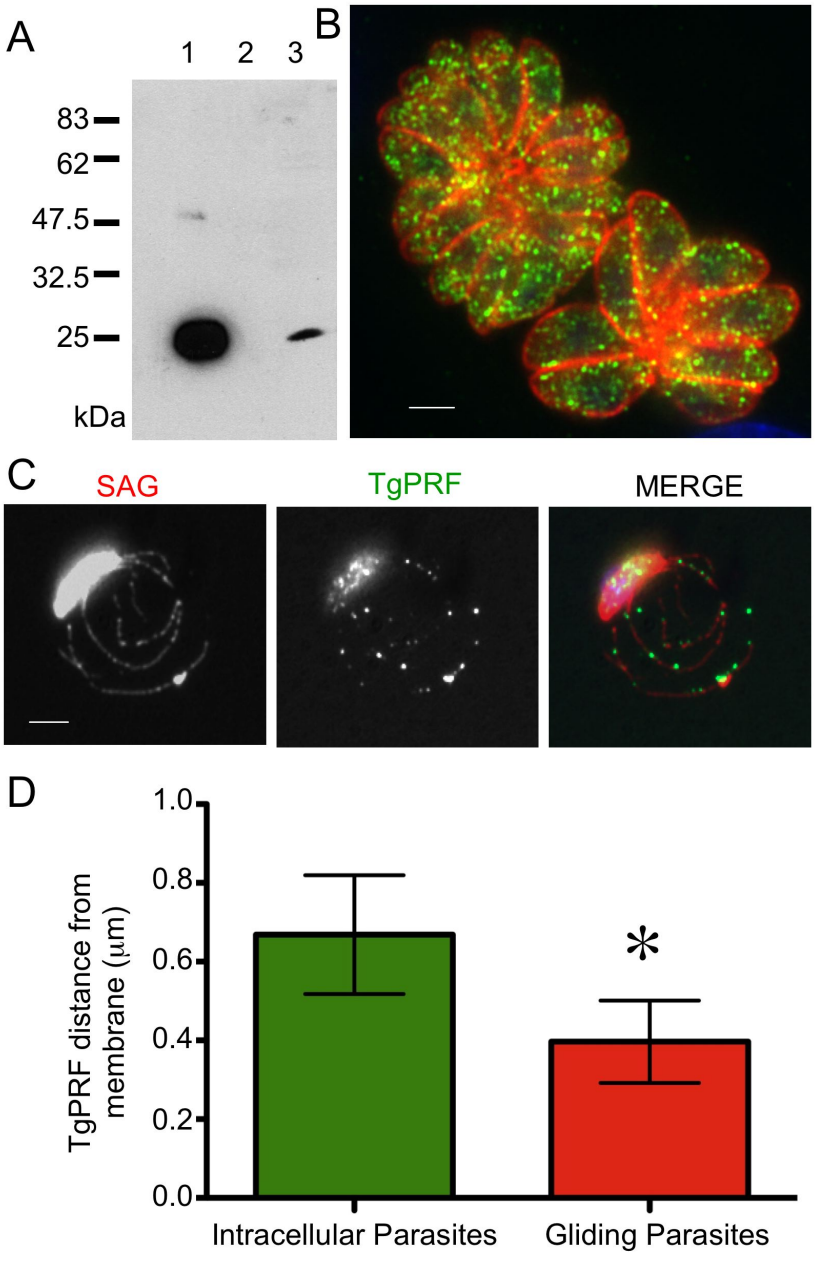
A
1
2
3
83
62
47.5
32.5
25
kDa
B
C
SAG
TgPRF
MERGE
D
TgPRF distance from membrane (μm)
1.0
0.8
0.6
0.4
0.2
0.0
*
Intracellular Parasites
Gliding Parasites

Figure 1. Expression and localization of TgPRF within *T. gondii*.

(A) Recombinant His-tagged TgPRF was purified on Ni-beads and used for polyclonal antibody production. The antibody was affinity purified and used to probe a Western blot where it detected recombinant TgPRF (lane 1), a band at the correct molecular weight for profilin from Toxoplasma lysate (lane 3), but nothing in host cell lysate (lane 2). (B) Localization of TgPRF within intracellular parasites using immunofluorescence microscopy with anti-TgPRF (green) and SAG1 (Surface antigen 1, red) to visualize the parasites. Scale bar, 2.5 μm. (C) Co-localization of TgPRF within protein trails of extracellular gliding parasites using immunofluorescence microscopy with anti-TgPRF (green) and SAG1 (red). Scale bar, 2.5 μm. (D) Quantitation of relocalization of TgPRF to parasite periphery during gliding. Distance of TgPRF from the parasite membrane was measured in intracellular parasites and extracellular gliding parasites. Average distance from the membrane for each condition is shown. * = Significantly less distance from membrane . Student's t-test $P < 0.0001$.

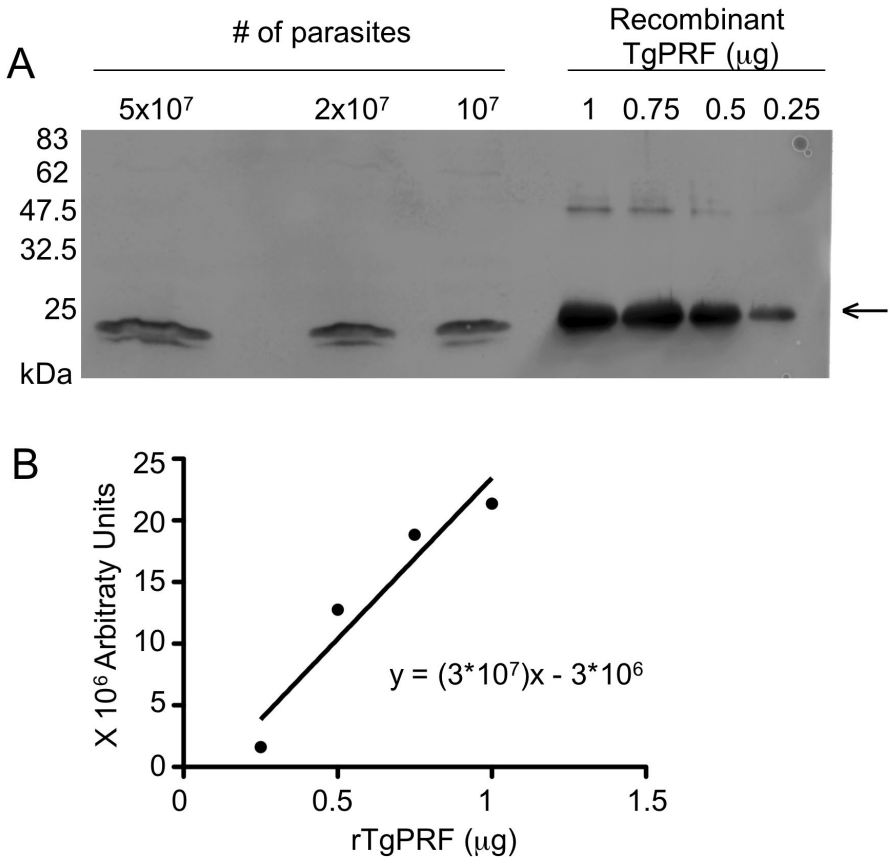

Figure 2. Calculation of intracellular concentration of TgPRF.

(A) Western blot to compare amount of TgPRF in parasite lysates to known concentrations of recombinant TgPRF. Parasite lysates and recombinant protein were resolved on a 12% SDS-PAGE gel, transferred to nitrocellulose and probed with rabbit αTgPRF. Arrow denotes TgPRF band. (B) Standard curve used to calculate amount of TgPRF within parasite lysate. Bands from Western in (A) were quantitated with a phosphorimager and used to calculate a standard curve from rTgPRF of known concentration. The rTgPRF values were fit with a linear regression curve.

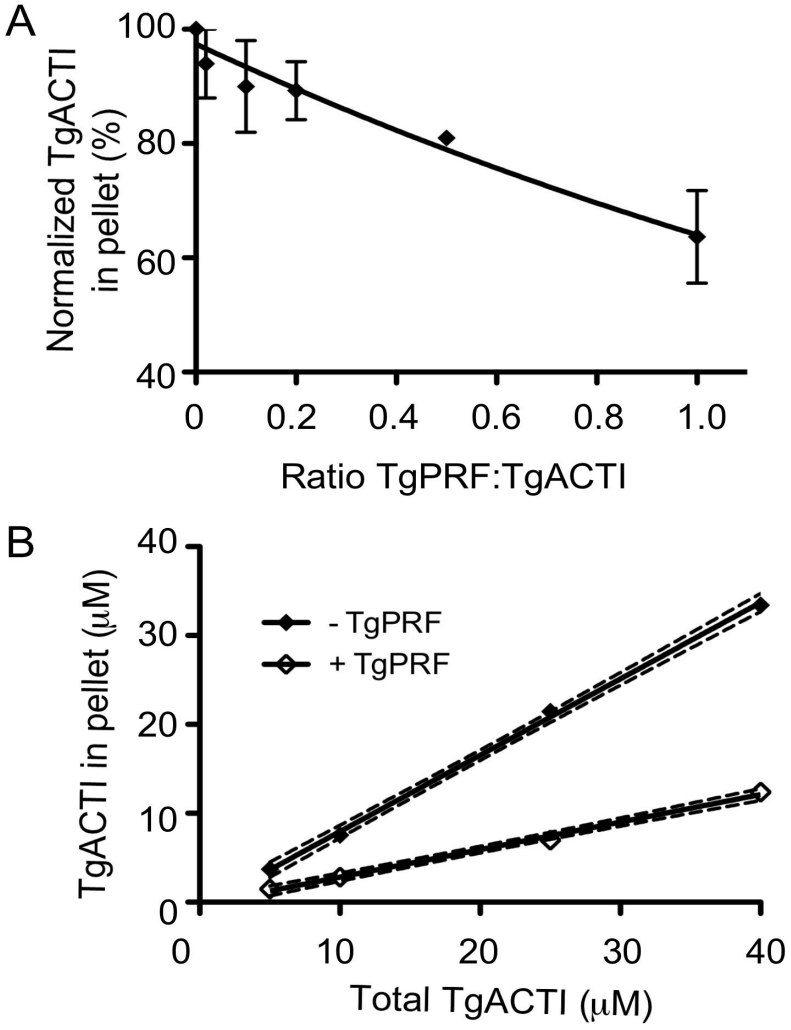
A
100
80
60
40
Normalized TgACTI in pellet (%)
0
0.2
0.4
0.6
0.8
1.0
Ratio TgPRF:TgACTI
B
40
30
20
10
0
TgACTI in pellet (μM)
- TgPRF
+ TgPRF
0
10
20
30
40
Total TgACTI (μM)

Figure 3. TgPRF acts to sequester TgACTI from polymerization.

(A) Sedimentation analysis of TgACTI polymerized with varying concentrations of TgPRF. 25 μM TgACTI was incubated in F buffer with TgPRF (0.1 –1 molar ratio) for 1.5 hr. Reactions were centrifuged at 350,000g, run on SDS-PAGE gels to determine the amount of protein in the pellet, stained with Sypro Ruby and visualized using a phosphoimager. Values were normalized to the amount of pelleted TgACTI in the absence of TgPRF. Means +/- S.D of three independent experiments are shown.

(B) Steady state sedimentation analysis of varying TgACTI concentrations polymerized with equimolar TgPRF. TgACTI was polymerized for 20 hrs +/- TgPRF, centrifuged at 350,000g, run on SDS-PAGE gels to determine the amount of protein in the pellet, stained with Sypro Ruby and visualized using a phosphorimager. 95% confidence interval of the best-fit line is shown. Data is combined from two independent experiments.

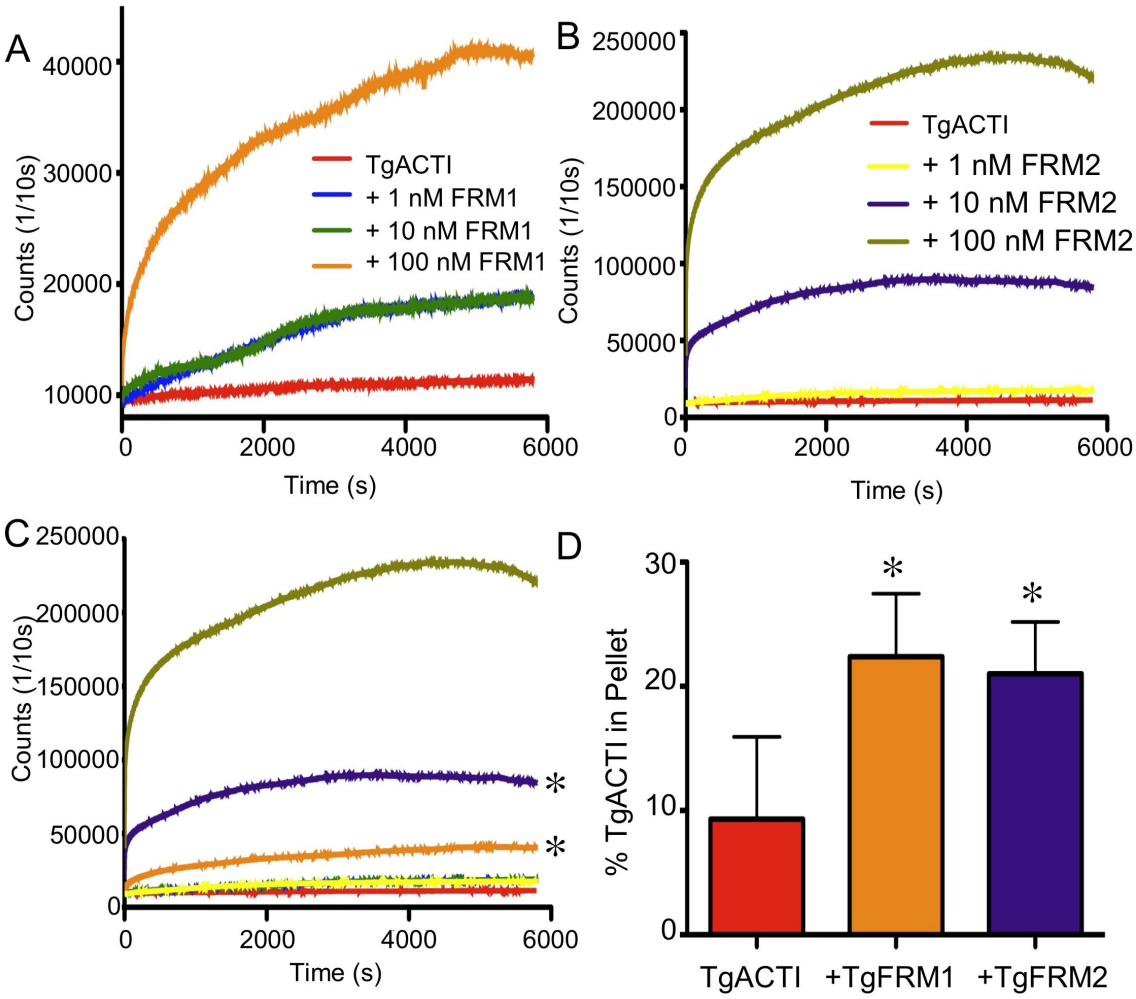
A
Counts (1/10s)
Time (s)
TgACTI
+ 1 nM FRM1
+ 10 nM FRM1
+ 100 nM FRM1
B
Counts (1/10s)
Time (s)
TgACTI
+ 1 nM FRM2
+ 10 nM FRM2
+ 100 nM FRM2
C
Counts (1/10s)
Time (s)
*
*
D
% TgACTI in Pellet
TgACTI
+TgFRM1
+TgFRM2
*
*

Figure 4. TgFRM1 and TgFRM2 enhance polymerization of TgACTI.

(A) Comparison of polymerization kinetics of TgACTI in the presence and absence of TgFRM1. Polymerization of 5 μM actin in F buffer alone (red) or with the addition of 1 μM (blue), 10 μM (green) or 100 μM (orange) TgFRM1 monitored by light scattering. Representative of 2 experiments. (B) Comparison of polymerization kinetics of TgACTI in the presence and absence of TgFRM2. Polymerization of 5 μM actin in F buffer alone (red) or with the addition of 1 μM (blue), 10 μM (green) or 100 μM (orange) TgFRM2 monitored by light scattering. Representative of 2 experiments. (C) Polymerization curves for TgACTI with addition of TgFRM1 or TgFRM2 plotted together for comparison of increase in polymerization kinetics. Concentrations chosen for subsequent experiments are denoted with asterisks. (D) Upon completion of light scattering, samples of TgACTI alone or in the presence of 100 nM TgFRM1 or 10 nM TgFRM2 were centrifuged for 1 hour at 100,000g to pellet actin filaments. Protein from the pellet or supernatants of all samples was resolved on a 12% SDS-PAGE gel, stained with SYPRO Ruby and quantified by phosphorimager analysis. The average percentage of protein in the pellet fraction from three replicate experiments is shown. Percent in the TgACTI pellet alone was compared to +TgFRM1 or +TgFRM2 and * denotes significance using Students two tailed t-test. $P < 0.05$.

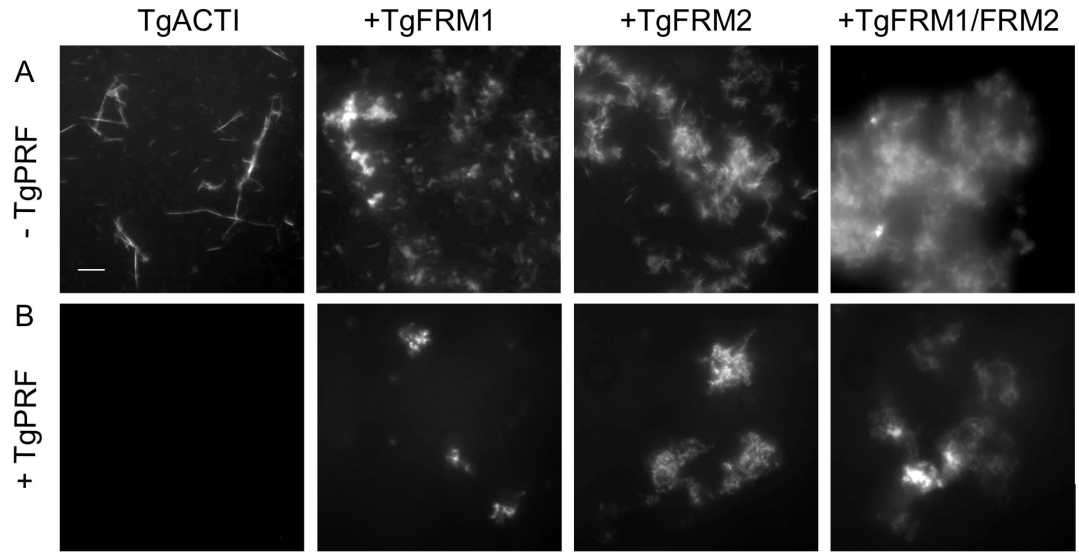

Figure 5. Influence of TgFRM1, TgFRM2, and TgPRF on formation of TgACTI filaments. (A) *In vitro* polymerization of TgACTI with formin. 25 μM TgACTI incubated in F buffer alone, with 500 nM TgFRM1, 50 nM TgFRM2, or 500 nM TgFRM1 with 50 nM TgFRM2 for 1 hour then visualized by fluorescence microscopy using 0.33 μM Alexa 488-phalloidin. (B) *In vitro* polymerization of TgACTI with formin and profilin. 25 μM TgACTI incubated in F buffer alone, with 500 nM TgFRM1, 50 nM TgFRM2, or 500 nM TgFRM1 with 50 nm TgFRM2 + 25 μM TgPRF for 1 hour then visualized by fluorescence microscopy using 0.33 μM Alexa 488-phalloidin. Scale bar, 5 μm. A representative of 2 similar experiments is shown.

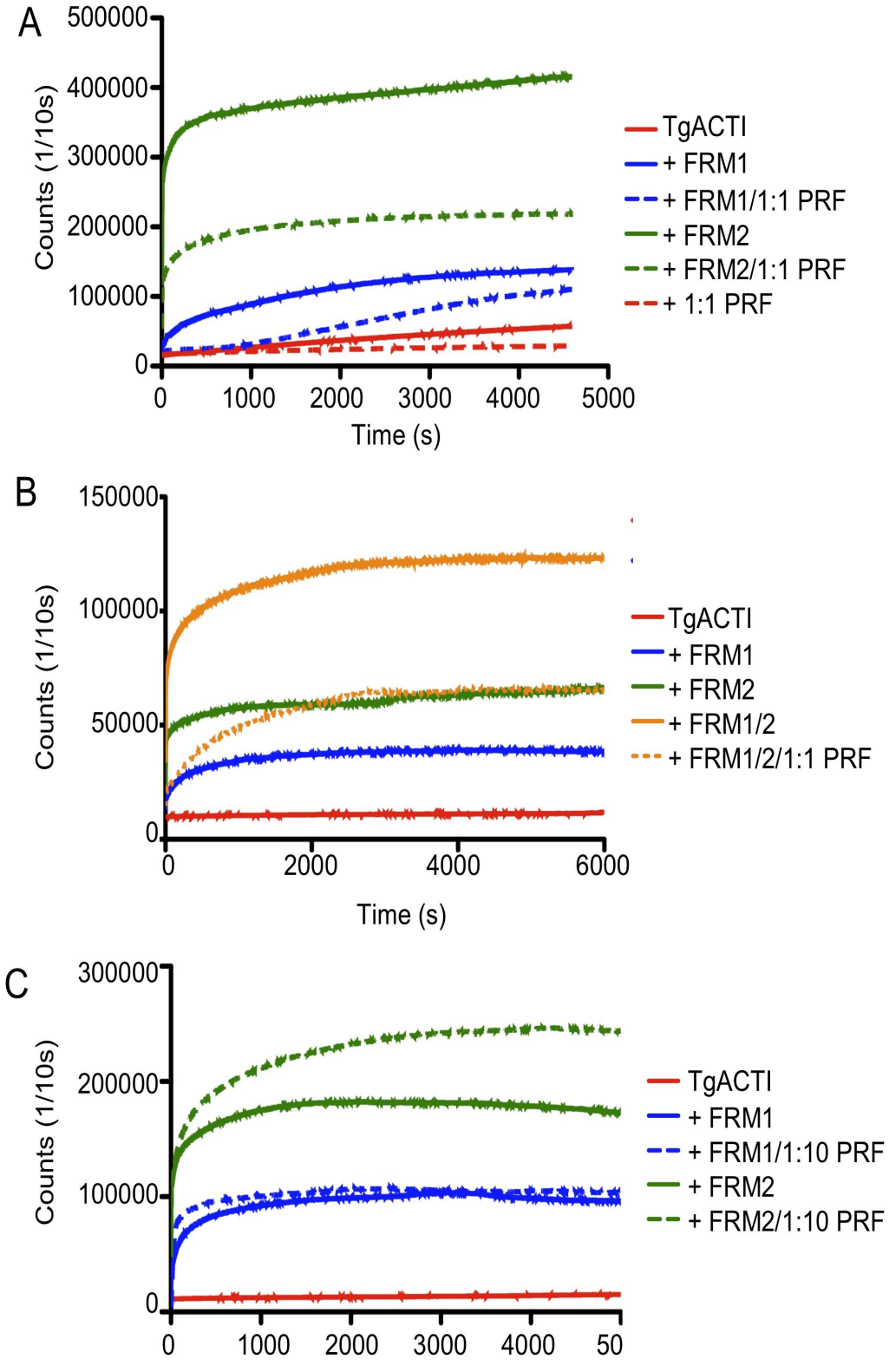
A
500000
400000
300000
200000
100000
0
Counts (1/10s)
0
1000
2000
3000
4000
5000
Time (s)
TgACTI
+ FRM1
+ FRM1/1:1 PRF
+ FRM2
+ FRM2/1:1 PRF
+ 1:1 PRF
B
150000
100000
50000
0
Counts (1/10s)
0
2000
4000
6000
Time (s)
TgACTI
+ FRM1
+ FRM2
+ FRM1/2
+ FRM1/2/1:1 PRF
C
300000
200000
100000
0
Counts (1/10s)
0
1000
2000
3000
4000
50
TgACTI
+ FRM1
+ FRM1/1:10 PRF
+ FRM2
+ FRM2/1:10 PRF

Figure 6. Effect of TgPRF on formin-mediated TgACTI polymerization.

(A) Comparison of polymerization kinetics of TgACTI in the presence or absence of formin with and without addition of equimolar TgPRF. Polymerization of 5 μM actin in F buffer alone (solid red), with 5 μM TgPRF (dashed red), with 100 nM TgFRM1 (solid blue), with 100 nM TgFRM1 and 5 μM TgPRF (dashed blue), with 10 nM TgFRM2 (solid green) or with 10 nM TgFRM2 and 5 μM TgPRF (dashed green) monitored by light scattering. (B) Comparison of polymerization kinetics of TgACTI in the presence or absence of TgFRM1 and TgFRM2 in combination with and without addition of TgPRF. Polymerization of 5 μM actin in F buffer alone (solid red), with 100 nM TgFRM1 (solid blue), with 10 nM TgFRM2 (solid green), with 100 nM TgFRM1 and 10 nM TgFRM2 (solid orange) or with 100 nM TgFRM1, 10 nM TgFRM2 and 5 μM TgPRF (dashed orange) monitored by light scattering. (C) Comparison of polymerization kinetics of TgACTI in the presence or absence of formin with and without addition of 1:10 concentration of TgPRF. Polymerization of 5 μM actin in F buffer alone (solid red), with 100 nM TgFRM1 (solid blue), with 100 nM TgFRM1 and 0.5 μM TgPRF (dashed blue), with 10 nM TgFRM2 (solid green) or with 10 nM TgFRM2 and 0.5 μM TgPRF (dashed green) monitored by light scattering. Representative data from 2 or 3 experiments are shown.

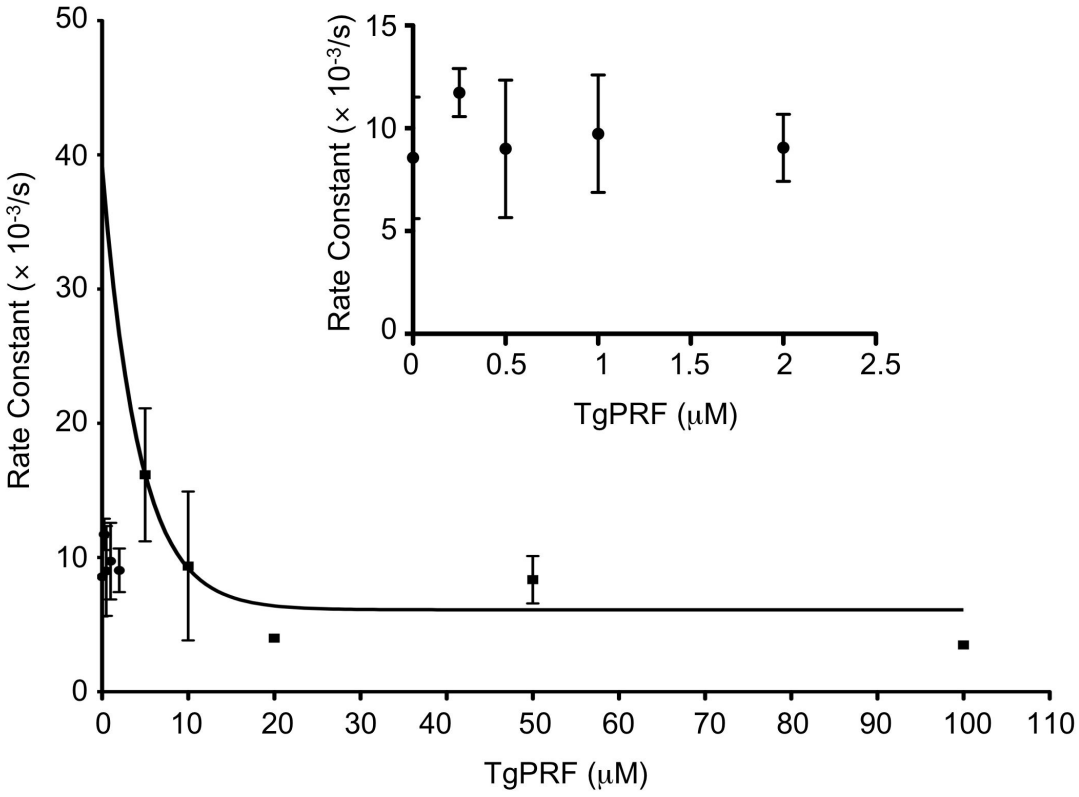

Figure 7. Nucleotide Exchange of TgACTI by TgPRF.

The effect of TgPRF on nucleotide exchange of TgACTI was examined using ε-ATP labeled TgACTI (1 μM) with various concentrations of TgPRF (0.25 μM – 100 μM) and examining the loss of fluorescence over time following addition of 1.25 mM unlabeled ATP. The initial rates of fluorescence loss were used to calculate rate constants and are plotted verses TgPRF concentration to obtain a curve of one phase decay. The effect of lower concentrations of TgPRF on TgACTI nucleotide exchange is expanded in the inset. Three independent experiments were averaged and values are mean +/- S.D.

Chapter V

Toxoplasma gondii Actin Undergoes Isodesmic Polymerization Rather than Nucleation-Elongation

PREFACE

Work presented in this chapter was conducted by KMS.

The first complete draft of this chapter was written by KMS. Comments from David Sibley were incorporated into the final version printed here.

ABSTRACT

Toxoplasma gondii is a protozoan pathogen that relies on actin polymerization for gliding motility, which powers its unique entry mechanism into host cells. Despite a requirement for actin filaments, studies with recombinant actin from *T. gondii* (TgACTI) have previously shown this actin forms filaments that are much shorter in length than those of conventional actins. Here, we demonstrate by fluorescence microscopy that at higher concentrations of protein, TgACTI is able to form filaments of more conventional length. However, the majority of TgACTI still fails to polymerize even at high concentrations as shown by sedimentation analysis and density centrifugation. Normally, actin filaments polymerize via a nucleation-elongation mechanism that utilizes cooperative assembly of filaments after formation of a trimeric nucleus, which is energetically favorable once the actin concentration reaches its critical concentration. The nucleation-elongation mechanism for polymerization is characterized by a lag phase, which is more pronounced at low protein concentration, and has a defined critical concentration for filament assembly above which elongation occurs. Analysis of TgACTI polymerization at varying protein concentrations revealed that TgACTI does not meet the criteria for filamentation via nucleation-elongation. Rather, these data indicate that TgACTI polymerizes in a concentration dependent manner that is most consistent with an isodesmic mode of polymerization. Isodesmic polymerization of TgACTI explains *in vivo* observations and suggests a fundamentally different regulatory mechanism for actin in protozoans.

INTRODUCTION

Toxoplasma gondii is a parasitic protozoan belonging to the phylum Apicomplexa. *T. gondii* is an obligate intracellular parasite and penetrates host cells in order to replicate within them. To accomplish entry, *T. gondii* utilizes an active gliding motility process that is dependent upon polymerization of its own actin into filaments (Dobrowolski and Sibley, 1996). Agents that influence actin polymerizaton such as the actin depolymerizing drug, cytochalasin-D, or the actin stabilizing agent, jasplakinolide, have a detrimental effect on the ability of *T. gondii* to enter into host cells (Dobrowolski and Sibley, 1996; Poupel and Tardieux, 1999; Wetzel et al., 2003). Despite a requirement for actin polymerization, sedimentation of *T. gondii* actin (TgACTI) from parasite lysates as well as *in vitro* polymerization studies with recombinant TgACTI, have demonstrated most parasite actin is unpolymerized or only forms short filaments (Dobrowolski and Sibley, 1996; Wetzel et al., 2003). In addition to its unconventional functional behavior, TgACTI contains a number of residues that diverge from conventional actins and shares only 83% sequence identity with mammalian muscle actin (Dobrowolski et al., 1997).

Conventional actins undergo cooperative assembly to polymerize head-to-tail into parallel helical strands that form filaments (Pollard et al., 2000). Polymerization is dependent on Mg^{2+}, salt (i.e. KCl), and ATP and only occurs when the actin concentration exceeds its critical concentration (Cc). Polymerization is initiated by a slow annealing step due to unstable dimer and trimer intermediates that fall apart resulting in a lag phase (Sept and McCammon, 2001). Once the protein concentration surpasses the Cc, nucleation is thermodynamically favored allowing nucleation followed by a rapid elongation phase (Pollard et al., 2000). Because elongation is highly efficient, long actin

filaments normally remain stable without the presence of small multimeric intermediates (Sept and McCammon, 2001). However, gradual hydrolysis of ATP and release of P_i increase disassembly from the pointed end, creating a pool of monomers (Pollard et al., 2000).

Similar to conventional actin, TgACTI also requires high salt, Mg^{2+} and ATP for polymerization (Sahoo et al., 2006). The polymerization of TgACTI was previously examined by tryptophan quenching and surprisingly, the Cc was calculated to be 0.04 μM, 3-4 fold lower than mammalian actin (Sahoo et al., 2006). Similar estimates were made from analyzing the amount of actin that pelleted at 100,000g (Sahoo et al., 2006). The low Cc suggests TgACTI initiates polymerization more readily, yet paradoxically, it only forms short, transient filaments *in vitro* (Sahoo et al., 2006). It was initially believed that this behavior could be explained by TgACTI having a greater capacity to initiate new filament formation but a reduced ability to establish inter-strand contacts and form stable filaments (Sahoo et al., 2006).

In contrast to a nucleation-elongation mechanism, polymers can form in an uncooperative manner via isodesmic polymerization, which does not require a nucleus for the initiation of filament formation (Miraldi et al., 2008; Oosawa and Kasai, 1962). While monomers that assemble cooperatively have a higher affinity for filament ends than for other monomers, in isodesmic polymerization, the affinity of monomers for filament ends does not change as the length of the filament grows (Miraldi et al., 2008). As the protein concentration increases, a range of filaments lengths are formed, resulting in an average polymer size that is shorter than those formed by a nucleation-elongation mechanism (Oosawa and Kasai, 1962). Additionally, during isodesmic polymerization

the population of both monomer and polymers increases with concentration, contrasting cooperative assembly where the monomer concentration plateaus upon reaching the Cc (Miraldi et al., 2008).

Actins undergoing nucleation-elongation are expected to rapidly assemble into filaments when the concentration exceeds the Cc. However, microscopy analyses have previously demonstrated TgACTI does not assemble into long filaments above its calculated Cc. This contradiction raises questions regarding the mechanism of TgACTI assembly into filaments. Here, we reexamined the ability of TgACTI to undergo polymerization via nucleation-elongation versus isodesmic polymerization.

RESULTS

TgACTI polymerizes more efficiently at higher concentrations

We have previously demonstrated that at a concentration of 5 μM, TgACTI fails to exhibit robust polymerization and requires the addition of phalloidin for filamentation (Chapter 1 and Figure 1A, B). However, when polymerization is allowed to proceed with higher concentrations of actin (10 μM, 25 μM or 40 μM), and monitored by light scattering, the protein undergoes more robust polymerization on its own in a dose-dependent manner (Figure 1A). Although there is a substantial increase in light scattering from 5 μM to 40 μM, even the polymerization at the highest concentration is significantly less robust than the kinetics observed for the conventionally studied actin, *Saccharomyces cerevisiae* actin (ScACT) (Chapter 2). Notably, upon addition of F buffer, there was no lag in the initiation of TgACTI polymerization. Consistent with the increase in light scattering, visualization of the filaments formed at these higher concentrations by fluorescence microscopy revealed longer filaments than what is observed at lower concentrations. (Figure 1B). TgACTI polymerized even more robustly in the presence of equimolar phalloidin, but it is clear that they do have increased ability to form filaments on their own when the concentration is sufficiently high.

TgACTI sediments only slightly more efficiently at higher concentration

When conventional actins are polymerized, the majority of the protein exists in long filaments and therefore sediments and is found in the pellet at 100,000g (Pardee and Spudich, 1982). Previous studies with TgACTI have reported that it requires higher force (i.e. 350,000g - 500,000g for 1 hour) for sedimentation following polymerization in F

buffer (Sahoo et al., 2006). We were interested to determine how sedimentation with higher force, or with addition of phalloidin, would influence polymerization of higher concentrations of TgACTI. When TgACTI at 5 μM was incubated in F buffer to induce polymerization and subsequently centrifuged at 100,000g, the majority of the protein remained in the supernatant, with only 29% in the pellet (Figure 2A). Addition of phalloidin at equimolar ratio shifted slightly more TgACTI to the pellet (61%) (Figure 2A). Centrifugation at 350,000g was sufficient to pellet the majority of TgACTI even in the absence of phalloidin (84%), demonstrating that this higher force efficiently sediments TgACTI oligomers. When TgACTI was polymerized in the presence of phalloidin and subsequently centrifuged at 350,000g, there was essentially no further sedimentation from that seen without phalloidin (90% TgACTI in the pellet). Surprisingly, at 30 μM the majority of TgACTI still remained in the supernatant after centrifugation at 100,000g (37% in pellet) (Figure 2B). Although more of the actin was pelleted than seen from 5 μM TgACTI, this increase was not significantly different (Student's t-test, $P = 0.26$). In contrast to the results of sedimentation at 5 μM, addition of phalloidin at 100,000g was sufficient to sediment nearly all of the TgACTI at 30 μM (90%). Centrifugation at 350,000g did not exhibit any further increase in pelletable actin with or without addition of phalloidin (90% versus 96%, respectively) (Figure 2B). The unusual behavior of TgACTI was not the result of baculovirus expression since ScACT was tested under the same conditions and more than 90% of the protein was found in the pellet regardless of the addition of phalloidin or speed of centrifugation (Figure 2C).

Sizing TgACTI filaments by density centrifugation

The sedimentation assays suggest that polymerized TgACTI filaments were of different size ranges than conventional actin. To evaluate this size distribution more fully, TgACTI was subjected to density centrifugation. When 5 μM TgACTI incubated in G buffer was run on the gradient, the majority of protein was found in a peak corresponding to the size expected for monomeric protein (Figure 3A, blue). Incubation of 5 μM TgACTI in F buffer shifted the protein slightly into higher fractions, although the majority was still in low molecular weight fractions (Figure 3A, red). A large low molecular weight peak was also seen following addition of phalloidin although a proportion of the actin (14.5%) was shifted to the pellet (Figure 3A, green). Similarly, 30 μM TgACTI incubated in G buffer showed a broad low molecular weight peak consistent with monomer and small oligomers (Figure 3B, blue). Incubation of 30 μM actin in F buffer resulted in spread of the protein along the gradient, although most protein still remained in lighter fractions (Figure 3B, red). However, addition of phalloidin to the F buffer incubation drove the 30 μM actin into the pellet (43.5%) with little remaining in lighter fractions of the gradient (Figure 3B, green).

In contrast to TgACTI, sucrose gradient analysis of ScACT gave results expected for conventional actin. In G buffer, the majority of the protein was found in fractions corresponding to monomeric protein (Figure 3C, blue). However, in F buffer, the majority of the protein was found in the pellet of the gradient, suggesting that most of the protein had polymerized into long filaments (Figure 3C, red).

In order to compare the efficiency of sedimentation to the fractions in the gradient, we determined the fractions in the gradients that correspond to the proportion of actin

found in the pellet at 100,000g and 350,000g (Figure 3, dashed line, solid line, respectively). This analysis indicates that oligomers < 4.0S sediment efficiently at 100,000g and yet only a minor percentage of TgACTI sediments (29% at 5 μM and 37% at 30 μM). In contrast, sedimentation at 350,000g sediments a majority of the smaller oligomers seen in TgACTI incubated in F buffer regardless of concentration. Collectively, these results are consistent with the presence of a stable population of small TgACTI oligomers in F-buffer.

TgACTI undergoes isodesmic polymerization

Using sedimentation analysis and tryptophan quenching, the critical concentration of TgACTI was previously determined to be 0.04 μM, which is three fold lower than that of conventional actins (Sahoo et al., 2006). Here, we have revisited the critical concentration in light of the observation that TgACTI polymerizes more robustly at higher concentrations than were used in the previous analysis. A range of protein concentrations from 0.25 to 40 μM were polymerized for 20 hours and the steady-state levels of polymerization were then measured by light scattering. A continued increase in polymerization versus protein concentration was observed and this data was best fit using a quadratic equation (Figure 4). The intercept of this curve crosses the x-axis at very low concentration, but there was no range where polymerization did not occur. Collectively, these results are inconsistent with a fixed critical concentration typical of a nucleation-elongation model, but rather resemble the kinetics of isodesmic polymerization.

To further examine the polymerization of TgACTI, we examined the amount of protein in the supernatant and pellet after centrifugation of various concentrations of

TgACTI at 100,000g. If TgACTI were undergoing nucleation-elongation, it would be expected that upon exceeding the Cc, the concentration of protein in the supernatant would plateau at the Cc (Oosawa and Kasai, 1962). Strikingly, this was not observed with TgACTI. Rather, the amount of protein in the supernatant continued to increase up to 40 μM TgACTI, the highest concentration tested (Figure 5, red). This response is again suggestive of an isodesmic mode of polymerization where increasing protein concentration results in increased polymerization.

DISCUSSION

Several features indicate TgACTI undergoes isodesmic polymerization rather than the more conventional nucleation-elongation process. First, a noticeable lack in a lag phase was not observed, which is inconsistent with a mechanism of cooperative assembly for formation of a nucleation step. Second, examination of the amount of TgACTI left in the supernatant after sedimentation with varying TgACTI concentrations revealed that the amount of unpolymerized TgACTI does not reach a plateau but rather increases continually with protein concentration. Third, density centrifugation shows evidence of small stable oligomers that would not be expected from nucleation-elongation. Collectively, these results suggest that TgACTI does not polymerize into by a nucleation-elongation model but is instead isodesmic.

Actins traditionally undergo cooperative assembly as evidenced by a lag phase in polymerization due to the unfavorable assembly of the required trimeric nucleus, formation of which is concentration dependent (Pollard et al., 2000). At protein concentrations exceeding the Cc, nucleation becomes favorable and elongation proceeds until reaching equilibrium between the monomeric state and actin filaments (Carlier, 1990). The remaining monomeric concentration at equilibrium is equal to the critical concentration (Carlier, 1990) and will be consistent regardless of the initial protein concentration.

Initial investigation of TgACTI polymerization reported a lag phase, albeit only at low concentration, and polymerization at low Cc, as determined by tryptophan quenching (Sahoo et al., 2006). When we repeated this analysis over a much wider range, it became more clear that there was no apparent critical concentration for TgACTI because the

unpolymerized TgACTI pool never reached a plateau but rather increased in a concentration dependent manner. We also did not observe a lag phase at any concentration tested. Instead, the properties of TgACTI fit an isodesmic process of polymerization where the distribution of actin monomers, oligomers and filaments are concentration dependent. At high concentration, some long filaments are formed, yet these are still a minority as seen in sedimentation analysis and density centrifugation.

Prokaryotic actins have also been described to have unconventional polymerization properties. For example, the bacterial actin homolog MreB forms both single stranded helices and linear protofilaments (Popp et al., 2010; van den Ent et al., 2001). However, polymerization of MreB occurs by nucleation-elongation and a critical concentration of ~ 900 nM has been determined for MreB from *Bacillus subtilis* (Mayer and Amann, 2009). The polymerization properties of TgACTI differ from both conventional actins and prokaryotic actin. To our knowledge, this is the first example of an actin that undergoes a mechanism other than cooperative assembly. It is possible that other unconventional actins may also undergo isodesmic polymerization. For example, many plant actins that maintain a highly monomeric state (Gibbon et al., 1999; Snowman et al., 2002) and actin from *Giardia intestinalis* that has been observed to form conventional helical filaments as well as single protofilaments (Paredez et al., 2011).

Questions remain as to the *in vivo* implications of the finding that TgACTI undergoes isodesmic polymerization. First, isodesmic polymerization occurs in a dose-dependent manner suggesting that the extent of polymerization will depend on available subunits. Recent calculations estimate the intracellular TgACTI concentration to be around 40 μM (Mehta and Sibley, 2011) which according to our current findings would suggest

filaments should be seen within the parasite. However, actin-binding proteins within *T. gondii* such as profilin (Chapter 4) and actin depolymerizing factor (Mehta and Sibley, 2011) function primarily to sequester the majority of TgACTI, restricting the pool of free monomers available to polymerize into long filaments *in vivo*.

Secondly, isodesmic polymerization also suggests that lateral contacts between individual TgACTI protofilaments within an actin helix play a minor role in filament interactions compared to longitudinal contacts between individual monomers. Weak lateral contacts within TgACTI have previously been predicted by molecular modeling and introduction of mutations into TgACTI to strengthen inter-monomer contacts resulted in longer, more stable filaments (Chapter 3). Weak lateral contacts are further supported by demonstration that addition of phalloidin to recombinant TgACTI increases filament size and stability, likely by stabilizing interactions between protomers (Chapter 2). Additionally, the presence of actin-binding proteins *in vivo* may act to stabilize interactions and drive the individual protofilaments into more stable helical conformations as well as bundles by strengthening these lateral contacts. One family of candidate proteins that may provide this function *in vivo* is formins. Experiments to analyze the role of *T. gondii* formin on heterologous chicken skeletal actin demonstrate these proteins participate in actin filament polymerization (Daher et al., 2010). However, if TgACTI undergoes isodesmic polymerization, there is no need for a nucleation step and formin may instead be contributing to the stability of the TgACTI filament through binding to the barbed end or by binding to the side of the filament as has been seen with mammalian and plant formins (Harris et al., 2006; Michelot et al., 2005). An *in vivo* role

for formin in stabilizing TgACTI filaments is consistent with the finding that TgACTI polymerization is greatly enhanced in the presence of formin (Chapter 4).

The realization that TgACTI undergoes isodesmic polymerization explains several perplexing behaviors of actin *in vivo*. First, homologs of the nucleating protein, Arp 2/3, have not been identified within the *T. gondii* genome (Gordon and Sibley, 2005) consistent with the lack of nucleation required for isodesmic polymerization. Second, following centrifugation of *T. gondii* lysate at 100,000g, the majority of TgACTI remains in the supernatant and higher speeds (350,000g) were required to sediment the protein suggesting TgACTI exists as monomers or smaller oligomers (Dobrowolski et al., 1997; Sahoo et al., 2006; Wetzel et al., 2003). Finally, *T. gondii* lacks long, stable TgACTI filaments based on microscopy examination (Wetzel et al., 2003) (Chapter 3). Collectively, this behavior implies the population of differentially sized oligomers are functionally important in parasites rather than a population of monomers versus highly stable, long filaments, typical of mammalian cells.

MATERIALS AND METHODS

Ninety Degree Light Scattering

Purified recombinant actin was clarified by centrifugation at 100,000g, 4°C, for 30 min using a TL100 rotor and a Beckman Optima TL ultracentrifuge (Becton Coulter, Fullerton, CA) to remove aggregates. TgACTI was diluted to the desired concentration in G buffer (5 mM Tris-Cl, pH 8.0, 0.2 mM $CaCl_2$, 0.2 mM ATP, 0.5 mM DTT) and preincubated with 1 mM EGTA and 50 μM $MgCl_2$ for 10 min (to replace bound Ca^{2+} with Mg^{2+}). Samples were placed in a 100 μl cuvette (Submicro Quartz Fluorometer cell, Starna Cells, Atascadero, CA) and light scattering was monitored with the PTI Quantmaster spectrofluorometer (Photon Technology International, Santa Clara, CA): excitation 310 nm (1 nm bandpass), emission 310 nm (1 nm bandpass). Once a steady reading was obtained, the acquisition was paused and $1/10^{th}$ volume of 10X F-buffer (500 mM KCl, 20 mM $MgCl_2$, 10 mM ATP) was added to induce polymerization. Light scattering counts were averaged with 10 neighbors to smooth curves using Prism.

Fluorescence Microscopy

Purified recombinant TgACTI was clarified as described above, diluted to final molarity with $1/10^{th}$ 10X F buffer and treated with or without equimolar amounts of unlabeled phalloidin (Molecular Probes, Eugene, OR). Final concentration 0.33 μM Alexa-488 phalloidin (Molecular Probes) was added to each sample and polymerization was allowed to proceed for 1 hr at room temperature in the dark following which 6 μl of the reaction was placed on a slide and viewed with a Zeiss Axioskop (Carl Zeiss, Thornwood, NY) microscope using 63X Plan-NeoFluar oil immersion lens (1.30 NA). Images were

collected using a Zeiss Axiocam with Axiovision v3.1. All Images were processed by linear adjustment in the same manner using Adobe Photoshop v8.0 (San Jose, CA).

Actin Sedimentation Assays

Purified recombinant TgACTI and ScACT proteins were clarified as described above and incubated in F buffer to initiate polymerization for 1 hr in the presence or absence of equimolar amounts of phalloidin (Molecular Probes) at room temperature. The samples were subsequently centrifuged at 100,000g or 350,000g for 1 hr at room temperature. Protein in the supernatant was acetone precipitated and washed with 70% ethanol. All pellets were resuspended in 1X sample buffer. Proteins were resolved on a 12% SDS-PAGE gels, stained with Sypro-Ruby (Molecular Probes), visualized using a FLA-5000 phosphorimager (Fuji Film Medical Systems), and quantitated using Image Gauge v4.23.

Density Centrifugation

Purified recombinant TgACTI or ScACT were clarified as described above, pre-incubated with 1 mM EGTA and 50 μM $MgCl_2$ for 10 min (to replace bound Ca^{2+} with Mg^{2+}). TgACTI or ScACT were then incubated in G buffer, F buffer or F buffer supplemented with equimolar phalloidin (Molecular Probes) for 1 hr at room temperature. Samples were placed on the top of an 11 ml 5-40% continuous sucrose gradient made in the corresponding buffer and generated with a gradient maker and Auto Densi-Flow Gradient Fractionator (LabConco, Kansas City, MO) and centrifuged at 100,000g, 4°C for 20 hrs using a SW41 rotor in a L-80 ultracentrifuge (Beckman Coulter). Amersham HMW Calibration kit for native electrophoresis (GE Healthcare,

Buckinghamshire, UK) containing bovine serum albumin, 4.4S, lactate dehydrogenase, 7S, catalase, 11.4S, thyroglobulin, 19.4S was resuspended in 500 µl G-buffer and used as molecular weight markers. Fractions were collected, the specific gravity of each was measured using a refractometer (Sper Scientific, Scottsdale, AZ), and then precipitated in 10% TCA for 1 hr. The precipitated protein was washed with 500 µl acetone, air dried, resuspended in 1X sample buffer, run on 12% SDS-PAGE gels, stained with Sypro-Ruby (Molecular Probes), visualized using a FLA-5000 phosphorimager (Fuji Film Medical Systems) and quantitated using Image Gauge v4.23.

Steady State Polymerization

Purified recombinant TgACTI was clarified as described above, diluted to a range of concentrations in F buffer and incubated at room temperature for 20 hours. Samples were placed in a 100 µl cuvette (Submicro Quartz Fluorometer cell, Starna Cells, Atascadero, CA) and monitored by light scattering using a PTI Quantmaster spectrofluorometer (Photon Technology International, Santa Clara, CA): excitation 310 nm (1 nm bandpass), emission 310 nm (1 nm bandpass). An average reading was plotted vs protein concentration and fit with a best-fit line.

ACKNOWLEDGEMENTS

We are grateful to John Cooper and Dave Sept for helpful comments and suggestions. We thank Jennifer Gordon for experimental advice regarding density centrifugation. Supported by predoctoral fellowships from the American Heart Association (0815645G to K.M.S.) and an Institutional Training Grant T32-AI007172 (to K.M.S.), and a grant from the NIH (AI073155 to L.D.S, D.S).

REFERENCES

Carlier, M.F. (1990). Actin polymerization and ATP hydrolysis. Adv Biophys *26*, 51-73.

Daher, W., Plattner, F., Carlier, M.F., and Soldati-Favre, D. (2010). Concerted action of two formins in gliding motility and host cell invasion by *Toxoplasma gondii*. PLoS Pathog *6*.

Dobrowolski, J.M., Niesman, I.R., and Sibley, L.D. (1997). Actin in the parasite *Toxoplasma gondii* is encoded by a single copy gene, *ACT1* and exists primarily in a globular form. Cell Motil Cytoskel *37*, 253-262.

Dobrowolski, J.M., and Sibley, L.D. (1996). Toxoplasma invasion of mammalian cells is powered by the actin cytoskeleton of the parasite. Cell *84*, 933-939.

Gibbon, B.C., Kovar, D.R., and Staiger, C.J. (1999). Latrunculin B has different effects on pollen germination and tube growth. Plant Cell *11*, 2349-2363.

Gordon, J.L., and Sibley, L.D. (2005). Comparative genome analysis reveals a conserved family of actin-like proteins in apicomplexan parasites. BMC Genomics *6*, e179.

Harris, E.S., Rouiller, I., Hanein, D., and Higgs, H.N. (2006). Mechanistic differences in actin bundling activity of two mammalian formins, FRL1 and mDia2. J Biol Chem *281*, 14383-14392.

Mayer, J.A., and Amann, K.J. (2009). Assembly properties of the Bacillus subtilis actin, MreB. Cell Motil Cytoskeleton *66*, 109-118.

Mehta, S., and Sibley, L.D. (2011). Actin depolymerizing factor controls actin turnover and gliding motility in Toxoplasma gondii. Molc Biol Cell *22*, 1290-1299.

Michelot, A., Guerin, C., Huang, S., Ingouff, M., Richard, S., Rodiuc, N., Staiger, C.J., and Blanchoin, L. (2005). The formin homology 1 domain modulates the actin nucleation and bundling activity of Arabidopsis FORMIN1. Plant Cell *17*, 2296-2313.

Miraldi, E.R., Thomas, P.J., and Romberg, L. (2008). Allosteric models for cooperative polymerization of linear polymers. Biophys J *95*, 2470-2486.

Oosawa, F., and Kasai, M. (1962). A theory of linear and helical aggregations of macromolecules. J Mol Biol *4*, 10-21.

Pardee, J.D., and Spudich, J.A. (1982). Purification of muscle actin. Methods Cell Biol *24*, 271-289.

Paredez, A.R., Assaf, Z.J., Sept, D., Timofejeva, L., Dawson, S.C., Wang, C.J.R., and Cande, W.J. (2011). An actin cytoskeleton with evolutionaryly conserved functions in the absence of cannonical actin-binding protiens. PNAS (USA) *in press*.

Pollard, T.D., Blanchoin, L., and Mullins, R.D. (2000). Molecular mechanisms controlling actin filament dynamics in nonmuscle cells. Annu Rev Biophys Biomol Struct *29*, 545 - 576.

Popp, D., Narita, A., Maeda, K., Fujisawa, T., Ghoshdastider, U., Iwasa, M., Maeda, Y., and Robinson, R.C. (2010). Filament structure, organization, and dynamics in MreB sheets. J Biol Chem *285*, 15858-15865.

Poupel, O., and Tardieux, I. (1999). *Toxoplasma gondii* motility and host cell invasiveness are drastically impaired by jasplakinolide, a cyclic peptide stabilizing F-actin. Microb Infect *1*, 653-662.

Sahoo, N., Beatty, W.L., Heuser, J.E., Sept, D., and Sibley, L.D. (2006). Unusual kinetic and structural properties control rapid assembly and turnover of actin in the parasite *Toxoplasma gondii*. Mol Biol Cell *17*, 895-906.

Sept, D., and McCammon, J.A. (2001). Thermodynamics and kinetics of actin filament nucleation. Biophys J *81*, 667-674.

Snowman, B.N., Kovar, D.R., Shevchenko, G., Franklin-Tong, V.E., and Staiger, C.J. (2002). Signal-mediated depolymerization of actin in pollen during the self-incompatibility response. Plant Cell *14*, 2613-2626.
van den Ent, F., Amos, L.A., and Lowe, J. (2001). Prokaryotic origin of the actin cytoskeleton. Nature *413*, 39-44.

Wetzel, D.M., Hakansson, S., Hu, K., Roos, D., and Sibley, L.D. (2003). Actin filament polymerization regulates gliding motility by apicomplexan parasites. Mol Biol Cell *14*, 396-406.

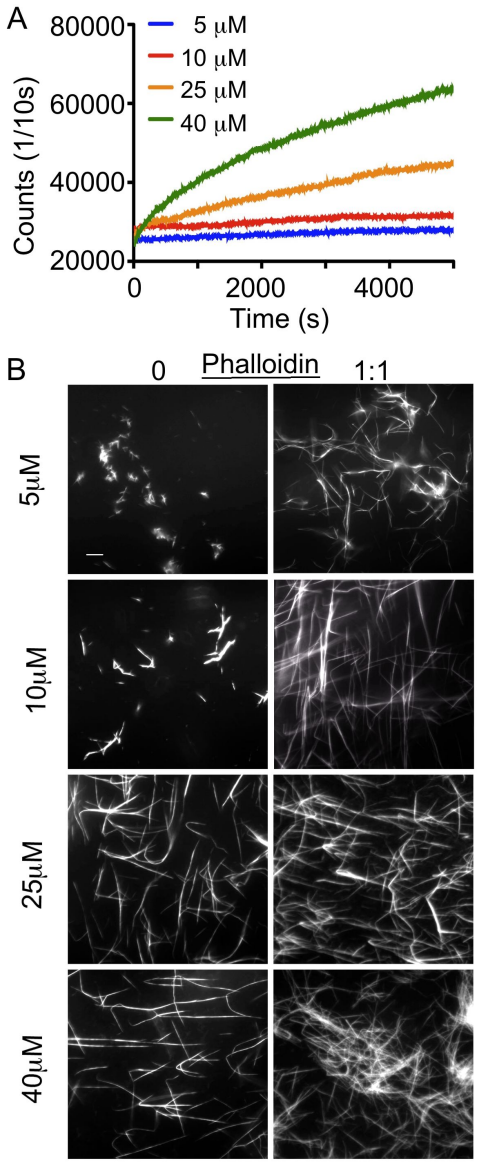

Figure 1. TgACTI polymerization at varying protein concentration.

(A) Comparison of polymerization kinetics. F buffer was added to induce polymerization that was monitored by light scattering. (B) *In vitro* polymerization of TgACTI at varying protein concentrations as visualized by fluorescence microscopy using 0.33 μM Alexa 488-phalloidin +/- equimolar amounts of unlabeled phalloidin (1:1). Scale bars, 5 μm. Representative of three or more similar experiments.

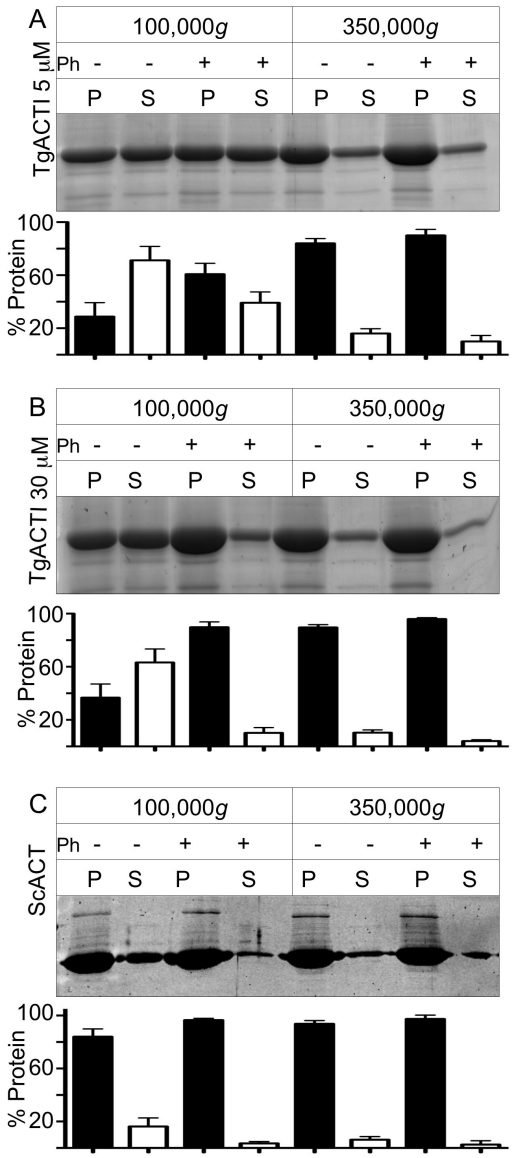

Figure 2. Sedimentation analysis of parasite (TgACTI) and yeast (ScACT) actins. (A) 5 μM or (B) 30 μM purified TgACTI was polymerized in F-buffer +/- equimolar phalloidin and centrifuged at 100,000g or 350,000g. Protein in the pellet or supernatant of all samples was resolved on a 12% SDS-PAGE gel, stained with SYPRO Ruby and quantified by phosphorimager analysis. (C) 5 μM ScACT was sedimented under the same conditions. The graphs above represent averages of 3 or more experiments with mean +/- S.D. and a representative gel is shown.

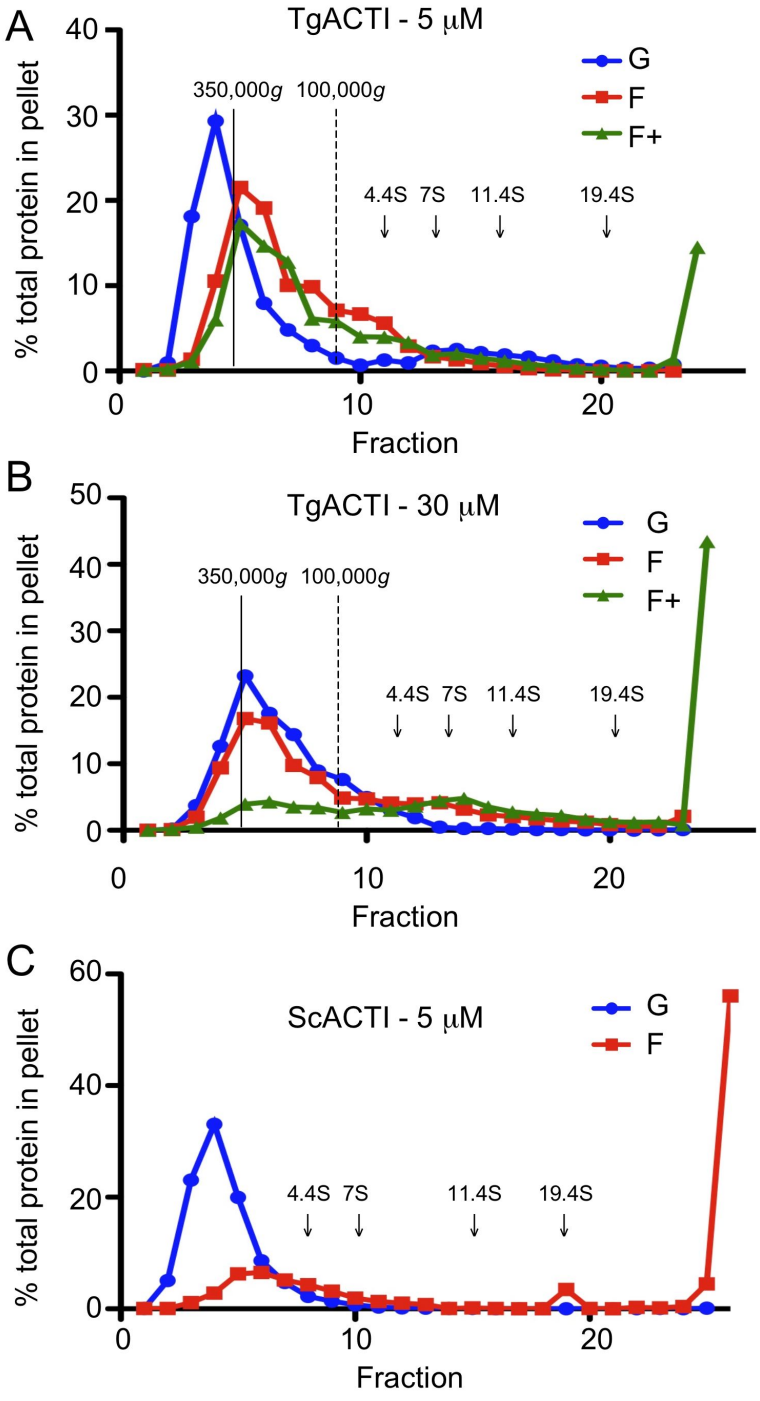
A
TgACTI - 5 μM
% total protein in pellet
350,000g
100,000g
G
F
F+
4.4S
7S
11.4S
19.4S
Fraction
B
TgACTI - 30 μM
% total protein in pellet
350,000g
100,000g
G
F
F+
4.4S
7S
11.4S
19.4S
Fraction
C
ScACTI - 5 μM
% total protein in pellet
G
F
4.4S
7S
11.4S
19.4S
Fraction

Figure 3. Size determination of TgACTI filaments by density centrifugation. (A) 5 μM TgACTI was incubated in G buffer (blue), F buffer (red) or F buffer with equimolar phalloidin (green) for 1 hr was placed on a 5-40% sucrose gradient made of the corresponding buffer and centrifuged at 100,000g for 20 hrs. Fractions were collected, precipated with 10% TCA and resolved on a 12% SDS-PAGE gel. This was repeated with (B) 30 μM TgACTI and (C) ScACT. The dashed black line corresponds to TgACTI oligomers expected to pellet at 100,000g based on sedimentation assays (Figure 3). The solid black line corresponds to TgACTI oligomers expected to pellet at 350,000g based on sedimentation assays. Protein standard markers (bovine serum albumin, 4.4S, lactate dehydrogenase, 7S, catalase, 11.4S, thyroglobulin, 19.4S) run in G buffer are denoted with black arrows. Representative of 2 similar experiments.

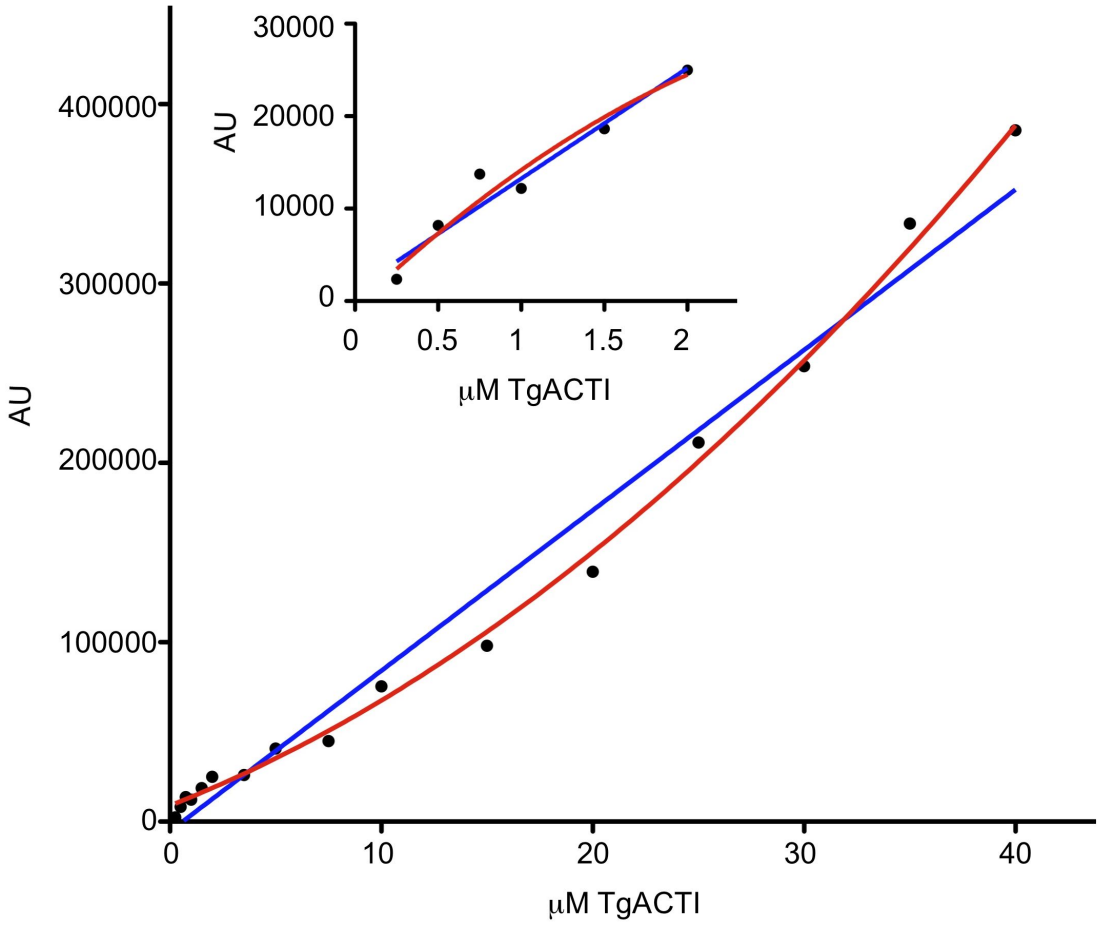

Figure 4. Determination of TgACTI polymerization versus concentration based on light scattering.

Increasing concentrations of TgACTI were incubated in F-buffer for 20 hours to allow polymerization to reach steady state and then monitored by ninety degree light scattering to determine the extent of polymerization. The values obtained were plotted against the protein concentration and a linear regression curve (blue) or quadratic curve (red) used to plot the relationship. Data points are averages from 2 or more experiments. Points from lower concentrations are expanded in inset.

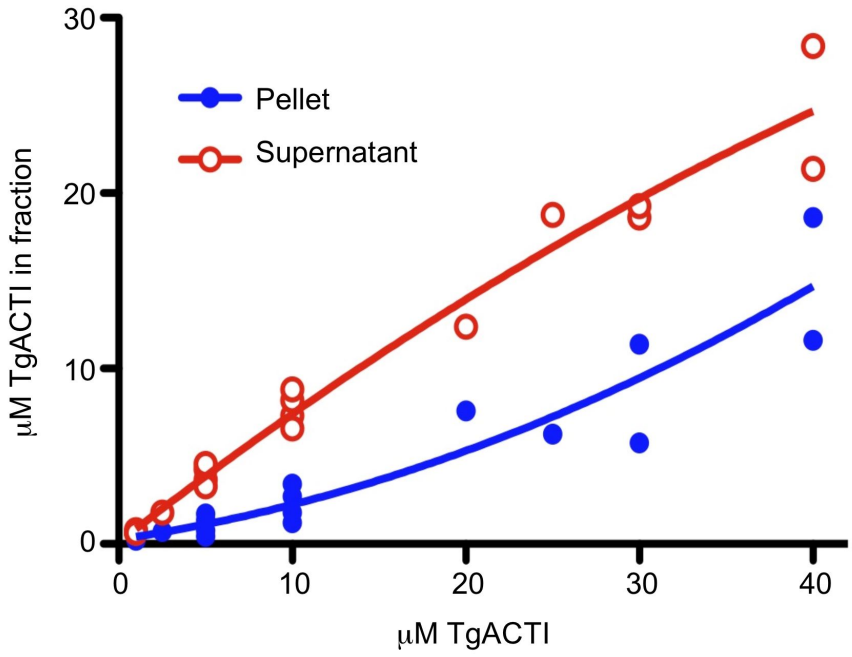

Figure 5. Comparison of extent of TgACTI polymerization versus concentration based on protein sedimentation.

Varying concentrations of purified TgACTI was polymerized in F-buffer and centrifuged at 100,000g. Protein in the pellet or supernatant of all samples was resolved on a 12% SDS-PAGE gel, stained with SYPRO Ruby and quantified by phosphorimager analysis. The molar amounts of protein in the pellet (blue) or supernatant (red) was plotted versus concentration and fit with a quadratic nonlinear regression. Data is combined from 3 experiments.

Chapter VI

Conclusions and Future Directions

This chapter was composed entirely by Kristen Skillman. Comments from David Sibley were incorporated into the final version printed here.

CONCLUSIONS

As obligate intracellular pathogens, apicomplexan parasites must enter into host cells to establish their replicative niche. Rather than relying on host cell phagocytosis for uptake and thereby alerting the host immune system, these parasite have evolved an active mechanism for host cell entry that is dependent on their own proteins for motility and allows entry into a protective compartment. Apicomplexan motility, termed gliding motility, is unique to the members of the phylum and differs from other forms of locomotion that involve flagella or amoeboid gliding. Rather, gliding motility depends on the actomyosin motor of the parasite, located within the inner membrane space of the parasite and linked to extracellular adhesins in contact with the host cell membrane. According to the currently proposed model, for gliding motility to occur, parasite actin must assemble into filaments that are translocated by the myosin motors toward the posterior of the cell (Sibley, 2004). However, examination of actin within both *Toxoplasma gondii* and *Plasmodium falciparum* has revealed this actin is unusual in the sense it does not polymerize into conventional filaments. Apicomplexan actins have been shown to be highly unpolymerized while the parasite is growing intracellularly (Dobrowolski and Sibley, 1996; Schmitz et al., 2005) and attempts to visualize polymerization of recombinant parasite actin have revealed the filaments formed are very short and potentially unstable (Sahoo et al., 2006; Schmitz et al., 2005; Schüler et al., 2005). Additionally, when *T. gondii* is treated with the stabilizing agent, jasplakinolide (JAS), the parasite was found to be unable to invade host cells and continue its life cycle (Poupel and Tardieux, 1999; Wetzel et al., 2003). More in depth analysis of this defect revealed the rate of motility of JAS treated parasites was actually increased but the

parasites lost their sense of directionality thereby impeding host cell invasion (Wetzel et al., 2003). Stabilization of parasite actin filaments appears to be toxic to the parasite, therefore, the formation of short filaments *in vitro* may reveal a critical role for short filaments *in vivo*.

Although previous attempts to visualize filaments within the parasite have failed, EM examination of protein left behind in trails of gliding parasites revealed filamentous structures that disappeared upon treatment with cytochalasin-D (CytD), consistent with actin filaments (Wetzel et al., 2003). The transient assembly of actin filaments suggests that filament formation is tightly regulated so filaments do not form unless the parasites are undergoing gliding motility. Searches of the apicomplexan genome have revealed the presence of a minimal set of actin-binding proteins that could potentially play a critical role in this regulation (Schüler and Matuschewski, 2006). Two specific contenders are profilin and formin of which isoforms have been found and purified from apicomplexan parasites. Mechanistic studies with both proteins in combination with heterologous actin revealed they function as canonical regulators. *T. gondii* profilin (TgPRF) promoted polymerization at rabbit actin barbed but not pointed ends while *T. gondii* formins (TgFRM1 and TgFRM2) enhanced nucleation of rabbit actin (Baum et al., 2008; Daher et al., 2010; Plattner et al., 2008).

Although numerous studies have been conducted to examine parasite actin filament formation and its regulation, the mechanism leading to limited polymerization kinetics and short filament formation remains elusive. Previous studies have not addressed whether reduced TgACTI polymerization is an intrinsic property within the actin itself, a consequence of interaction with regulatory proteins within the parasite, or most likely, if

it is a combination of both. The goal of this thesis was to address both of these questions with more in depth studies of polymerization of parasite actins as well as a mutational approach of TgACTI to determine if divergent residues within the parasite actin might account for unconventionally short filament formation. In addition, the function of parasite actin-binding proteins has previously only been tested with heterologous actins. Experiments conducted within this thesis were the first to look at regulation directly using TgACTI.

Low levels of fluorescent phalloidin are traditionally added to actin polymerization reactions to allow binding to the actin filament and subsequent visualization by fluorescence microscopy (Wulf et al., 1979). Previous studies with both recombinant TgACTI and PfACTI have employed this method to reveal formation of short actin filaments (Sahoo et al., 2006; Schmitz et al., 2005; Schüler et al., 2005). The present studies confirmed short filament formation by TgACTI and PfACTI, but also examined the polymerization capabilities of the second actin from *P. falciparum*, PfACTII, which has not previously been studied. Fluoresence microscopy studies with PfACTII revealed it is capable of forming slightly longer filaments than TgACTI and PfACTI; however, polymerization was still not very robust and the kinetics of polymerization were almost identical to those of PfACTI (Chapter 2). Although TgACTI, PfACTI and PfACTII did not polymerize robustly and formed filaments shorter than conventional actins, addition of equimolar phalloidin resulted in formation of much longer filaments that more closely resembled filaments formed by conventionally studied actins (Chapter 2). Phalloidin binds in a pocket that contacts three actin monomers within the filament thereby aiding to pin the monomers together (Faulstich et al., 1993) and we wanted to determine where

phalloidin bound parasite actin. The phalloidin-binding pocket within the parasites actin filaments was modeled to be in a similar location as that predicted for binding to conventional actin filaments (Chapter 2). The rescue of parasite actin polymerization by equimolar phalloidin revealed that the lack of robust polymerization by parasite actins is at least in part due to an intrinsic property of this actin itself. TgACTI contains a number of divergent residues within its sequence, some that have been predicted to result in reduced contacts between monomers within the filament (Sahoo et al., 2006). The divergent residues may prevent formation of stable contacts within the filament or alternatively play a role in monomer turnover. Either scenario could result in shorter filaments and account for the differences observed in polymerization of parasite actin compared with yeast actin (Chapter 2). Phalloidin rescue is consistent with such a model as binding to the filament may help to overcome a defect within the actin that keeps it from elongating or causes filaments to disassemble, likely through interaction with multiple monomers thereby increasing stability and compensating for intrinsic properties that reduce polymerization.

The model that intrinsic properties of the parasite actins result in reduced filament formation prompted the question of what features within the actin might be contributing to this instability. To address this question, molecular modeling was used to uncover residues that diverge from conventional actin, specifically in residues predicted to be involved in inter-strand contacts that had potential to be critical for actin filament stability (Chapter 3). The modeling identified two regions of interest, an inter-strand hydrogen bonding interaction that occurs in muscle actin, but not TgACTI, and reduced hydrophobicity within the hydrophobic loop of TgACTI (Chapter 3). Mutational analysis

substituting the residues within TgACTI with those from conventional mammalian muscle actin revealed that TgACTI substituted in either region polymerized more robustly than wild type TgACTI, with the substitution restoring the hydrogen bond interaction being the most pronounced polymerization increase (Chapter 3). The rescue in polymerization by single amino acid substitutions was quite striking and suggested only a few changes within TgACTI may be responsible for its unconventional polymerization properties. Both of the substitutions tested were predicted to strengthen monomer-monomer contacts and in fact they rescued polymerization in a similar manner to phalloidin, although to a lesser extent. Enhancement of *in vitro* polymerization through amino acid substitutions provides further evidence that intrinsic properties within parasite actins influence overall polymerization.

Substituted TgACTI was introduced into *T. gondii* with an N-terminal destabilization domain for conditional expression to determine the impact of substituted TgACTI *in vivo*. Videomicroscopy of *T. gondii* expressing the stabilized mutant revealed the parasites exhibited both aberrant circular and helical gliding motility (Chapter 3). Additionally, the overall speed of gliding for *T. gondii* expressing stabilized TgACTI was reduced compared to control parasites. The observation that proper gliding motility is disrupted by introduction of substituted alleles of TgACTI into *T. gondii* provides insight into a molecular basis for the intrinsic instability of TgACTI that results in formation of short actin filaments. The exact mechanism for how these substitutions affect gliding motility is still undetermined. One model for the impact on gliding is that the substituted actin monomers result in strengthened monomer-monomer stable contacts, creating longer, more stable filaments. Stabilization of TgACTI could then influence the gliding ability

of the parasite by inhibiting the tight turning radius required for productive motility, resulting in aberrant motons and reduced speed. The substitutions could also stabilize the filaments by preventing monomer turnover affecting the control of timing of gliding. Alternatively, the substitutions have an indirect impact on gliding by altering interactions with actin-binding proteins and disrupting TgACTI regulation.

Failure to visualize filaments within the stabilized-TgACTI expressing parasites suggests that the length of these filaments was still not above the level of detection of microscopy approaches, yet, expression of the mutant alleles had a detrimental effect on the ability of the parasites to undergo productive gliding motility. Small alterations in filamentation appear to lead to defects on the *T. gondii* life cycle, reminiscent of the toxic effect of JAS treatment (Wetzel et al., 2003), although JAS treatment results in a more severe effect (i.e. complete loss of directionality) and leads to visualization of filaments within the parasite. It appears both small and large perturbations of TgACTI polymerization dynamics disrupt proper gliding motility further demonstrating actin polymerization is a very precise process.

It is apparent that control of the timing and extent of actin polymerization within *T. gondii* is critical and these events must be strictly regulated. *T. gondii* encodes fewer actin-binding proteins than other more conventional systems. *T. gondii* profilin (TgPRF) and formins (TgFRM1 and TgFRM2) exhibit canonical behaviors on heterologous actin (Daher et al., 2010; Plattner et al., 2008) although their effect on TgACTI polymerization was unknown. Because TgACTI is divergent from conventional actins and polymerization is less robust, it was unclear if TgPRF and TgFRMs would function in the same manner with TgACTI as they do with conventional actin. Therefore, the current

studies examined the function of TgPRF, TgFRM1 and TgFRM2 on TgACTI polymerization. TgPRF decreased TgACTI polymerization in a dose dependent manner as assayed by light scattering and sedimentation analysis (Chapter 4). Nucleotide exchange assays with TgPRF also demonstrated that this protein exerts a slight inhibition for exchanging nucleotide on TgACTI, consistent with results reported from these assays conducted using rabbit actin (Kucera et al., 2010), but contrasting the impact of many more conventional profilins (Mockrin and Korn, 1980). TgPRF was able to inhibit TgACTI polymerization but did not enhance nucleotide exchange, suggesting the major function of TgPRF is to sequester TgACTI. Further evidence of TgPRF function in TgACTI sequesteration was observed when a 1:1 concentration of TgPRF to TgACTI was added to light scattering assays in the presence of TgFRM. This combination of regulators resulted in an inhibition of polymerization indicating TgPRF does not enhance TgFRM mediated polymerization at this concentration. Decreasing the amount of TgPRF to a 1:10 ratio to TgACTI reversed the inhibitory impact suggesting there is a threshold of TgPRF concentration above which TgACTI is efficiently sequestered. Actin depolymerizing factor (TgADF) also functions within *T. gondii* to sequester TgACTI (Mehta and Sibley, 2010). Both TgPRF and TgADF are in roughly 1:1 concentration with TgACTI and are expected to sequester the majority of TgACTI. The combination of sequestering by both of these proteins is likely to account for the high percent of unpolymerized actin found in intracellular parasites.

TgFRM1 and TgFRM2 acted to greatly enhance light scattering in the presence of TgACTI, suggesting these proteins are influencing polymerization (Chapter 4). Addition of TgFRM to TgACTI provides the first evidence of robust parasite actin polymerization

in the absence of non-physiological agents (i.e. phalloidin, JAS). The amount of light scattering by TgACTI increased dramatically in the presence of TgFRM suggesting additional mechanisms other than simply polymerization were being measured. Certain formins have been demonstrated to stimulate actin filament bundling and this may be occurring with the TgFRM proteins to robustly increase polymerization. In *Arabidopsis*, one formin, AFH1, induced bundling via side-binding to actin filaments to mediate bundling (Michelot et al., 2006; Michelot et al., 2005) and it remains to be determined if a similar phenomena occurs with TgFRMs. Demonstration of the impact of TgPRF and TgFRMs on TgACTI polymerization suggest that these two actin-binding proteins perform functions that can account for major regulation of TgACTI *in vitro* by allowing control between sequestering of monomers and the enhancement of polymerization. Although apicomplexan parasites encode a more minimal set of regulatory proteins, the small repetoire appears to contain proteins that can sequester TgACTI as well as promote polymerization and are therefore likely to be sufficient for proper regulation of TgACTI.

TgACTI was initially reported to have a critical concentration (Cc) of 0.04 μM, about three fold lower than that of mammalian actins, suggesting it should polymerize robustly at low concentrations (Sahoo et al., 2006). Yet, few filaments were formed at 5 μM, a concentration that far exceeds the calculated Cc (Sahoo et al., 2006) (Chapter 2 and 3). This contradiction raised questions about the exact mechanism of polymerization employed by TgACTI. Actins traditionally polymerize via a nucleation-elongation mechanism where polymerization does not occur until the actin concentration exceeds its Cc. However, closer examination of the features of TgACTI polymerization demonstrated polymerization in a concentration dependent manner with no lag phase, no

Cc and formed a range of filament sizes, properties that are inconsistent with nucleation-elongation (Chapter 5). Rather, the polymerization characteristics of TgACTI provide striking evidence that TgACTI is the first actin shown to undergo isodesmic polymerization. Polymerization via an isodesmic mechanism explains the lack of long, stable filaments within *T. gondii* as this type of polymerization would not require exceeding a concentration threshold to initiate polymerization but rather be expected to result in concentration dependent polymerization. Actin-binding proteins with sequestering roles within *T. gondii* are predicted to remove the majority of TgACTI from the free monomer pool thereby preventing the intracellular TgACTI concentration from becoming high enough for polymerization.

The results from the work of this thesis indicate that TgACTI does not polymerize robustly on its own, is regulated by actin-binding proteins, and polymerizes in a dose-dependent manner via isodesmic polymerization and these properties of TgACTI collectively result in a lack of long, stable filaments within the parasite. The efforts of this thesis provide evidence for multiple mechanisms used by *T. gondii* to maintain high levels of unpolymerized TgACTI *in vivo* and to ensure spontaneous polymerization of long filaments does not occur. TgACTI contains divergent residues to reduce monomer-monomer contacts within the filament and ensure long filaments do not form by TgACTI alone. Many of these divergent residues are within regions of inter-strand contacts and may account for the ability of TgACTI to assemble via isodesmic polymerization rather than conventional nucleation-elongation. Isodesmic polymerization may result from weakened inter-strand contacts within the filament and would aid to prevent robust polymerization by requiring a high concentration of TgACTI to form long filaments.

Finally, TgACTI polymerization is specifically regulated by actin-binding proteins to sequester TgACTI from polymerization and also by actin-binding proteins with an opposing function to promote polymerization.

Together, presence of divergent residues within TgACTI and regulation by actin-binding proteins predict a model to explain both unusual *in vitro* and *in vivo* findings for TgACTI. In the absence of actin binding proteins *in vitro*, TgACTI does not polymerize robustly and forms short filaments due to divergent residues. Lack of inter-strand contacts to stabilize TgACTI filaments may result in formation of a looser helix and concentration dependent polymerization due to an isodesmic mode of assembly (Figure 1A). The addition of phalloidin or substitution of divergent residues with those from conventional actin reverses these effects and allow for formation of more conventional filaments. Support for this model comes from recent modeling of the helix of PfACTI that suggests the pitch of the helix is larger than that of conventional actin. A larger pitch could be evidence of a looser helical interactions but the reported results are confounded by the addition of phalloidin and therefore this finding requires further analysis (Schmitz et al., 2010). *In vivo*, TgACTI has an additional level of regulation by actin binding proteins where TgPRF exists at high intracellular concentrations to act in TgACTI sequestration and inhibit spontaneous TgACTI polymerization. Upon initiation of gliding motility, TgFRM function becomes activated to bind TgACTI, potentially acting as a capper or side binder to enable filament formation and possibly bundling. If a looser helix is formed by TgACTI alone, it is possible that TgFRMs aid to orient the filaments into a more conventional helix (Figure 1B).

SUMMARY

Apicomplexan invasion of host cells involves a gliding motility mechanism that is dependent on polymerization of parasite actin. Studies involving *T. gondii* actin, TgACTI, have demonstrated that parasite actin does not readily polymerize and forms only short filaments (Sahoo et al., 2006). Treatment of *T. gondii* with actin stabilizing drugs, such as jasplakinolide, disrupts motility (Poupel and Tardieux, 1999), suggesting that stabilization of actin filaments may inhibit gliding motility and be toxic for the parasite. The present work has demonstrated that divergent residues within TgACTI contribute to its lack of robust polymerization. Changes to a minimal set of divergent residues negatively impacted gliding motility suggesting the process of filament formation is tightly controlled. The sequestering properties of TgPRF as well as polymerization enhancement by TgFRMs appear to play a critical role in the balance between unpolymerized actin and filaments for gliding. Reevaluation of the polymerization properties of TgACTI also reveal they are more consistent with isodesmic polymerization than traditional nucleation-elongation. Together, these mechanisms control TgACTI filament formation so polymerization occurs only when required for gliding motility ensuring proper host cell invasion and continuation of the parasite life cycle. The conclusions from this thesis work advance our understanding of apicomplexan cell biology and gliding motility and potentially provide targets unique to *Toxoplasma* for therapeutic intervention to block infection.

FUTURE DIRECTIONS

Mechanism of motility defect for parasites expressing TgACTI mutants

The mutational analysis in Chapter 3 demonstrated that introduction of amino acid substitutions within an intermonomer hydrogen bond and hydrophobic plug resulted in increased TgACTI filament length *in vitro* as well as defects in gliding motility *in vivo*. However, while filaments formed by the substituted TgACTI alleles showed increased sensitivity to jasplakinolide, all attempts to visualize filaments in the absence of stabilization agent failed. Therefore, we were unable to definitely conclude the negative impact on gliding motility was directly an effect of expressing stabilized TgACTI within the parasite and other models were proposed that could be used to explain the motility defect. However, further experimental testing could lend additional support for the model that stabilized filaments disrupt gliding and determine the merit of the alternative hypotheses.

Detection of Filaments within T. gondii stability mutants

Multiple techniques for the detection of filaments in the absence of stabilizing agents have been attempted including confocal microscopy and total internal refection (TIRF) microscopy of parasites expressing the DD-mutant alleles or these alleles transfected with YFP-TgACTI or GFP-LifeACT (Riedl et al., 2008) for aiding in visualization. Despite these efforts, filaments could not be detected within the control or mutant parasites. However, the one method that has proven promising was to use electron microscopy of Shld1 treated DD-TgACTI expressing parasites. The mutant parasites, but not control parasites, were observed to form membrane blebs that extended from the apical end of

the parasite, similar but less pronounced than the apical projections observed upon treatment with jasplakinolide (Chapter 3). Intriguingly, these membrane blebs contained filamentous structures within them. Immuno-electron microscopy would be insightful to identify if these structures are in fact actin filaments and if so, would be evidence that there are more stable filaments within the mutant TgACTI expressing parasites that are not observed within control parasites.

Defect in structural flexibility

Consistent with the model that expression of stabilized filaments within the parasite are the cause of the gliding defects observed, is the fact that the parasites move in larger arcs during circular gliding and are unable to undergo the tight turning radius of helical gliding. This hypothesis could be tested by modeling the forces applied on the surface and changing the flexibility of the surface on which the parasite is gliding. Glass coverslips may make these motions more difficult but using alternative substrates may reveal that the parasites are able to compensate and undergo more normal motility.

Turnover of actin monomers

If the TgACTI stability mutants are in fact more stable than wild type TgACTI, they would be expected to undergo less turnover than wild type TgACTI. To investigate this hypothesis, fluorescence recovery after photobleaching would be used to examine the ability of YFP-tagged mutant TgACTI expressing parasites to recover from photobleaching relative to the YFP-TgACTI control. A caveat with using FRAP in cells of small size such as *T. gondii* is the fact that bleaching even a small region of interest

often results in a loss of fluorescence within the entire parasite due to rapid protein diffusion. Previous use of FRAP within *T. gondii* has accounted for this by monitoring a second region of interest that was not bleached to account for loss in fluorescence and to use to subtract this loss in fluorescence from the FRAP results (Gordon et al., 2010). The prediction would be that the stabilized mutants would recover less quickly because there would be a slower rate of turnover so slower recovery in binding new monomers.

Impact of actin-binding proteins on TgACTI substitutions

An alternative model for the effect of the TgACTI substitutions on gliding motility is that the aberrant motility is due to changes in interactions with actin binding proteins. To test if TgPRF or TgFRMs function differently on wild type TgACTI or the stability mutants light scattering and fluorescence phalloidin microscopy would be utilized. If disruption of interaction with these proteins is the cause of the gliding defects, light scatter of mutant TgACTI would be expected to increase in the presence of TgPRF or decrease in the presence of TgFRM. TgADF has also been shown to act in TgACTI sequesteration (Mehta and Sibley, 2010) and therefore light scattering assays with the mutant actins would also be conducted with TgADF. If there are differences in these assays compared to what has been seen with wild type TgACTI, this would confirm the alternative hypothesis that the mutations disrupt either sequestering by TgACTI or TgADF, or polymerization enhancement by TgFRM.

Other life cycle stages impacted

In Chapter 3, the impact the stability mutants have on gliding motility was fully characterized but there are other life cycle stages that require gliding motility that remain to be examined. Another process that could potentially be affected by the mutant TgACTI alleles is host cell invasion. Invasion of *T. gondii* into host cells can be assayed using two-color immunofluorescence. After allowing the parasites to invade, the cells would be fixed and stained with an antibody against a surface protein conjugated to one fluorophore, then permeabilized and stained with the same antibody conjugated to a second fluorophore. This method allows differential staining of intracellular and extracellular parasites and to determine whether or not the parasites expressing the mutant TgACTI allele are able to invade host cells. Initial attempts to conduct invasion assays with mutant and control parasites did not result in a significant difference (Skillman and Sibley, unpublished data). However, using the standard assay protocol, parasites are given a large window of time for invasion. Even though there is a severe defect on plaque formation over time, it is possible that initially the parasites can use the slow, aberrant motility to enter into host cells especially if added to confluent monolayers where they do not have to use extensive gliding to enter the host cells. To alleviate these concerns, subconfluent monolayers would be used and *T. gondii* would be given a shorter time window for invasion to determine if these parasites are capable of gliding to the host cell and invading.

After completing endodyogeny, *T. gondii* must egress from the host cell and use gliding motility to move to a new cell for invasion and replication. Intracellular calcium levels signal to the parasite to initiate egress and this process can be induced using a

calcium ionophore to increase intracellular calcium concentration. The time for parasites to egress as well as their ability to undergo gliding to move from the lysed vacuole could be measured for parasites expressing the mutant TgACTI alleles compared to control parasites. The gliding defects observed in videomicroscopy would be expected to disrupt the migration to a new host cell.

Modulate levels of stability mutants expressed within T. gondii

Using the degradation domain system to tag TgACTI, we were able to express the TgACTI alleles at about 70% of the endogenous TgACTI expression level. Even with less than 1:1 expression, we were able to characterize a substantial phenotype in terms of gliding motility. However, it is possible that the mutant TgACTI was still able to copolymerize with endogenous TgACTI and therefore dilute the effect of the mutants. Non-productive interactions may also occur between the tagged proteins and endogenous proteins that disrupt the ability of the tagged proteins to assemble into more stable filaments. To alleviate these issues, the mutant constructs that were transfected into parasites would be reengineered to contain the A136G point mutant that has been shown to confer resistance to CytD (Dobrowolski and Sibley, 1996). These plasmids would then be transfected into parasites and clones isolated. Using this strategy, the parasites would be treated with Shld1 to stabilize and express the mutants but also treated with CytD just prior to experimentation to disrupt polymerization of the CytD-sensitive endogenous protein. CytD treatment would create a chemical knockdown of the endogenous protein so only the effects of the DD-tagged proteins will be monitored and the level of mutant expression will no longer be a concern.

The advantage of the degradation domain system is that it requires fewer steps of manipulating the parasite but the limitation is the presence of the endogenous allele. A more direct method of analyzing the impact of the TgACTI mutants would be to create a conditional knockout of endogenous wild type TgACTI using the tetracycline inducible-transactivator system, which has been adapted for use in parasites (Meissner et al., 2002). This strategy would be untaken rather than a direct knock out as TgACTI appears to be essential for completion of the *T. gondii* life cycle since cytD treatment inhibits invasion (Dobrowolski and Sibley, 1996). First, a plasmid containing the Tet operator upstream of an HA9 tagged version of the wild type *TgACTI* allele along with a selectable marker would be transfected into the *Toxoplasma* cell line that expresses the tetracycline transactivator. Parasites would be cloned to establish a cell line that now expresses both the transactivator as well as the tagged version of wild-type *TgACTI*. Merodiploid parasites would be tested to determine if expression of this tagged copy of the gene can be repressed in the absence of tetracycline. Second, these cloned parasites would be transfected with a construct containing a selectable marker with 5' and 3' UTRs homologous to the endogenous *TgACTI* gene allowing integration of this construct into the genome and deleting the endogenous gene through homologous recombination. Finally, the mutant *TgACTI* allele would be transfected into parasites and allowed to integrate anywhere in the genome. YFP would be cloned downstream of the mutant allele under control of its own promoter to use for selection of parasites that have integrated the mutant actin. When tetracycline is added, the transactivator will be unable to bind the operator resulting in a conditional knockout. Creation of this conditional-expression system would allow testing of the phenotypes of expression of TgACTI

mutants with no confounding effects of the wild type TgACTI. Without having the endogenous TgACTI present, phenotypes of the stabilized mutants may become stronger and it may be more feasible to uncover actin filaments within the parasite if they are not diluted with endogenous TgACTI. Conversely, expression of the mutant actins alone may toxic to resulting in severe defects in host cell invasion. In this case, we will have developed a scale to measure phenotypes that occur upon expressing variable levels of the TgACTI mutants.

Additionally, parasites depleted of wild type TgACTI could be used as a powerful tool to study the function of endogenous TgACTI by expressing a regulatable copy of wild type TgACTI. Little is known about the role of TgACTI within the parasite other than its role in gliding motility. Actins often play a role in cell divison but in *T. gondii* this process has been demonstrated to be driven by microtubules rather than actin (Shaw et al., 2000). TgACTI depletion would allow determination if cell division really is exclusively a microtubular process or whether TgACTI plays any role. Conditional expression of TgACTI would reveal if the actin contributes to any intracellular mechanisms independent of its role in gliding motility.

Nucleotide turnover and TgACTI stability

In addition to residues in the salt bridge and hydrophobic plug, the initial molecular modeling of TgACTI also revealed divergent residues within the nucleotide-binding pocket of TgACTI (Sept and Sibley, unpublished data). A methionine at amino acid 16 corresponds with asparagine-17 in TgACTI. This substituted residue is modeled to protrude into the nucleotide binding pocket thereby potentially affecting ATP hydrolysis

or P_i dissociation. The end result of such a substitution may be increased filament turnover that could account for the unstable TgACTI filaments observed. Serine 14 is a conserved residue located within the nucleotide binding pocket and is proposed to make contact with the gamma phosphate of ATP (Kabsch et al., 1990). Mutation of Serine 14 within yeast resulted in decreased affinity for ATP as well as temperature sensitive defects in polymerization (Chen et al., 1995; Chen and Rubenstein, 1995) adding merit to the hypothesis that the N17 residue in the binding pocket could influence stability.

Preliminary data using a phosphate release assay suggests that this divergent substitution in TgACTI results in release of phosphate four times greater than the amount of protein in the reaction (Sahoo and Sibley, unpublished results). When this assay was performed with rabbit actin or with a TgACTI mutant, N17M, where the asparagine is mutated back to the conventional residue of methionine, equimolar concentration of phosphate to protein was released (Sahoo and Sibley, unpublished results). If this finding is reproducible, it would suggest that TgACTI is undergoing rapid turnover since it must go through multiple steps including polymerization, hydrolysis of ATP, dissociation of P_i, depolymerization, exchange of nucleotide and repolymerization four times in the amount of time conventional actins would go through the process once (Figure 3). Both TgACTI and PfACTI contain the asparagine substitution but interestingly, PfACTII retains the methionine found in conventional actins.

The divergent N17 residue within TgACTI has the potential to impact a number of steps within the process of monomer turnover including ATP hydrolysis, phosphate release and nucleotide binding (Figure 2). To examine the phosphate release of TgACTI, the Enz-chek phosphate release assay kit (Molecular Probes) would be utilized to

determine the molar ratio of phosphate released from TgACTI. An N17M TgACTI mutant was previously created by site-directed mutagenesis and has been expressed in baculovirus allowing purification of recombinant His-tagged protein. The phosphate release assay would be compared with wildtype TgACTI, rabbit actin and the N17M mutant of TgACTI to determine if the preliminary results suggesting increased phosphate release in TgACTI are correct.

Additionally, the presence of non-hydrolyzable ATP and additional ATP analogs will be used in these assays to examine if this would affect the results seen with TgACTI. Previous studies have demonstrated that addition of beryllium fluoride can rescue polymerization defects from reduced hydrophobicity within the hydrophobic loop (Kuang and Rubenstein, 1997). Beryllium fluoride acts as a phosphate analog and binds within the P_i site after ATP hydrolysis. Beryllium fluoride has been suggested to add stability to the filament via enhanced contact between subdomain 2 of one actin monomer and the monomer above it within the helix (Orlova and Egelman, 1992).

To better understand the rate of phosphate release, it will also be important to determine the nucleotide exchange rate of TgACTI in the G-actin state versus the F-actin state since this is one of the steps that could be influencing turnover. Determining how this step compares to what is seen with conventional actins will be important in understanding any differences observed with TgACTI. A fluorescent ATP analog, ε-ATP (1,N,6-ethenoadenosine 5'-triphosphate), is commonly used for measurement of nucleotide exchange (Wang and Taylor, 1981). Unlabeled ADP-actin is first depleted of any unbound ATP. The actin is then incubated with an excess of ε-ATP and the levels of fluorescence are monitored using a plate reader giving the nucleotide exchange rate.

In addition to analysis of the effects on ATP hydrolysis and exchange, fluorescent phalloidin staining and sedimentation assays will be conducted on the N17M mutant. Preliminary analysis of this mutant by fluorescent phalloidin microscopy did not reveal a striking increase in filament length, however, addition of equimolar levels of unlabeled phalloidin resulted in filaments that were much more kinked than seen with wild type TgACTI (Skillman and Sibley, unpublished data). Therefore, this mutant merits closer examination by other means such as tryptophan quenching, light scattering, and electron microscopy.

If it is confirmed that TgACTI has an increased intrinsic nucleotide turnover rate, it would provide another mechanism for maintaining short filaments as rapid turnover would make actin filaments susceptible to polymerization and prevent them from becoming exceedingly long. Such a finding would also explain why TgPRF does not appear to function in enhancing nucleotide exchange as other profilins do since TgACTI would be capable to perform this function on its own and not require an actin-binding protein to do so.

Also related to nucleotide turnover is the methylation of His-73 that occurs in many eukaryotic actins. This methylation adds positive charge to this histidine, which allows it to act within a network of interactions strengthening a hydrogen bond between H73 and G158 aiding to bind the terminal phosphate of ATP and contributing to conformational changes of the nucleotide binding pocket (Nyman et al., 2002). Mutation of histidine-73 to alanine in mammalian β-actin uncoupled ATP hydrolysis and phosphate release from polymerization. These studies led to speculation regarding whether the effect of methylation at this point is to aid in keeping the actin in a polymerization competent

formation so filamentation can rapidly occur. Mass spectrometry to examine modifications of PfACTI extracted from the parasite revealed this methylation is not present (Schmitz et al., 2005). Therefore, it would be of interest to confirm this within TgACTI isolated from *T. gondii*. If this modification is missing, it may be another factor contributing to overall filament instability through divergence in the nucleotide binding pocket.

Mechanisms of profilin and formin function *in vitro* and *in vivo*

TgFRM mechanism of polymerization enhancement

Light scattering assays examining the impact of TgFRM1 and TgFRM2 on TgACTI polymerization reveal a dramatic increase in light scatter (Chapter 4). These results make it apparent that *T. gondii* formins influence TgACTI, however, as ninety degree light scattering would be influenced by filament elongation or bundling, the exact mechanism of TgFRM function is still unresolved. Therefore, it is important to differentiate between possible mechanisms that explain the influence of TgFRMs on TgACTI polymerization such as binding the barbed end acting to cap filaments thereby providing stability or binding the sides of filaments to promote bundling. Understanding these mechanisms also entails determining if TgFRMs move processively or nonprocessively along the TgACTI filament.

In nonplant systems, binding of formin to the barbed end of filament lowers the affinity of capping protein binding to the actin filament (Kovar et al., 2003). Therefore, if TgFRMs act to cap filaments and stay associated with the barbed end, addition of capping protein should not lead to a dramatic decrease in polymerization. In the case of

AFH1, which has been shown to move to the side of actin filaments following barbed end binding, the presence of capping protein inhibits polymerizatin in a dose dependent manner (Michelot et al., 2005). Light scattering assays combining TgACTI, either TgFRM and a conventional capping protein (from a different organism) would be used to reveal the accessibility of the TgACTI barbed end and decipher if TgFRMs stay associated with the barbed end to block it from binding of capping protein.

TIRF microscopy would also be employed to differentiate between potential mechanisms of the TgFRMs. The caveat to these assays would be the need to add a fluorescent label to TgACTI. Low yields of TgACTI from purification have hindered these experiments in the past but only low levels of actin would be required for these assays and it may therefore be feasible to obtain labeled TgACTI. The labeled TgACTI would be incubated with either TgFRM1 or TgFRM2 and changes in polymerization would be observed over time. These assays would be a direct observation to determine if TgFRMs increase initiation of polymerization. By observing the growth of the filaments, the question of processivity can also be addressed. If either formin is aiding filamentation in a processive manner, the growth of the filament should be remain the brightest at the originial point of assembly. However, if the formin is acting non-processively, the brightest point of the actin will move away from the initiation point. If the TgFRMs can promote bundling through side binding, similar to AFH1, they should exhibit non-processive polymerization (Michelot et al., 2006), as the formin moves from the barbed end to the side of the filament.

To confirm or deny the side binding hypothesis, GFP-tagged TgFRMs would be used in fluorescence microscopy of phalloidin labeled TgACTI to observe if the formins are

observed interacting with the filaments on the sides or only at the filaments ends. It is possible from the results of Chapter 5 regarding the finding that TgACTI utilizes an isodesmic mode of polymerization that even low levels of phalloidin may influence the polymerization results. To verify a potential side binding interaction, immuno gold electron microscopy of TgACTI polymerized in the presence of formin would also be required.

The light scattering results from Chapter 4 strongly suggest filament bundling is occurring *in vitro*, however, it is unclear if this occurs *in vivo* and what significance it would have. Therefore, it would be of interest to identify regions of TgFRMs that contribute to bundling. Regions of importance could be achieved via comparison of the FH1-FH2 portions of TgFRMs against formins known to bundle actin filaments such as AFH1 (Michelot et al., 2006; Michelot et al., 2005), FRL1 and mDia2 (Harris et al., 2006) as well as comparison to more conventional processive formins to potentially identify residues important for side binding. Mutational analysis could then be performed to attempt to separate barbed end binding from side binding and bundling to determine the impact of each role on TgACTI polymerization.

In vivo analysis of TgPRF interactions

If TgPRF is acting primarily to sequester TgACTI within *T. gondii*, it would be expected that parasites depleted for TgPRF would reveal longer filaments. *T. gondii* cell lines expressing a regulatable copy of TgPRF have been created (Plattner et al., 2008) by a collaborator. In the published work with this cell line, staining was conducted using an anti-actin antibody but no difference was observed between wild type parasites and those

depleted for TgPRF. If filaments become as long as those within jasplakinolide treated parasites, they would be immediately apparent but if they were of a more intermediate length, more in depth analysis of the parasite could be required for visualization. Therefore, the TgPRF-depleted parasites would be subjected to confocal microscopy with z-slices taken to determine if filaments can be detected that are not seen in wild type parasites.

Regulation mechanisms for controlling TgFRM function

While it appears TgFRMs function to regulate TgACTI polymerization, the regulation of TgFRM is unknown. Formin proteins often contain Rho-GTPase domains or diaphanous autoinhibitory domains (DAD) to control the timing of their function in actin assembly (Kovar, 2006) but both of these domains are lacking in apicomplexan formins (Schüler and Matuschewski, 2006). TgFRMs must be regulated in some manner to dictate when they are capable of promoting polymerization *in vivo* because filaments are not observed in intracellular parasites. To determine what other parasite factors are interacting with TgFRM and controlling their function, parasite lysates would be used for co-immunoprecipitations with an anti-TgFRM antibody. The proteins within the resulting complex would be identified using mass spectrometry. Identified proteins may reveal binding partners that interact with conventional formins, such as Rho or cdc42, but bind to previously unidentified domains within the formin or these assays have the potential to identify novel binding partners that regulate TgFRM function.

Impact of isodesmic polymerization of TgACTI filaments *in vivo*

The key requirements of a nucleation-elongation mechanism of actin assembly (i.e, lag phase in elongation, critical concentration for assembly, plateau in unpolymerized actin) were shown not to be met by TgACTI and rather the polymerization features of TgACTI are more consistent with isodesmic polymerization (Chapter 5). Polymerization through an isodesmic mechanism should be concentration dependent and not require a lag phase for nucleation. Isodesmic polymerization would also be expected to produce filaments of various lengths whereas nucleation-elongation polymerization would produce two populations, monomers or long filaments. Density centrifugation analysis with TgACTI was consistent with isodesmic polymerization in that incubation of TgACTI on F buffer did not induce a large population of pelletable filaments as observed with yeast actin, but rather an slight increase in the molecular weight of the protein was observed (Chapter 5). However a more precise analysis of the population of filament lengths upon polymerization of TgACTI would further confirm the hypothesis of isodesmic polymerization and this would be achieved using dynamic light scattering.

Another possible property of isodesmic polymerization is the formation of single protofilaments rather than helical filaments. To date, all visualization of TgACTI filaments have been in the presence of either low or high levels of phalloidin. EM images of phalloidin stabilized TgACTI filaments show characteristics of helical actin filaments (Chapter 2), but it is possible phalloidin may influence polymerization and could alter the native filament structure. It is unclear how these filaments are structured in the absence of phalloidin as attempts to visualize them have been unsuccessful. With the knowledge that longer TgACTI filaments form at higher protein concentrations,

attempts to visualize the filaments by EM using these concentrations will be attempted as they may be more successful. In addition to negative staining EM, freeze fracture EM is another potential mechanism to observe filaments. If filaments are not captured by negative staining EM due to instability and disruption during the drying process, freeze fracture may overcome this limitation and reveal information about the filament structure.

While the TgACTI sequence does diverge from more conventional actins, it seems unlikely that the difference would result in formation of single protofilaments. However, it is possible that TgACTI relies more on intrastrand contacts than on interstrand contacts and forms a somewhat looser helix than conventional actins. In this case, the molecular modeling done to determine inter-strand contacts that may influence filament stability could be utilized to examine intra-strand contacts and how disruption of these residues may influence TgACTI polymerization. Specifically, the DNase I loop of actin contributes to intra-strand contacts and this region of the apicomplexan actins is highly divergent and may be important for creating a filament that is able to undergo isodesmic polymerization rather than nucleation-elongation.

Finally, the kinetics of increase in polymerization of different concentrations by light scattering will be used for modeling the polymerization of TgACTI to confirm if these kinetics are consistent with isodesmic polymerization. In addition to wild type TgACTI, these kinetics will also be determined for the TgACTI stability mutants in order to determine if the divergent residues are contributing to isodesmic polymerization.

REFERENCES

Baum, J., Tonkin, C.J., Paul, A.S., Rug, M., Smith, B.J., Gould, S.B., Richard, D., Pollard, T.D., and Cowman, A.F. (2008). A malaria parasite formin regulates actin polymerization and localizes to the parasite-erythrocyte moving junction during invasion. Cell Host Microbe *3*, 188-198.

Chen, X., Peng, J., Pedram, M., Swenson, C., and Rubenstein, P.A. (1995). The effect of the S14A mutation on the conformation and thermostability of *Saccharomyces cerevisiae* G-actin and its interaction with adenine nucleotides. J Biol Chem *270*, 11415-11423.

Chen, X., and Rubenstein, P. (1995). A mutation in an ATP-binding loop of *Saccharomyces cerevisiae* actin (S14A) casues a temperature-sensitive phenotype *in vivo* and *in vitro*. J Biol Chem *270*, 11406-11414.

Daher, W., Plattner, F., Carlier, M.F., and Soldati-Favre, D. (2010). Concerted action of two formins in gliding motility and host cell invasion by *Toxoplasma gondii*. PLoS Pathog *6*.

Dobrowolski, J.M., and Sibley, L.D. (1996). Toxoplasma invasion of mammalian cells is powered by the actin cytoskeleton of the parasite. Cell *84*, 933-939.

Faulstich, H., Zobeley, S., Heintz, D., and Drewes, G. (1993). Probing the phalloidin binding site of actin. FEBS Lett *318*, 218-222.

Gordon, J.L., Buguliskis, J.S., Buske, P.J., and Sibley, L.D. (2010). Actin-like protein 1 (ALP1) is a component of dynamic, high molecular weight complexes in Toxoplasma gondii. Cytoskeleton *67*, 23-31.

Harris, E.S., Rouiller, I., Hanein, D., and Higgs, H.N. (2006). Mechanistic differences in actin bundling activity of two mammalian formins, FRL1 and mDia2. J Biol Chem *281*, 14383-14392.

Kabsch, W., Mannherz, H.G., Suck, D., Pai, E.F., and Holmes, K.C. (1990). Atomic structure of actin: DNAseI complex. Nature *347*, 37-43.

Kovar, D.R. (2006). Molecular details of formin-mediated actin assembly. Curr Opin Cell Biol *18*, 11-17.

Kovar, D.R., Kuhn, J.R., Tichy, A.L., and Pollard, T.D. (2003). The fission yeast cytokinesis formin Cdc12p is a barbed end actin filament capping protein gated by profilin. J Cell Biol *161*, 875 - 887.

Kuang, B., and Rubenstein, P.A. (1997). Beryllium fluoride and phalloidin retore polymerizability of a mutant yeast actin (V266G, L267G) with severely decreased hydrophobicty in a subdomain 3/4 loop. J Biol Chem *272*, 1237-1247.

Kucera, K., Koblansky, A.A., Saunders, L.P., Frederick, K.B., De La Cruz, E.M., Ghosh, S., and Modis, Y. (2010). Structure-based analysis of Toxoplasma gondii profilin: a parasite-specific motif is required for recognition by Toll-like receptor 11. J Mol Biol *403*, 616-629.

Mehta, S., and Sibley, L.D. (2010). *Toxoplasma gondii* actin depolymerizing factor acts primarily to sequester G-actin. J Biol Chem *285*, 6835-6847.

Meissner, M., Schluter, D., and Soldati, D. (2002). Role of *Toxoplasma gondii* myosin A in powering parasite gliding and host cell invasion. Science *298*, 837-840.

Michelot, A., Derivery, E., Paterski-Boujemaa, R., Guerin, C., Huang, S., Parcy, F., Staiger, C.J., and Blanchoin, L. (2006). A novel mechanism for the formation of actin-filament bundles by a nonprocessive formin. Curr Biol *16*, 1924-1930.

Michelot, A., Guerin, C., Huang, S., Ingouff, M., Richard, S., Rodiuc, N., Staiger, C.J., and Blanchoin, L. (2005). The formin homology 1 domain modulates the actin nucleation and bundling activity of Arabidopsis FORMIN1. Plant Cell *17*, 2296-2313.

Mockrin, S.C., and Korn, E.D. (1980). Acanthamoeba profilin interacts with G-actin to increase the rate of exchange of actin-bound adenosine 5'-triphosphate. Biochemistry *19*, 5359-5362.

Nyman, T., Schuler, H., Korenbaum, E., Schutt, C.E., Karlsson, R., and Lindberg, U. (2002). The role of MeH73 in actin polymerization and ATP hydrolysis. J Mol Biol *317*, 577-589.

Orlova, A., and Egelman, E.H. (1992). Structural basis for the destabilization of F-actin by phosphate release following ATP hydrolysis. J Mol Biol *227*, 1043-1053.

Plattner, F., Yarovinsky, F., Romero, S., Didry, D., Carlier, M.F., Sher, A., and Soldati-Favre, D. (2008). *Toxoplasma* profilin is essential for host cell invasion and TLR11-dependent induction of an interleukin-12 response. Cell Host Microbe *3*, 77-87.

Poupel, O., and Tardieux, I. (1999). *Toxoplasma gondii* motility and host cell invasiveness are drastically impaired by jasplakinolide, a cyclic peptide stabilizing F-actin. Microb Infect *1*, 653-662.

Riedl, J., Crevenna, A.H., Kessenbrock, K., Yu, J.H., Neukirchen, D., Bista, M., Bradke, F., Jenne, D., Holak, T.A., Werb, Z., *et al*. (2008). Lifeact: a versatile marker to visualize F-actin. Nat Methods *5*, 605-607.

Sahoo, N., Beatty, W.L., Heuser, J.E., Sept, D., and Sibley, L.D. (2006). Unusual kinetic and structural properties control rapid assembly and turnover of actin in the parasite *Toxoplasma gondii*. Mol Biol Cell *17*, 895-906.

Schmitz, S., Grainger, M., Howell, S.A., Calder, L.J., Gaeb, M., Pinder, J.C., Holder, A.A., and Veigel, C. (2005). Malaria parasite actin filaments are very short. J Mol Biol *349*, 113-125.

Schmitz, S., Schaap, I.A., Kleinjung, J., Harder, S., Grainger, M., Calder, L., Rosenthal, P.B., Holder, A.A., and Veigel, C. (2010). Malaria parasite actin polymerisation and filament structure. J Biol Chem.

Schüler, H., and Matuschewski, K. (2006). Regulation of apicomplexan microfilament dynamics by minimal set of actin-binding proteins. Traffic *7*, 1433-1439.

Schüler, H., Mueller, A.K., and Matuschewski, K. (2005). Unusual properties of *Plasmodium falciparum* actin: new insights into microfilament dynamics of apicomplexan parasites. FEBS Lett *579*, 655-660.

Shaw, M.K., Compton, H.L., Roos, D.S., and Tilney, L.G. (2000). Microtubules, but not actin filaments, drive daughter cell budding and cell division in *Toxoplasma gondii*. J Cell Sci *113*, 1241-1254.

Sibley, L.D. (2004). Invasion strategies of intracellular parasites. Science *304*, 248-253.

Wang, Y.L., and Taylor, D.L. (1981). Exchange of 1,N6-etheno-ATP with actin-bound nucleotides as a tool for studying the steady-state exchange of subunits in F-actin solutions. Proc Natl Acad Sci U S A *78*, 5503-5507.

Wetzel, D.M., Håkansson, S., Hu, K., Roos, D.S., and Sibley, L.D. (2003). Actin filament polymerization regulates gliding motility by apicomplexan parasites. Mol Biol Cell *14*, 396-406.

Wulf, E., Deboben, A., Bautz, F.A., Faulstich, H., and Wieland, T. (1979). Fluorescent phallotoxin, a tool for the visualization of cellular actin. Proc Natl Acad Sci U S A *76*, 4498-4502.

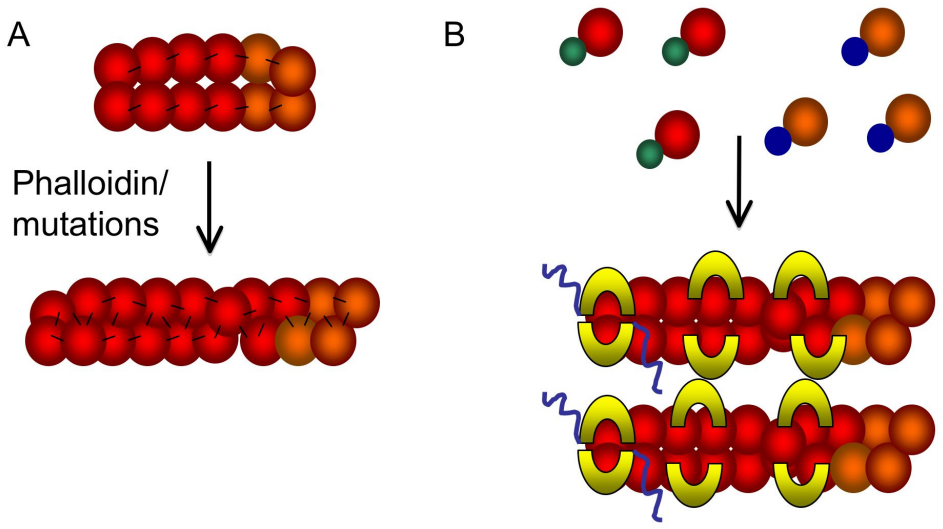

Figure 1. Models of *in vitro* and *in vivo* TgACTI polymerization.

(A) TgACTI polymerization *in vitro*. On its own, TgACTI assembles into short, loose actin helices due to a small number of divergent residues that weaken inter-strand contacts. The introduction of phalloidin to stabilize weak contacts or substitution of divergent residues with conventional residues restores the length and helical nature of the TgACTI filaments to appear more conventional. (B) TgACTI polymerization *in vivo*. During intracellular growth, TgPRF (green) and other actin-binding proteins sequester actin monomers ensuring there is no spontaneous polymerization. Upon intiation of gliding motility, TgFRMs (yellow) interact with TgACTI to stabilize interactions and potentially interact with the sides of filaments for added stability and bundle formation, also pulling the monomers into a conventional helix.

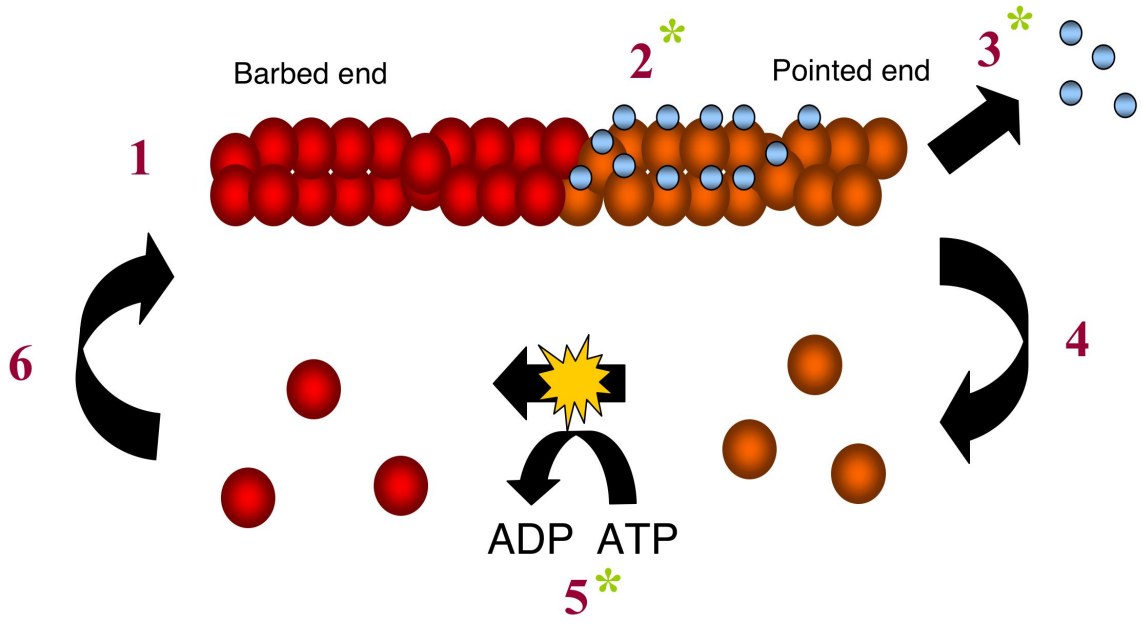

Figure 2. Multiple steps must occur for rapid nucleotide turnover.

1. Polymerization 2. ATP hydrolysis 3. P_i dissociation 4. Depolymerization 5. Nucleotide exchange 6. Repolymerization. Asteriks indicate steps that may be influenced by the divergent asparagine at position 17 in TgACTI.